Halogen Bonding Interlocked Host Systems for Recognition and Sensing of Anions

Benjamin R. Mullaney

Wolfson College, University of Oxford



A thesis submitted for the degree of Doctor of Philosophy

Inorganic Chemistry Laboratory
University of Oxford

Trinity Term, 2014

Halogen Bonding Interlocked Host Systems for Recognition and Sensing of Anions

Benjamin R. Mullaney, Wolfson College, University of Oxford

Abstract of thesis submitted for the degree of D.Phil., Trinity Term 2014

This thesis describes the synthesis of halogen bonding receptors for integration within interlocked anion host systems.

Chapter 1 introduces the field of supramolecular chemistry, with a particular focus on anion recognition and sensing, halogen bonding, and the synthesis of mechanically interlocked structures.

Chapter 2 describes the preparation and anion binding properties of carbazole-based receptor molecules. A systematic anion binding study on a series of halogen- and hydrogen-bonding 3,6-bis-triazolium carbazole acyclic receptors is described initially, followed by the development of a halogen bonding rotaxane. The anion and metal complexation properties of acyclic and macrocyclic systems incorporating the 1,8-bis-triazole carbazole motif are also presented.

Chapter 3 details the synthesis and anion complexation investigations of halogen and hydrogen bonding naphthalene-based acyclic and interlocked rotaxane host molecules.

Chapter 4 presents receptors based on the 4,4′-bis-triazole-2,2′-bipyridyl motif. A halogen bonding rhenium(I) bipyridyl complex is exploited in the development of a rotaxane host system which optically senses anions *via* luminescence purely through halogen bonding interactions. The anion recognition and sensing properties of diquat-based receptors are also investigated, and shown to exhibit optical and electrochemical responses to anions.

Chapter 5 summarises the major conclusions from Chapters 2–4.

Chapter 6 describes the experimental procedures used in the work, and includes characterisation data for the synthesised compounds.

Supplementary information relating to crystallographic data, and absorption, luminescence and electrochemical studies, is provided in the Appendices.

Acknowledgments

For all his time, effort, support, patience, ideas, encouragement and excellent humour, my sincerest thanks are owed to my supervisor, Prof. Paul Beer. These past years in his research group have been very rewarding, and I leave a wiser man.

The group have all left their mark on me as well – the help and friendship of members past and present have made life in the CRL thoroughly enjoyable. Particular thanks are due to Drs Chris Serpell, Lydia Gilday, Simon Picot, Nick White and Asha Brown, all of whose synthetic knowledge and experience were essential in teaching me the dark arts of organic synthesis. The other members of S8 have also been an absolute pleasure to work (and have fun) with, including DPhil students Tim Barendt, Sean Robinson, Tom Mole and Remi Tirfoin, and the various Part II students who have come and gone through those glass doors. Dr Amber Thompson has also been of immense help in teaching me crystallography, and solving structures beyond my skills.

I had the priviledge of supervising an excellent Part II student, Ben Partridge. He started the year knowing that he needed to accomplish 3 terms of work in 2, and exceeded all expectations, even managing to synthesise a halogen bonding rotaxane before he finished (although getting it pure was another matter…). A fun lab-mate and an extremely capable chemist, he has my thanks and my respect.

The staff of Wolfson College have been very supportive during my time in Oxford, and were particularly helpful in getting me through my final year here. My housemates, especially over the past year, deserve special mention for keeping my sane throughout my self-imposed write-up seclusion.

For proofreading various chunks of this thesis, I thank Matt, Sean, Asha, Chris, Nick, Ben P, Tim and Tom, and of course Paul, who had the (un)enviable pleasure of reading it all.

Finally, I would like to thank all my family and friends, both here and elsewhere. Without their support in all their various different ways, my Oxford experience would not have been as enjoyable and rewarding as it was.

Table of Contents

Abstract.....i

Acknowledgments.....ii

Table of Contents.....iv

Abbreviations and Symbols.....x

Chapter 1: Introduction.....1

1.1 Supramolecular Chemistry.....2

1.1.1 Intermolecular Interactions.....3

1.1.2 Design Principles for Host–Guest Chemistry.....7

1.2 Anion Recognition.....10

1.2.1 Importance of Anions.....10

1.2.2 Properties of Anions.....11

1.2.3 Biological Anion Receptors.....12

1.2.4 Synthetic Anion Receptors.....13

1.2.4.1 Cationic Anion Receptors.....14

1.2.4.2 Neutral Anion Receptors.....16

1.2.4.3 Metal-Containing Anion Receptors.....18

1.2.5 Sensing of Anions.....19

1.2.5.1 Colorimetric Anion Sensors.....19

1.2.5.2 Luminescent Sensors.....21

1.2.5.3 Electrochemical Sensors.....24

1.3 Halogen Bonding.....25

1.3.1 Halogen Bonding with Anions....26

1.4 Interlocked Structures....29

1.4.1 Synthesis of Catenanes and Rotaxanes....30

1.4.1.1 Cationic Templated Synthesis....32

1.4.1.2 Neutral Templation....35

1.4.1.3 Anion Templation....37

1.4.2 Applications of Interlocked Molecules....39

1.5 Outline of Project....43

1.6 References....44

Chapter 2: Carbazole-Based Anion Receptors....54

2.1 Introduction....55

2.2 Outline....55

2.3 3,6-Bis-substituted Carbazole Model Systems....56

2.3.1 Synthesis of Acyclic Model Receptors....57

2.3.1.1 Prototriazole Receptor Precursors....59

2.3.1.2 Bromotriazole Receptor Precursors....60

2.3.1.3 Iodotriazole Receptor Precursors....60

2.3.1.4 Prototriazolium and Iodotriazolium Receptors....63

2.3.2 Anion Binding Properties....64

2.3.2.1 Anion Recognition Properties of Prototriazolium Receptors....65

2.3.2.2 Anion Recognition Properties of Iodotriazolium Receptors....68

2.4 Interpenetrated and Interlocked Molecules....71

2.4.1 Pseudorotaxane Assembly Investigations....71

2.4.2 Attempted Rotaxane Synthesis by Stoppering....73

2.4.3 Rotaxane Synthesis by Ring-Clipping 76

2.4.3.1 Macrocycle Precursor and Axle Components 76

2.4.3.2 N-linked Rotaxane Synthesis 79

2.4.3.3 C-linked Rotaxane Synthesis 81

2.4.4 Anion Recognition Properties of Rotaxane **60**·$2PF_6$ 83

2.5 Optical Properties 86

2.5.1 Absorption Behaviour 86

2.5.2 Fluorescence Behaviour 87

2.6 Acyclic 1,8-Substituted Carbazole Systems 89

2.6.1 Synthesis of 1,8-Substituted Acyclic Carbazole Systems 89

2.6.2 Crystal Structures of Model Systems 90

2.6.3 Anion Binding Studies 91

2.6.4 Metal Complexation Studies 92

2.6.5 Macrocycles and Pseudorotaxanes 95

2.7 Conclusions and Future Work 101

2.8 References 103

Chapter 3: Naphthalene-Based Anion Receptors 105

3.1 Introduction 106

3.2 Outline 106

3.3 Naphthalene-Based Hydrogen Bonding Receptors 107

3.3.1 Synthesis of Acyclic Receptors 107

3.3.2 Anion Recognition Properties of HB Naphthalene-Based Receptors **82**·2BF_4 and **83**·2BF_4.....109

3.3.3 Macrocycles and Pseudorotaxanes 111

3.4 Naphthalene-Based XB Receptor.....116

3.4.1 Synthesis of Acyclic XB Bis-Iodotriazolium Naphthalene Receptor.....116

3.4.2 Anion Recognition Properties of XB Naphthalene-Based Receptor **98**·2BF_4.118

3.5 XB Interpenetrated and Interlocked Molecules 120

3.5.1 Pseudorotaxane Assembly Investigations.....120

3.5.2 Attempted Synthesis of Napthalene-Based Rotaxane by Stoppering Methodology.....121

3.5.3 Synthesis of Naphthalene-Based Rotaxane by Clipping Methodology.....122

3.5.4 Anion Recognition Properties of Rotaxane **106**·2PF_6.....124

3.6 Fluorescence Properties of XB Napthalene-Based Receptors 127

3.7 Conclusions.....128

3.8 References.....129

Chapter 4: Halogen Bonding Rhenium(I) Bipyridyl- and Diquat-Based Anion Receptors 130

4.1 Introduction.....131

4.2 Outline.....131

4.3 Acyclic Rhenium(I) Bipyridyl Receptors 132

4.3.1 Synthesis of Acyclic Receptors 132

4.3.2 Anion Recognition Properties of Acyclic Complex Receptors 135

4.4 XB Rhenium(I)-Containing Interpenetrated and Interlocked Structures 138

4.4.1 Pseudorotaxane Assembly Investigations 138

4.4.2 Rhenium(I)-Based All-XB Rotaxane Synthesis 140

4.4.3 Anion Binding Studies of All-XB Rotaxane **128**$^{2+}$ 145

4.5 Acyclic Diquat-Based Anion Receptors 149

4.5.1 Synthesis of Diquat-Based Acyclic Receptors 150

4.5.2 Anion Recognition and Sensing Properties 150

4.5.2.1 ^{1}H NMR Spectroscopic Studies 150

4.5.2.2 Absorption Studies 153

4.5.2.3 Electrochemical Studies 154

4.6 Attempted Synthesis of a Diquat-Containing All-XB Rotaxane 159

4.7 Conclusions and Future Work 160

References 162

Chapter 5: Conclusions 163

Conclusions 164

Chapter 6: Experimental Methods 166

6.1 Titration Protocols 167

6.1.1 NMR Titrations 167

6.1.2 UV-vis Titrations 167

6.1.3 Luminescence Titrations 168

6.2 X-ray Crystallography....168
6.3 Synthesis and Characterisation....170
6.3.1 Reactants and Reagents....170
6.3.2 Characterisation....170
6.4 Synthesis of Compounds from Chapter 2....171
6.5 Synthesis of Compounds from Chapter 3....221
6.6 Synthesis of Compounds from Chapter 4....242
6.7 References....262
Appendices....264
Appendix A: Crystallography Data....265
Crystallographic Information Files (CIF)....265
Data Tables....266
Appendix B: Absorption and Luminescence Spectra....268
Appendix C: Electrochemical Data....276

Abbreviations and Symbols

°	degrees
Å	angstroms
A	Ampere
a, *b*, *c*	length unit cell parameters (SCXRD)
α, *β*, *γ*	angle unit cell parameters (SCXRD)
AcOH	acetic acid
AIBN	azobisisobutyronitrile
aq.	aqueous
au	arbitrary units (luminescence) absorbance units (absorbance)
br.	broad (NMR)
C	Celsius
cf.	*confer*, compare/contrast
CIF	crystallographic information file
CuAAC	Cu(I)-catalysed azide–alkyne cycloaddition
CV	cyclic voltammogram
d	deuterated (NMR solvents)
d	doublet (NMR)
dd	doublet of doublets (NMR)
dt	doublet of triplets (NMR)
DBU	1,8-diazabicyclo[5.4.0]undec-7-ene
DIPEA	*N*,*N*-diisopropylethylamine
DMAP	4-dimethylaminopyridine
DMSO	dimethylsulfoxide
DNA	deoxyribonucleic acid
$E_{1/2}$	half-wave potential
E_{pa}	potential at the anodic peak
E_{pc}	potential at the cathodic peak
eq. / equiv.	equivalent/s
ESI	electrospray ionisation (MS)
FI	field ionisation (MS)
equiv.	equivalent
g	grams
GOF	goodness of fit (SCXRD)
Grubbs' I	Grubbs' 1st generation catalyst
Grubbs' II	Grubbs' 2nd generation catalyst

h	hours
HB	hydrogen bonding
HRMS	high-resolution mass spectrometry
Hz	Hertz
K	Kelvin
K_a	association constant
J	coupling constant
^3J	three bond coupling constant
^4J	four bond coupling constant
M	moles per litre
m	multiplet (NMR)
MALDI	matrix assisted laser desorption ionisation (MS)
MeOH	methanol
mg	milligrams
min	minutes
mL	millilitres
mm	millimetres
mmol	millimoles
MS	mass spectrometry
Ms	mesyl
mV	millivolts
NaHMDS	sodium hexamethyldisilazide; or sodium bis(trimethylsilyl)amide
NB	*nota bene*, note well no binding
NMR	nuclear magnetic resonance
$PdCl_2(PPh_3)_2$	bis(triphenylphosphine)palladium(II) dichloride
ppm	parts per million
q	quartet (NMR)
quin	quintet (NMR)
R	residual (SCXRD)
RCM	ring-closing metathesis
ROESY	rotating-frame nuclear Overhauser effect spectroscopy
RT	room temperature
sat.	saturated
SCXRD	single crystal X-ray diffraction
spt	septet (NMR)
St	stopper (of a molecular axle or rotaxane)
Stewart–Grubbs'	Stewart–Grubbs' catalyst, dichloro[1,3-bis(2-methylphenyl)-2-imidazolidinylidene](2-isopropoxyphenylmethylene)ruthenium(II)

sxt	sextet
T	Temperature
t	triplet (NMR)
TBA	tetra-*n*-butylammonium
TBTA	tris[(1-benzyl-1,2,3-triazol-4-yl)methyl]amine
^{t}Bu	tertiary butyl
THF	tetrahydrofuran
TLC	thin layer chromatography
TMS	trimethylsilyl
Ts	tosyl
UV	ultraviolet
V	unit cell volume (SCXRD) voltage (Electrochemistry)
vs	versus (against)
XB	halogen bonding
Z	formula units per unit cell (SCXRD)
δ	chemical shift
Δδ	change in chemical shift
θ	angle (diffraction)
λ	wavelength
μ	absorption coefficient (SCXRD)
ρ	density
$\%vdW_{x,y}$	% of the sum of the van der Waals radii of two atoms *x* and *y*
° C	degrees Celsius
§	section
≈	approximately equal to

Chapter 1: Introduction

1.1 *Supramolecular Chemistry*

The nature of supramolecular chemistry was eloquently expressed by Lehn in his 1987 Nobel lecture: "One may say that supermolecules are to molecules and the intermolecular bond what molecules are to atoms and the covalent bond".[1] This field is concerned with the study of non-covalent interactions between molecules, and the assembly of molecular architectures and the properties that arise as a consequence of these interactions.

Since its beginnings originating from the work of Pedersen on crown ethers and their ability to complex alkali metal cations,[2] the field of supramolecular chemistry has developed enormously, enabling the construction of highly complex structures, which can exhibit a plethora of desirable properties. Supramolecular chemistry may be divided into two main branches: *host–guest recognition*, in which a host molecule is designed and synthesised to bind a particular guest species using intermolecular interactions (**Figure 1-1a**); and *self-assembly*, in which simple components interact with one another in such a way that a larger composite structure is assembled (**Figure 1-1b**).

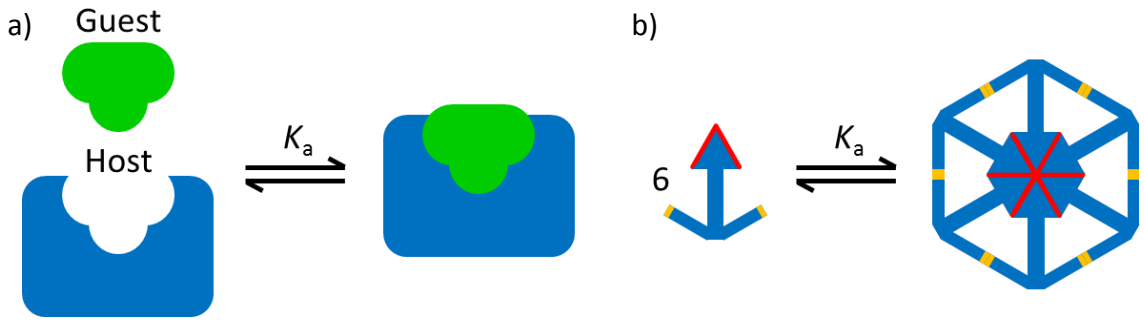


Figure 1-1: Cartoons representing the supramolecular principles of **a)** host–guest recognition; and **b)** self-assembly, where K_a is the equilibrium constant.

1.1.1 *Intermolecular Interactions*

In the design of supramolecular systems, there are many types of non-covalent interactions which can be exploited, according to the desired structure and functionality of the assembly.

Electrostatic Interactions: This class of interactions can be divided into three major categories: ion–ion, ion–dipole, and dipole–dipole. Ion–ion interactions are the attractive force between two oppositely-charged species. These are of comparable strength to covalent bonds, and tend to have no directionality (**Figure 1-2a**).[3] Of particular interest to the research theme of this thesis, ion–dipole interactions are used extensively in the host–guest chemistry of charged species (**Figure 1-2b**). Dipole–dipole are the weakest of the electrostatic interactions, but are nevertheless found extensively in nature, such as in the folding of proteins (**Figure 1-2c**).[4]

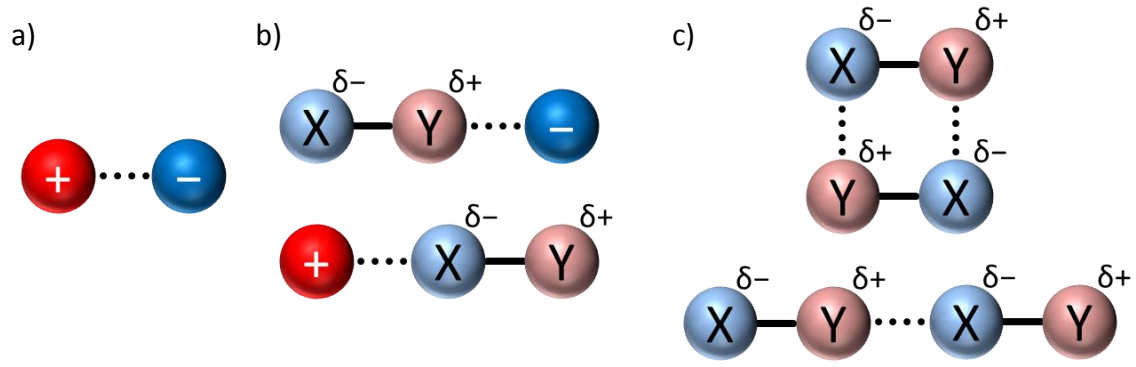


Figure 1-2: Schematic representations of the three types of electrostatic interactions, where X is an atom or region with partial negative charge, and Y is an atom or region with partial positive charge: **a)** ion–ion; **b)** ion–dipole; and **c)** two modes of dipole–dipole.

Hydrogen Bonding: This is a special class of dipole interaction. When a hydrogen atom is covalently bonded to an electronegative atom, such as O or N, or an electron-withdrawing

functional group, then a dipole is formed as the hydrogen develops a partial positive charge. This is able to interact with an electron-rich species, forming a so-called 'hydrogen bond' (**Figure 1-3a**). These intermolecular interactions tend to be highly directional due to the polarisation of the hydrogen atom, with linear hydrogen bonds being the strongest.[5] This interaction is the dominant ubiquitous structure-directing force in many biological macromolecules, such as the double-helix of DNA (**Figure 1-3b**).

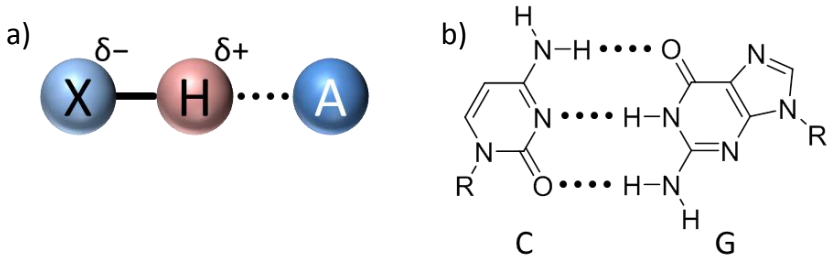


Figure 1-3: a) Schematic representation of hydrogen bonding (X = electronegative atom, H = hydrogen atom, A = hydrogen bond acceptor); **b)** hydrogen bonding between the cytosine (C) and guanine (G) base pairs of DNA.

Halogen Bonding: This is the intermolecular interaction formed between an electron-deficient halogen atom and an electron-rich Lewis Base. In a similar manner to the formation of a hydrogen bond, halogen atoms covalently bonded to electron-withdrawing groups can lead to polarisation of the halogen's electron distribution, producing a region of positive electrostatic potential (termed the 'σ hole') on the pole of the halogen. This electron-deficient region is able to interact with an electron-rich species, forming a stringently linear halogen bond. As the halogen atom size increases, the halogen bonding strength also increases due to the greater polarisability of the atom, with iodine providing the strongest halogen bonds. As halogen bonding is a central theme in the research presented in this thesis, a more comprehensive discussion on the subject is given in **§1.3**.

Aromatic Stacking Interactions: The terms 'π stacking' and 'π–π interactions' have been historically used to indicate a type of intermolecular attraction between aromatic molecules which was understood to be somehow distinct from other non-covalent interactions. However, it has recently come to light that such interactions arise from a combination of solvation effects, dispersion forces and, in particular, electrostatic interactions.[6] Nevertheless, there is an important class of interactions in donor–acceptor aromatic stacking, whereby there is an attractive force between electron-deficient and electron-rich aromatic systems (**Figure 1-4a**). A seminal example of using this effect in supramolecular chemistry is Stoddart's [2]pseudorotaxane shown in **Figure 1-4b**, which is assembled through donor–acceptor interactions between the electron-deficient 4,4′-bipyridinium-containing macrocycle, and the electron-rich 1,5-dimethoxynaphthalene thread component.[7]

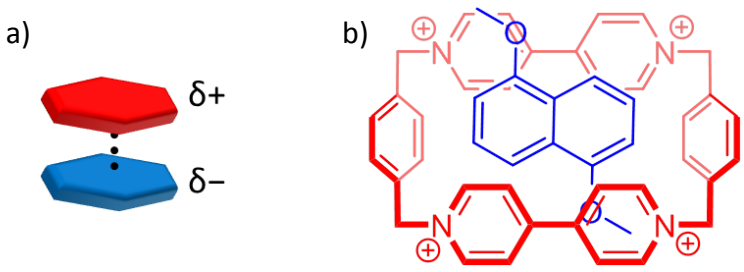


Figure 1-4: a) Schematic representation of donor–acceptor interactions between electron-rich and electron-deficient aromatic systems; **b)** Stoddart's [2]pseudorotaxane, which is assembled by donor–acceptor aromatic interactions between the thread and macrocycle.[7]

Cation– and Anion–π Interactions: The attractive force between cations and electron-rich π systems is well established, and arises primarily through an electrostatic interaction between the cation and the quadrupole of the π system (**Figure 1-5a**).[8-10] The interactions between anions and electron-deficient aromatic π systems have been observed and studied in the solid state, but are generally less well-explored, especially in the solution phase,

where they usually complement other anion recognition interactions within receptor motifs (**Figure 1-5b**).[11-17]

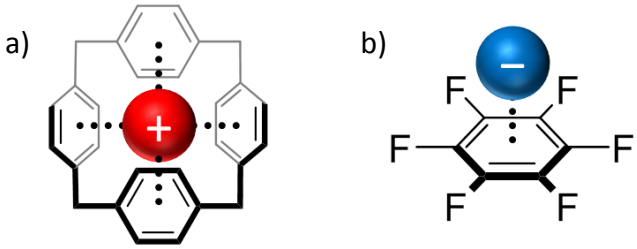


Figure 1-5: Examples of **a)** cation–π;[10] and **b)** anion–π[18] interactions.

Coordinate Bond: Although the coordination of ligands to metals is not non-covalent, the coordinate bond has been widely exploited in developing supramolecular systems. The advantages of these bonds lie in the structure-directing features of both the metal ions, which have specific coordination geometry requirements, as well as the design of the polydentate ligands (**Figure 1-6**).

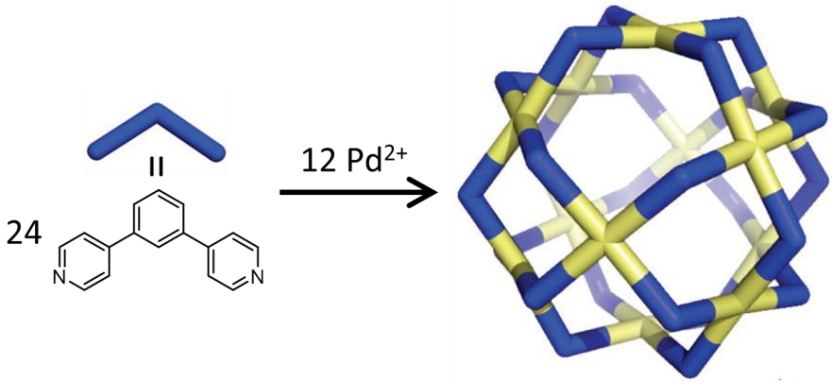


Figure 1-6: A supramolecular cage structure assembled by coordinate bonds between simple components.[19]

Solvophobic Effects: The influence of solvent on the assembly of supramolecular species is of great importance. Interactions between the components must be more thermodynamically favourable than interactions with the solvent, in order for the

supramolecular assembly to form. Assembly of a supramolecular system is entropically favoured if it results in the expulsion of ordered solvent molecules. Furthermore, there is also an enthalpic gain if the interactions are stronger between the component species, and/or between the solvent molecules. Where the solvent and solute molecules have significantly different polarities, aggregation or self-assembly can occur in order to maximise favourable solvophobic interactions.[20] For example, micelles are supramolecular structures formed from surfactant molecules aggregating in aqueous solution to form globular structures, with the surfactant lipophilic 'tails' producing a hydrophobic interior and the hydrophilic 'head' portion exposed to the aqueous solvent environment (**Figure 1-7**).

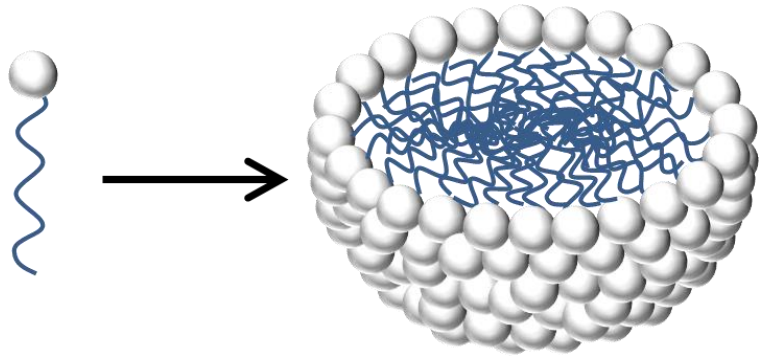


Figure 1-7: Cut-out illustration of a micelle, which is formed by aggregation of surfactant molecules, with the assembly driven by the solvophobic effect.

1.1.2 *Design Principles for Host–Guest Chemistry*

Since the inception of host–guest supramolecular chemistry, there are certain structural design principles which have been proven to produce host systems which effectively bind desired substrates.

When the binding sites in the host cavity are of a complementary size and shape to the

target guest, the overall stability of the favourable host–guest complex is increased. This *complementarity* design principle can be utilised to achieve enhanced selectivity for the optimised guest species over other substrates. This is demonstrated by proteins in biological systems which, through a combination of different non-covalent interactions arranged in a complementary geometry, exhibit impressive selectivity for specific substrates.[21,22] Cryptands[23] are a synthetic class of group 1 metal cation receptors which illustrate this concept (**Figure 1-8**): the [2.1.1]cryptand, with its relatively small binding cavity, is selective for Li^+; the [2.2.1]cryptand binds Na^+ selectively; and the larger [2.2.2]cryptand binds K^+ preferentially over the other alkali metal ions.

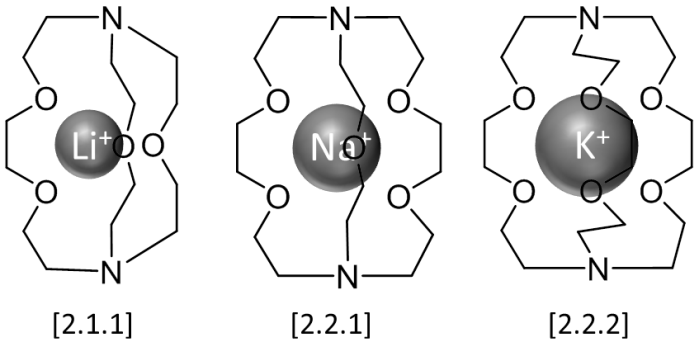


Figure 1-8: The size of the cryptand host cavity determines the preferential size of the alkali metal cation guest.[23]

The *chelate effect* refers to the phenomenon whereby complexes containing multidentate ligands are more stable than those composed of ligands of lower denticity. This is primarily due to favourable entropy of solvation when multiple solvent molecules are released upon complexation. There is also an enthalpic contribution to this effect, as the energetic cost of bringing two donor groups together has already been paid in the ligand synthesis. An example of the chelate effect in the context of anion binding is the isophthalamide receptor (**Figure 1-9a**), which preferentially recognises chloride in CD_2Cl_2

through cooperative binding of two amide groups.[24]

The concept of *preorganisation* refers to the observation that the binding strength of a guest is increased when the host is designed to adopt a rigid favourable binding conformation prior to guest complexation. In an extension of the isophthalamide receptor motif, it has been shown that hydroxyl groups appended to the phenyl ring can undergo intramolecular hydrogen bonding interactions with the carbonyl groups of the amide moieties (**Figure 1-9b**). These interactions result in a preorganised convergent orientation of the amide N–H bonds prior to guest complexation, greatly enhancing the halide anion binding strength compared to a non-preorganised receptor.[25]

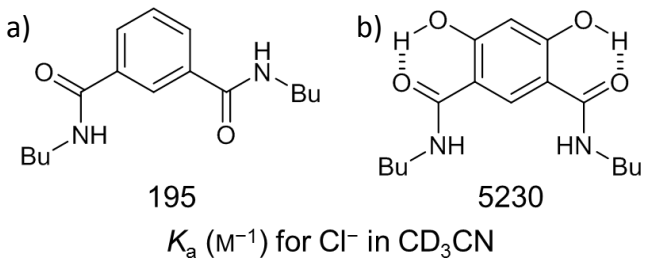


Figure 1-9: a) Crabtree's isophthalamide receptor; and **b)** the same receptor substituted with hydroxyl groups, which preorganise the amides for anion binding, significantly increasing the anion complexation strength (errors < 10%).[25]

The *macrocyclic effect* is an extension of the chelate effect principle, in which the ligand donors are incorporated within a macrocyclic framework, resulting in a more stable complex than its acyclic analogue. Fewer degrees of freedom are lost upon complexation with macrocyclic ligands, which is entropically favourable, and enthalpic contributions arise from the lower solvation of macrocycles. This effect is demonstrated by Jurczak's macrocyclic anion receptor (**Figure 1-10**), which was shown to bind Cl^- about 40 times more strongly than an acyclic analogue.

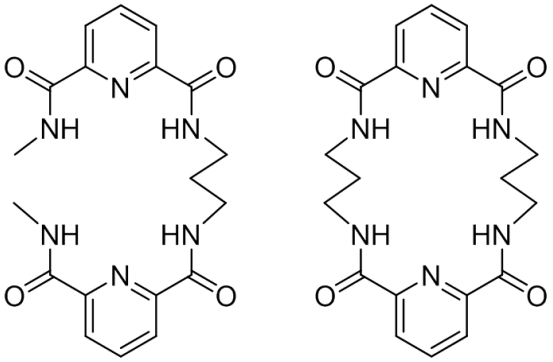


Figure 1-10: Jurczak's macrocyclic tetra(amide)-based receptor binds Cl^- with much higher affinity than an acyclic analogue.

1.2 *Anion Recognition*

1.2.1 *Importance of Anions*

The many varied roles that anions play in biology and the environment are well known. From the polyanionic DNA, the genetic code of life, to ATP, the energy currency of life, anions play an integral role in the function of biological systems. Chloride has essential roles in respiration and metabolism,[26] and misregulation of chloride channels can lead to cystic fibrosis.[27] Iodide is essential for proper thyroid function,[28] and fluoride is used in toothpaste to strengthen teeth against decay.[29] Pollution of the environment with anions can lead to serious problems, including eutrophication of water sources, which is caused by excess nitrate and phosphate from agricultural sources.[30] In addition to their presence in the environment, anions are also prevalent in many chemical and industrial processes.

Given the essential functions of anions, it is imperative that host systems be developed. Studying the interactions of anions with synthetic hosts could lead to practical solutions to

the various problems related to anions, through the development of anion receptors, sensors and sequestering agents.[31-33]

1.2.2 *Properties of Anions*

Due to the physical properties of anions, the task of developing effective anion receptors for strong and selective binding is arguably more challenging than for cations. Anions are larger than their isoelectronic cations due to the lower effective nuclear charge, Z_{eff}, so host cavities must be larger to accommodate the guest. This also leads to a decrease in the charge density of the anion, and so the strength of electrostatic interactions is reduced, requiring stronger and/or additional interactions for effective recognition.

While the majority of common cations are spherical, anions are often polyatomic, and adopt a range of geometries, thus requiring more demanding structural features in the host binding cavity. Anion geometries include spherical (halides), linear (N_3^-, CN^-), trigonal planar (CO_3^{2-}, NO_3^-), tetrahedral (PO_4^{3-}, SO_4^{2-}, BF_4^-), square planar ($AuCl_4^-$, $PtCl_4^{2-}$), octahedral (PF_6^-, $Fe(CN)_6^{4-}$), or more complex structures (keggin anions, DNA, etc.) (**Figure 1-11**).

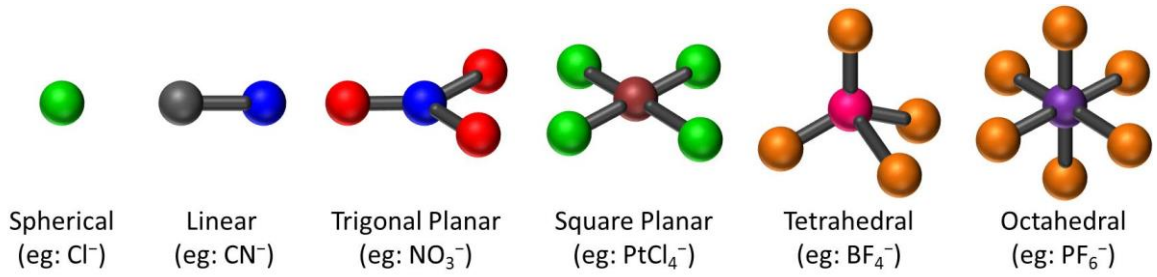


Figure 1-11: Examples of different anion geometries.

Many anions only exist within a particular pH range, such as sulfates, phosphates and carboxylates. This effect is of particular importance for anion recognition in aqueous

solvents, as even at neutral pH very basic anions, such as fluoride and acetate, may deprotonate acidic sites on receptors.[34] Receptors can also be pH-dependent, and many polyammonium-based receptors are only active within a certain pH window, limiting their efficacy (see **§1.2.4.1**).

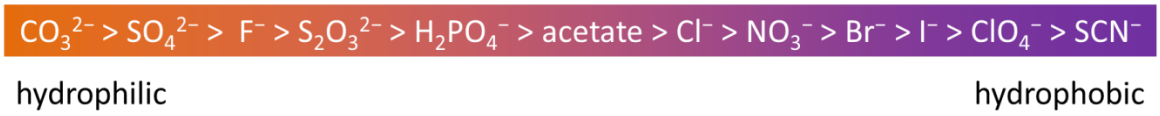


Figure 1-12: The Hofmeister Series of anion hydrophilicity/hydrophobicity.

Another challenge is that anions are generally more highly solvated than cations, giving a higher enthalpic barrier to complexation. Their degree of solvation is related to the Hofmeister series, which is a qualitative comparison of the relative hydrophobicity of anions (**Figure 1-12**).[26] For a receptor to bind an anion it must compete effectively with the solvent. As a consequence, designing receptors to recognise anions in competitive solvent media, such as DMSO or water, is a particular challenge to overcome.

1.2.3 *Biological Anion Receptors*

In order to strongly and selectively bind anions, evolution has produced proteins with highly preorganised binding pockets, in which the sequence of amino acids in the protein structure results in a precise geometric arrangement of complementary hydrogen bond donor and acceptor binding sites in the host cavity. Phosphate is an important biological anion, due to its structural role in DNA and function as an energy provider in ATP. The Phosphate Binding Protein (PBP), which transports phosphate in bacteria, forms 12 strong hydrogen bonds between the host cavity and the guest anion.[21] The protein binds both HPO_4^{2-} and $H_2PO_4^-$, depending on the pH of the solution, with a slight modification of the

binding cavity to accommodate the difference in the hydrogen bonding requirements. In the case of HPO_4^{2-}, a negatively charged aspartate residue accepts a hydrogen bond from the phosphate proton, while the positively charged guanidinium group of an arginine residue provides an additional electrostatic component to the anion binding (**Figure 1-13a**).

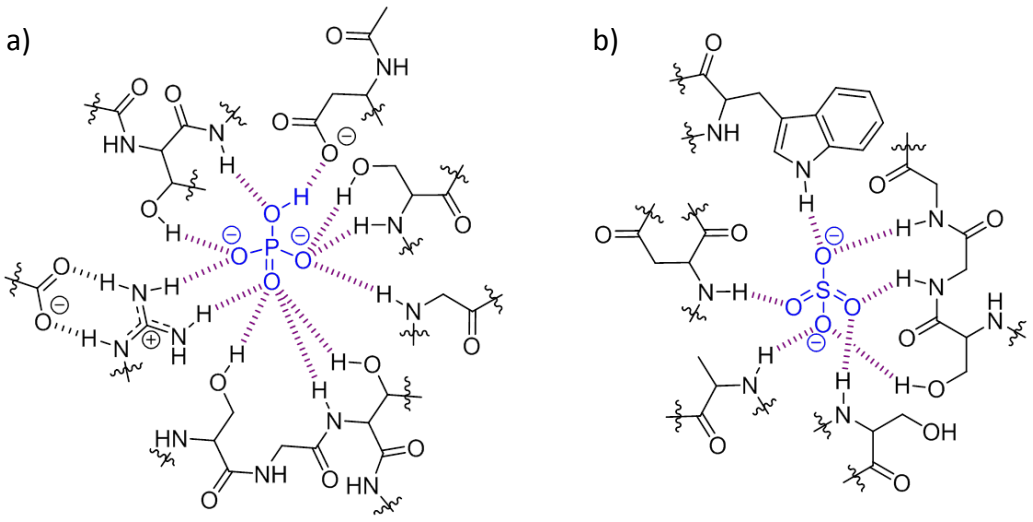


Figure 1-13: Structures of the active sites of **a)** Phosphate Binding Protein; and **b)** Sulfate Binding Protein.

The Sulfate Binding Protein (SBP) of *Salmonella typhimurium* is an example of a highly selective biological anion receptor which binds sulfate purely through seven hydrogen bonding interactions of neutral residues in a complementary tetrahedral fashion (**Figure 1-13b**).[35]

1.2.4 *Synthetic Anion Receptors*

In the development of abiotic anion receptor host systems, many of the supramolecular interactions described in **§1.1.1** have been exploited, including electrostatics, hydrogen bonding, halogen bonding, Lewis acid–base interactions and anion–π interactions. In

general, anion binding motifs are either cationic or neutral, with a positive charge generally leading to stronger host–guest association, but at the expense of selectivity, unless directional anion receptor motifs are also incorporated into the binding cavity.

1.2.4.1 Cationic Anion Receptors

Some of the earliest work on anion receptors involved the development of positively-charged ammonium-based host systems. Influenced by the seminal work of Park and Simmons (**Figure 1-14a**),[36] Lehn constructed macrocyclic and cryptand-like polyammonium receptors, which demonstrated anion selectivity based on the size of the anion binding cavity (**Figure 1-14b**).[37,38] These polyammonium receptors bind anions through a combination of electrostatics and multiple hydrogen bonding interactions.

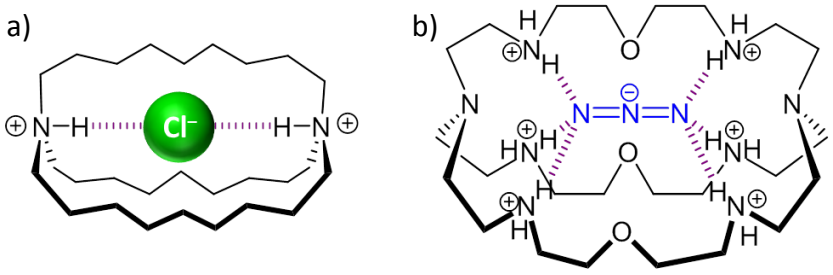


Figure 1-14: Ammonium-based receptors **a)** Park and Simmons' bis-ammonium cryptand; and **b)** Lehn's macrotricyclic receptor, which is selective for linear anions.

The major drawback of receptors containing protonated amines is their pH dependence. One strategy to avoid this limitation is to use pH-independent positively charged quaternary ammonium groups such as Schmidtchen's tetracationic quaternary ammonium cage, which was demonstrated to bind halides in water (**Figure 1-15a**).[39] In order to avoid competition with counterions, a neutral zwitterionic host was subsequently developed (**Figure 1-15b**), which recognises iodide selectively in water, with a significantly enhanced binding affinity compared to the tetracationic host system.[40]

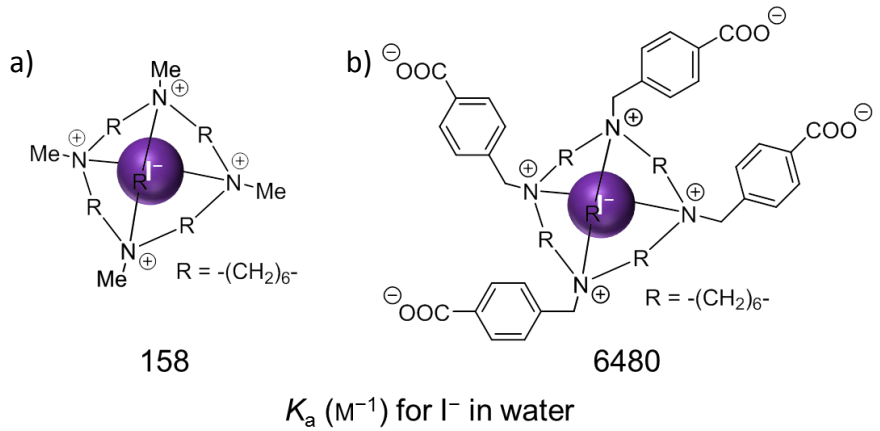


Figure 1-15: a) Schmidtchen's tetraammonium anion cage receptor; and **b)** the neutral zwitterionic receptor form. In the absence of competitive counterions, the neutral receptor binds iodide significantly more strongly than the charged receptor.

Guanidinium has also been investigated as an anion receptor motif, having the advantage of a much higher pK_a value (13.6) than ammonium (9.3) due to the greater degree of charge delocalisation, and can thus remain protonated over a larger pH range.[41,42] The guanidinium-based receptor shown in **Figure 1-16a** demonstrated strong binding of carboxylates in water at pH 7.4, with a particularly strong affinity for citrate.[42]

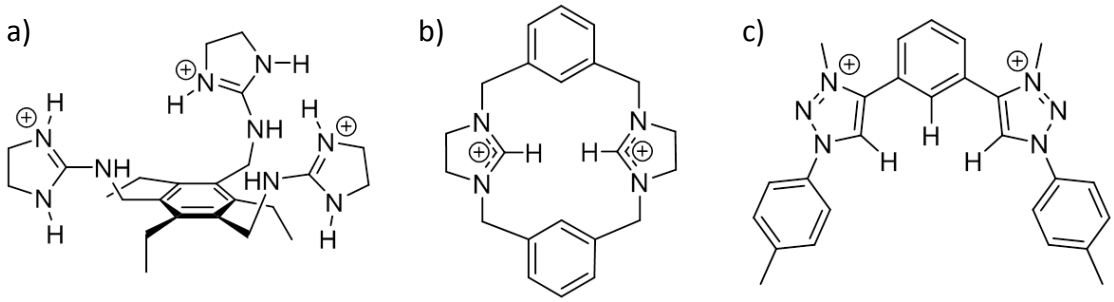


Figure 1-16: a) Anslyn's guanidinium-based receptor;[42] **b)** Alcalde's imidazolium-containing receptor;[43] and **c)** Schubert's triazolium-based receptor.[44]

Charged C–H hydrogen bond donors have also been studied: imidazolium has been incorporated into a variety of anion receptors,[45,46] including Alcade's imidazolium macrocycle (**Figure 1-16b**), which is selective for F^- in d_6-DMSO.[43] More recently,

triazolium has also been used,[44,47] exemplified by Schubert's bis-triazolium receptor (**Figure 1-16c**), which binds SO_4^{2-} strongly in 4:1 CD_3CN/CH_3OH.[44]

1.2.4.2 Neutral Anion Receptors

Although neutral anion receptor motifs generally bind anions more weakly than positively charged groups, they have the distinct advantage that such interactions are more directional, and can lead to greater anion selectivity. As demonstrated by the anion binding proteins in **§1.2.3**, an appropriate combination and arrangement of neutral binding sites in a receptor cavity can produce strong and highly selective anion binding behaviour.

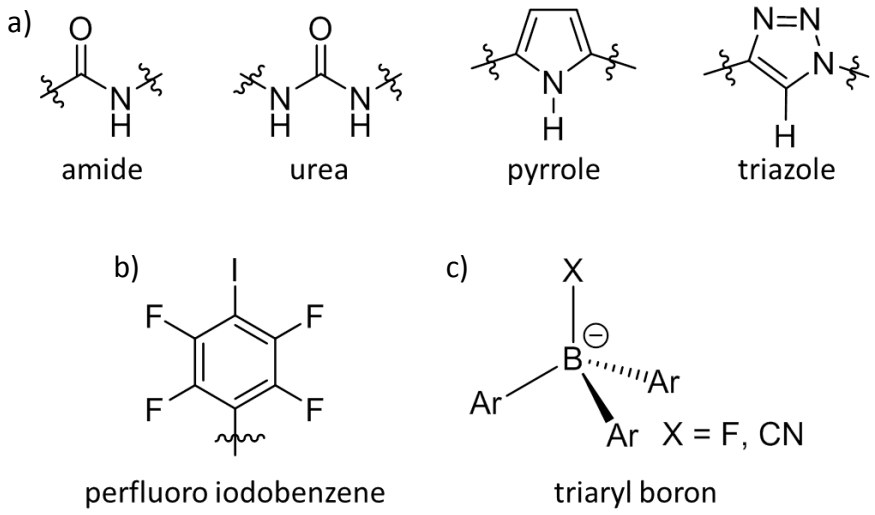


Figure 1-17: Anion binding motifs which utilise **a)** hydrogen bonding; **b)** halogen bonding; and **c)** Lewis acid–base interactions

There are many neutral hydrogen bond donor moieties which have been exploited in the design of anion receptors, including amide,[24,48,49] urea,[50] pyrrole,[51,52] and triazole[53,54] groups (**Figure 1-17a**). Perfluorinated iodoaromatic compounds have been shown to be effective halogen bonding anion receptors[55] (**Figure 1-17b**), and Lewis acids, such as triarylboron species, are also exploited for anion recognition, especially for F^- and CN^-

(**Figure 1-17c**).[56]

A popular motif for incorporation into synthetic anion receptors is the amide functional group. Since Pascal's cyclophane host (**Figure 1-18a**),[48] which was the first synthetic anion receptor to incorporate amides, there has been an abundance of amide-containing anion receptors reported.[57]

While neutral N–H hydrogen bond donors are relatively common in anion receptors, the exploitation of a neutral C–H unit as a potential hydrogen bond donor for anion recognition is rarer. The most notable neutral C–H anion receptor motif is the triazole group,[58,59] used effectively by Flood in the development of a macrocyclic triazolophane host (**Figure 1-18b**).[60] The cyclic cavity was demonstrated to be of a complementary size to bind chloride over the other halides in CD_2Cl_2. Neutral O–H donors have also been incorporated into anion receptors, including Jeong's indolocarbazole-based anion host (**Figure 1-18c**), which binds anions through both N–H and O–H hydrogen bond donors.[61] The receptor was selective for acetate in 1% H_2O/CD_3CN, and the presence of the O–H units enhanced the anion binding strength by up to three orders of magnitude.

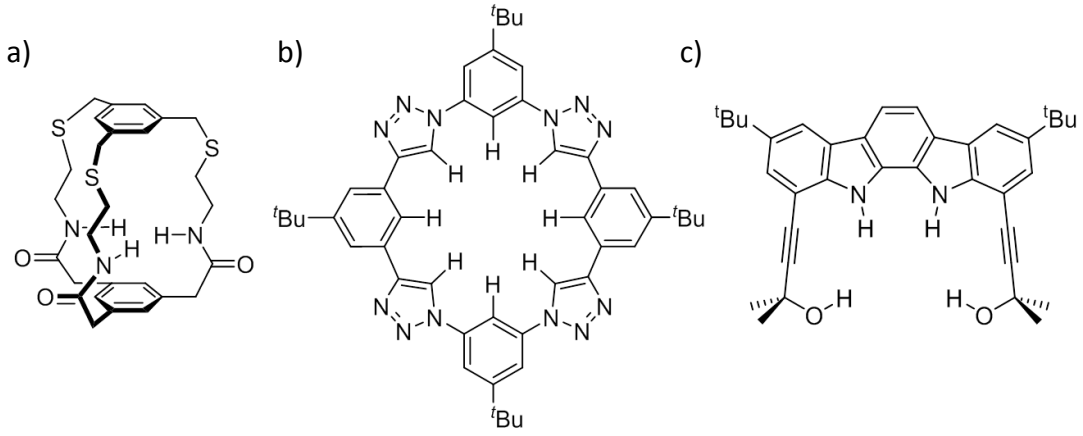


Figure 1-18: a) Pascal's cyclophane host;[48] **b)** Flood's triazolophane macrocycle;[60] and Jeong's indolocarbazole receptor.[61]

1.2.4.3 *Metal-Containing Anion Receptors*

Incorporation of metals into an anion receptor can improve the anion binding properties, by providing an additional electrostatic component, preorganising the receptor by appropriately orienting the binding motifs, directly binding to the anion if the metal is coordinatively unsaturated, and/or acting as a reporter group to sense the anion binding event.[62-64]

Gale and Loeb's platinum(II)-based tetra-urea receptor (**Figure 1-19a**) was shown to bind strongly to the tetrahedral anions $H_2PO_4^-$ and SO_4^{2-} in d_6-DMSO.[65] The Pt^{2+} metal ion coordinates to four ligands in a square planar geometry, structurally preorganising the ligand urea groups for convergent hydrogen bonding to the oxoanion. In addition to the structural influence of the metal, it also provides an electrostatic contribution to the anion binding strength of the receptor.

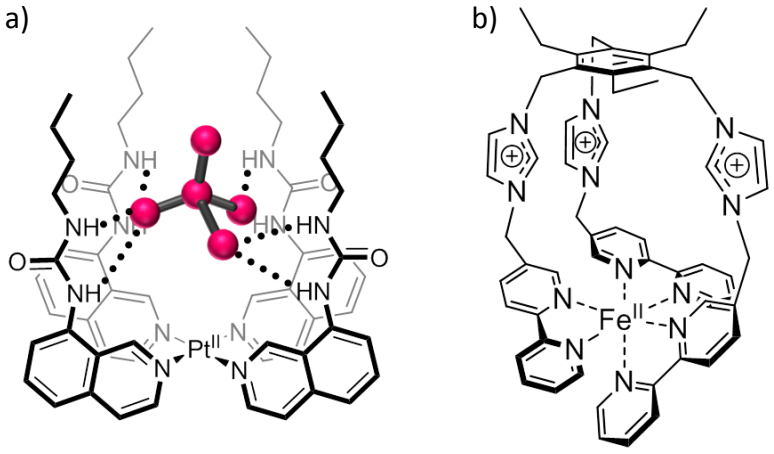


Figure 1-19: Metal-containing anion receptors, **a)** Gale and Loeb's urea-containing receptor;[65] and **b)** Fabbrizzi's imidazolium-containing Fe(II) complex cage.[66]

Fabbrizzi's metal-directed tripodal cage (**Figure 1-19b**) is another example of using a metal to preorganise a receptor for convergent anion binding.[66] The three 2,2′-bipyridyl ligand units coordinate to Fe(II) in an octahedral geometry, which induces the three ligand

imidazolium units to assume a conformation which is effectively setup for cooperative anion binding. UV-vis spectrophotometric titration experiments determined the Fe(II) receptor to exhibit a preference for chloride in CH_3CN, with $\log(K_a) > 7$.

1.2.5 *Sensing of Anions*

While the fundamental development of anion receptors is important, in order for such receptors to be utilised for practical sensing applications, they can be modified with an integrated reporter group such that anion complexation induces a measureable physical response, usually an optical or electrochemical output. Other methods of sensing anions include displacement assays,[67-69] chemodosimeters,[70-72] and ion-selective electrodes.[73,74]

1.2.5.1 *Colorimetric Anion Sensors*

Anion sensors which operate using the displacement and chemodosimeter approaches often produce a colorimetric response.[67,69,70,72] Perhaps the most noteworthy application of the displacement approach is its use in selectively detecting cyanide. These systems operate on the general principle whereby a dye molecule is complexed to a metal ion, typically Cu(II). Addition of cyanide sequesters the metal ion *via* displacement of the dye. For example in **Figure 1-20**, a naked eye detectable colour change from light yellow to deep red occurs upon cyanide addition to the Cu(II) complex of a diazo-functionalised ligand.[75] Importantly, no other anion was observed to give such a response, making this method a highly selective cyanide detection technique.

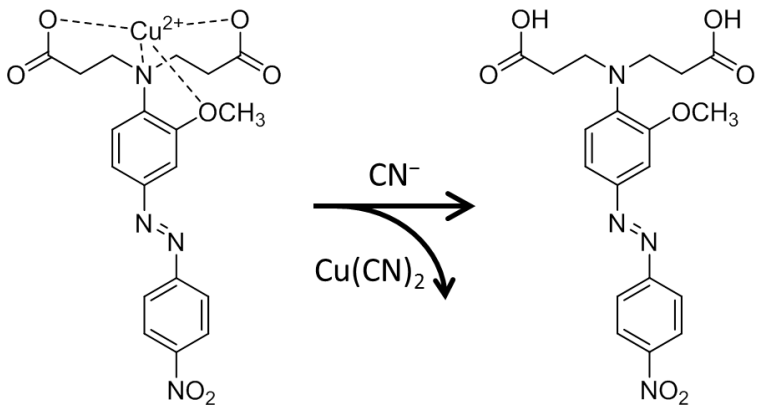


Figure 1-20: Example of the displacement approach to anion sensing, in which addition of cyanide results in removal of the Cu(II) from the complex, changing the colour of the molecule from light yellow to red.

Numerous colorimetric sensors operate *via* deprotonation by basic anions.[76-79] A recent example of such a molecule is Kumar's glyoxylamide-based anion sensor (**Figure 1-21a**), which changes from colourless to yellow upon addition of F^- in acetone.[80]

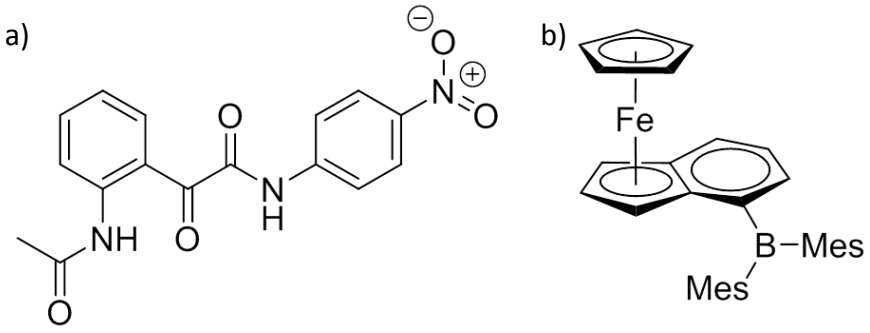


Figure 1-21: Colorimetric anion sensors, **a)** Kumar's glyoxylamide-based sensor;[80] and **b)** Aldridge's ferrocenyl borane-based sensor.[81]

Anion receptors based on triarylboron have been widely exploited for sensing F^- and CN^-, which directly coordinate to the Lewis acidic boron centre. A recent example of a CN^--selective sensor is Aldridge's ferrocenyl borane (**Figure 1-21b**), which demonstrates a green-to-red colorimetric response to only CN^- in 1:1 H_2O/THF.[81]

1.2.5.2 Luminescent Sensors

While colorimetric anion sensors have the advantage that the anion binding event can be visible to the naked eye, luminescent sensors are desirable due to the high sensitivity of the detection techniques.

Luminescence is the phenomenon where an electronically excited species releases energy in the form of light, to return to a lower-energy state (**Figure 1-22**). Where the electronic transition is a singlet–singlet relaxation, which often occurs in organic fluorophores, the light emission is called *fluorescence*.[82] In some systems, the singlet excited state may undergo intersystem crossing to a triplet state. Transition from a triplet excited state to the singlet ground state is formally forbidden but will occur due to quantum mechanical effects, such as spin–orbit coupling, resulting in longer lifetimes of the excited state. This behaviour is called *phosphorescence*, and occurs in many metal complexes which have a triplet metal-to-ligand charge transfer (^{3}MLCT) excited state.

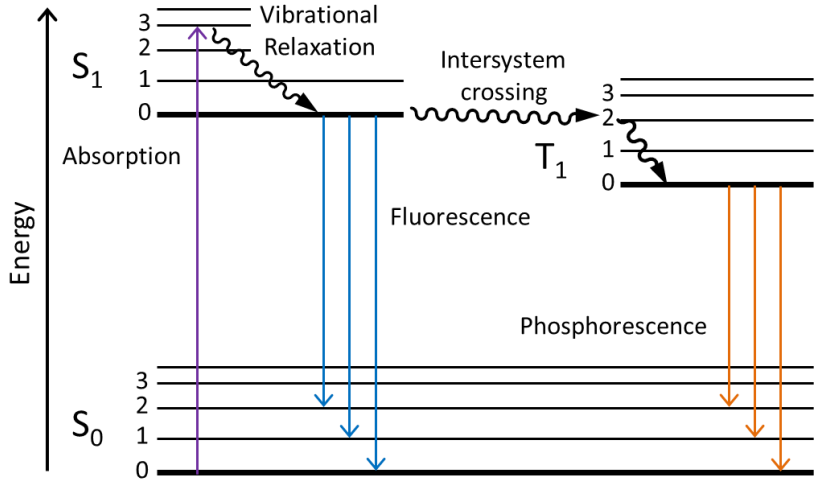


Figure 1-22: Jablonski diagram, pictorially representing the origins of fluorescence and phosphorescence.

Depending on the nature of the luminescent moiety, there are different mechanisms by

which the emission properties may be altered upon binding of anions to the receptor. Photo-induced electron transfer (PET), electronic energy transfer, excimer formation, and the rigidity effect have all been exploited in the development of luminescent anion sensors.[83-85]

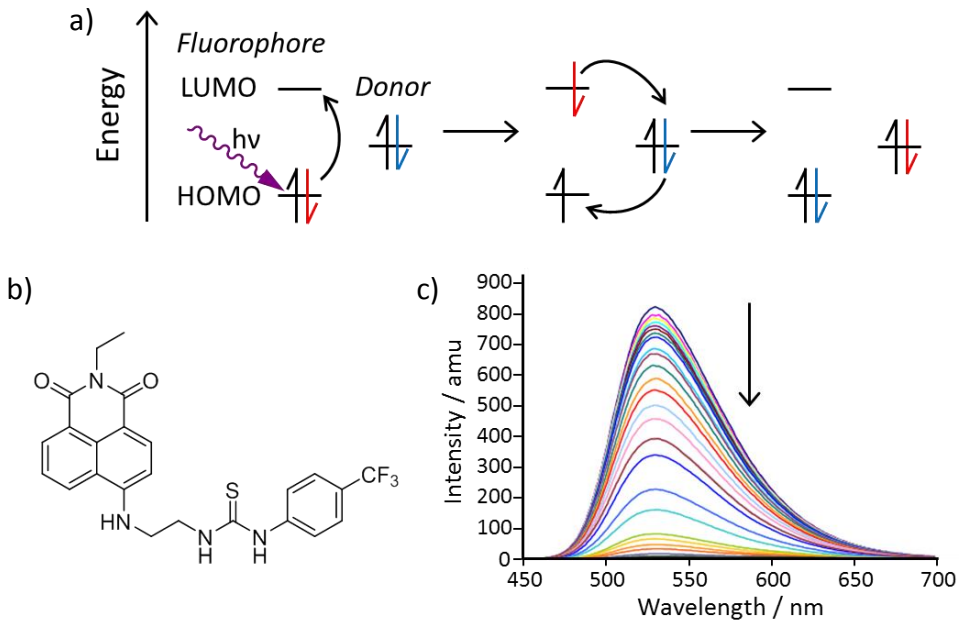


Figure 1-23: a) The mechanism for PET quenching of a fluorophore by a donor group; **b)** Gunnlaugsson's naphthalamide-based F^- sensor; and **c)** fluorescence emission spectra of the sensor upon addition of F^-.[86]

PET is a quenching mechanism, which competes with radiative decay. When a proximal donor group possesses an orbital energy that is intermediate between the HOMO and LUMO of the fluorophore, photo-induced electron excitation does not lead to fluorescence, but instead relaxes to the ground state *via* transfer to the donor species, quenching the fluorescence (**Figure 1-23a**). This behaviour can be exploited as a luminescent sensing method, in which the donor group has an electronic energy level which can be modified by anion binding. In a demonstration of the application of this principle to anion binding, Gunnlaugsson and co-workers have developed a series of anion sensors which incorporate

the fluorescent naphthalamide motif, connected to a thiourea receptor.[87,88] The receptor shown in **Figure 1-23b** is able to selectively sense F^- in DMSO, as the anion deprotonates the thiourea receptor, enhancing the PET quenching ability of the receptor, leading to a dramatic decrease in the fluorescence emission intensity (**Figure 1-23c**).[86]

Metal-based luminescent receptors have also been studied for their anion sensing potential. Tris(2,2′-bipyridine)ruthenium(II) complexes have well-established luminescence properties, which have been exploited to sense anions when incorporated into an anion receptor.[89-92] Beer's ruthenium(II)-based calix[4]diquinone macrocycle (**Figure 1-24a**) is an early example of such a system, which demonstrated a significant increase in the MLCT emission intensity upon addition of acetate in CH_3CN.[93] The cause of this emission intensity increase is purported to arise from rigidification of the receptor upon anion binding, which reduces non-radiative decay mechanisms by enforcing vibrational and rotational restraints on the molecule.

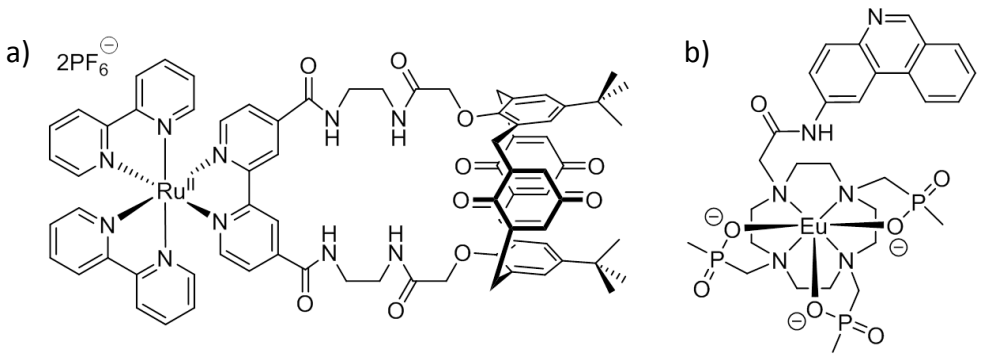


Figure 1-24: a) Beer's ruthenium(II)-based anion sensor;[93] and **b)** Parker's europium-based anion sensor.[94]

Lanthanide-based luminescent anion sensors have also been studied, though these 'receptors' bind anions through direct bonds to the metal.[95-97] Parker's europium-containing receptor (**Figure 1-24b**) is an early example of a lanthanide-based anion sensor,

which was shown to sense halides and hydroxide in water, by means of quenching of the europium emission.[94]

1.2.5.3 Electrochemical Sensors

Electrochemically-active receptors are another class of anion sensor which has been studied extensively. In these systems, a redox-active group is combined with an anion recognition site in such a way that anion binding perturbs the redox couple.

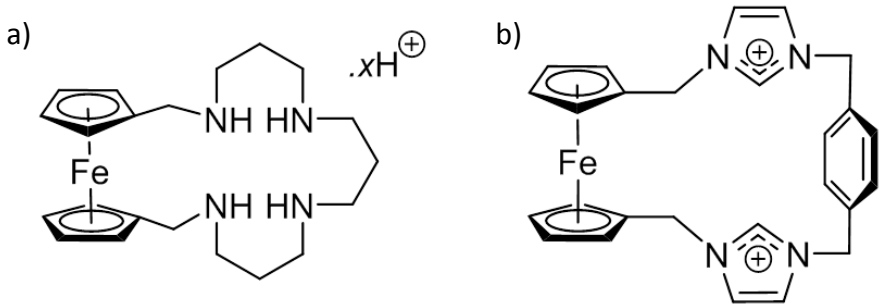


Figure 1-25: Electrochemical anion sensors, **a)** Beer's polyaza ferrocene macrocycle;[98] **b)** Cheng's bis(imidazolium) ferrocene macrocycle.[99]

Perhaps the most widely-exploited electrochemical motifs used to sense anions are ferrocene and cobaltocenium, which have well established redox properties.[92,100-106] Beer's polyaza-ferrocene macrocycle was demonstrated to give an electrochemical response upon binding of phosphate anions in water of pH 6–8, a range within which multiple amine sites of the macrocycle are protonated (**Figure 1-25a**).[98] Binding of anions induced a cathodic shift of the ferrocene/ferrocenium redox couple, due to stabilisation of the positively-charged ferrocenium species by the anionic guest. Cheng's bis(imidazolium) ferrocene macrocycle also demonstrated a significant cathodic shift upon addition of anions in CH_3CN, with the greatest magnititude of perturbation (ΔE = −276 mV) observed for fluoride (**Figure 1-25b**).[99]

1.3 *Halogen Bonding*

IUPAC recently codified the formal definition of halogen bonding (XB): "A halogen bond occurs when there is evidence of a net attractive interaction between an electrophilic region associated with a halogen atom in a molecular entity and a nucleophilic region in another, or the same, molecular entity".[107] When a halogen is attached to an electron-withdrawing substituent, the electron density of the halogen is polarised in such a way that a region of positive electrostatic potential develops on the atomic terminus (**Figure 1-26a**). This region is termed the 'σ-hole', and its relative size increases as the halogen becomes larger, due to the corresponding increase in atomic polarisability.

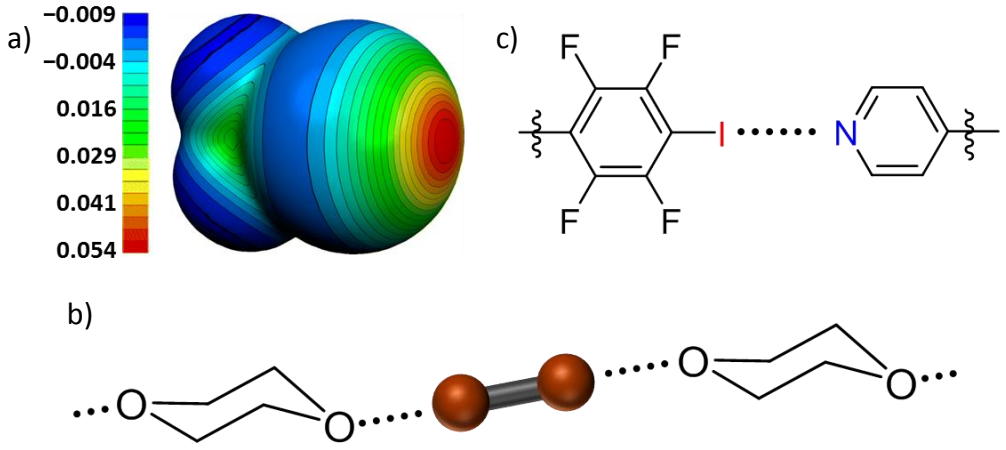


Figure 1-26: a) Calculated molecular electrostatic potential in Hartrees, at the 0.001 electrons Bohr^{-3} isodensity surface of CF_3I;[108] **b)** XB shown in the solid state chains of alternating Br_2 and 1,4-dioxane molecules;[109] and **c)** XB interaction between iodotetrafluorobenzene and a pyridyl unit.

Interactions between the σ-hole of the halogen and Lewis basic species have been studied extensively in the solid state. Since Hassel's pioneering work in the study of charge-transfer interactions in cocrystals of bromine and 1,4-dioxane (**Figure 1-26b**),[109] the field of crystal engineering has utilised the XB interaction as a supramolecular synthon[110] to

great effect, producing many interesting material structures and topologies.[111-116]

The power of XB to affect material properties has been exploited in the design and study of various solid state functional materials,[117-119] including conducting,[120,121] magnetic,[122-124] porous,[111,125] gel-phase[126] and liquid crystalline[127-129] materials, surface relief gratings,[130,131] and for solid state synthesis[132,133] and polymerisation.[134,135] In particular, the XB interaction between iodoperfluorobenzene- and nitrogen-containing components, especially pyridyl-based moieties, has been incorporated into many of these functional systems (**Figure 1-26c**).

In contrast to the vast library of solid state applications of XB, studies of this interaction in the solution phase are few in number.[136] Preliminary work is being conducted on the potential of XB in catalytic systems,[137,138] and the effect of XB has also been investigated in protein–ligand complexes.[139] The central theme in this thesis is the application of XB in solution phase anion receptors, which warrants a more detailed treatment of the subject.

1.3.1 *Halogen Bonding with Anions*

Though XB interactions with anions had been previously observed in the solid state,[140] solution phase experiments on a XB anion receptor were first reported by Resnati and co-workers on 1,2-diiodotetrafluoroethane,[141] which demonstrated a shift in the ^{19}F NMR signal in $CDCl_3$, in the presence of different anions. This was followed by a heterodipotic receptor, which simultaneously bound alkali metals through ether donors, and halides through iodine halogen bond donors (**Figure 1-27a**).[142] The ion pair binding behaviour was monitored using ^{1}H NMR titration studies in $CDCl_3$, and demonstrated significantly stronger binding of NaI compared to an analogous receptor without the halogen bond

donors.

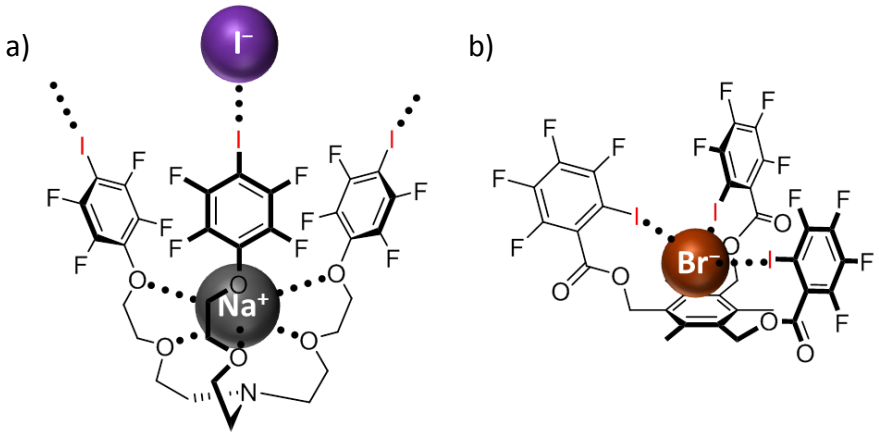


Figure 1-27: a) Resnati's heteroditopic XB receptor;[142] and **b)** Taylor's tripodal convergent XB anion receptor.[55]

Taylor and co-workers incorporated the iodoperfluorobenzene-based motif into various multidentate receptors in which the iodine XB donor atoms are positioned for convergent binding to an anion in the central cavity.[55,143,144] The tripodal XB receptor (**Figure 1-27b**) was reported to be selective for Cl^- in acetone. An analogous mixed XB and hydrogen bonding anion receptor (**Figure 1-28**) was shown in CD_3CN to preferentially bind the benzoate anion through both hydrogen and halogen bonding interactions with the carboxylate moiety, as well as favourable aromatic donor–acceptor interactions with the electron-deficient perfluorobenzene rings.[145]

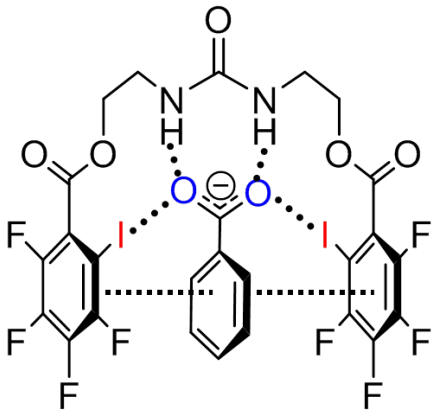


Figure 1-28: Schematic of the benzoate complex of Taylor's mixed hydrogen bonding and XB receptor.[145]

Introducing charge into halogen bond donor systems imparts a stronger electrostatic component to the XB interaction, enhancing the anion association. The *syn* conformer of Beer's bromoimidazolium macrocycle (**Figure 1-29a**) was reported to be selective for Br^- in 9:1 CD_3OD/D_2O through cooperative convergent binding of the bromine halogen bond donors.[146] This result is in contrast to the hydrogen bonding imidazolium analogue, which showed very little discrimination between the halides, and bound bromide significantly more weakly than the XB receptor.

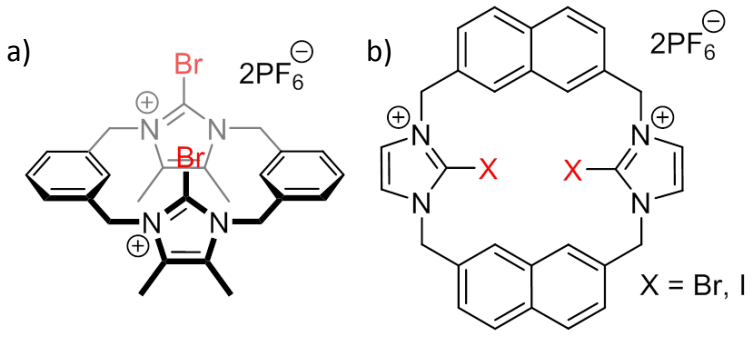


Figure 1-29: a) Bromoimidazoliophane receptor; and **b)** naphthalene-containing haloimidazoliophane sensors.

In an extension of this work, the naphthalene-based bromo- and *syn* iodo-imidazolium

macrocycles (**Figure 1-29b**) were shown to sense selectively the heavier halide anions through perturbations in the fluorescence behaviour of the naphthalene spacer units.[147] In 9:1 CD_3OD/D_2O, both receptor molecules only gave a fluorescence response for Br^- and I^-, with the bromoimidazolium macrocycle being I^--selective, while the iodoimidazolium macrocycle was Br^--selective. The hydrogen bonding imidazolium analogue exhibited no fluorescent change to any anion, demonstrating the superiority of XB for recognising the larger halides in these systems.

1.4 *Interlocked Structures*

Interlocked molecules are of major interest in supramolecular chemistry, not just for their aesthetic appeal and the synthetic challenge, but also because they are promising targets for nanotechnological applications.[148] Interlocked molecules are supramolecular systems in which two or more molecular components are mechanically interlocked; that is, they are not covalently bonded to each other, but they nevertheless cannot be separated without breaking a chemical bond. The two most common types of interlocked species are [*n*]catenanes and [*n*]rotaxanes, where *n* is the number of interlocked components. Catenanes consist of two or more mechanically interlocked macrocycles (**Figure 1-30a**), and rotaxanes are composed of one or more macrocycles threaded over one or more axle components, which are terminated by stopper groups of sufficient bulk to prevent the macrocycles from slipping off (**Figure 1-30b**). Other, less common interlocked molecules include Borromean rings[149] and knots[150-152] (**Figure 1-30d**,**e**).

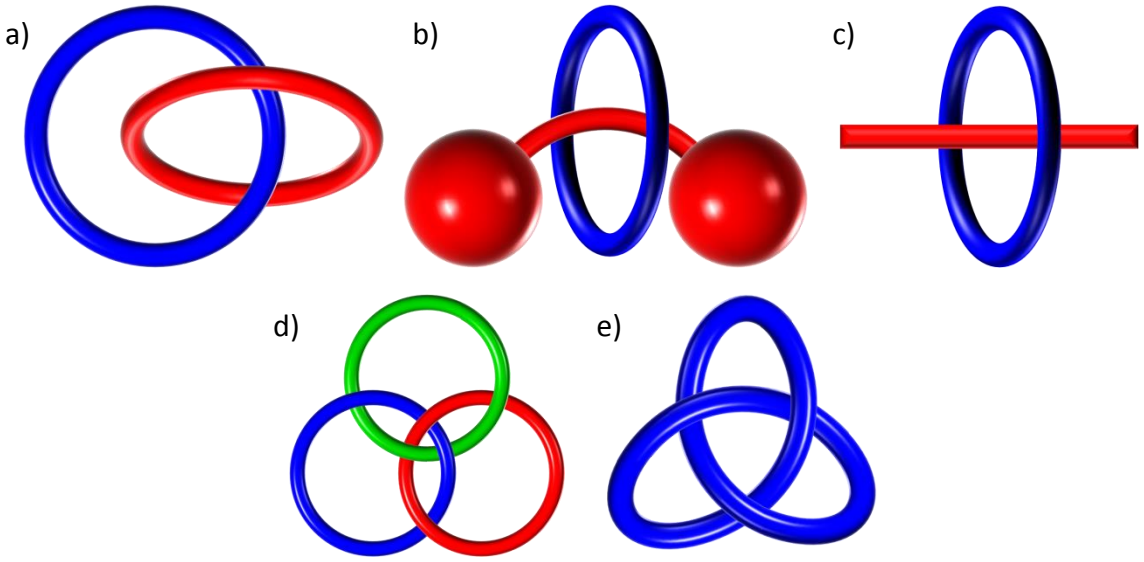


Figure 1-30: Interlocked and interpenetrated topologies, **a)** [2]rotaxane; **b)** [2]catenane; **c)** [2]pseudorotaxane; **d)** Borromean rings; and **e)** trefoil knot.

A rotaxane-like assembly which does not have stopper groups is called a pseudorotaxane (**Figure 1-30c**), which is regarded as *interpenetrated* rather than interlocked, as it is possible for dethreading of the macrocycle to occur. Pseudorotaxanes are often used as precursor assemblies for the formation of interlocked structures, as the thread component can be closed to form a catenane, or stoppered to form a rotaxane. Studying the stability of the formation of pseudorotaxanes can give valuable information about their potential to form interlocked molecules.

1.4.1 *Synthesis of Catenanes and Rotaxanes*

Due to intense interest in interlocked molecules, multiple strategies have been developed to synthesise these supramolecular systems. As mentioned above, [2]catenanes are usually synthesised by the 'clipping' of a pseudorotaxane, or by 'double-clipping' an orthogonal precursor complex (**Figure 1-31a**),[153] although a 'magic ring' route has also been reported,[154-158] whereby one or both macrocycles may dynamically open and close in

solution, and a catenane may be formed due to favourable interactions between the macrocycles.

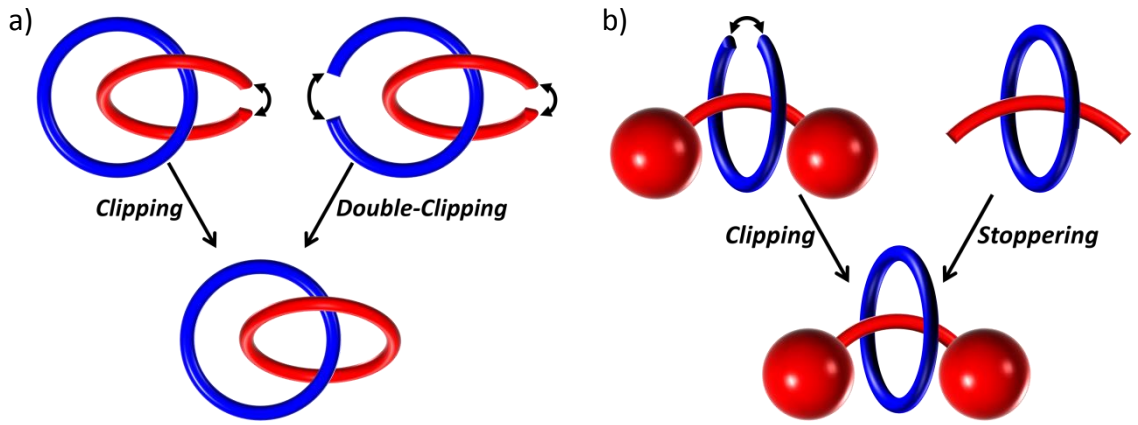


Figure 1-31: Major synthetic routes two form **a)** [2]catenanes; and **b)** [2]rotaxanes.

The most commonly employed methods used for the synthesis of [2]rotaxanes include 'clipping' a macrocycle closed over the axle, or 'stoppering' of the thread component in a pseudorotaxane (**Figure 1-31b**). Other methods reported include 'slippage' of a macrocycle over the axle stopper groups at high temperature or pressure,[159,160] 'magic ring/rod' approaches which are similar to the analogous method for catenanes,[161,162] 'snapping' two half-axle components together within the macrocycle,[163] 'swelling' of the stopper groups after a macrocycle has been threaded in a pseudorotaxane,[164,165] and 'shrinking' the macrocycle size once it has slipped onto the axle.[166,167]

The most successful strategy to form interlocked molecules is by using various templating methodologies, of which there are three major classes. *Discrete passive templation* is where the templating species is separate to the interlocked components, does not take part directly in the mechanical bond forming reaction, and is able to be removed following the interlocking synthesis (**Figure 1-32a**). When the templating species does take part in the interlocking synthetic step, this is termed *active templation* (**Figure 1-32b**). Structure-

directing template motifs may be incorporated into the respective interlocking components themselves which upon association lead to mechanical bond formation (**Figure 1-32c**).

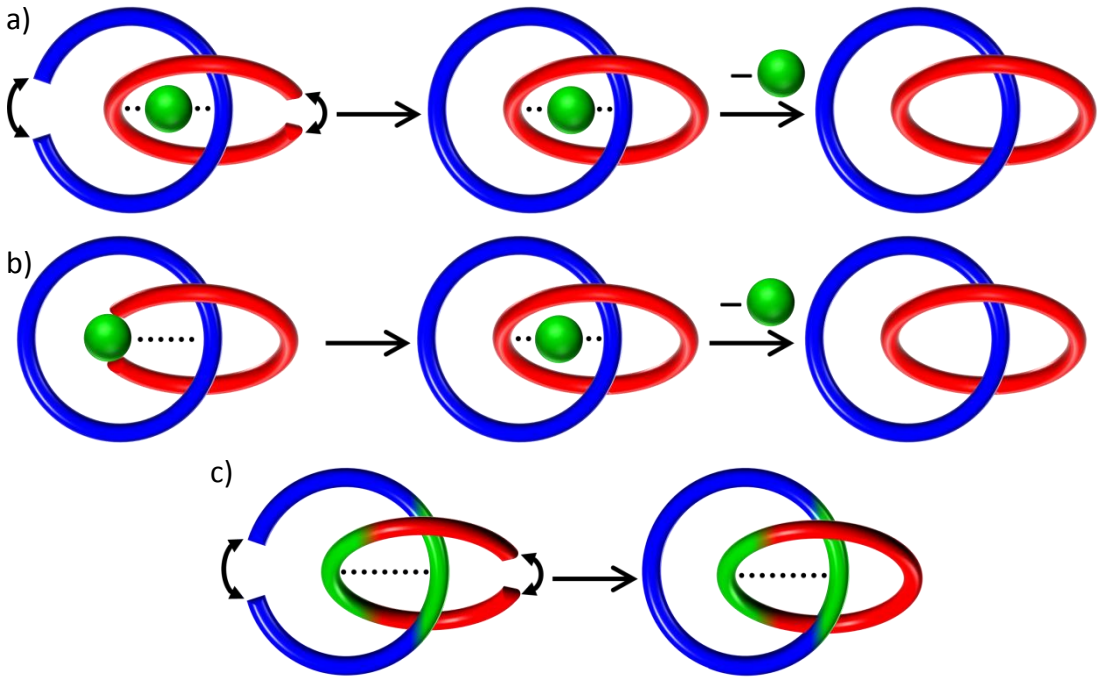


Figure 1-32: Schematic representations of the major types of templated synthesis of interlocked structures, **a)** discrete passive templation; **b)** active templation; and **c)** where interactions between the interlocked components template the assembly.

1.4.1.1 Cationic Templated Synthesis

While the statistical synthesis of catenanes[168] and rotaxanes[169] had been previously reported, it was not until 1983 that an efficient templation approach was described by Sauvage and co-workers. The tetrahedral coordination preference of Cu(I) was exploited in its use as a template, initially forming an orthogonal bis(phenanthroline) complex. Both ligand units were then cyclised to form a [2]catenane in 27% yield (**Figure 1-33a**).[170] More recently, employing a ring-closing metathesis (RCM) clipping approach increased the yield significantly to 92% (**Figure 1-33b**).[171] Many rotaxanes, catenanes, and higher-order exotic interlocked structures have since been made using the Cu(I)-templated

phenanthroline-based system.[172-179]

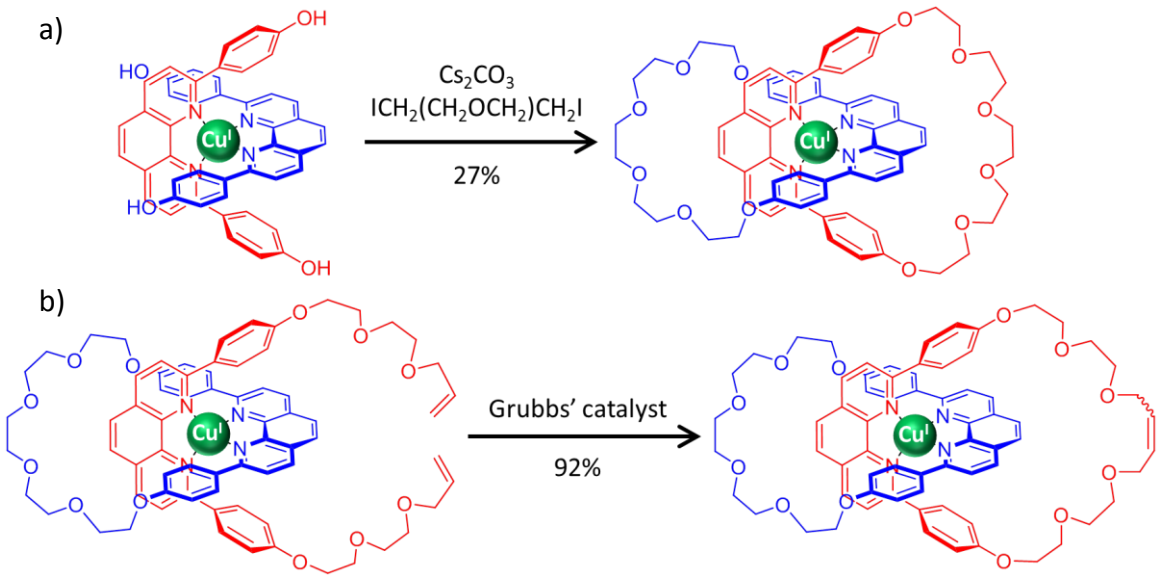


Figure 1-33: Synthesis of Cu(I)-templated phenanthroline-based catenanes, **a)** original synthesis;[170] and **b)** ring-closing metathesis synthesis.[171]

In addition to tetrahedral Cu(I), many other transition metal cations have been used to template interlocked structures, due to the strength of the metal–ligand coordinate bond, and the coordination geometric preferences of the metal.[180] Examples include using transition metals with linear,[181] square planar,[182] trigonal bipyramidal[183] and octahedral[184] coordination geometries (**Figure 1-34**).

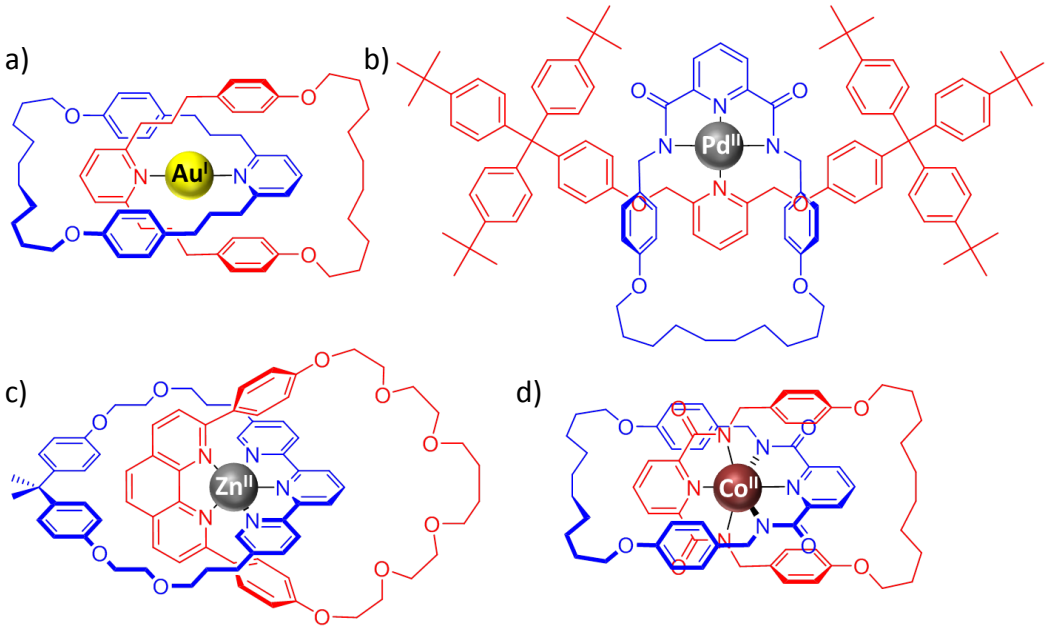


Figure 1-34: Transition metal-templated interlocked structures, demonstrating **a)** linear;[181] **b)** square planar;[182] **c)** trigonal bipyramidal;[183] and **d)** octahedral[184] coordination geometries.

Certain transition metals are known to catalyse organic reactions, which has led to their use as active templates in the formation of interlocked molecules.[163] Leigh and co-workers reported the first active metal templated interlocked structure, in which a rotaxane was assembled using Cu(I) as a template, which catalysed an azide-alkyne 1,3-cycloaddition reaction to form the axle within the macrocycle cavity.[185] Since then, this route has been used to make a range of interlocked molecules.[186-188] The Cu(I)-catalysed Glaser coupling of two terminal alkynes has also been exploited,[189-193] as well as the similar Pd(II)-catalysed homocoupling of alkynes.[194] Other active templation reactions involving Pd(II) include the oxidative Heck cross-coupling reaction[195] and the Pd(II)-mediated Michael addition,[196] which has been used to form a [2]rotaxane in 99% yield, from a four component assembly.

Cationic organic molecules are another template class which has been exploited in the

assembly of interlocked molecules. The strong hydrogen bonding interactions between secondary dialkylammonium cations and crown ether species was first used by Stoddart and co-workers to template the formation of an interlocked structure (**Figure 1-35a**),[197] and these motifs have since been incorporated into many interlocked systems.[157,198,199] Charge-assisted aromatic donor–acceptor interactions between electron-deficient and electron-rich aromatic systems have also been employed extensively to template the formation of interlocked structures.[200,201] The seminal example of this work is Stoddart's [2]catenane (**Figure 1-35b**),[202] in which the electron-deficient cyclobis(4,4′-bipyridinium) macrocycle is templated by the electron-rich hydroquinone units of a polyether paracyclophane.

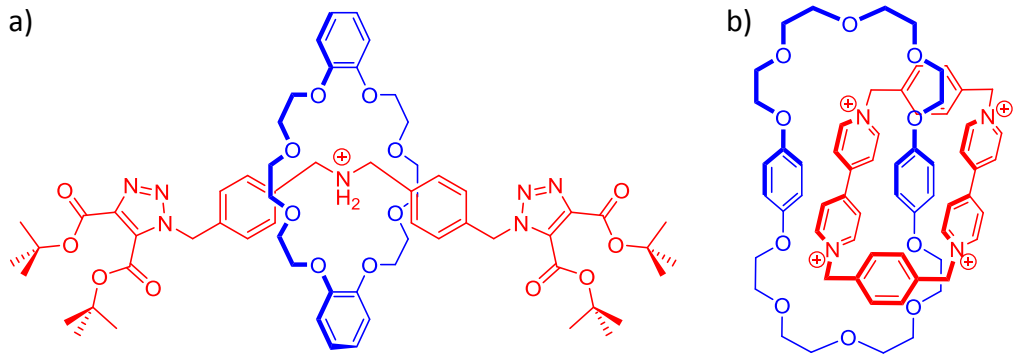


Figure 1-35: Interlocked structures templated by interactions with organic cations, **a)** dialkylammonium–polyether;[197] and **b)** aromatic donor–acceptor.[202]

1.4.1.2 Neutral Templation

While the strong electrostatic interaction of charged species can produce highly stable interpenetrated assemblies, thus favouring the synthesis of interlocked molecules, the use of charged templates is not absolutely necessary. Hydrogen bonding interactions of amides have proven to be effective structure-directing units,[203-207] exemplified by Leigh's simple [2]rotaxane (**Figure 1-36**), which is assembled by complementary hydrogen bonding

interactions between the isophthalamide units of the macrocycle, and the amides of the axle component, giving the rotaxane in 97% yield.[208]

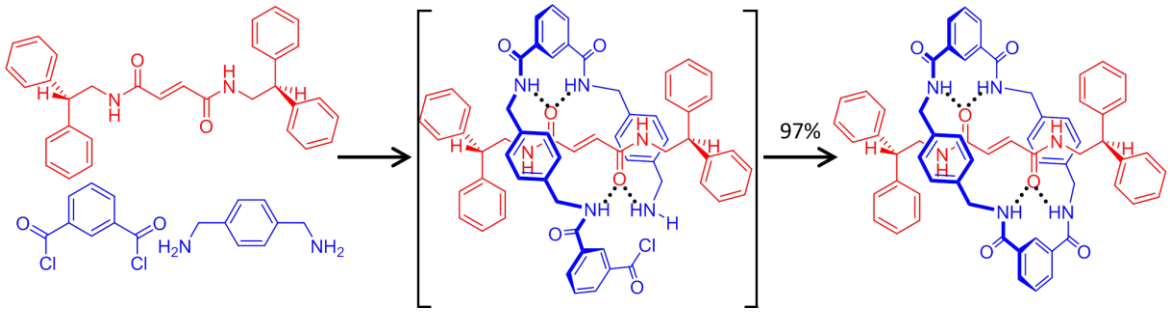


Figure 1-36: Synthesis of Leigh's neutral amide-templated [2]rotaxane.

Aromatic donor–acceptor interactions have also been used, in which the acceptor component is a neutral electron-deficient aromatic system. The naphthalene diimide (NDI)-containing [2]catenane, reported by Sanders and co-workers, is an example of such a system, in which the electron-deficient NDI units of one macrocycle interact with the electron-rich naphthaquinone motifs of the other macrocycle, in an alternating donor–acceptor stacking mode (**Figure 1-37a**).[209] It is interesting to note that aqueous dynamic combinatorial library studies of the synthesis of catenanes formed using NDI and naphthaquinone-containing components produced [2]catenanes with unexpected stacking arrangements of the motifs (**Figure 1-37b**), suggesting that hydrophobic interactions also have an influence on the assembly of these catenane systems.[210,211]

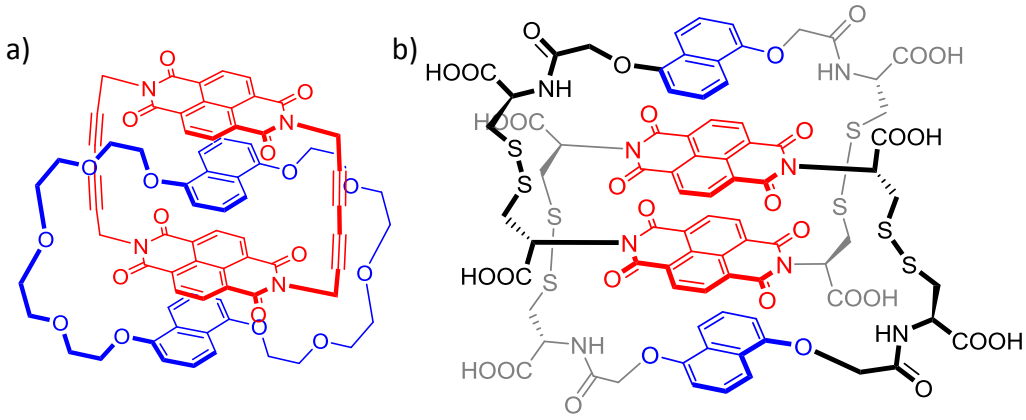


Figure 1-37: a) Sanders' original neutral aromatic donor–acceptor [2]catenane;[209] **b)** [2]catenane assembled by donor–acceptor and hydrophobic interactions.[210]

1.4.1.3 Anion Templation

While cation templation has been exploited to construct a vast number of interlocked systems, the use of anion templation has been comparatively underexplored. The first anion-templated interlocked structure was reported by Vögtle in 1999,[212] in which an anionic phenolate axle precursor was complexed by a bis(isophthalamide)-based macrocycle. A subsequent S_N2 reaction of the phenolate with another axle segment results in formation of the axle within the macrocycle, generating the [2]rotaxane (**Figure 1-38**).

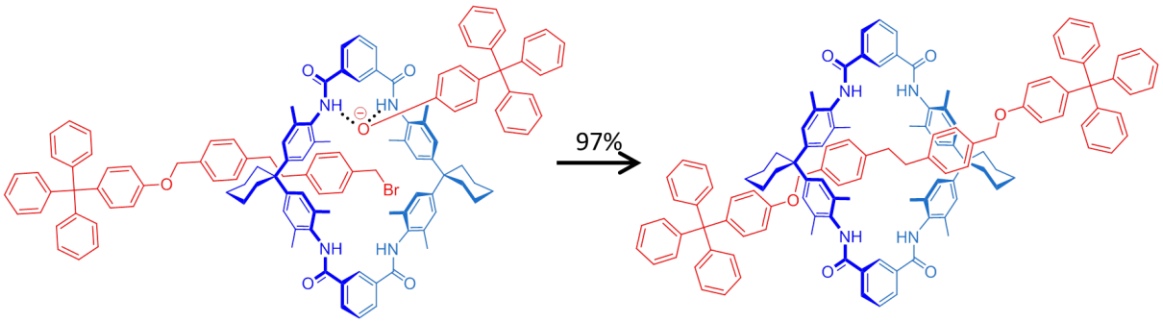


Figure 1-38: Synthesis of Vögtle's anion-templated [2]rotaxane.[212]

Taking inspiration from the successful use of transition metals to template interlocked structures, Beer and co-workers have pioneered the analogous use of discrete anionic

templates.[213,214] The potential of anion templates was first demonstrated by the formation of a stable pseudorotaxane, incorporating a bis(amide)pyridinium-based thread and a neutral isophthalamide-based macrocycle, with both coordinating to a chloride anion template (**Figure 1-39a**).[215] Based on this precedent, a rotaxane,[216] and catenane (**Figure 1-39b**)[217] were prepared using chloride anion templation. In these and other anion-templated interlocked systems, upon removal of the anion template, the resulting interlocked cavity selectively recognises the templating anion. Since then, many topologically diverse anion-templated interlocked structures have been reported, including a 'handcuff' [2]catenane,[218] Janus [2]rotaxane,[219] porphyrin-containing rotaxanes,[220] and [3]rotaxanes.[221,222]

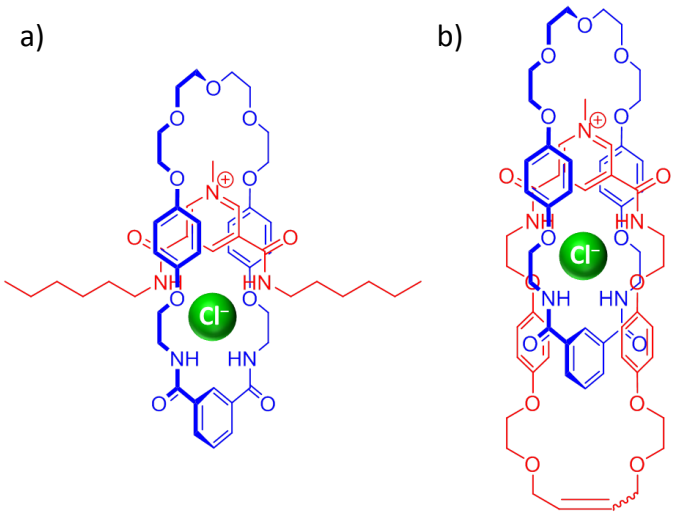


Figure 1-39: Anion-templated interpenetrated and interlocked structures, **a)** Beer's original [2]pseudorotaxane;[215] and **b)** the analogous anion-templated [2]catenane.

The vast majority of anion-templated interlocked molecules use the hydrogen bonding amide group as the anion receptor moiety. Following demonstration of the anion binding potential of the triazolium group (**§1.2.4.1**), this motif has also been exploited as a C–H hydrogen bond donor in interlocked systems,[223,224] such as the rotaxane in **Figure 1-40a**

(X = H), shown to be selective for Br^- in 1:1 $CDCl_3/CD_3OD$.[225]

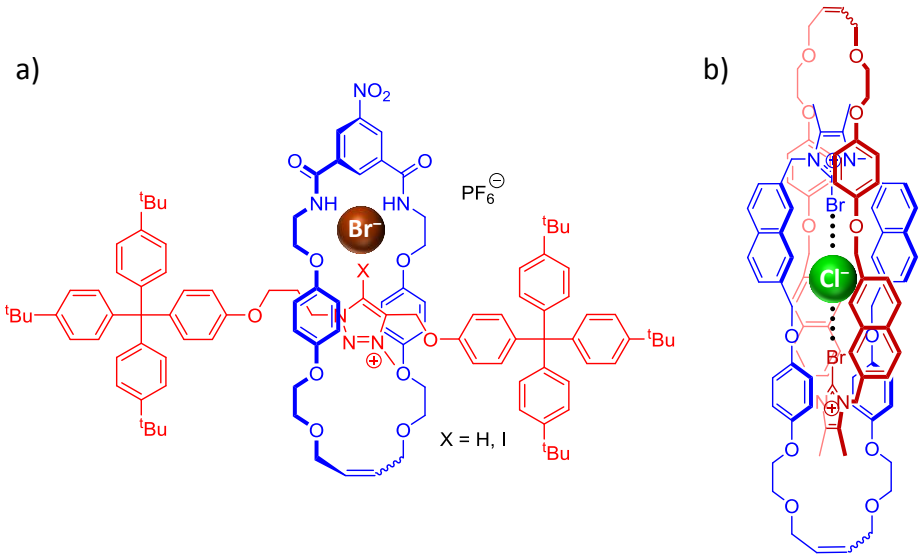


Figure 1-40: a) [2]rotaxane containing prototriazolium (X = H) or iodotriazolium (X = I) anion receptor motifs;[225,226] and **b)** bromoimidazolium-containing [2]catenane.[227]

Halogen bonding (XB) (**§1.3**) is a very recent addition to the interactions utilised in interlocked anion receptors. The potential of using XB to form interlocked structures was first noted when haloimidazolium-based threads were shown to form interpenetrated pseudorotaxane assemblies with a neutral isophthalamide-based macrocycle and a halide anion template.[228,229] Shortly thereafter, the first anion-templated XB rotaxane host system was reported (**Figure 1-40a**, X = I), which incorporated an iodotriazolium halogen bond donor group in the axle component, and was selective for I^- in 45:45:10 $CDCl_3/CD_3OD/D_2O$.[226] A bromide-templated bromoimidazolium-containing catenane has also been reported (**Figure 1-40b**). This interlocked host system was shown to exclusively sense Br^- and Cl^- by fluorescence in acetonitrile, with a binding preference for Cl^-.[227]

1.4.2 *Applications of Interlocked Molecules*

As the molecular components of interlocked molecules are not covalently bonded to each

other, they have the potential to be dynamic, and to undergo molecular motion induced by various stimuli. Stoddart's [2]rotaxane shown in **Figure 1-41** undergoes molecular motion *via* redox control.[230] The axle component contains a 1,5-dioxynaphthalene (DNP) unit and a redox-active tetrathiafulvalene (TTF) group, which is interlocked with the electron-deficient cyclobis(paraquat-*p*-phenylene) macrocycle. In the neutral state the macrocycle resides around the electron-rich TTF. However, upon oxidation of the TTF motif, mutual electrostatic repulsion results in the macrocycle moving to the DNP group.

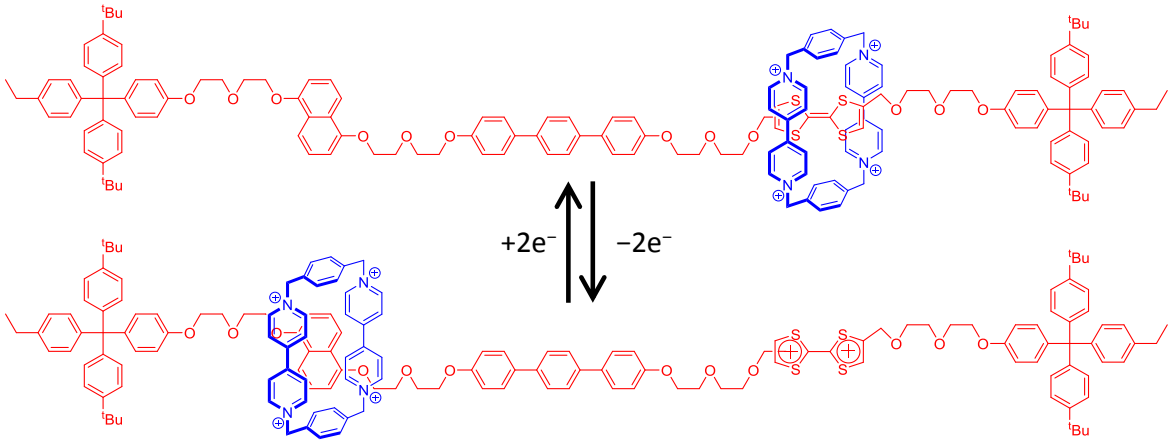


Figure 1-41: Stoddart's redox-switchable [2]rotaxane molecular shuttle.[230]

Many interlocked molecular machines have been developed which exhibit complex dynamic behaviours, including molecular muscles,[231,232] which can expand or contract upon some external stimulus, a [3]catenane 4-station unidirectional molecular rotor,[233] and a machine capable of sequence-specific peptide synthesis.[234]

Interlocked molecules have been shown to be effective hosts for molecular guest recognition, exhibiting greater binding strength and selectivity compared to non-interlocked systems.[213,214] However, the potential of using interlocked hosts for guest recognition is relatively underexplored. Nevertheless, progress has been made in the

development of these host systems, particularly rotaxanes and catenanes which can bind and sense charged guest species.

The ability of interlocked host molecules to exhibit a guest-induced dynamic response has been exploited for sensing cations. Hiratani's [3]rotaxane (**Figure 1-42**) consists of two polyether-containing 'crownophane' macrocycles interlocked around an anthracene-stoppered axle.[235] Upon complexation of Cs^+, the relative positions of the macrocycles undergo conformational changes to form a 'sandwich' complex with the cation, enhancing the anthracene fluorescence emission to give an optical response to binding of the cation.

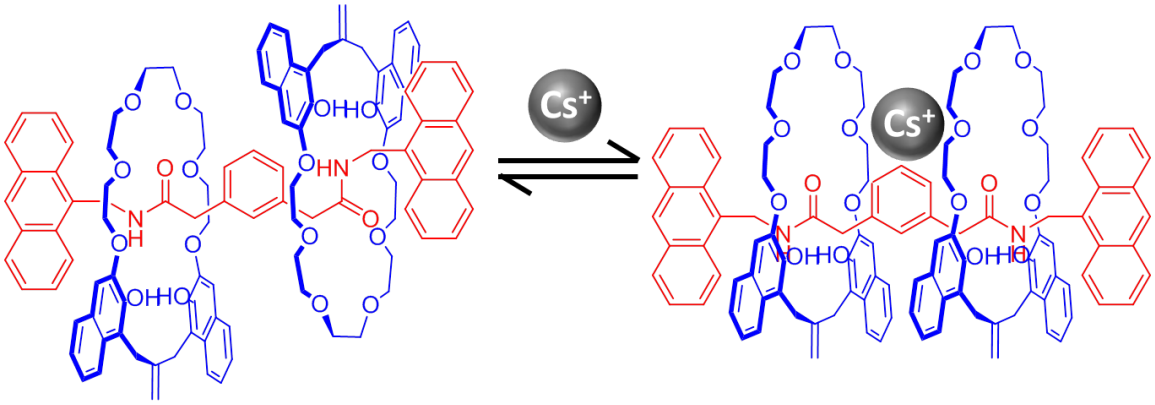


Figure 1-42: Hiratani's Cs^+ sensing [3]rotaxane.

A similar principle is used in Li's transition metal-sensing [2]rotaxane (**Figure 1-43**).[236] In the absence of a metal, the anthracene fluorescence emission is quenched by PET from the axle amine group, and the macrocycle resides predominantly over the axle amide motif. Addition of Zn(II) was shown to induce shuttling of the macrocycle over the axle amine group, which negated PET quenching through metal coordination to the amine, enhancing the anthracene emission.

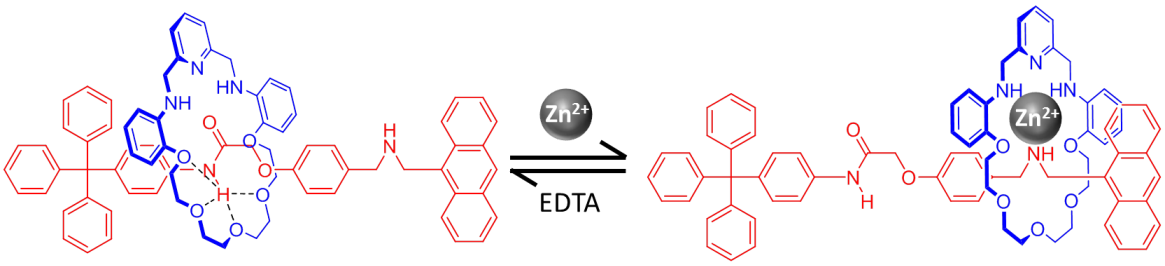


Figure 1-43: Li's transition metal-sensing [2]rotaxane.

As mentioned in the previous section, one of the major objectives of using anion templation (**§1.4.1.3**) to form interlocked systems is to develop synthetic receptors to strongly and selectively recognise anions by encapsulating them within a three-dimensional binding cavity. In an extension of this work, interlocked anion receptors which incorporate reporter groups have been developed, which provide an easily measurable response to anion binding.[237] Ferrocene-functionalised rotaxanes and catenanes have been reported (**Figure 1-44a**), which electrochemically sense anions through a cathodic shift in the ferrocene redox couple upon anion complexation.[221,238,239] These systems have also been confined on surfaces as self-assembled monolayers.[240,241]

Interlocked receptors containing optically-active groups are another research avenue in the development of anion sensors. The $[Re(CO)_3(2,2'\text{-bipyridine})Cl]$ and $[Ru(2,2'\text{-bipyridine})_3]^{2+}$ complex motifs have been used as luminescent reporter groups, which sense anions through changes in their luminescence emission properties.[242,243] The rotaxane shown in **Figure 1-44b** demonstrated selectivity for Cl^-, with an association constant of $K_a = 1.2 \times 10^6\ M^{-1}$ in 9:1 acetone/water, calculated using luminescence titration data.[243] Luminescent lanthanide-containing rotaxanes have also been reported,[244] and organic fluorophores have been successfully used to study anion binding in interlocked systems,[223,245,246] such as Jeong's indolocarbazole-based catenane (**Figure 1-44c**), which

selectively senses chloride over oxoanions in 99:1 acetone/water, and is a rare example of a neutral interlocked anion receptor.[247]

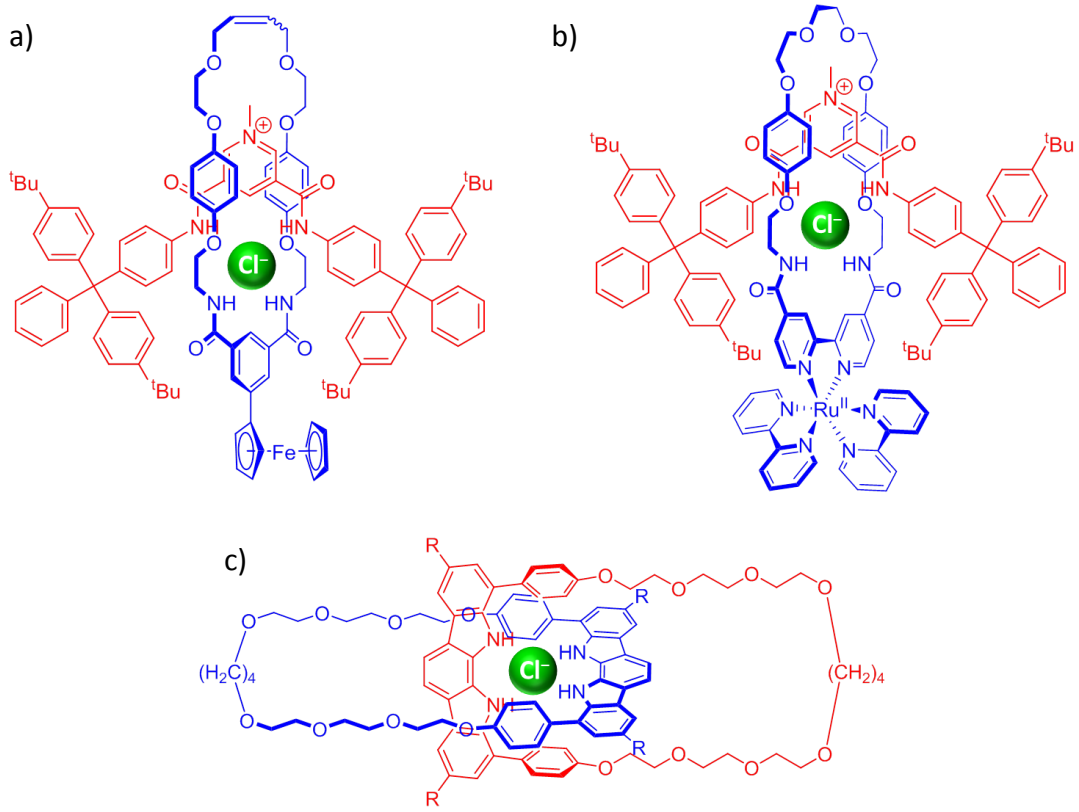


Figure 1-44: a) Beer's ferrocene-appended redox-active [2]rotaxane;[238] **b)** Ru(2,2′-bipyridine)$_3$-containing luminescent [2]rotaxane sensor;[243] and **c)** Jeong's indolocarbazole-based fluorescent [2]catenane.[247]

1.5 *Outline of Project*

As noted in **§1.3**, the exploitation of halogen bonding (XB) for molecular recognition applications is underdeveloped, and examples of XB host systems for anion binding are especially rare when compared to the vast array of hydrogen bonding anion receptors in the current literature (**§1.3.1**). Furthermore, at the time of writing there have only been two interlocked XB anion receptors reported to date, both of which exhibit superior anion binding affinities in comparison to hydrogen bonding host analogues (**§1.4.1.3**). With this

in mind, the general aim of this project was to integrate halogen bond donor groups into various acyclic, macrocyclic and ultimately interlocked host structural frameworks that contain redox- and photo-active reporter groups, and investigate their anion recognition and sensing capabilities.

Chapter 2 describes anion receptors containing the carbazole spacer unit, which is well known to have interesting and potentially useful fluorescent properties. A systematic study on the anion binding properties of a series of both XB and hydrogen bonding anion receptors is presented. Following these results, a XB rotaxane was then synthesised and its anion binding properties explored.

Chapter 3 presents the construction of XB receptors containing the naphthalene spacer. The synthesis and anion binding properties of both acyclic and interlocked systems are discussed.

Chapter 4 describes the syntheses of receptors containing photo-active $Re(I)(CO)_3Cl(bpy)$ and redox-active diquat reporter groups. An all-XB rotaxane consisting of a $Re(I)(CO)_3Cl(bpy)$ macrocycle and a carbazole-based axle component is prepared, and demonstrated to sense anions in competitive aqueous solutions. The electrochemical anion recognition properties of diquat-based receptors are studied, and the synthesis of a diquat-containing rotaxane attempted.

1.6 *References*

(1) Lehn, J.-M. *Angew. Chem. Int. Ed. Eng.* **1988**, *27*, 89.
(2) Pedersen, C. J. *J. Am. Chem. Soc.* **1967**, *89*, 2495.
(3) Steed, J. W.; Atwood, J. L. *Supramolecular Chemistry*; John Wiley & Sons, Ltd., 2000.
(4) Anfinsen, C. B. *Biochem. J.* **1972**, *128*, 737.

(5) Arunan, E.; Desiraju, G. R.; Klein, R. A.; Sadlej, J.; Scheiner, S.; Alkorta, I.; Clary, D. C.; Crabtree, R. H.; Dannenberg, J. J.; Hobza, P.; Kjaergaard, H. G.; Legon, A. C.; Mennucci, B.; Nesbitt, D. J. *Pure Appl. Chem.* **2011**, *83*, 1637.
(6) Martinez, C. R.; Iverson, B. L. *Chem. Sci.* **2012**, *3*, 2191.
(7) Reddington, M. V.; Slawin, A. M. Z.; Spencer, N.; Stoddart, J. F.; Vicent, C.; Williams, D. J. *J. Chem. Soc., Chem. Commun.* **1991**, 630.
(8) Ma, J. C.; Dougherty, D. A. *Chem. Rev.* **1997**, *97*, 1303.
(9) Gokel, G. W.; Barbour, L. J.; Ferdani, R.; Hu, J. *Acc. Chem. Res.* **2002**, *35*, 878.
(10) Salonen, L. M.; Bucher, C.; Banner, D. W.; Haap, W.; Mary, J.-L.; Benz, J.; Kuster, O.; Seiler, P.; Schweizer, W. B.; Diederich, F. *Angew. Chem. Int. Ed.* **2009**, *48*, 811.
(11) Lin, C.-H.; Radhakrishnan, K. *Chem. Commun.* **2005**, 504.
(12) Gil-Ramírez, G.; Escudero-Adán, E. C.; Benet-Buchholz, J.; Ballester, P. *Angew. Chem. Int. Ed.* **2008**, *47*, 4114.
(13) Chifotides, H. T.; Dunbar, K. R. *Acc. Chem. Res.* **2013**, *46*, 894.
(14) Watt, M. M.; Zakharov, L. N.; Haley, M. M.; Johnson, D. W. *Angew. Chem. Int. Ed.* **2013**, *52*, 10275.
(15) Zhao, Y.; Beuchat, C.; Domoto, Y.; Gajewy, J.; Wilson, A.; Mareda, J.; Sakai, N.; Matile, S. *J. Am. Chem. Soc.* **2014**, *136*, 2101.
(16) Wang, D.-X.; Wang, M.-X. *J. Am. Chem. Soc.* **2012**, *135*, 892.
(17) Frontera, A. *Coord. Chem. Rev.* **2013**, *257*, 1716.
(18) Berryman, O. B.; Bryantsev, V. S.; Stay, D. P.; Johnson, D. W.; Hay, B. P. *J. Am. Chem. Soc.* **2006**, *129*, 48.
(19) Harris, K.; Fujita, D.; Fujita, M. *Chem. Commun.* **2013**, *49*, 6703.
(20) Blokzijl, W.; Engberts, J. B. F. N. *Angew. Chem. Int. Ed. Eng.* **1993**, *32*, 1545.
(21) Luecke, H.; Quiocho, F. A. *Nature* **1990**, *347*, 402.
(22) Dutzler, R.; Campbell, E. B.; Cadene, M.; Chait, B. T.; MacKinnon, R. *Nature* **2002**, *415*, 287.
(23) Lehn, J. M. *Acc. Chem. Res.* **1978**, *11*, 49.
(24) Kavallieratos, K.; de Gala, S. R.; Austin, D. J.; Crabtree, R. H. *J. Am. Chem. Soc.* **1997**, *119*, 2325.
(25) Santacroce, P. V.; Davis, J. T.; Light, M. E.; Gale, P. A.; Iglesias-Sánchez, J. C.; Prados, P.; Quesada, R. *J. Am. Chem. Soc.* **2007**, *129*, 1886.
(26) Sessler, J. L.; Gale, P. A.; Cho, W.-S. *Anion Receptor Chemistry*; Royal Society of Chemistry, Cambridge, 2006.
(27) Davis, A. P.; Sheppard, D. N.; Smith, B. D. *Chem. Soc. Rev.* **2007**, *36*, 348.
(28) Axelrad, A. A.; Leblond, C. P. *Cancer* **1955**, *8*, 339.
(29) Loskill, P.; Zeitz, C.; Grandthyll, S.; Thewes, N.; Müller, F.; Bischoff, M.; Herrmann, M.; Jacobs, K. *Langmuir* **2013**, *29*, 5528.
(30) Beer, P. D.; Gale, P. A. *Angew. Chem. Int. Ed.* **2001**, *40*, 486.
(31) Wenzel, M.; Hiscock, J. R.; Gale, P. A. *Chem. Soc. Rev.* **2012**, *41*, 480.
(32) Gale, P. A.; Pérez-Tomás, R.; Quesada, R. *Acc. Chem. Res.* **2013**, *46*, 2801.
(33) Gale, P. A.; Busschaert, N.; Haynes, C. J. E.; Karagiannidis, L. E.; Kirby, I. L. *Chem. Soc. Rev.* **2014**, *43*, 205.
(34) Caltagirone, C.; Bates, G. W.; Gale, P. A.; Light, M. E. *Chem. Commun.* **2008**, 61.
(35) Pflugrath, J. W.; Quiocho, F. A. *Nature* **1985**, *314*, 257.
(36) Park, C. H.; Simmons, H. E. *J. Am. Chem. Soc.* **1968**, *90*, 2431.

(37) Graf, E.; Lehn, J. M. *J. Am. Chem. Soc.* **1976**, *98*, 6403.
(38) Lehn, J. M.; Sonveaux, E.; Willard, A. K. *J. Am. Chem. Soc.* **1978**, *100*, 4914.
(39) Schmidtchen, F. P. *Angew. Chem. Int. Ed. Eng.* **1977**, *16*, 720.
(40) Worm, K.; Schmidtchen, F. P. *Angew. Chem. Int. Ed. Eng.* **1995**, *34*, 65.
(41) Schiessl, P.; Schmidtchen, F. P. *J. Org. Chem.* **1994**, *59*, 509.
(42) Metzger, A.; Lynch, V. M.; Anslyn, E. V. *Angew. Chem. Int. Ed. Eng.* **1997**, *36*, 862.
(43) Alcalde, E.; Mesquida, N.; Pérez-García, L. *Eur. J. Org. Chem.* **2006**, *2006*, 3988.
(44) Schulze, B.; Friebe, C.; Hager, M. D.; Günther, W.; Köhn, U.; Jahn, B. O.; Görls, H.; Schubert, U. S. *Org. Lett.* **2010**, *12*, 2710.
(45) Yoon, J.; Kim, S. K.; Singh, N. J.; Kim, K. S. *Chem. Soc. Rev.* **2006**, *35*, 355.
(46) Xu, Z.; Kim, S. K.; Yoon, J. *Chem. Soc. Rev.* **2010**, *39*, 1457.
(47) Kumar, A.; Pandey, P. S. *Org. Lett.* **2007**, *10*, 165.
(48) Pascal Jr, R. A.; Spergel, J.; Van Engen, D. *Tetrahedron Lett.* **1986**, *27*, 4099.
(49) Bak, K. M.; Chmielewski, M. J. *Chem. Commun.* **2014**, *50*, 1305.
(50) Li, A.-F.; Wang, J.-H.; Wang, F.; Jiang, Y.-B. *Chem. Soc. Rev.* **2010**, *39*, 3729.
(51) Sessler, J. L.; Camiolo, S.; Gale, P. A. *Coord. Chem. Rev.* **2003**, *240*, 17.
(52) Ghosh, S. K.; Ishida, M.; Li, J.; Cha, W.-Y.; Lynch, V. M.; Kim, D.; Sessler, J. L. *Chem. Commun.* **2014**, *50*, 3753.
(53) Hua, Y.; Flood, A. H. *Chem. Soc. Rev.* **2010**, *39*, 1262.
(54) Schulze, B.; Schubert, U. S. *Chem. Soc. Rev.* **2014**, *43*, 2522.
(55) Sarwar, M. G.; Dragisic, B.; Sagoo, S.; Taylor, M. S. *Angew. Chem. Int. Ed.* **2010**, *49*, 1674.
(56) Wade, C. R.; Broomsgrove, A. E. J.; Aldridge, S.; Gabbaï, F. P. *Chem. Rev.* **2010**, *110*, 3958.
(57) Bondy, C. R.; Loeb, S. J. *Coord. Chem. Rev.* **2003**, *240*, 77.
(58) Juwarker, H.; Lenhardt, J. M.; Pham, D. M.; Craig, S. L. *Angew. Chem. Int. Ed.* **2008**, *47*, 3740.
(59) Meudtner, R. M.; Hecht, S. *Angew. Chem. Int. Ed.* **2008**, *47*, 4926.
(60) Li, Y.; Flood, A. H. *J. Am. Chem. Soc.* **2008**, *130*, 12111.
(61) Ju, J.; Park, M.; Suk, J.-m.; Lah, M. S.; Jeong, K.-S. *Chem. Commun.* **2008**, 3546.
(62) Amendola, V.; Fabbrizzi, L. *Chem. Commun.* **2009**, 513.
(63) Mercer, D. J.; Loeb, S. J. *Chem. Soc. Rev.* **2010**, *39*, 3612.
(64) Custelcean, R. *Chem. Soc. Rev.* **2014**, *43*, 1813.
(65) Bondy, C. R.; Gale, P. A.; Loeb, S. J. *J. Am. Chem. Soc.* **2004**, *126*, 5030.
(66) Amendola, V.; Boiocchi, M.; Colasson, B.; Fabbrizzi, L.; Rodriguez Douton, M.-J.; Ugozzoli, F. *Angew. Chem. Int. Ed.* **2006**, *45*, 6920.
(67) Wiskur, S. L.; Ait-Haddou, H.; Lavigne, J. J.; Anslyn, E. V. *Acc. Chem. Res.* **2001**, *34*, 963.
(68) Comes, M.; Aznar , E.; Moragues, M.; Marcos, M. D.; Martínez-Máñez, R.; Sancenón, F.; Soto, J.; Villaescusa, L. A.; Gil, L.; Amorós, P. *Chem. Eur. J.* **2009**, *15*, 9024.
(69) Lou, X.; Ou, D.; Li, Q.; Li, Z. *Chem. Commun.* **2012**, *48*, 8462.
(70) Ros-Lis, J. V.; Martinez-Manez, R.; Soto, J. *Chem. Commun.* **2002**, 2248.
(71) Kaur, K.; Saini, R.; Kumar, A.; Luxami, V.; Kaur, N.; Singh, P.; Kumar, S. *Coord. Chem. Rev.* **2012**, *256*, 1992.
(72) Cho, D.-G.; Kim, J. H.; Sessler, J. L. *J. Am. Chem. Soc.* **2008**, *130*, 12163.

(73) Bühlmann, P.; Pretsch, E.; Bakker, E. *Chem. Rev.* **1998**, *98*, 1593.
(74) Antonisse, M. M. G.; Reinhoudt, D. N. *Electroanalysis* **1999**, *11*, 1035.
(75) Lou, X.; Qin, J.; Li, Z. *Analyst* **2009**, *134*, 2071.
(76) Esteban-Gómez, D.; Fabbrizzi, L.; Licchelli, M. *J. Org. Chem.* **2005**, *70*, 5717.
(77) Taner, B.; Alici, O.; Deveci, P. *Supramol. Chem.* **2013**, *26*, 119.
(78) Emami Khansari, M.; Wallace, K. D.; Hossain, M. A. *Tetrahedron Lett.* **2014**, *55*, 438.
(79) Ema, T.; Okuda, K.; Watanabe, S.; Yamasaki, T.; Minami, T.; Esipenko, N. A.; Anzenbacher, P. *Org. Lett.* **2014**, *16*, 1302.
(80) Suryanti, V.; Bhadbhade, M.; Chawla, H. M.; Howe, E.; Thordarson, P.; Black, D. S.; Kumar, N. *Spectrochim. Acta A* **2014**, *121*, 662.
(81) Tirfoin, R.; Aldridge, S. *Dalton Trans.* **2013**, *42*, 12836.
(82) Lakowicz, J. R. *Principles of Fluorescence Spectroscopy*; 3rd ed.; Springer, New York, 2006.
(83) de Silva, A. P.; Gunaratne, H. Q. N.; Gunnlaugsson, T.; Huxley, A. J. M.; McCoy, C. P.; Rademacher, J. T.; Rice, T. E. *Chem. Rev.* **1997**, *97*, 1515.
(84) Callan, J. F.; de Silva, A. P.; Magri, D. C. *Tetrahedron* **2005**, *61*, 8551.
(85) Gunnlaugsson, T.; Glynn, M.; Tocci, G. M.; Kruger, P. E.; Pfeffer, F. M. *Coord. Chem. Rev.* **2006**, *250*, 3094.
(86) Duke, R. M.; Gunnlaugsson, T. *Tetrahedron Lett.* **2007**, *48*, 8043.
(87) Veale, E. B.; Gunnlaugsson, T. *J. Org. Chem.* **2008**, *73*, 8073.
(88) Veale, E. B.; Tocci, G. M.; Pfeffer, F. M.; Kruger, P. E.; Gunnlaugsson, T. *Org. Biomol. Chem.* **2009**, *7*, 3447.
(89) Beer, P. D.; Mortimer, R. J.; Stradiotto, N. R.; Szemes, F.; Weightman, J. S. *Anal. Proc.* **1995**, *32*, 419.
(90) Beer, P. D.; Szemes, F. *J. Chem. Soc., Chem. Commun.* **1995**, 2245.
(91) Beer, P. D.; Szemes, F.; Balzani, V.; Salà, C. M.; Drew, M. G. B.; Dent, S. W.; Maestri, M. *J. Am. Chem. Soc.* **1997**, *119*, 11864.
(92) Beer, P. D.; Cadman, J. *Coord. Chem. Rev.* **2000**, *205*, 131.
(93) Beer, P. D.; Timoshenko, V.; Maestri, M.; Passaniti, P.; Balzani, V. *Chem. Commun.* **1999**, 1755.
(94) Parker, D.; Senanayake, K.; Williams, J. A. G. *Chem. Commun.* **1997**, 1777.
(95) Montalti, M.; Prodi, L.; Zaccheroni, N.; Charbonnière, L.; Douce, L.; Ziessel, R. *J. Am. Chem. Soc.* **2001**, *123*, 12694.
(96) Cable, M. L.; Kirby, J. P.; Gray, H. B.; Ponce, A. *Acc. Chem. Res.* **2013**, *46*, 2576.
(97) Tropiano, M.; Blackburn, O. A.; Tilney, J. A.; Hill, L. R.; Placidi, M. P.; Aarons, R. J.; Sykes, D.; Jones, M. W.; Kenwright, A. M.; Snaith, J. S.; Sørensen, T. J.; Faulkner, S. *Chem. Eur. J.* **2013**, *19*, 16566.
(98) Beer, P. D.; Chen, Z.; Drew, M. G. B.; Johnsona, A. O. M.; Smith, D. K.; Spencer, P. *Inorg. Chim. Acta* **1996**, *246*, 143.
(99) Niu, H.-T.; Yin, Z.; Su, D.; Niu, D.; Ao, Y.; He, J.; Cheng, J.-P. *Tetrahedron* **2008**, *64*, 6300.
(100) Beer, P. D.; Keefe, A. D. *J. Organomet. Chem.* **1989**, *375*, C40.
(101) Beer, P. D.; Hesek, D.; Hodacova, J.; Stokes, S. E. *J. Chem. Soc., Chem. Commun.* **1992**, 270.
(102) Beer, P. D.; Graydon, A. R.; Johnson, A. O. M.; Smith, D. K. *Inorg. Chem.* **1997**, *36*, 2112.

(103) Altmann, R.; Gausset, O.; Horn, D.; Jurkschat, K.; Schürmann, M.; Fontani, M.; Zanello, P. *Organometallics* **2000**, *19*, 430.
(104) Willener, Y.; Joly, K. M.; Moody, C. J.; Tucker, J. H. R. *J. Org. Chem.* **2008**, *73*, 1225.
(105) Romero, T.; Caballero, A.; Tárraga, A.; Molina, P. *Org. Lett.* **2009**, *11*, 3466.
(106) Lorenzo, Á.; Aller, E.; Molina, P. *Tetrahedron* **2009**, *65*, 1397.
(107) Desiraju, G. R.; Ho, P. S.; Kloo, L.; Legon, A. C.; Marquardt, R.; Metrangolo, P.; Politzer, P.; Resnati, G.; Rissanen, K. *Pure Appl. Chem.* **2013**, *85*, 1711.
(108) Clark, T.; Hennemann, M.; Murray, J.; Politzer, P. *J. Mol. Model.* **2007**, *13*, 291.
(109) Hassel, O.; Hvoslef, J. *Acta Chem. Scand.* **1954**, *8*, 873.
(110) Desiraju, G. R. *Angew. Chem. Int. Ed. Eng.* **1995**, *34*, 2311.
(111) Rissanen, K. *CrystEngComm* **2008**, *10*, 1107.
(112) Fourmigué, M. *Curr. Opin. Solid State Mater. Sci.* **2009**, *13*, 36.
(113) Aakeroy, C. B.; Champness, N. R.; Janiak, C. *CrystEngComm* **2010**, *12*, 22.
(114) Bertani, R.; Sgarbossa, P.; Venzo, A.; Lelj, F.; Amati, M.; Resnati, G.; Pilati, T.; Metrangolo, P.; Terraneo, G. *Coord. Chem. Rev.* **2010**, *254*, 677.
(115) Metrangolo, P.; Resnati, G. *Cryst. Growth Des.* **2012**, *12*, 5835.
(116) Troff, R. W.; Mäkelä, T.; Topić, F.; Valkonen, A.; Raatikainen, K.; Rissanen, K. *Eur. J. Org. Chem.* **2013**, *2013*, 1617.
(117) Metrangolo, P.; Resnati, G.; Pilati, T.; Liantonio, R.; Meyer, F. *J. Polym. Sci. A: Polym. Chem.* **2007**, *45*, 1.
(118) Meyer, F.; Dubois, P. *CrystEngComm* **2013**, *15*, 3058.
(119) Priimagi, A.; Cavallo, G.; Metrangolo, P.; Resnati, G. *Acc. Chem. Res.* **2013**, *46*, 2686.
(120) Fourmigué, M.; Batail, P. *Chem. Rev.* **2004**, *104*, 5379.
(121) Shin, K.-S.; Brezgunova, M.; Jeannin, O.; Roisnel, T.; Camerel, F.; Auban-Senzier, P.; Fourmigué, M. *Cryst. Growth Des.* **2011**, *11*, 5337.
(122) Clemente-Juan, J. M.; Coronado, E.; Minguez Espallargas, G.; Adams, H.; Brammer, L. *CrystEngComm* **2010**, *12*, 2339.
(123) Espallargas, G. M.; Recuenco, A.; Romero, F. M.; Brammer, L.; Libri, S. *CrystEngComm* **2012**, *14*, 6381.
(124) Awwadi, F. F.; Haddad, S. F.; Turnbull, M. M.; Landee, C. P.; Willett, R. D. *CrystEngComm* **2013**, *15*, 3111.
(125) Metrangolo, P.; Meyer, F.; Pilati, T.; Resnati, G.; Terraneo, G. *Chem. Commun.* **2008**, 1635.
(126) Meazza, L.; Foster, J. A.; Fucke, K.; Metrangolo, P.; Resnati, G.; Steed, J. W. *Nat. Chem.* **2013**, *5*, 42.
(127) Nguyen, H. L.; Horton, P. N.; Hursthouse, M. B.; Legon, A. C.; Bruce, D. W. *J. Am. Chem. Soc.* **2003**, *126*, 16.
(128) Prasang, C.; Nguyen, H. L.; Horton, P. N.; Whitwood, A. C.; Bruce, D. W. *Chem. Commun.* **2008**, 6164.
(129) McAllister, L. J.; Prasang, C.; Wong, J. P. W.; Thatcher, R. J.; Whitwood, A. C.; Donnio, B.; O'Brien, P.; Karadakov, P. B.; Bruce, D. W. *Chem. Commun.* **2013**, *49*, 3946.
(130) Priimagi, A.; Cavallo, G.; Forni, A.; Gorynsztejn–Leben, M.; Kaivola, M.; Metrangolo, P.; Milani, R.; Shishido, A.; Pilati, T.; Resnati, G.; Terraneo, G. *Adv. Funct. Mater.* **2012**, *22*, 2572.

(131) Priimagi, A.; Saccone, M.; Cavallo, G.; Shishido, A.; Pilati, T.; Metrangolo, P.; Resnati, G. *Adv. Mater.* **2012**, *24*, OP345.
(132) Caronna, T.; Liantonio, R.; Logothetis, T. A.; Metrangolo, P.; Pilati, T.; Resnati, G. *J. Am. Chem. Soc.* **2004**, *126*, 4500.
(133) Meazza, L.; Marti-Rujas, J.; Terraneo, G.; Castiglioni, C.; Milani, A.; Pilati, T.; Metrangolo, P.; Resnati, G. *CrystEngComm* **2011**, *13*, 4427.
(134) Sun, A.; Lauher, J. W.; Goroff, N. S. *Science* **2006**, *312*, 1030.
(135) Lauher, J. W.; Fowler, F. W.; Goroff, N. S. *Acc. Chem. Res.* **2008**, *41*, 1215.
(136) Beale, T. M.; Chudzinski, M. G.; Sarwar, M. G.; Taylor, M. S. *Chem. Soc. Rev.* **2013**, *42*, 1667.
(137) Jungbauer, S. H.; Schindler, S.; Kniep, F.; Walter, S. M.; Rout, L.; Huber, S. M. *Synlett* **2013**, *24*, 2624.
(138) Kniep, F.; Jungbauer, S. H.; Zhang, Q.; Walter, S. M.; Schindler, S.; Schnapperelle, I.; Herdtweck, E.; Huber, S. M. *Angew. Chem. Int. Ed.* **2013**, *52*, 7028.
(139) Scholfield, M. R.; Zanden, C. M. V.; Carter, M.; Ho, P. S. *Protein Sci.* **2013**, *22*, 139.
(140) Weiss, R.; Schwab, O.; Hampel, F. *Chem. Eur. J.* **1999**, *5*, 968.
(141) Liantonio, R.; Metrangolo, P.; Pilati, T.; Resnati, G. *Cryst. Growth Des.* **2003**, *3*, 355.
(142) Mele, A.; Metrangolo, P.; Neukirch, H.; Pilati, T.; Resnati, G. *J. Am. Chem. Soc.* **2005**, *127*, 14972.
(143) Dimitrijevic, E.; Kvak, O.; Taylor, M. S. *Chem. Commun.* **2010**, *46*, 9025.
(144) Sarwar, M. G.; Dragisić, B.; Dimitrijević, E.; Taylor, M. S. *Chem. Eur. J.* **2013**, *19*, 2050.
(145) Chudzinski, M. G.; McClary, C. A.; Taylor, M. S. *J. Am. Chem. Soc.* **2011**, *133*, 10559.
(146) Caballero, A.; White, N. G.; Beer, P. D. *Angew. Chem. Int. Ed.* **2011**, *50*, 1845.
(147) Zapata, F.; Caballero, A.; White, N. G.; Claridge, T. D. W.; Costa, P. J.; Félix, V.; Beer, P. D. *J. Am. Chem. Soc.* **2012**, *134*, 11533.
(148) van Dongen, S. F. M.; Cantekin, S.; Elemans, J. A. A. W.; Rowan, A. E.; Nolte, R. J. M. *Chem. Soc. Rev.* **2014**, *43*, 99.
(149) Chichak, K. S.; Peters, A. J.; Cantrill, S. J.; Stoddart, J. F. *J. Org. Chem.* **2005**, *70*, 7956.
(150) Lukin, O.; Vögtle, F. *Angew. Chem. Int. Ed.* **2005**, *44*, 1456.
(151) Ayme, J.-F.; Beves, J. E.; Leigh, D. A.; McBurney, R. T.; Rissanen, K.; Schultz, D. *Nat. Chem.* **2012**, *4*, 15.
(152) Ayme, J.-F.; Beves, J. E.; Leigh, D. A.; McBurney, R. T.; Rissanen, K.; Schultz, D. *J. Am. Chem. Soc.* **2012**, *134*, 9488.
(153) Dietrich-Buchecker, C. O.; Sauvage, J. P. *Chem. Rev.* **1987**, *87*, 795.
(154) Fujita, M.; Ibukuro, F.; Hagihara, H.; Ogura, K. *Nature* **1994**, *367*, 720.
(155) G. Hamilton, D.; Feeder, N.; J. Teat, S.; K. M. Sanders, J. *New J. Chem.* **1998**, *22*, 1019.
(156) Kilbinger, A. F. M.; Cantrill, S. J.; Waltman, A. W.; Day, M. W.; Grubbs, R. H. *Angew. Chem. Int. Ed.* **2003**, *42*, 3281.
(157) Guidry, E. N.; Cantrill, S. J.; Stoddart, J. F.; Grubbs, R. H. *Org. Lett.* **2005**, *7*, 2129.
(158) Wong, W. W. H.; Cookson, J.; Evans, E. A. L.; McInnes, E. J. L.; Wolowska, J.;

Maher, J. P.; Bishop, P.; Beer, P. D. *Chem. Commun.* **2005**, 2214.
(159) Ashton, P. R.; Belohradsky, M.; Philp, D.; Spencer, N.; Stoddart, J. F. *J. Chem. Soc., Chem. Commun.* **1993**, 1274.
(160) Händel, M.; Plevoets, M.; Gestermann, S.; Vögtle, F. *Angew. Chem. Int. Ed. Eng.* **1997**, *36*, 1199.
(161) Hannam, J. S.; Kidd, T. J.; Leigh, D. A.; Wilson, A. J. *Org. Lett.* **2003**, *5*, 1907.
(162) Zheng, H.; Li, Y.; Zhou, C.; Li, Y.; Yang, W.; Zhou, W.; Zuo, Z.; Liu, H. *Chem. Eur. J.* **2011**, *17*, 2160.
(163) Crowley, J. D.; Goldup, S. M.; Lee, A.-L.; Leigh, D. A.; McBurney, R. T. *Chem. Soc. Rev.* **2009**, *38*, 1530.
(164) Chiu, C.-W.; Lai, C.-C.; Chiu, S.-H. *J. Am. Chem. Soc.* **2007**, *129*, 3500.
(165) Ko, J.-L.; Ueng, S.-H.; Chiu, C.-W.; Lai, C.-C.; Liu, Y.-H.; Peng, S.-M.; Chiu, S.-H. *Chem. Eur. J.* **2010**, *16*, 6950.
(166) Yoon, I.; Narita, M.; Shimizu, T.; Asakawa, M. *J. Am. Chem. Soc.* **2004**, *126*, 16740.
(167) Hsueh, S.-Y.; Ko, J.-L.; Lai, C.-C.; Liu, Y.-H.; Peng, S.-M.; Chiu, S.-H. *Angew. Chem. Int. Ed.* **2011**, *50*, 6643.
(168) Wasserman, E. *J. Am. Chem. Soc.* **1960**, *82*, 4433.
(169) Harrison, I. T.; Harrison, S. *J. Am. Chem. Soc.* **1967**, *89*, 5723.
(170) Dietrich-Buchecker, C. O.; Sauvage, J. P.; Kern, J. M. *J. Am. Chem. Soc.* **1984**, *106*, 3043.
(171) Mohr, B.; Sauvage, J.-P.; Grubbs, R. H.; Weck, M. *Angew. Chem. Int. Ed. Eng.* **1997**, *36*, 1308.
(172) Chambron, J.-C.; Heitz, V.; Sauvage, J.-P. *J. Chem. Soc., Chem. Commun.* **1992**, 1131.
(173) Nierengarten, J. F.; Dietrich-Buchecker, C. O.; Sauvage, J. P. *J. Am. Chem. Soc.* **1994**, *116*, 375.
(174) Diederich, F.; Dietrich-Buchecker, C.; Nierengarten, J.-F.; Sauvage, J.-P. *J. Chem. Soc., Chem. Commun.* **1995**, 781.
(175) Jimenez-Molero, M. C.; Dietrich-Buchecker, C.; Sauvage, J.-P. *Chem. Commun.* **2003**, 1613.
(176) Frey, J.; Kraus, T.; Heitz, V.; Sauvage, J.-P. *Chem. Eur. J.* **2007**, *13*, 7584.
(177) Collin, J.-P.; Durola, F.; Frey, J.; Heitz, V.; Reviriego, F.; Sauvage, J.-P.; Trolez, Y.; Rissanen, K. *J. Am. Chem. Soc.* **2010**, *132*, 6840.
(178) Durola, F.; Lux, J.; Sauvage, J.-P.; Wenger, O. S. *Supramol. Chem.* **2010**, *23*, 42.
(179) Roche, C.; Sauvage, J.-P.; Sour, A.; Strutt, N. L. *New J. Chem.* **2011**, *35*, 2820.
(180) Beves, J. E.; Blight, B. A.; Campbell, C. J.; Leigh, D. A.; McBurney, R. T. *Angew. Chem. Int. Ed.* **2011**, *50*, 9260.
(181) Goldup, S. M.; Leigh, D. A.; Lusby, P. J.; McBurney, R. T.; Slawin, A. M. Z. *Angew. Chem.* **2008**, *120*, 7107.
(182) Fuller, A.-M.; Leigh, D. A.; Lusby, P. J.; Oswald, I. D. H.; Parsons, S.; Walker, D. B. *Angew. Chem.* **2004**, *116*, 4004.
(183) Hamann, C.; Kern, J.-M.; Sauvage, J.-P. *Inorg. Chem.* **2003**, *42*, 1877.
(184) Leigh, D. A.; Lusby, P. J.; McBurney, R. T.; Morelli, A.; Slawin, A. M. Z.; Thomson, A. R.; Walker, D. B. *J. Am. Chem. Soc.* **2009**, *131*, 3762.
(185) Aucagne, V.; Hänni, K. D.; Leigh, D. A.; Lusby, P. J.; Walker, D. B. *J. Am. Chem. Soc.* **2006**, *128*, 2186.

(186) Aucagne, V.; Berná, J.; Crowley, J. D.; Goldup, S. M.; Hänni, K. D.; Leigh, D. A.; Lusby, P. J.; Ronaldson, V. E.; Slawin, A. M. Z.; Viterisi, A.; Walker, D. B. *J. Am. Chem. Soc.* **2007**, *129*, 11950.
(187) Goldup, S. M.; Leigh, D. A.; McGonigal, P. R.; Ronaldson, V. E.; Slawin, A. M. Z. *J. Am. Chem. Soc.* **2009**, *132*, 315.
(188) Barran, P. E.; Cole, H. L.; Goldup, S. M.; Leigh, D. A.; McGonigal, P. R.; Symes, M. D.; Wu, J.; Zengerle, M. *Angew. Chem. Int. Ed.* **2011**, *50*, 12280.
(189) Saito, S.; Takahashi, E.; Nakazono, K. *Org. Lett.* **2006**, *8*, 5133.
(190) Sato, Y.; Yamasaki, R.; Saito, S. *Angew. Chem. Int. Ed.* **2009**, *48*, 504.
(191) Langton, M. J.; Matichak, J. D.; Thompson, A. L.; Anderson, H. L. *Chem. Sci.* **2011**, *2*, 1897.
(192) Movsisyan, L. D.; Kondratuk, D. V.; Franz, M.; Thompson, A. L.; Tykwinski, R. R.; Anderson, H. L. *Org. Lett.* **2012**, *14*, 3424.
(193) Weisbach, N.; Baranova, Z.; Gauthier, S.; Reibenspies, J. H.; Gladysz, J. A. *Chem. Commun.* **2012**, *48*, 7562.
(194) Berná, J.; Crowley, J. D.; Goldup, S. M.; Hänni, K. D.; Lee, A.-L.; Leigh, D. A. *Angew. Chem. Int. Ed.* **2007**, *46*, 5709.
(195) Crowley, J. D.; Hänni, K. D.; Lee, A.-L.; Leigh, D. A. *J. Am. Chem. Soc.* **2007**, *129*, 12092.
(196) Goldup, S. M.; Leigh, D. A.; Lusby, P. J.; McBurney, R. T.; Slawin, A. M. Z. *Angew. Chem. Int. Ed.* **2008**, *47*, 3381.
(197) Aston, P. R.; Glink, P. T.; Stoddart, J. F.; Tasker, P. A.; White, A. J. P.; Williams, D. J. *Chem. Eur. J.* **1996**, *2*, 729.
(198) Martínez-Díaz, M. V.; Spencer, N.; Stoddart, J. F. *Angew. Chem. Int. Ed. Eng.* **1997**, *36*, 1904.
(199) Hsueh, S.-Y.; Cheng, K.-W.; Lai, C.-C.; Chiu, S.-H. *Angew. Chem. Int. Ed.* **2008**, *47*, 4436.
(200) Anelli, P. L.; Spencer, N.; Stoddart, J. F. *J. Am. Chem. Soc.* **1991**, *113*, 5131.
(201) Fang, L.; Olson, M. A.; Benitez, D.; Tkatchouk, E.; Goddard Iii, W. A.; Stoddart, J. F. *Chem. Soc. Rev.* **2010**, *39*, 17.
(202) Ashton, P. R.; Goodnow, T. T.; Kaifer, A. E.; Reddington, M. V.; Slawin, A. M. Z.; Spencer, N.; Stoddart, J. F.; Vicent, C.; Williams, D. J. *Angew. Chem. Int. Ed. Eng.* **1989**, *28*, 1396.
(203) Hunter, C. A. *J. Am. Chem. Soc.* **1992**, *114*, 5303.
(204) Vögtle, F.; Meier, S.; Hoss, R. *Angew. Chem. Int. Ed. Eng.* **1992**, *31*, 1619.
(205) Johnston, A. G.; Leigh, D. A.; Pritchard, R. J.; Deegan, M. D. *Angew. Chem. Int. Ed. Eng.* **1995**, *34*, 1209.
(206) Johnston, A. G.; Leigh, D. A.; Nezhat, L.; Smart, J. P.; Deegan, M. D. *Angew. Chem. Int. Ed. Eng.* **1995**, *34*, 1212.
(207) Tron, A.; Thornton, P. J.; Rocher, M.; Jacquot de Rouville, H.-P.; Desvergne, J.-P.; Kauffmann, B.; Buffeteau, T.; Cavagnat, D.; Tucker, J. H. R.; McClenaghan, N. D. *Org. Lett.* **2014**, *16*, 1358.
(208) Gatti, F. G.; Leigh, D. A.; Nepogodiev, S. A.; Slawin, A. M. Z.; Teat, S. J.; Wong, J. K. Y. *J. Am. Chem. Soc.* **2001**, *123*, 5983.
(209) G. Hamilton, D.; K. M. Sanders, J.; E. Davies, J.; Clegg, W.; J. Teat, S. *Chem. Commun.* **1997**, 897.
(210) Au-Yeung, H. Y.; Pantoş, G. D.; Sanders, J. K. M. *Proc. Natl. Acad. Sci.* **2009**,

106, 10466.
(211) Cougnon, F. B. L.; Au-Yeung, H. Y.; Pantoş, G. D.; Sanders, J. K. M. *J. Am. Chem. Soc.* **2011**, *133*, 3198.
(212) Hübner, G. M.; Gläser, J.; Seel, C.; Vögtle, F. *Angew. Chem. Int. Ed.* **1999**, *38*, 383.
(213) Spence, G. T.; Beer, P. D. *Acc. Chem. Res.* **2012**, *46*, 571.
(214) Caballero, A.; Zapata, F.; Beer, P. D. *Coord. Chem. Rev.* **2013**, *257*, 2434.
(215) Wisner, J. A.; Beer, P. D.; Drew, M. G. B. *Angew. Chem. Int. Ed.* **2001**, *40*, 3606.
(216) Wisner, J. A.; Beer, P. D.; Drew, M. G. B.; Sambrook, M. R. *J. Am. Chem. Soc.* **2002**, *124*, 12469.
(217) Sambrook, M. R.; Beer, P. D.; Wisner, J. A.; Paul, R. L.; Cowley, A. R. *J. Am. Chem. Soc.* **2004**, *126*, 15364.
(218) Evans, N. H.; Serpell, C. J.; Beer, P. D. *Angew. Chem. Int. Ed.* **2011**, *50*, 2507.
(219) Evans, N. H.; Beer, P. D. *Chem. Eur. J.* **2011**, *17*, 10542.
(220) Brown, A.; Beer, P. D. *Dalton Trans.* **2012**, *41*, 118.
(221) Evans, N. H.; Serpell, C. J.; Beer, P. D. *Chem. Commun.* **2011**, *47*, 8775.
(222) Langton, M. J.; Beer, P. D. *Chem. Eur. J.* **2012**, *18*, 14406.
(223) Spence, G. T.; Pitak, M. B.; Beer, P. D. *Chem. Eur. J.* **2012**, *18*, 7100.
(224) White, N. G.; Costa, P. J.; Carvalho, S.; Félix, V.; Beer, P. D. *Chem. Eur. J.* **2013**, *19*, 17751.
(225) Mullen, K. M.; Mercurio, J.; Serpell, C. J.; Beer, P. D. *Angew. Chem. Int. Ed.* **2009**, *48*, 4781.
(226) Kilah, N. L.; Wise, M. D.; Serpell, C. J.; Thompson, A. L.; White, N. G.; Christensen, K. E.; Beer, P. D. *J. Am. Chem. Soc.* **2010**, *132*, 11893.
(227) Caballero, A.; Zapata, F.; White, N. G.; Costa, P. J.; Félix, V.; Beer, P. D. *Angew. Chem. Int. Ed.* **2012**, *51*, 1876.
(228) Serpell, C. J.; Kilah, N. L.; Costa, P. J.; Félix, V.; Beer, P. D. *Angew. Chem. Int. Ed.* **2010**, *49*, 5322.
(229) Caballero, A.; Bennett, S.; Serpell, C. J.; Beer, P. D. *CrystEngComm* **2013**, *15*, 3076.
(230) Tseng, H.-R.; Vignon, S. A.; Stoddart, J. F. *Angew. Chem. Int. Ed.* **2003**, *42*, 1491.
(231) Jiménez, M. C.; Dietrich-Buchecker, C.; Sauvage, J.-P. *Angew. Chem. Int. Ed.* **2000**, *39*, 3284.
(232) Liu, Y.; Flood, A. H.; Bonvallet, P. A.; Vignon, S. A.; Northrop, B. H.; Tseng, H.-R.; Jeppesen, J. O.; Huang, T. J.; Brough, B.; Baller, M.; Magonov, S.; Solares, S. D.; Goddard, W. A.; Ho, C.-M.; Stoddart, J. F. *J. Am. Chem. Soc.* **2005**, *127*, 9745.
(233) Leigh, D. A.; Wong, J. K. Y.; Dehez, F.; Zerbetto, F. *Nature* **2003**, *424*, 174.
(234) Lewandowski, B.; De Bo, G.; Ward, J. W.; Papmeyer, M.; Kuschel, S.; Aldegunde, M. J.; Gramlich, P. M. E.; Heckmann, D.; Goldup, S. M.; D'Souza, D. M.; Fernandes, A. E.; Leigh, D. A. *Science* **2013**, *339*, 189.
(235) Nagawa, Y.; Suga, J.-i.; Hiratani, K.; Koyama, E.; Kanesato, M. *Chem. Commun.* **2005**, 749.
(236) Zhou, W.; Li, J.; He, X.; Li, C.; Lv, J.; Li, Y.; Wang, S.; Liu, H.; Zhu, D. *Chem. Eur. J.* **2008**, *14*, 754.
(237) Langton, M. J.; Beer, P. D. *Acc. Chem. Res.* **2014**.
(238) Evans, N. H.; Beer, P. D. *Org. Biomol. Chem.* **2011**, *9*, 92.
(239) Evans, N. H.; Serpell, C. J.; White, N. G.; Beer, P. D. *Chem. Eur. J.* **2011**, *17*,

12347.
(240) Bayly, S. R.; Gray, T. M.; Chmielewski, M. J.; Davis, J. J.; Beer, P. D. *Chem. Commun.* **2007**, 2234.
(241) Evans, N. H.; Rahman, H.; Leontiev, A. V.; Greenham, N. D.; Orlowski, G. A.; Zeng, Q.; Jacobs, R. M. J.; Serpell, C. J.; Kilah, N. L.; Davis, J. J.; Beer, P. D. *Chem. Sci.* **2012**, *3*, 1080.
(242) Curiel, D.; Beer, P. D. *Chem. Commun.* **2005**, 1909.
(243) Hancock, L. M.; Marchi, E.; Ceroni, P.; Beer, P. D. *Chem. Eur. J.* **2012**, *18*, 11277.
(244) Allain, C.; Beer, P. D.; Faulkner, S.; Jones, M. W.; Kenwright, A. M.; Kilah, N. L.; Knighton, R. C.; Sorensen, T. J.; Tropiano, M. *Chem. Sci.* **2013**, *4*, 489.
(245) Gassensmith, J. J.; Matthys, S.; Lee, J.-J.; Wojcik, A.; Kamat, P. V.; Smith, B. D. *Chem. Eur. J.* **2010**, *16*, 2916.
(246) Raju, M. V. R.; Lin, H.-C. *Org. Lett.* **2013**, *15*, 1274.
(247) Chae, M. K.; Suk, J.-m.; Jeong, K.-S. *Tetrahedron Lett.* **2010**, *51*, 4240.

Chapter 2: Carbazole-Based Anion Receptors

2.1 *Introduction*

Carbazole is an attractive component for incorporation into anion receptor structural frameworks.[1-5] The pyrollic N–H group is a hydrogen bond donor for anion recognition; carbazole is a rigid, preorganised structural scaffold; and its fluorescence properties provide the potential for anion sensing. For example, all of these properties of carbazole were exploited in Sessler's calix[4]pyrrole[2]carbazole macrocycle (**Figure 2-1**), which was shown to preferentially sense acetate over a range of other oxoanions in CH_2Cl_2.[6]

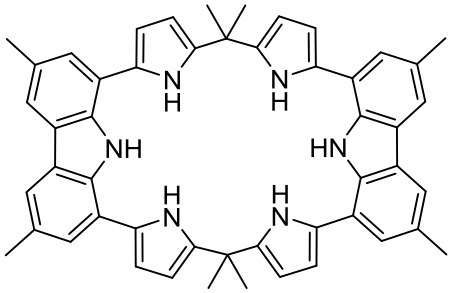


Figure 2-1: Sessler's calix[4]pyrrole[2]carbazole receptor.

As discussed in the previous chapter, neutral triazole and cationic triazolium groups have been utilised as C–H hydrogen bond donor groups in anion host systems reported by Flood[7] (**§1.2.4.2**) and Schubert[8] (**§1.2.4.1**). In addition, the halogen bonding (XB) interaction is beginning to be exploited for anion recognition applications.[9,10]

2.2 *Outline*

This chapter describes the development of new acyclic and interlocked anion receptors incorporating the carbazole motif.

A series of acyclic carbazole-based anion receptors substituted with cationic prototriazolium or halotriazolium (X = Br, I) groups at the 3,6-positions, to promote convergent anion

binding, were targeted (**Figure 2-2a**).

A second carbazole-based anion receptor design, involving triazole substitution at the 1,8-positions, was also devised (**Figure 2-2b**). Such a receptor would combine the pyrrolic N–H donor of the carbazole, as well as the two triazole C–H donors, for cooperative anion binding.

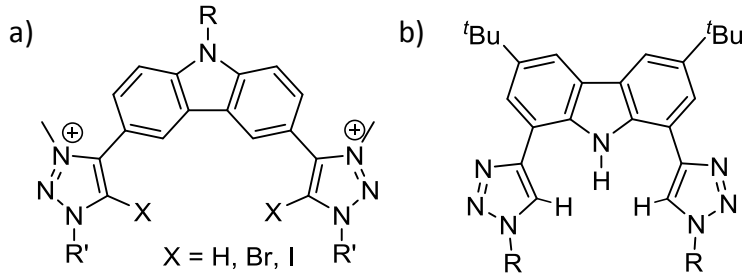


Figure 2-2: The carbazole-based motifs under investigation, **a)** 3,6-bis-triazolium carbazole derivatives; and **b)** 1,8-bis-triazole carbazole.

Having investigated the synthesis and anion coordination properties of these acyclic triazole- and triazolium-functionalised carbazole derivatives, attempts to integrate them into interlocked host systems were undertaken in order to produce receptor systems with enhanced anion selectivity resulting from their unique, constrained three-dimensional binding cavities.

It should be noted that much of the research on the 3,6-bis-triazolium-substituted systems was carried out in collaboration with Benjamin Partridge, a Part II undergraduate student.

2.3 *3,6-Bis-substituted Carbazole Model Systems*

A systematic study of the anion recognition capabilities of a series of acyclic 3,6-bis-triazole carbazole derivatives was undertaken initially, investigating the effects of hydrogen bonding (HB) and halogen bonding (XB) through the attachment of proto-triazolium or halo-triazolium groups, which are connected to the carbazole backbone by the C- or N-terminus,

and varying the triazolium-appended R-group, aryl or alkyl (**Figure 2-3**).

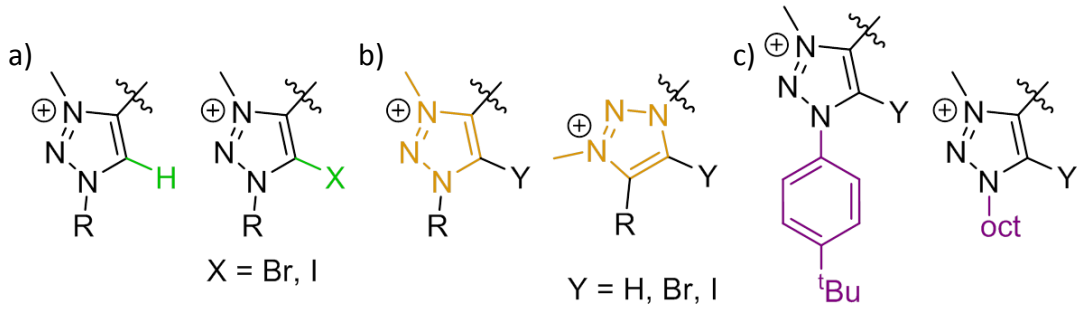
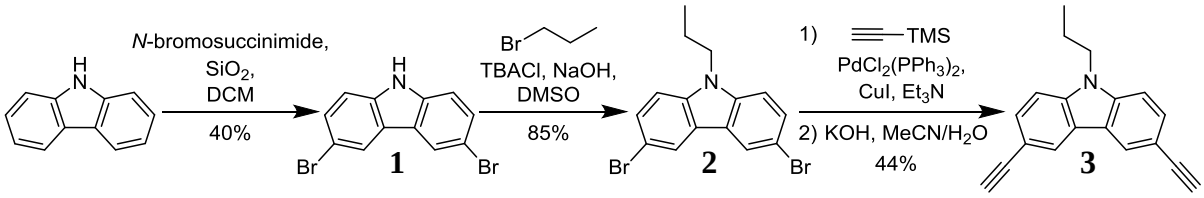


Figure 2-3: The structural properties varied in the study of the acyclic carbazole-containing anion receptor models, **a)** iodo- or proto-triazolium; **b)** C- or N-linked; and **c)** aryl- or alkyl-appended.

2.3.1 *Synthesis of Acyclic Model Receptors*

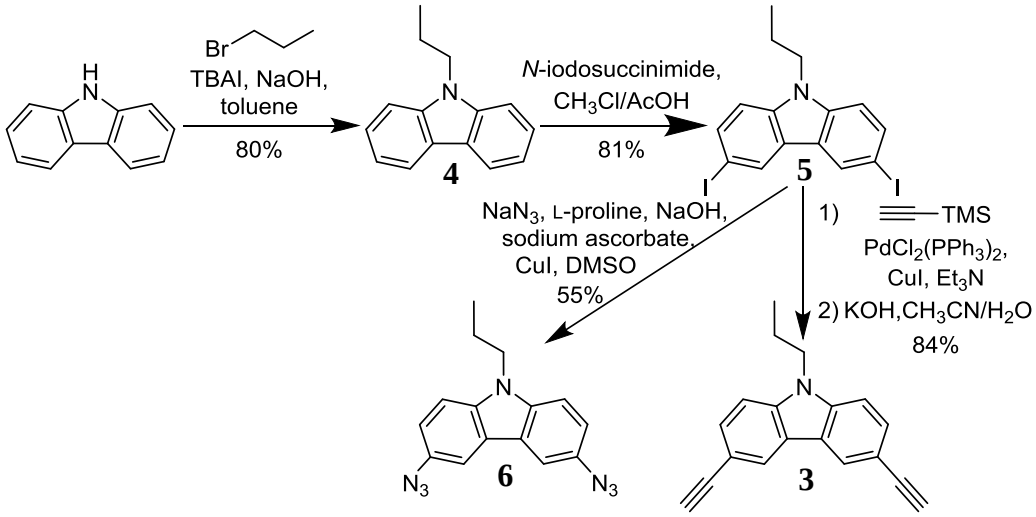
The 3,6-dibromo-substituted carbazole derivative **2** was targeted as a precursor to the 3,6-diethynylcarbazole intermediate compound **3**. The reaction of carbazole with *N*-bromosuccinimide in CH_2Cl_2 afforded 3,6-dibromocarbazole **1** in 40% yield.[11] To avoid competition of anions binding to the pyrrolic N–H hydrogen bond donor and to improve solubility, carbazole **2** was alkylated using *n*-bromopropane in the presence of base in DMSO to form **2** in 85% yield.[12] This compound was then reacted with TMS-acetylene under Sonogashira conditions,[13] followed by removal of the TMS group using KOH, to form bis-alkyne **3** in 44% overall yield for the two steps (**Scheme 2-1**).



Scheme 2-1: Synthesis of 3,6-diethynylcarbazole **3**.

Unfortunately, bromide proved not to be a sufficiently good leaving group for the preparation

of 3,6-diazidocarbazole. Attempts to form this compound by reaction of the bis-bromo precursor with NaN_3 in the presence of CuI, L-proline, NaOH and sodium ascorbate in DMSO,[14] only gave the mono-azide substituted product. The corresponding 3,6-diiodo substituted derivative **5** was therefore prepared (**Scheme 2-2**). In this case, the pyrollic nitrogen was alkylated first using *n*-bromopropane,[15] giving *N*-propylcarbazole **4** in 80% yield. This compound was then treated with *N*-iodosuccinimide in a $CHCl_3/AcOH_{(glacial)}$ solvent mixture,[15] producing 3,6-diiodocarbazole **5** in 81% yield. To make the bis-azide substituted compound, **5** was reacted under the same conditions as used for the bis-bromo substituted precursor,[14] to give bis-azide **6** in 55% yield. This material proved to be highly unstable to light, and necessitated its immediate use in subsequent triazole-forming reactions (*vide infra*).

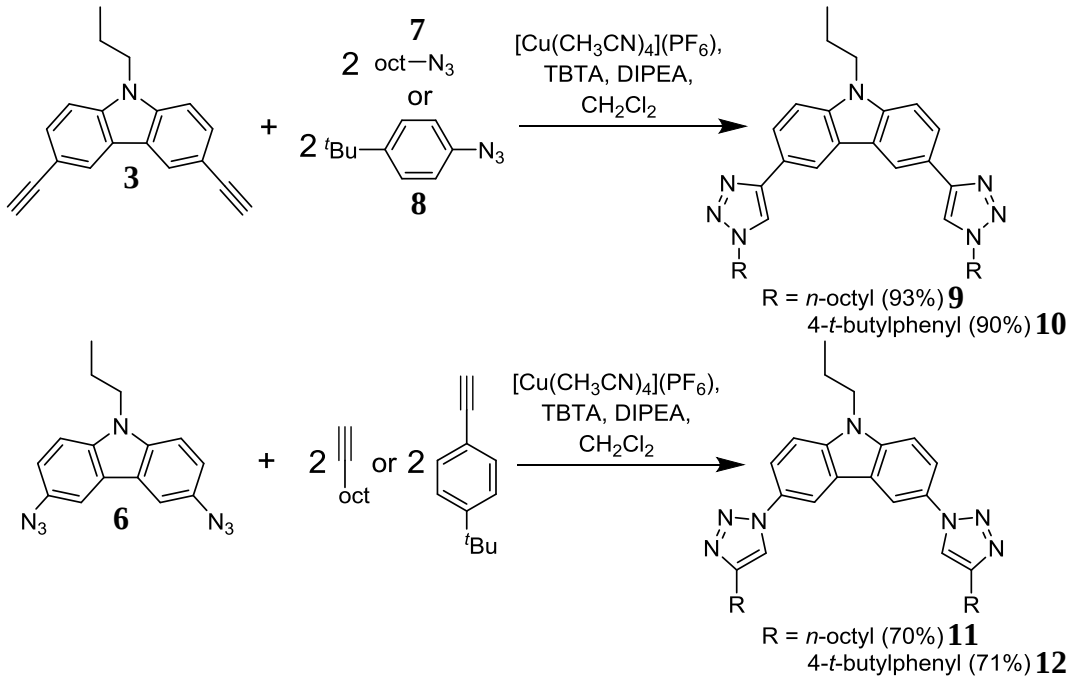


Scheme 2-2: Synthesis of diazidocarbazole **6** and diethynylcarbazole **3**.

Iodinated aromatic compounds are known to take part in Sonogashira couplings, with an activity that can be superior to their brominated analogues.[16] Compound **5** was reacted with two equivalents of TMS-acetylene under Songashira conditions, to form 3,6-diethynyl-carbazole **3** in an improved yield of 84% (**Scheme 2-2**).

2.3.1.1 Prototriazole Receptor Precursors

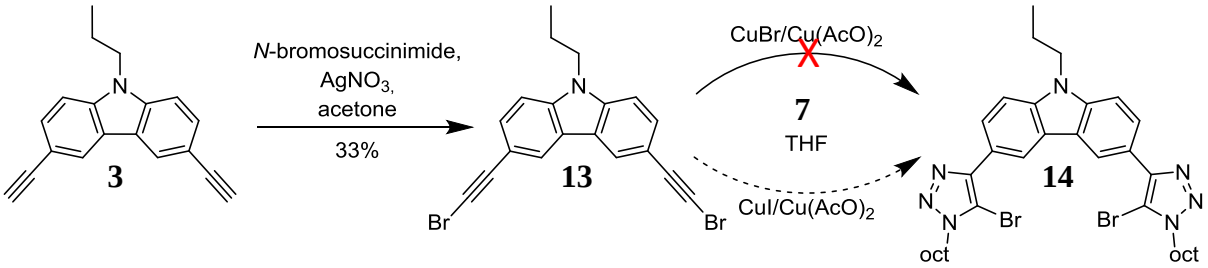
The C-linked prototriazole precursors **9**–**12** were synthesised using Cu(I)-catalysed azide–alkyne cycloaddition (CuAAC) reactions (**Scheme 2-3**). Bis-alkyne **3** was treated with two equivalents of either *n*-octyl azide[17] **7** (for the alkyl-substituted precursor), or 1-(*tert*-butyl)-4-azidobenzene[18] **8** (for the aryl-substituted precursor), in the presence of $[Cu(CH_3CN)_4](PF_6)$, TBTA and DIPEA in CH_2Cl_2,[19] giving the C-linked bis-triazole products **9** and **10**, in 93% and 90% respective yields. The corresponding N-linked prototriazole precursors were made using an analogous synthetic procedure: bis-azide **6** was reacted with two equivalents of either 1-decyne (for the alkyl-substituted compound), or 1-(*tert*-butyl)-4-ethynylbenzene (for the aryl-substituted compound), under the same CuAAC conditions as for the C-linked prototriazole reactions, to afford the N-linked bis-triazole products **11** and **12** in good yields.



Scheme 2-3: Synthesis of bis-triazole carbazole precursors **9**–**12**.

2.3.1.2 Bromotriazole Receptor Precursors

In an initial step toward preparing halogen bonding triazole-functionalised carbazole analogues, attempts were made to synthesise a bis-bromotriazole carbazole precursor. Diethynylcarbazole **3** was reacted with *N*-bromosuccinimide in the presence of $AgNO_3$ in acetone in the dark,[20] giving bis(bromoethynyl)carbazole **13** in 33% yield. In an initial attempt to form the bromotriazole, **13** was treated with two equivalents of *n*-octyl azide **7** in the presence of CuBr and $Cu(AcO)_2$ in THF.[21] However, no evidence of bromotriazole formation was observed by mass spectrometry analysis after two weeks. With the understanding that CuBr can have a lower catalytic activity than CuI,[21] the same reaction between **13** and *n*-octyl azide **7** was attempted using CuI and $Cu(AcO)_2$ in THF (**Scheme 2-4**). This reaction did give some bromotriazole product **14**, however, it was contaminated with significant quantities of iodotriazole-containing side-products resulting from halogen exchange, an observation noted in the literature.[21] The impurities could not be separated, and as a consequence the synthesis of iodotriazole systems was targeted instead.



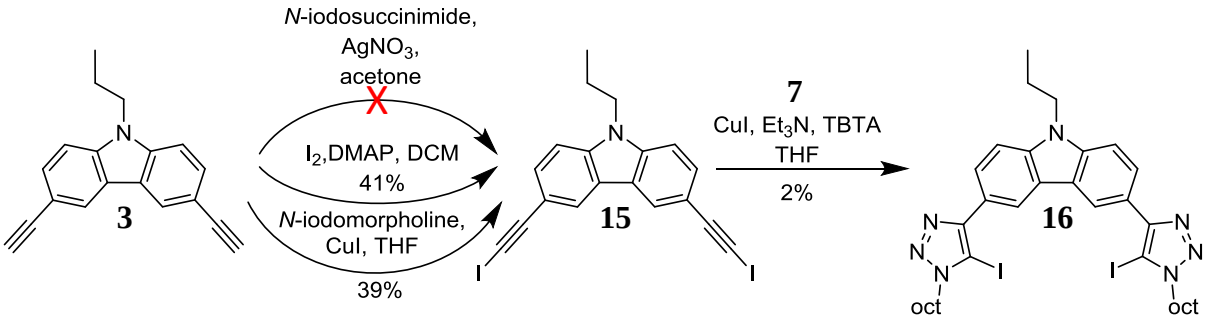
Scheme 2-4: Attempted synthesis of bis-bromotriazole carbazole **14**.

2.3.1.3 Iodotriazole Receptor Precursors

The investigations into the synthesis of bis(iodotriazole)carbazole systems encountered new challenges (**Scheme 2-5**). A common route to form iodotriazoles requires the corresponding iodoalkyne as the precursor,[22] and initially the synthesis of 3,6-bis(iodoethynyl)carbazole **15**

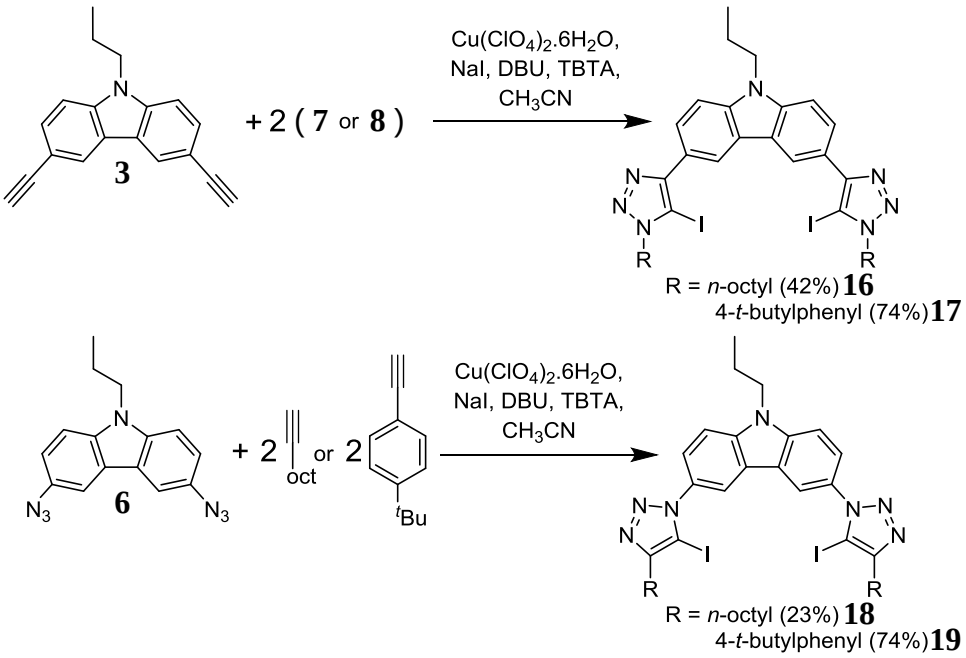
was explored. Three different synthetic methods to produce this compound were undertaken. The first method involved reacting the protoalkyne precursor **3** with *N*-iodosuccinimide in the presence of $AgNO_3$ in acetone in the dark.[20] Unfortunately, this method did not produce the desired product. The second method reacted the protoalkyne precursor **3** with molecular iodine, in the presence of DMAP under reflux in CH_2Cl_2 for 6 h,[23] and successfully produced the iodoalkyne product **15** in 41% yield after column chromatographic purification. However, the iodoalkyne product proved to be severely light-sensitive, readily decomposing to the protoalkyne form, which was a problem during the lengthy chromatographic purification procedure. The third method involved reaction of **3** with *N*-iodomorpholine in the presence of CuI in THF[22] producing the iodoalkyne product **15** in 39% yield, of sufficient purity not to require column chromatography.

Although an effective procedure had been found to form the iodoalkyne **15**, subsequent iodotriazole synthesis was achieved in poor yields. Using the conditions originally reported by Sharpless,[22] reaction of iodoalkyne **15** with two equivalents of *n*-octyl azide **7** in the presence of CuI, Et_3N and TBTA in THF in the dark gave the desired bis-iodotriazole carbazole **16** in only 2% isolated yield, with significant quantities of prototriazole side-product, and the protoalkyne decomposition product of the starting material, also observed.



Scheme 2-5: Synthesis of bis-iodotriazole carbazole *via* the bis-iodoalkyne precursor.

Fortunately, during the time of these synthetic investigations, Brotherton and co-workers reported a one-pot procedure to synthesise iodotriazoles from protoalkyne precursors, removing the necessity of isolation of an iodoalkyne intermediate.[24] This CuAAC reaction between an alkyne and azide takes place in the presence of two equivalents of $Cu(ClO_4)_2 \cdot 6H_2O$, four equivalents of NaI, one equivalent of DBU or Et_3N as a base, and a catalytic amount of TBTA, in either CH_3CN or THF. The NaI generates the triiodide anion I_3^- *in situ*, which reduces Cu(II) to Cu(I), the necessary oxidation state to catalyse the cycloaddition reaction. DBU acts as a base to deprotonate the alkyne, and the Cu(I)-triazolide intermediate is iodinated by the I_3^-, resulting in formation of the iodotriazole. Please note that throughout the remainder of this thesis, this synthetic procedure will henceforth be referred to as the 'Brotherton one-pot click' reaction.



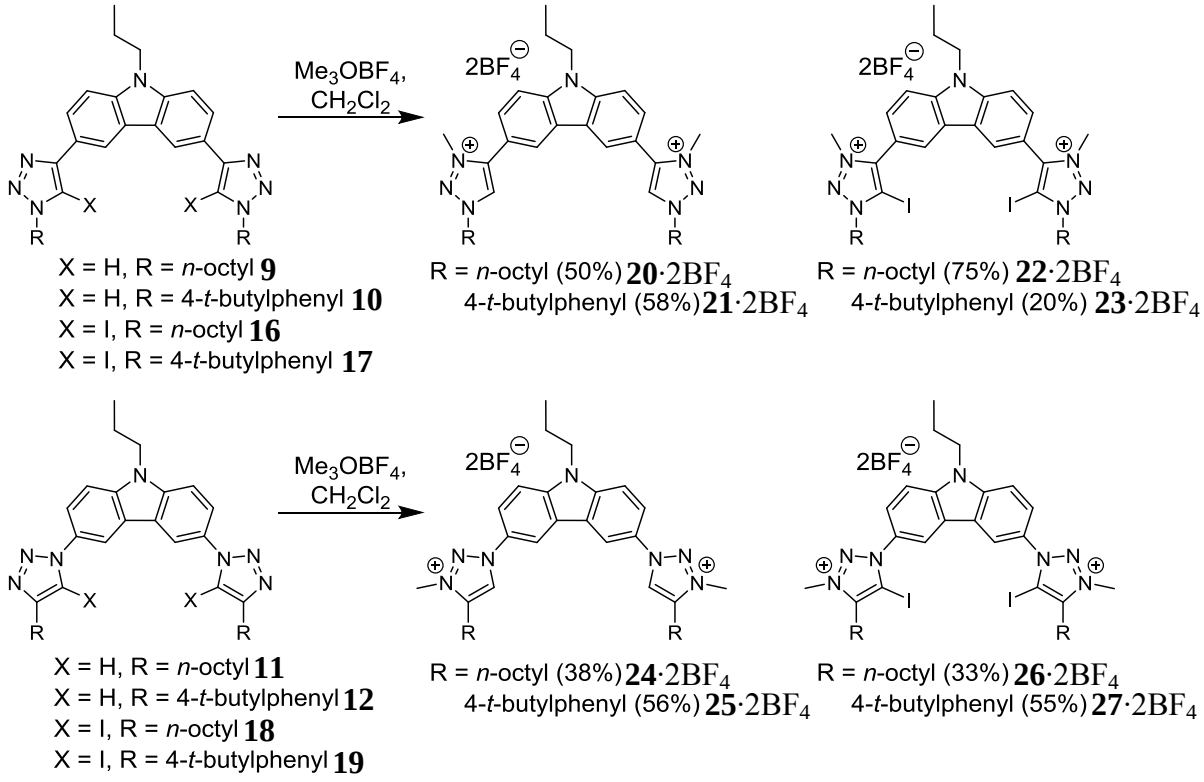
Scheme 2-6: Synthesis of bis-iodotriazole carbazole precursors **16**–**19**.

After optimisation of the reaction conditions to avoid any unwanted prototriazole side-product, this procedure was successfully implemented to produce the iodotriazole-

functionalised carbazole systems, using the same starting materials as the prototriazole-containing systems described above. For the C-linked iodotriazole precursors, diethynylcarbazole **3** was reacted with two equivalents of the appropriate azide in the presence of the Brotherton one-pot reagents, giving the iodotriazole products **16** and **17** in 42% and 74% respective yields. For the N-linked precursors, diazidocarbazole **6** was reacted with the appropriate alkyne, under analogous conditions, affording the iodotriazole products **18** (23%) and **19** (74%) (**Scheme 2-6**).

2.3.1.4 Prototriazolium and Iodotriazolium Receptors

To synthesise the acyclic proto- and iodo-triazolium receptors, the neutral triazole precursors were methylated using two equivalents of $Me_3O{\cdot}BF_4$ in CH_2Cl_2, giving receptors **20**·2BF_4–**27**·2BF_4 (**Scheme 2-7**).



Scheme 2-7: Synthesis of carbazole-based anion receptors **20**·2BF_4–**27**·2BF_4.

2.3.2 *Anion Binding Properties*

The anion recognition properties of the eight acyclic receptors **20**·2BF_4–**27**·2BF_4 were studied *via* ^{1}H NMR titration experiments. The association strengths of all receptors with chloride, bromide, iodide and sulfate anions were investigated, and the prototriazolium-containing receptors were also tested with nitrate. In all cases, anions were added as tetra-*n*-butylammonium (TBA) salts.

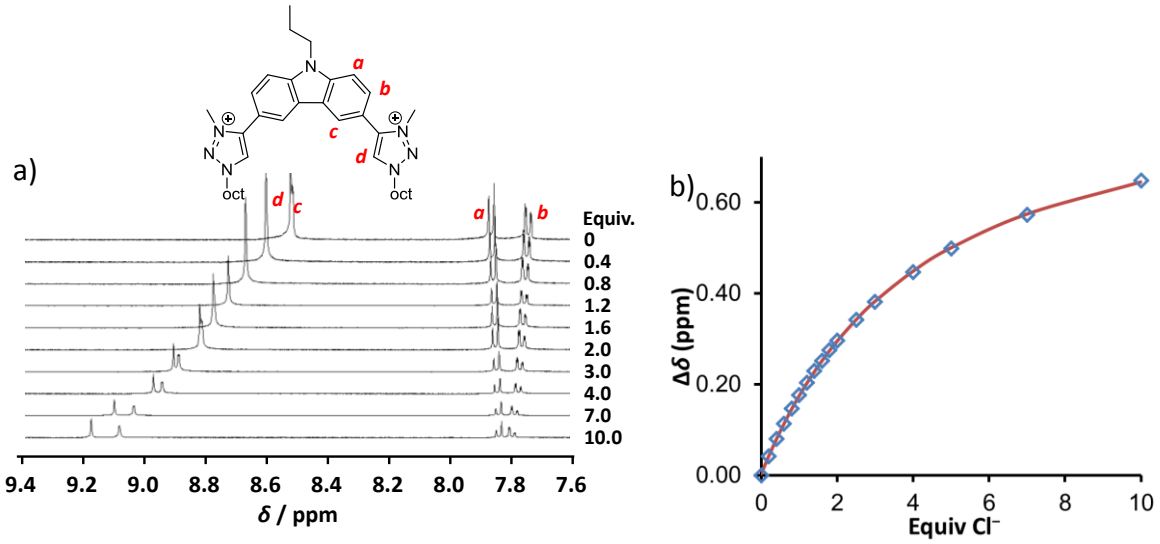


Figure 2-4: a) Truncated ^{1}H NMR spectra of **20**·2BF_4 upon addition of TBA·Cl; and **b)** the experimental titration data (points) following proton *d*, and the fitted binding isotherm (line) (CD_3CN, 293 K, 500 MHz).

Anion binding typically resulted in significant downfield shifts of the respective receptor's triazolium and carbazole aromatic proton signals, which is indicative of favourable anion–hydrogen bonding interactions. The rate of exchange between complexed and uncomplexed species was observed to be fast on the NMR timescale in all cases, resulting in a single time-averaged proton resonance. This is exemplified by the addition of Cl^- to the HB receptor **20**·2BF_4 in CD_3CN (**Figure 2-4a**), which results in a significant downfield shift of the triazolium proton *d* and internal carbazole proton *c*, which are directly involved in anion

binding.

WinEQNMR2[25] is a computer program which uses a least-squares refinement protocol to fit a specific host–guest stoichiometric binding model to the experimental changes in the proton chemical shifts, determining an association constant for the host–guest complexation process. WinEQNMR2 analysis of the chemical shift data of receptor $\mathbf{20}^{2+}$ triazolium proton *d* (**Figure 2-4b**) determined a 1:1 stoichiometric association constant for binding chloride of $K_a = 141(15)\ \text{M}^{-1}$.

2.3.2.1 Anion Recognition Properties of Prototriazolium Receptors

For the prototriazolium receptors $\mathbf{20}^{2+}$, $\mathbf{21}^{2+}$, $\mathbf{24}^{2+}$ and $\mathbf{25}^{2+}$, ^{1}H NMR anion titration experiments were conducted in CD_3CN. WinEQNMR2 analysis of the titration data, monitoring the triazolium proton chemical shift (**Figure 2-5**), determined 1:1 stoichiometric anion association constants, which are presented in **Table 2-1**.

Table 2-1: Association constants, K_a (M^{-1}), obtained from ^{1}H NMR titrations, for prototriazolium-containing model receptors with different anions. Errors are given in parentheses (CD_3CN, 293 K, 500 MHz).

	$\mathbf{20}^{2+}$ C-linked, alkyl	$\mathbf{21}^{2+}$ C-linked, aryl	$\mathbf{24}^{2+}$ N-linked, alkyl	$\mathbf{25}^{2+}$ N-linked, aryl
Cl^-	141(15)	430(40)	198(9)	313(40)
Br^-	200(5)	337(7)	274(5)	287(7)
I^-	161(4)	214(6)	233(5)	310(20)
NO_3^-	121(2)	295(14)	244(1)	213(6)
SO_4^{2-} [a]	341(35)	1450(50)	282(10)	1030(130)

[a] Titrations conducted in 10% D_2O/d_6-DMSO. K_a values were determined by monitoring the triazolium proton resonance.

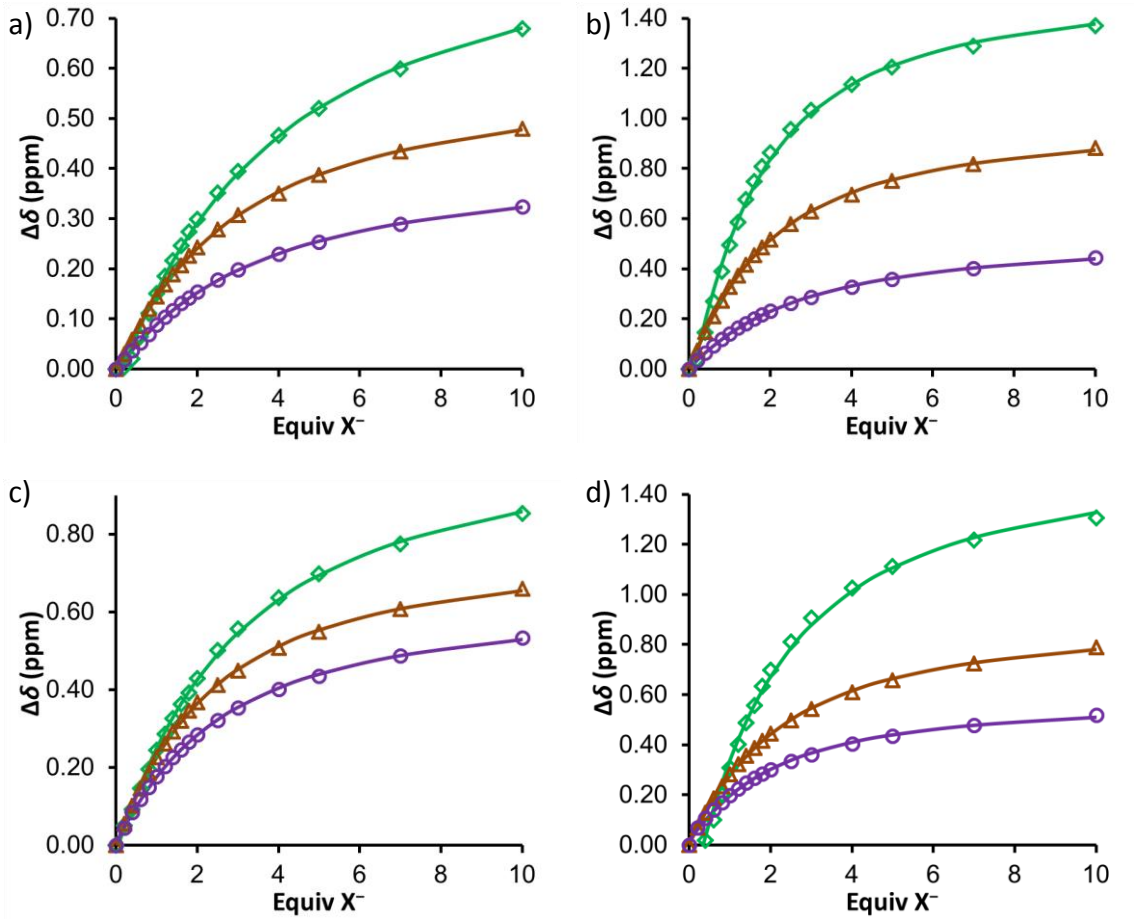


Figure 2-5: Experimental titration data (points) and fitted binding isotherms (lines) for receptors **a**) **20**·2BF_4; **b) 21**·2BF_4; **c) 24**·2BF_4; and **d) 25**·2BF_4 following the triazolium proton, upon addition of ◇ Cl^-, △ Br^- and ○ I^- (CD_3CN, 293 K, 500 MHz).

All the receptors bind halides and the oxoanions, nitrate and sulfate. The data in **Table 2-1** indicate that the aryl-appended receptors $\mathbf{21}^{2+}$ and $\mathbf{25}^{2+}$ form slightly stronger complexes with almost all anions studied, compared to alkyl-appended receptors $\mathbf{20}^{2+}$ and $\mathbf{24}^{2+}$. This result is consistent with previously-reported anion binding behaviour of triazole-based receptors,[26] and may be due to greater preorganisation of the binding cavity in the aryl-appended receptors. Polarised aryl C–H groups can also take part in HB interactions with the anion guest. Indeed, in addition to the downfield shift of the triazolium proton *d* and inner carbazole proton *c*, a downfield perturbation of phenyl proton signal *e* of aryl-appended receptor $\mathbf{21}^{2+}$ is

observed upon addition of Cl^- (**Figure 2-6**).

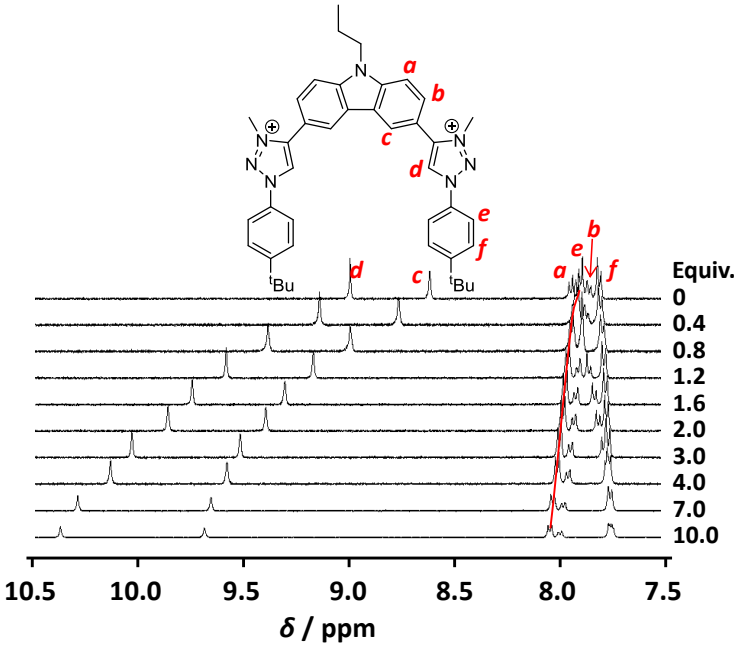


Figure 2-6: Truncated ^{1}H NMR spectra of **21**·2BF_4 upon addition of TBA·Cl (CD_3CN, 293 K, 500 MHz).

Somewhat surprisingly, **Table 2-1** reveals that the receptors exhibit no significant binding preferences between the monoanionic guests, although the alkyl-appended receptors $\mathbf{20}^{2+}$ and $\mathbf{24}^{2+}$ appear to follow a modest halide selectivity trend of $Br^- > I^- > Cl^-$. Conversely, C-linked aryl receptor $\mathbf{21}^{2+}$ demonstrated the trend $Cl^- > Br^- > I^-$, while the N-linked aryl receptor $\mathbf{25}^{2+}$ showed a negligible difference in halide binding strengths. The nitrate anion was also bound with comparable strength to the halides. While there do appear to be minor differences in halide anion preferences between the C-linked and N-linked receptors, no general selectivity trends can be drawn from these results.

As expected on the basis of charge effects, sulfate is bound strongly even in the competitive solvent mixture of 10% D_2O/d_6-DMSO. The dominant driving force for this strong association is the Coulombic attraction of a dicationic receptor to a dianionic guest. It is

noteworthy that the aryl-appended receptors $\mathbf{21}^{2+}$ and $\mathbf{25}^{2+}$ exhibit an affinity for sulfate approximately four-fold larger than their alkyl-appended analogues, suggesting that supplementary aryl C–H hydrogen bonding interactions are contributing significantly to binding this oxodianion guest (**Figure 2-7**).

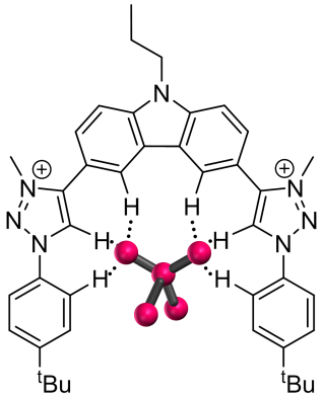


Figure 2-7: Possible binding behaviour of receptor $\mathbf{21}^{2+}$ with SO_4^{2-}.

2.3.2.2 Anion Recognition Properties of Iodotriazolium Receptors

While quantitative anion binding information was obtained from the prototriazolium receptor systems by monitoring the triazolium proton, ^{1}H NMR titration analysis of the anion binding properties of iodotriazolium systems relied on following changes in the proton signals adjacent to the iodotriazolium units. Hence, anion association constants for the iodotriazolium-containing receptors $\mathbf{22}^{2+}$, $\mathbf{23}^{2+}$, $\mathbf{26}^{2+}$ and $\mathbf{27}^{2+}$ were determined from WinEQNMR2 analysis of the internal carbazole proton *c* titration data (**Figure 2-8**).

Preliminary ^{1}H NMR titration experiments were conducted between receptor $\mathbf{22}^{2+}$ and Cl^- and Br^- in CD_3CN (**Figure 2-8a**). As shown in **Figure 2-8b**, addition of Cl^- results in a significant downfield shift of internal carbazole proton *c* until ~1 equivalent of anion, which is indicative of a strong 1:1 stoichiometric association. Upon further addition of anion the signal shifts back upfield, which suggests a significant 1:2 stoichiometric host:guest binding

component. In order to determine quantitative association constant data, further studies were conducted in the more competitive solvent, d_6-DMSO.

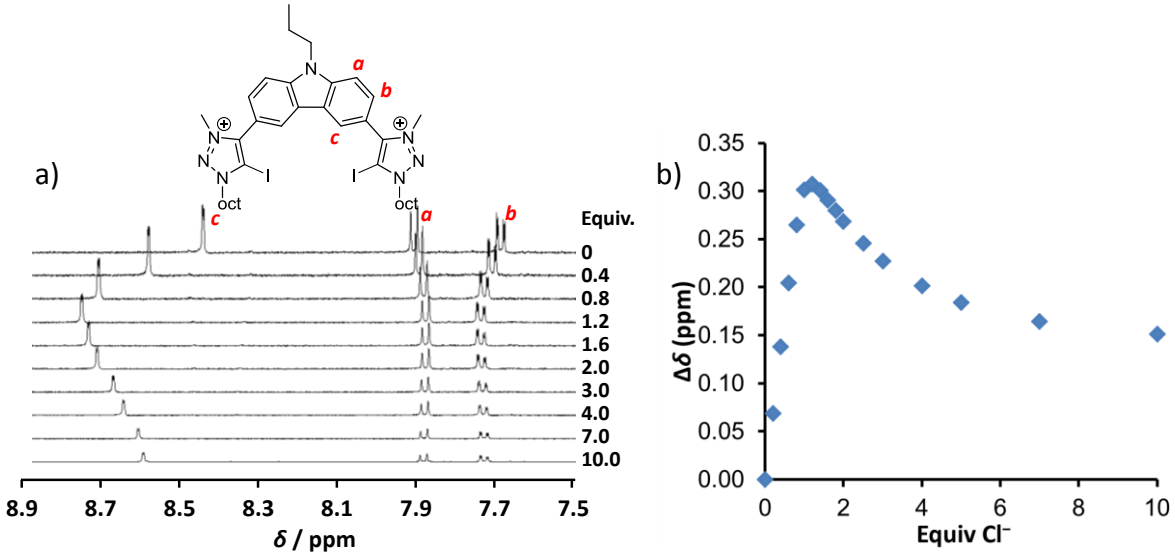


Figure 2-8: a) Truncated ^{1}H NMR spectra of **22**·2BF$_4$ upon addition of TBA·Cl; and **b)** the experimental titration data (points) following internal carbazole proton *c* (CD_3CN, 293 K, 500 MHz).

Association constants could be obtained for Br^- and I^- in d_6-DMSO, while Cl^- was too strong and required the more competitive 5% D_2O/d_6-DMSO solvent mixture, and SO_4^{2-} was studied in 10% D_2O/d_6-DMSO. For comparison, a plot of the binding curves of **26**$^{2+}$ upon addition of the halides in d_6-DMSO is shown in **Figure 2-9**.

Table 2-2: Association constants, K_a (M^{-1}), obtained from ^{1}H NMR titrations, for iodotriazolium-containing model receptors with different anions. Errors are given in parentheses (d_6-DMSO, 293 K, 500 MHz).

	22^{2+} C-linked, alkyl	**23**$^{2+}$ C-linked, aryl	**26**$^{2+}$ N-linked, alkyl	**27**$^{2+}$ N-linked, aryl
Cl^- [a]	217(11)	332(2)	341(26)	303(1)
Br^-	567(4)	893(4)	367(31)	900(70)
I^-	115(2)	254(3)	99(1)	222(1)
SO_4^{2-} [b]	348(8)	493(10)	363(13)	652(19)

[a] Titrations conducted in 5% D_2O/d_6-DMSO; [b] Titrations conducted in 10% D_2O/d_6-DMSO. K_a values were determined by monitoring the internal carbazole proton resonance.

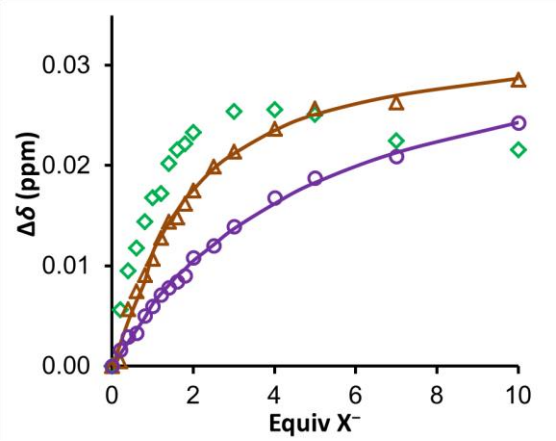


Figure 2-9: Experimental titration data (points) and fitted binding isotherms (lines) for receptor $\mathbf{26}^{2+}$ monitoring internal carbazole proton *c*, upon addition of ◇ Cl^-, △ Br^- and ○ I^- (d_6-DMSO, 293 K, 500 MHz). The binding behaviour of Cl^- was too strong to be accurately modelled.

In stark contrast to the HB prototriazolium receptors, the iodotriazolium receptors show clear selectivity trends which are consistent for all model systems: $SO_4^{2-} > Cl^- > Br^- > I^-$. The marked selectivity between the halides may reflect the increased potency of XB over HB for these anions, and the more efficient host–guest size complementarity of the respective XB iodotriazolium receptor.

There are only minor differences in the binding behaviour of the C-linked and N-linked receptors, and no general trends can be inferred from the data. However, similar to their HB analogues, the aryl-substituted receptors $\mathbf{23}^{2+}$ and $\mathbf{27}^{2+}$ generally bind more strongly than the alkyl-substituted receptors, especially for Br^-, I^- and SO_4^{2-}. It is possible that these anions are large enough to also interact with the acidic aromatic protons within the receptor cavity, which would enhance the binding affinity of the receptor for these anions.

Although the halides are bound significantly more strongly by the XB receptors compared to their HB counterparts, it is interesting to note that the strongest binding of sulfate is observed in the aryl-appended prototriazolium receptors $\mathbf{21}^{2+}$ and $\mathbf{25}^{2+}$, implying that the binding

cavities in these molecules are complementary for this anion.

In summary, the XB receptors importantly exhibited a far superior binding affinity for the halides, compared to the HB receptors, however, sulfate was bound most strongly by the HB receptors $\mathbf{21}^{2+}$ and $\mathbf{25}^{2+}$. The halide selectivity trend of $Cl^- > Br^- > I^-$ was consistent for all XB receptors. The aryl-appended receptors showed a minor increase in the binding strength of the receptors compared to the alkyl-appended analogues, and while there were minor differences in the anion binding affinities of the C-linked and N-linked receptors, no general trends could be established.

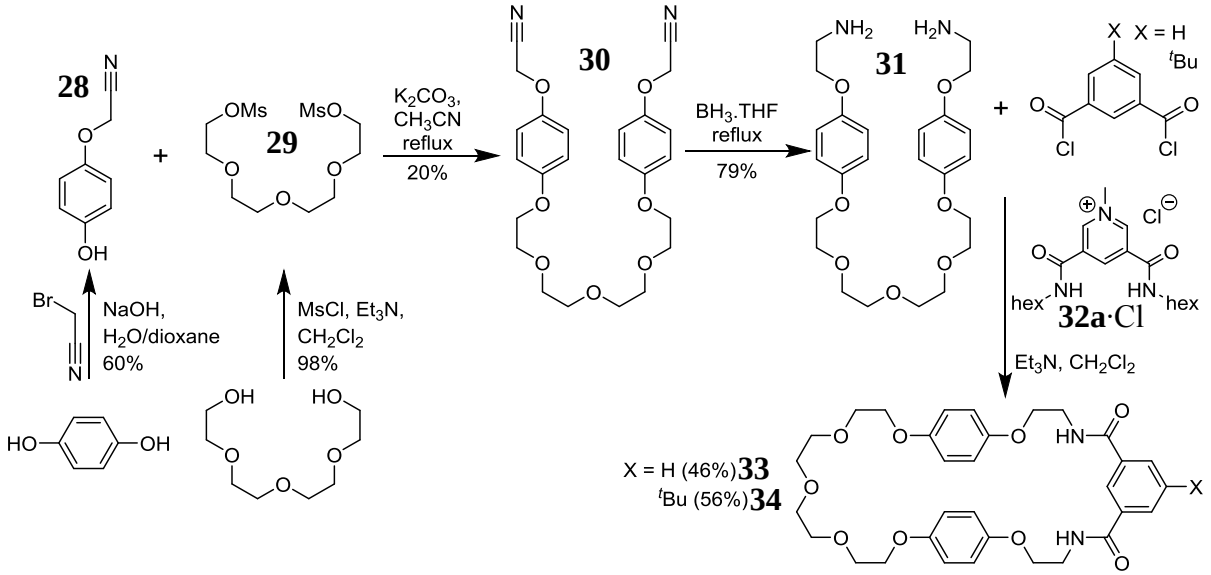
2.4 *Interpenetrated and Interlocked Molecules*

2.4.1 *Pseudorotaxane Assembly Investigations*

Having demonstrated the XB and HB acyclic triazolium carbazole receptors to be capable of recognising anions, the integration of such motifs into interlocked host structures was undertaken. The formation of an anion-templated pseudorotaxane assembly between a bis-iodotriazolium carbazole-based thread, and an isophthalamide-containing macrocycle, was studied initially.

The macrocycle synthesis was performed according to a literature procedure,[27] and is shown in **Scheme 2-8**. Hydroquinone was first reacted with bromoacetonitrile under basic conditions, to give the mono-subsituted hydroquinone **28** in 60% yield. Tetraethylene glycol was reacted with mesyl chloride to give the mesylated polyether **29** in near-quantitative yield. The reaction of **28** and **29** in the presence of K_2CO_3 in CH_3CN gave the bis-nitrile intermediate **30** (20% yield), which was reduced using borane in THF to form the bis-amine precursor **31** (79% yield). A condensation reaction between **31** and an isophthaloyl

dichloride derivative, in the presence of 3,5-bis(hexylamide)pyridinium chloride template **32a**·Cl,[28] afforded the target isophthalamide macrocycles **33** and **34** in 46% and 56% respective yields.



Scheme 2-8: Synthesis of isophthalamide-containing macrocycles **33** and **34**.[27]

A qualitative ^{1}H NMR pseudorotaxane assembly experiment was conducted, by mixing equimolar amounts of thread **22**·2BF$_4$, macrocycle **33** and TBA·Cl in d_6-acetone. As shown in the ^{1}H NMR spectra in **Figure 2-10**, there is a significant upfield shift and splitting of the hydroquinone proton peaks *5* and *6* of the macrocycle. This is diagnostic of interpenetration, and is due to favourable aromatic donor–acceptor interactions between the electron-rich hydroquinone units of the macrocycle, and the electron-deficient triazolium motifs of the thread.

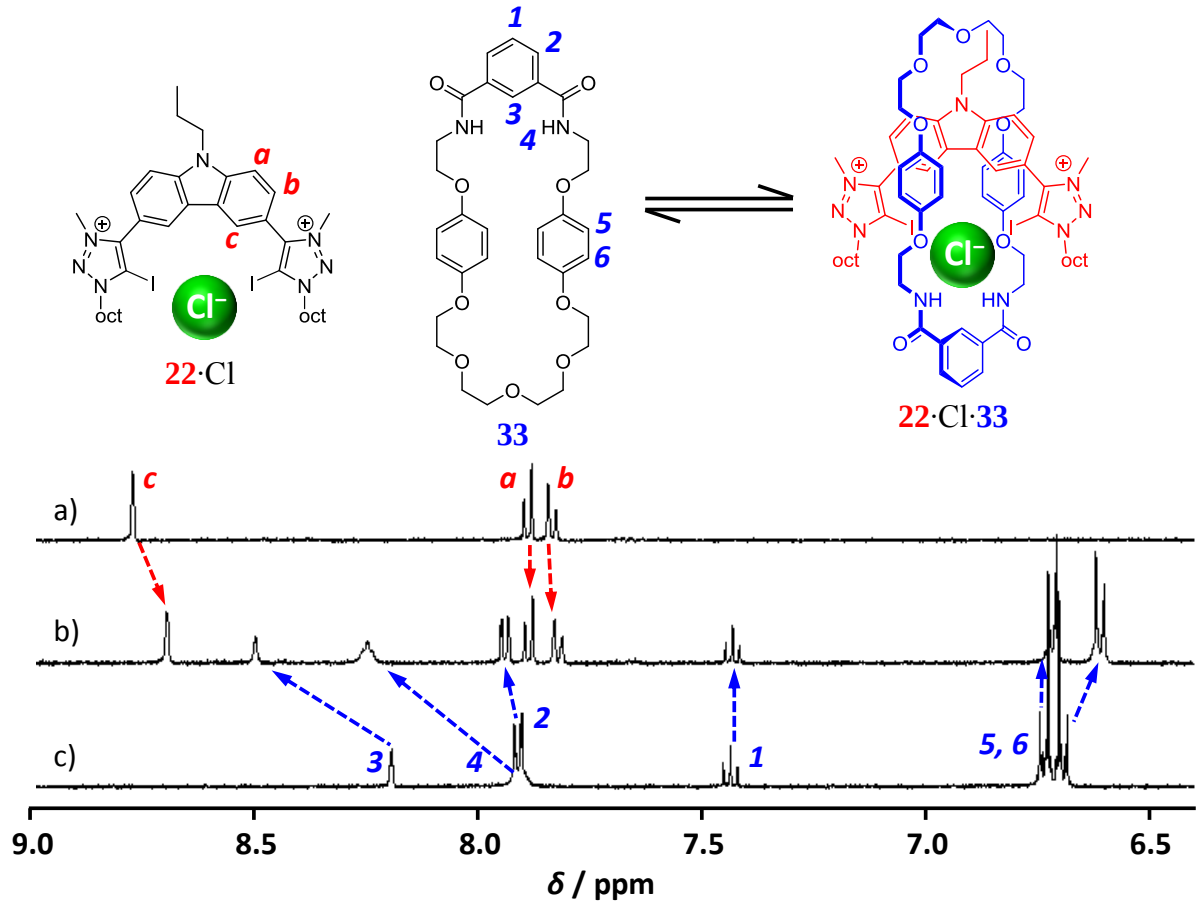


Figure 2-10: ^{1}H NMR pseudorotaxane study of **a)** carbazole-based thread $\mathbf{22}^{2+}$**,** and **c)** isophthalamide-containing macrocycle **33**, to form **b)** an interpenetrated assembly templated with Cl^{-} (d_6-acetone, 293 K, 500 MHz).

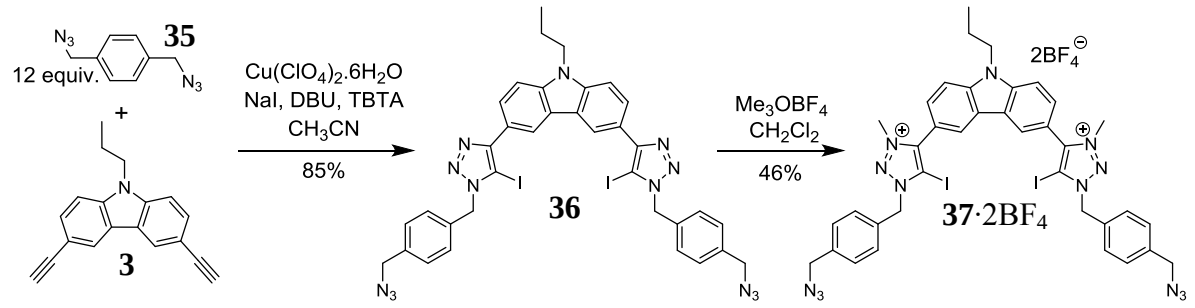
The thread internal carbazole proton *c* also shifts upfield, as the HB interaction with the chloride is weakened, due to 'sharing' of the anion with the macrocycle. Conversely, the HB interactions between protons *3* and *4* of the isophthalamide macrocycle and the halide anion result in significant downfield shifts of these proton resonances.

2.4.2 *Attempted Rotaxane Synthesis by Stoppering*

Encouraged by the qualitative ^{1}H NMR chloride-templated pseudorotaxane assembly observations above, attempts were made to construct a rotaxane containing a bis-

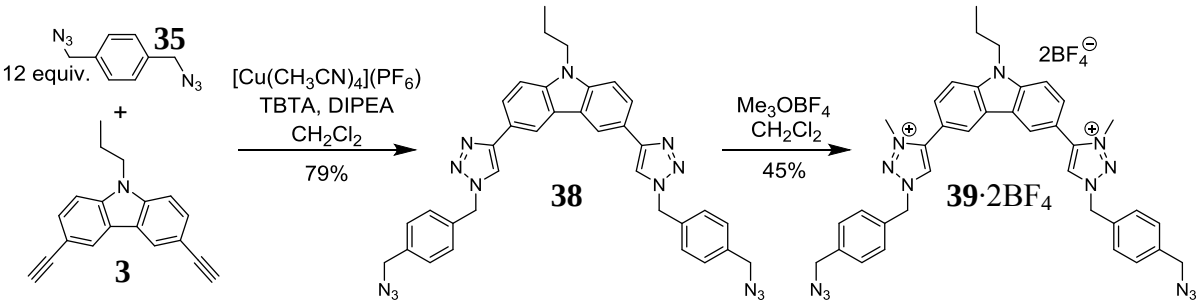
iodotriazolium carbazole axle and isophthalamide macrocycle components. Initial attempts were undertaken using a CuAAC (click) stoppering synthetic methodology via a bis-azide functionalised axle precursor which, following formation of the pseudorotaxane, would be stoppered with bulky alkyne-appended terphenyl groups.

3,6-Diethynylcarbazole **3** was reacted with an excess of 1,4-bis(azidomethyl)benzene **35**, under the Brotherton one-pot click conditions in CH_3CN, to afford bis-azide-appended bis-iodotriazole **36** in 85% yield. Methylation using $Me_3O{\cdot}BF_4$ gave bis-iodotriazolium compound **37** in 46% yield (**Scheme 2-9**).



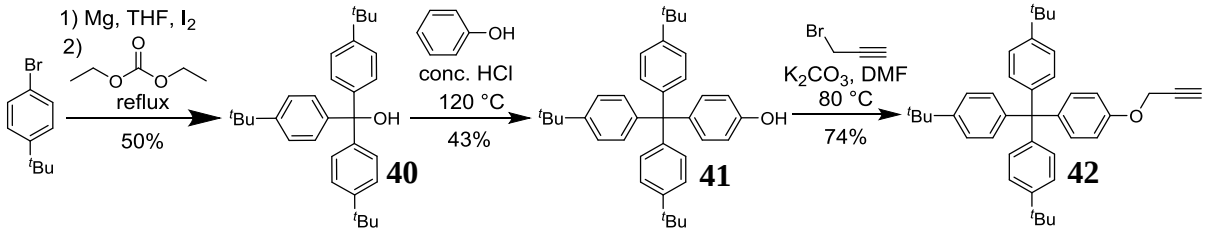
Scheme 2-9: Synthesis of bis-azide-appended axle precursor **37**.

The corresponding HB bis-azide-appended bis-triazolium derivative **39** was prepared similarly using the catalyst $[Cu(CH_3CN)_4](PF_6)$, TBTA and DIPEA in CH_2Cl_2, followed by methylation (**Scheme 2-10**).



Scheme 2-10: Synthesis of bis-azide-appended axle precursor **39**.

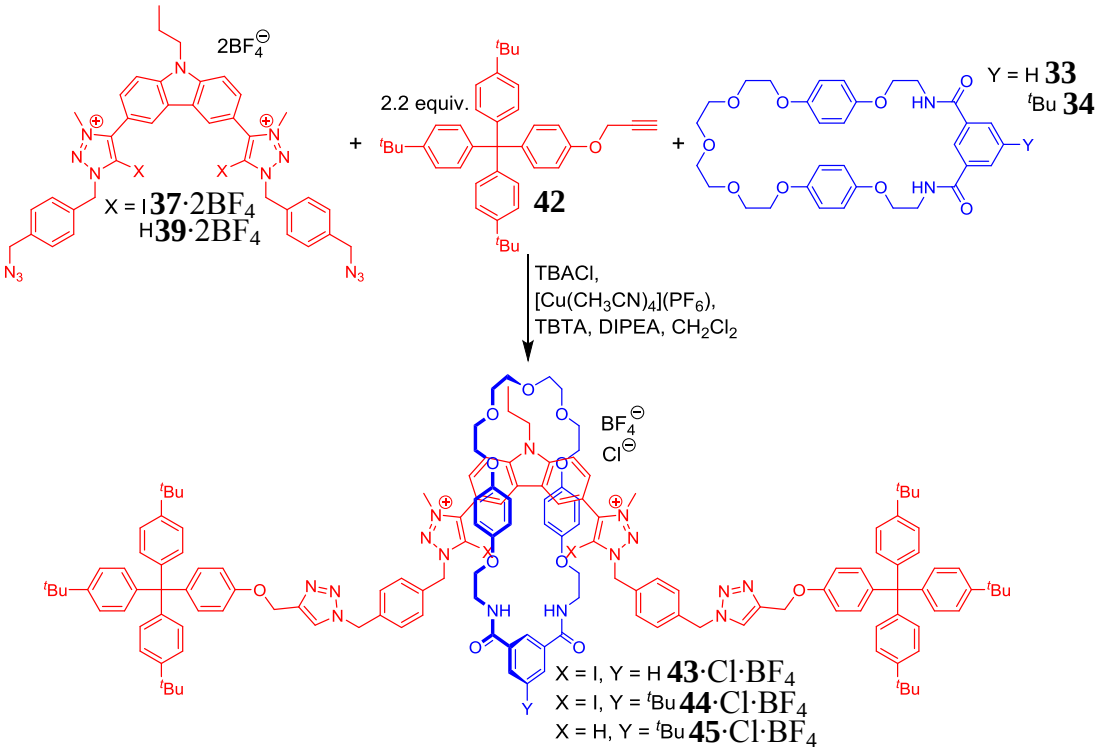
The alkyne-functionalised terphenyl stopper was synthesised according to a literature procedure (**Scheme 2-11**).[29,30] 1-Bromo-4-*tert*-butylbenzene was reacted with magnesium in the presence of iodine, to form a Grignard intermediate *in situ*, which was treated with diethylcarbonate to form trityl alcohol **40** in 50% yield. This was reacted with acidified molten phenol to produce stopper alcohol **41** (43% yield), which was subsequently suspended in hot DMF and reacted with propargyl bromide and excess K_2CO_3, affording the stopper alkyne **42** in 74% yield.



Scheme 2-11: Synthesis of alkyne-appended stopper **42**.

The stoppering method to form the target rotaxane was attempted twice, with the isophthalamide-containing macrocycle **33**, and the analogous *tert*-butyl-functionalised macrocycle **34**. An equimolar solution of axle precursor **37**·2BF_4, macrocycle **33** or **34** and TBA·Cl was treated with 2.2 equivalents of stopper alkyne **42**, in the presence of [Cu(CH_3CN)$_4$](PF_6), TBTA and DIPEA in CH_2Cl_2. While there was mass spectrometric evidence of the formation of rotaxanes **43**$^{2+}$ and **44**$^{2+}$ (**Scheme 2-12**), attempts to isolate the interlocked products by preparative TLC were not successful, which indicated that only trace amounts had been formed.

An analogous stoppering procedure undertaken to synthesise the HB rotaxane also failed to produce any interlocked material.



Scheme 2-12: Attempted synthesis of carbazole-containing rotaxanes by stoppering.

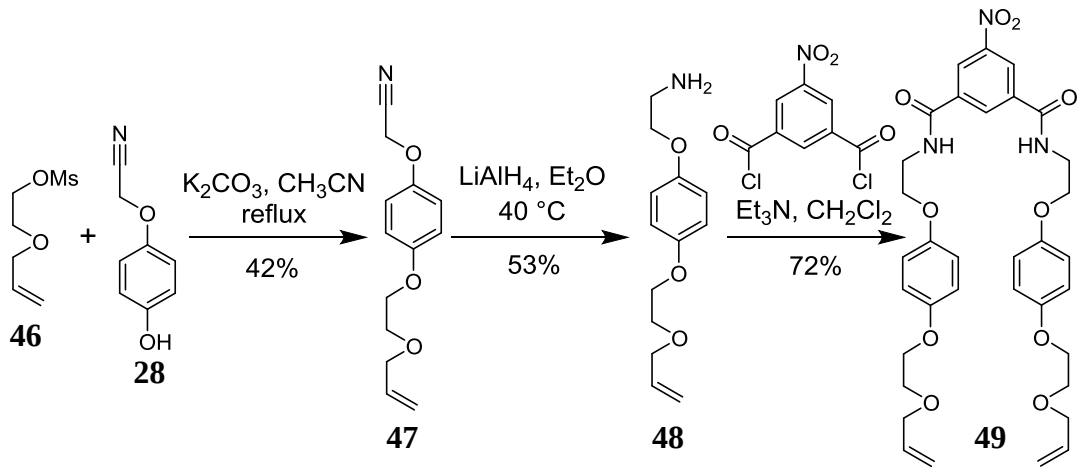
In light of the above, an alternative method of rotaxane synthesis was investigated using a 'clipping' approach, which involved ring-closing a macrocycle precursor component around an axle (**§1.4.1**).

2.4.3 *Rotaxane Synthesis by Ring-Clipping*

2.4.3.1 Macrocycle Precursor and Axle Components

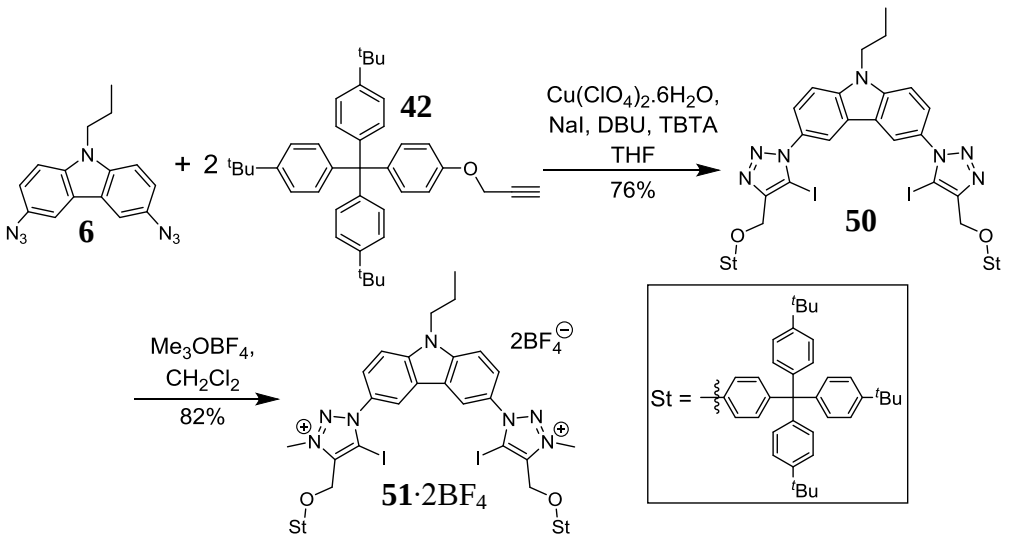
The bis-vinyl functionalised nitro-substituted isophthalamide derivative **49** has been previously used to form anion-templated rotaxanes *via* a ring-closing metathesis reaction.[10,31,32] Vinyl-appended mesylate **46** was reacted with mono-substituted hydroquinone **28** in the presence of K_2CO_3 in CH_3CN, to afford nitrile **47** in 42% yield. Reduction using $LiAlH_4$ in Et_2O gave amine **48** (53% yield), which was condensed with 5-nitroisophthaloyl dichloride in the presence of Et_3N in CH_2Cl_2 to give macrocycle precursor **49** in 72% yield

(**Scheme 2-13**)



Scheme 2-13: Synthesis of macrocycle precursor **49**.[31]

For the XB carbazole-based axle component, three different iodotriazolium-containing axle compounds were targeted, in which the stopper groups were connected to the iodotriazolium moieties through either the C- or N-terminus.

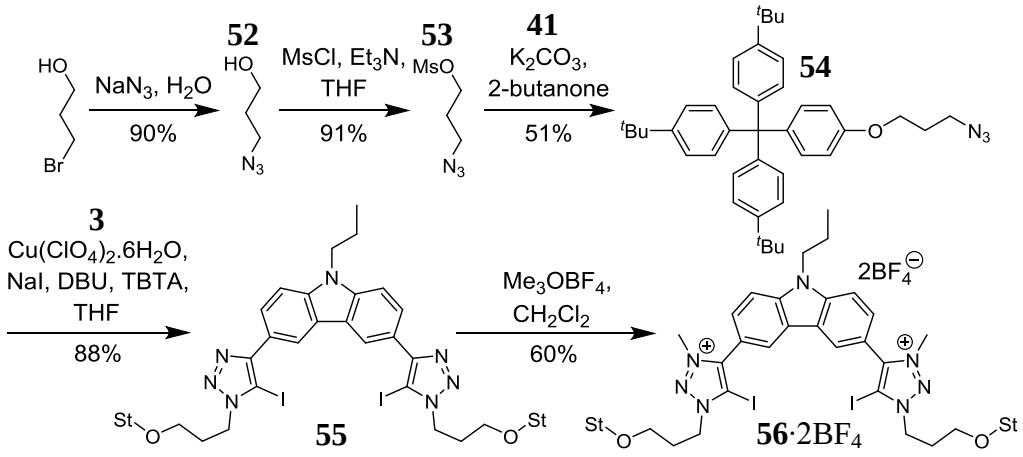


Scheme 2-14: Synthesis of N-linked carbazole-based axle **51**·2BF_4.

The preparation of the N-linked axle is given in **Scheme 2-14**. Diazidocarbazole **6** was

reacted with two equivalents of stopper alkyne **42** using the Brotherton one-pot reaction conditions to form neutral axle precursor **50** (76% yield), which was subsequently methylated using $Me_3O{\cdot}BF_4$ to form bis-iodotriazolium axle **51**$\cdot 2BF_4$ (82% yield).

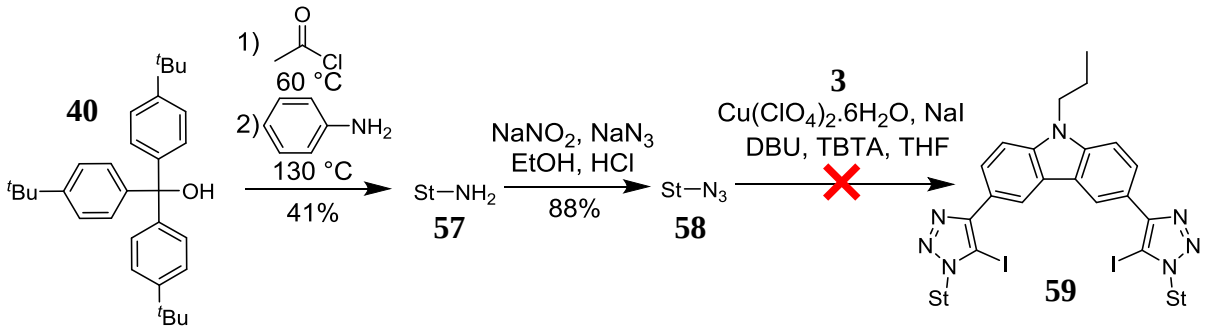
A similar C-linked axle was synthesised as shown in **Scheme 2-15**. 3-Bromo-1-propanol was reacted with NaN_3 in water to form 3-azido-1-propanol **52** (90%), which was then treated with mesyl chloride and triethylamine in THF to give 3-azidopropyl mesylate **53** (91%). Reaction with stopper alcohol **41** afforded propyl azide-appended stopper **54** in 51% yield. The Brotherton one-pot click reaction conditions were employed to react two equivalents of azide **54** with bis-alkyne carbazole **3**, to give bis-iodotriazole derivative **55** (88%), which was methylated using two equivalents of $Me_3O{\cdot}BF_4$ to form bis-iodotriazolium axle **56**$\cdot 2BF_4$.



Scheme 2-15: Synthesis of C-linked carbazole-based axle **56**$\cdot 2BF_4$.

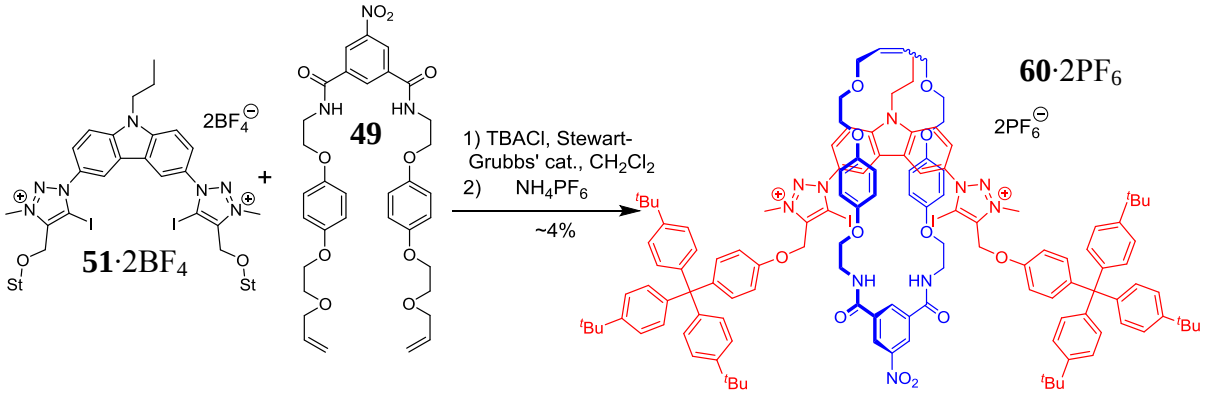
To increase preorganisation of the resulting rotaxane, a more rigid axle component was also envisaged, in which the stopper groups are directly connected to the iodotriazolium motifs (**Scheme 2-16**). Trityl alcohol **40** was first activated with acetyl chloride, followed by reaction with aniline, giving the stopper amine **57** in 41% yield. This was acidified and treated with $NaNO_2$ to form a diazonium intermediate, which was subsequently reacted with

NaN_3 to form the stopper azide **58** (88% yield). Multiple attempts were made to react stopper azide **58** with diethynylcarbazole **3** using the Brotherton one-pot reaction to form bis-iodotriazole carbazole **59**, but the syntheses did not produce the desired product. It is possible that direct attachment of azide to the aryl stopper may be sterically unfavourable.



Scheme 2-16: Attempted synthesis of C-linked carbazole-based axle precursor **59**.

2.4.3.2 N-linked Rotaxane Synthesis



Scheme 2-17: Synthesis of bis-iodotriazolium carbazole-based rotaxane **60**·$2PF_6$.

An equimolar mixture of N-linked axle **51**·$2BF_4$, macrocycle precursor **49** and TBA·Cl in dry dichloromethane in the presence of Stewart–Grubbs' catalyst afforded rotaxane **60**·Cl·BF_4 (**Scheme 2-17**). After an arduous purification employing multiple iterations of preparative silica TLC and recrystallisation, the rotaxane was anion exchanged using aqueous NH_4PF_6, to give **60**·$2PF_6$ in 4% isolated yield. This rotaxane was characterised by ^{1}H NMR and

^{13}C NMR spectroscopy, high-resolution mass spectrometry and ^{1}H–^{1}H ROESY NMR spectroscopy.

The ^{1}H NMR spectrum of rotaxane **60**·2PF$_6$ (**Figure 2-11**) clearly shows proton signals for both the axle and macrocycle. The proton resonances can be fully assigned, and the peak integrations are consistent with those expected for the rotaxane. Of particular interest is the observation that the hydroquinone protons *5* and *6* at ~6.6 ppm are split, which indicates that the macrocycle is part of an interlocked molecule.[33]

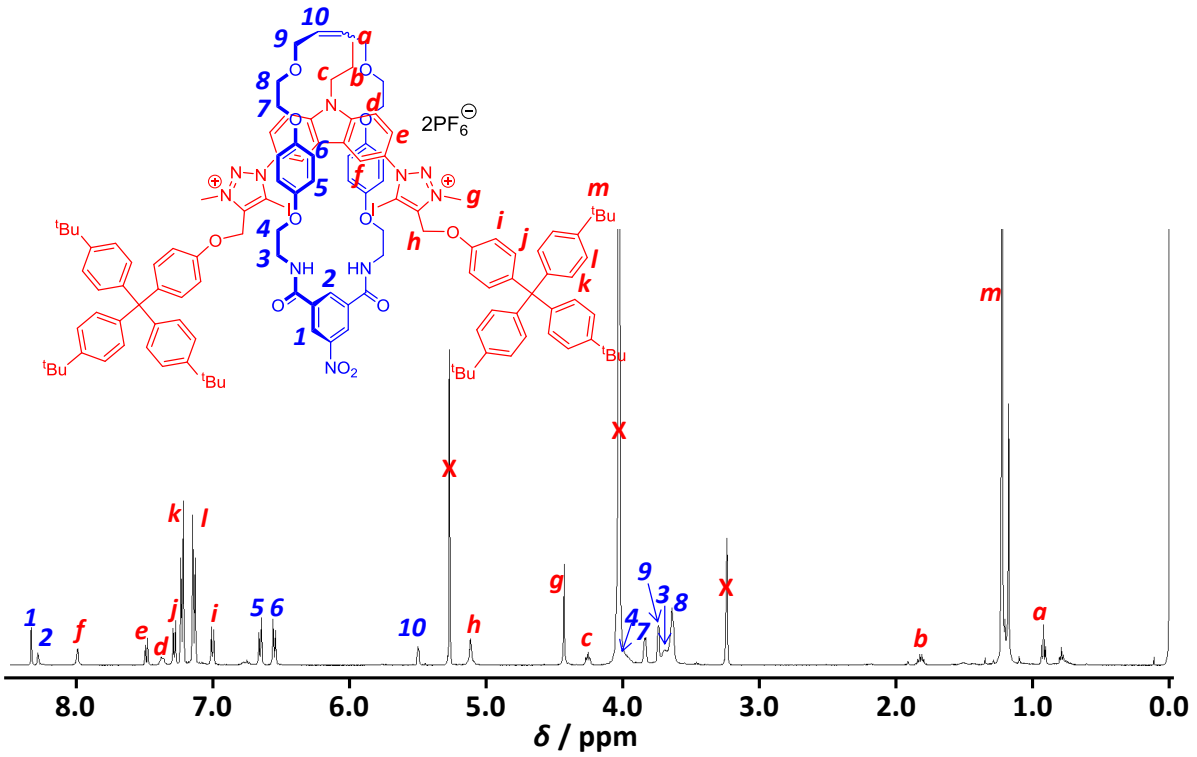


Figure 2-11: Assigned ^{1}H NMR spectrum of rotaxane **60**·2PF$_6$ (4:1 CD_2Cl_2/MeOD, 298 K, 500 MHz). Red 'X's denote solvent peaks.

Further evidence for the interlocked nature of the rotaxane molecule was obtained by ^{1}H–^{1}H ROESY NMR, as shown in **Figure 2-12**. Within the range shown, there are cross-component interactions observed between macrocycle alkene proton *10* and axle triazolium methyl

proton *g* (cross-peak 1), macrocycle hydroquinone proton *6* and axle methylene proton *h* (cross-peak 2), and macrocycle hydroquinone proton *5* and axle internal carbazole proton *f* (cross-peak 3).

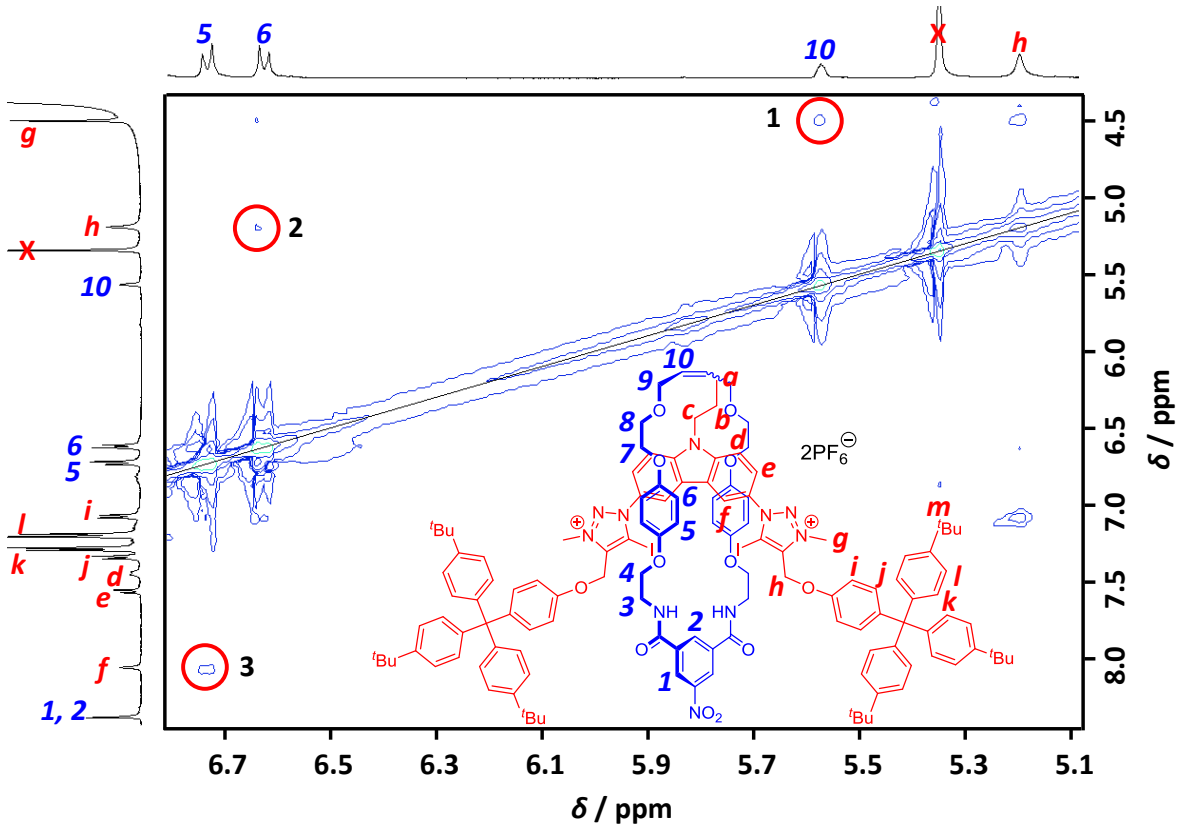
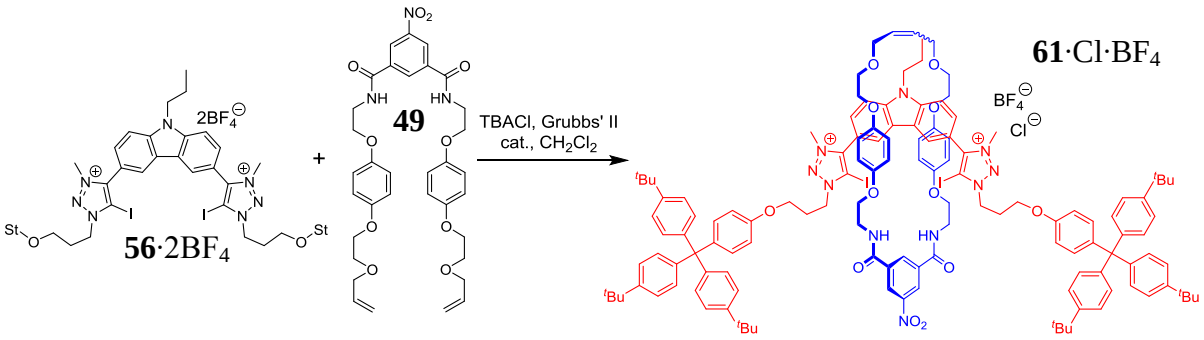


Figure 2-12: Trunctated ^{1}H–^{1}H ROESY NMR spectrum of rotaxane **60**·2PF_6 (4:1 CD_2Cl_2/MeOD, 298 K, 500 MHz). Red 'X's denote solvent peaks.

2.4.3.3 C-linked Rotaxane Synthesis

Attempts to prepare the C-linked rotaxane **61**$^{2+}$ involved reacting an equimolar mixture of axle **56**·2BF_4, macrocycle precursor **49** and TBA·Cl in dry dichloromethane with Grubbs' II RCM catalyst (**Scheme 2-18**). This reaction did afford some impure rotaxane **61**·Cl·BF_4, but it was not possible to isolate a completely pure sample, as the quantity of product was reduced to a trace amount as a consequence of repeated chromatographic purification procedures.



Scheme 2-18: Synthesis of C-linked rotaxane **61**·Cl·BF_4.

Although a pure ^{1}H NMR spectrum of rotaxane $\mathbf{61}^{2+}$ was not obtained, there is clear evidence for its formation in the ^{1}H NMR spectrum shown in **Figure 2-13**. While the impurities preclude a full assignment of the spectrum, signals can be clearly seen which correspond to the stopper aromatic protons (*A*) and the macrocycle hydroquinone (*1*) and ether (*2*) protons. Of particular note is the observation that the hydroquinone protons (*1*) are split and shifted upfield, which is diagnostic of an interlocked molecule containing this macrocycle. The proton resonances observed at ~6.8 ppm are likely to arise from the hydroquinones of both the non-interlocked macrocycle, and the macrocycle precursor impurities. Further confirmation that the rotaxane was successfully synthesised was also obtained by high resolution mass spectrometry, which displayed an *m*/*z* peak centred at 1168.4821, corresponding to the $[M]^{2+}$ ion.

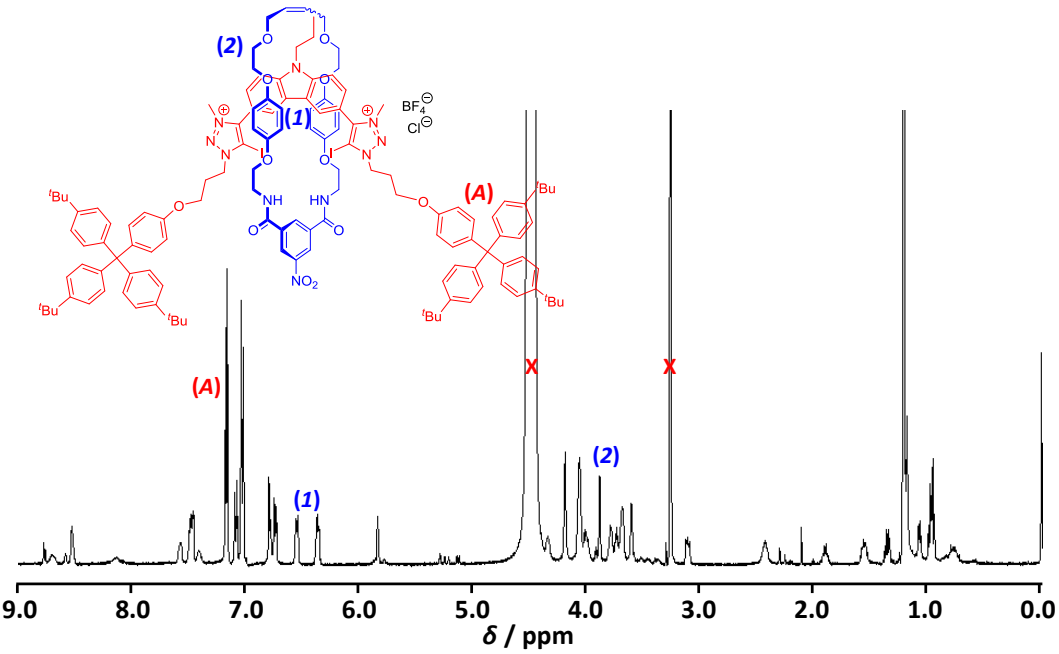


Figure 2-13: ^{1}H NMR spectrum of impure rotaxane **61**·Cl·BF_4 (4:1 CD_2Cl_2/MeOD, 298 K, 500 MHz). Red 'X's denote solvent peaks.

2.4.4 *Anion Recognition Properties of Rotaxane 60·2PF$_6$*

The anion binding behaviour of rotaxane **60**$^{2+}$ was studied using ^{1}H NMR titration experiments in 45:45:10 $CDCl_3$/CD_3OD/D_2O. Aliquots of a solution of the TBA salt of the anion were added to the rotaxane, most notably causing a downfield shift in the internal isophthalamide proton signal *2*, which is directly involved in anion binding (**Figure 2-14**). The titration data were analysed using WinEQNMR2[25] software, by following the macrocycle internal isophthalamide proton *2*, giving the binding isotherms shown in **Figure 2-15**, and determining the 1:1 stoichiometric association constants shown in **Table 2-3**.

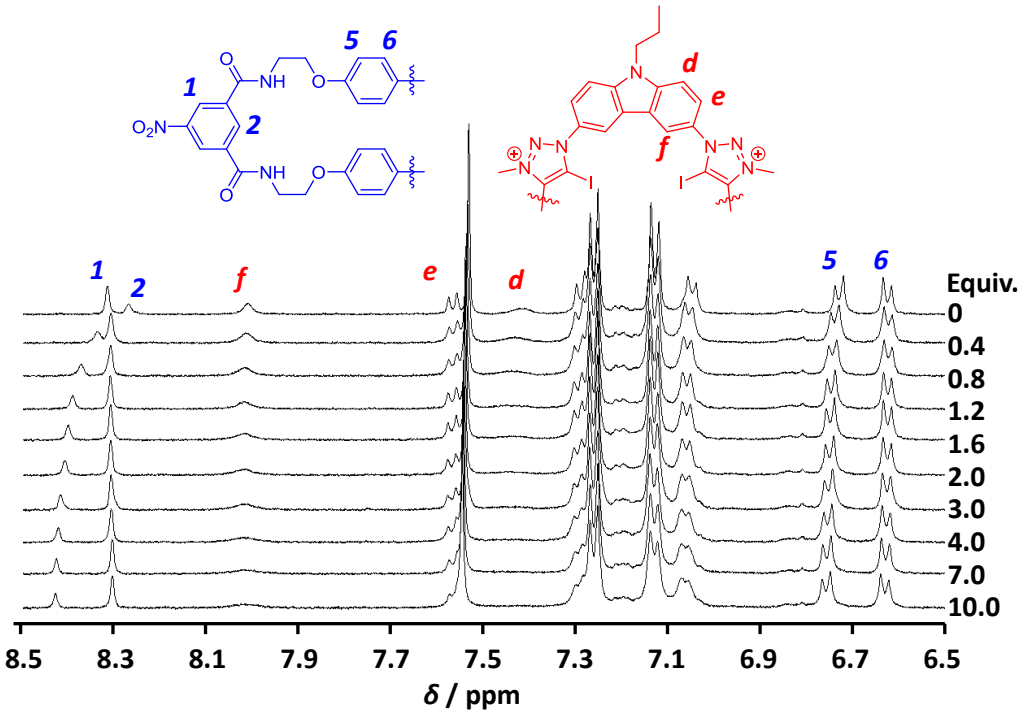


Figure 2-14: Partial ^{1}H NMR spectra of **60**·2PF$_6$ upon addition of TBA·Cl (45:45:10 $CDCl_3/CD_3OD/D_2O$, 293 K, 500 MHz).

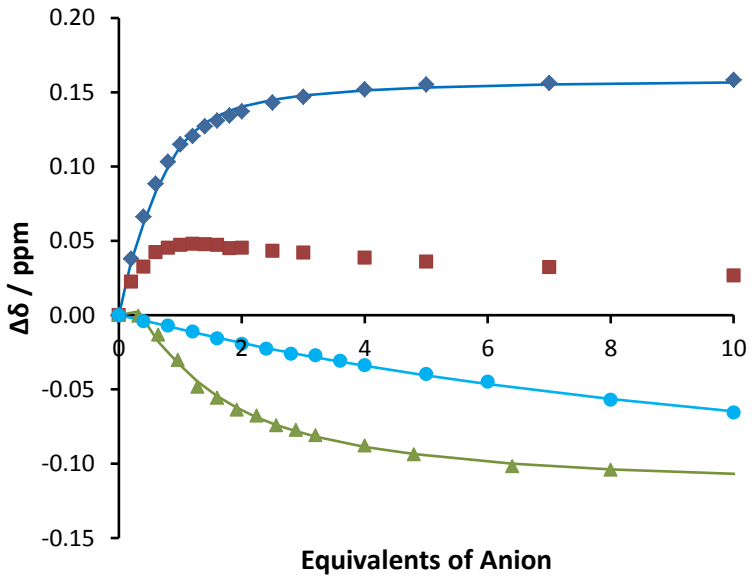


Figure 2-15: Experimental titration data (points) and fitted binding isotherms (lines) for the addition of ◆Cl^-, ■ Br^-, ▲ I^- and ●AcO^- anions to rotaxane **60**·2PF$_6$, monitoring the internal isophthalamide proton signal. Association of **60**·2PF$_6$ with bromide was too strong for WinEQNMR2[25] to accurately quantify (45:45:10 $CDCl_3/CD_3OD/D_2O$, 293 K, 500 MHz).

Of the anions studied, there is a remarkably strong preference for the halides over the oxoanions. The rotaxane is selective for Br^- over the other halides studied, with Cl^- in turn binding more strongly than I^-. The strong preference for Br^- is interesting when compared to the acyclic receptor behaviour, as all of the XB model systems were strongly selective for Cl^-.

Table 2-3: Association constants, K_a (M^{-1}), obtained from ^1H NMR titrations, for rotaxane **60**·2PF_6 with different anions (45:45:10 $CDCl_3/CD_3OD/D_2O$, 293 K, 500 MHz). Errors < 10%.

	60^{2+} [a]
Cl^-	2300
Br^-	> 10^4
I^-	750
AcO^-	25
$H_2PO_4^-$	[b]

[a] K_a values were determined by monitoring the internal carbazole proton resonance; [b] negligible shifts were observed, which is indicative of very weak binding.

It is noteworthy that addition of the anions Cl^- and Br^- induce downfield shifts in the monitored proton resonance, while AcO^- and I^- induce upfield shifts, and $H_2PO_4^-$ binding was found to be negligible. This observation may be indicative of the binding mode, wherein the downfield shifts imply that the binding cavity is of sufficient size and/or complementary shape to accommodate the anion, while the upfield shifts suggest the opposite effect, and the anion resides outside the cavity. Indeed, the external isophthalamide proton signal *1* also shifted upfield upon addition of AcO^- and I^-.

Furthermore, the Br^--selectivity is an interesting contrast to our previously-reported XB rotaxane (**Figure 2-16**), which contained a single iodotriazolium unit in the axle component, and was selective for I^-. The selectivity of rotaxane **60**$^{2+}$ for Br^- may be attributed to the specific binding cavity created between the axle and macrocycle, which results in good size complementarity for Br^-.

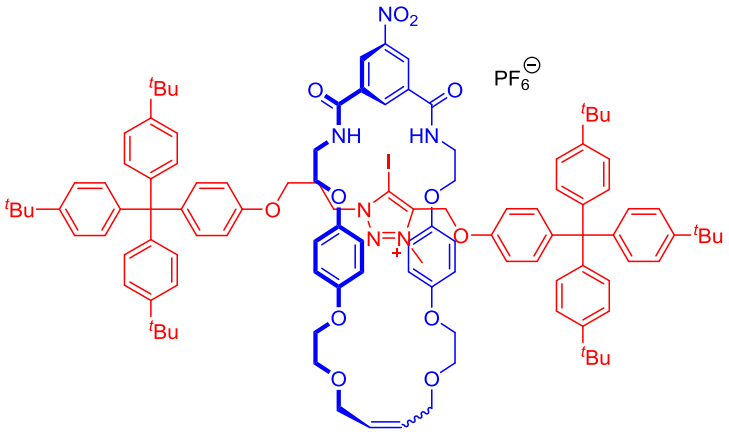


Figure 2-16: The previously-reported iodotriazolium-containing rotaxane.[10]

2.5 *Optical Properties*

The optical properties of carbazole are a major motivation for its incorporation into anion receptor designs. Preliminary optical anion sensing investigations were undertaken with two acyclic receptors: C-linked, alkyl prototriazolium receptor $\mathbf{20}^{2+}$; and C-linked, alkyl iodotriazolium receptor $\mathbf{22}^{2+}$, as well as rotaxane $\mathbf{60}^{2+}$.

2.5.1 *Absorption Behaviour*

UV-vis absorption titration experiments were undertaken in acetonitrile as an initial investigation into the anion sensing potential of the receptors. Although the absorption spectrum of acyclic prototriazolium receptor $\mathbf{20}^{2+}$ showed no significant change upon addition of TBA·Cl, the analogous iodotriazolium-containing receptor $\mathbf{22}^{2+}$ did give an anion-induced absorption response (**Figure 2-17a**). Specifically, the presence of Cl^- resulted in significant decreases in the absorption intensities at ~245 nm and ~280 nm, concomitant with bathochromic shifts of the absorption peaks. The data were analysed using the computer program SpecFit,[34] which determined a stoichiometric 1:1 association constant of $K_a > 10^4$ M^{-1},[35] in agreement with the ^{1}H NMR titration results.

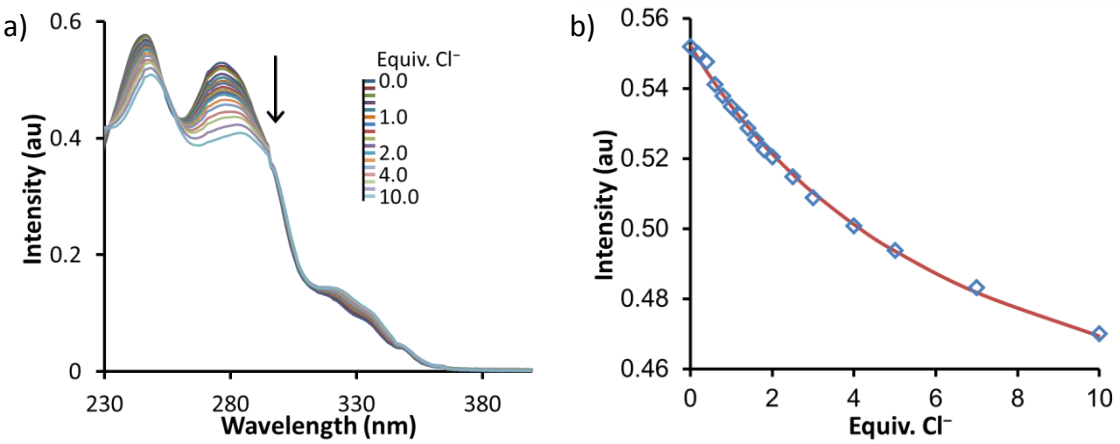


Figure 2-17: a) UV-vis spectra for bis-iodotriazolium receptor **22**·2BF_4 upon addition of Cl^-; and **b)** experimental titration intensity data (points) and the fitted binding model (line) at 245 nm (10 μM host, CH_3CN, 293 K).

Although the absorbance properties of acyclic iodotriazolium-containing receptor $\mathbf{22}^{2+}$ exhibited a response to anions, no spectral changes were observed upon TBA·Cl addition to a CH_3CN solution of the bis-iodotriazolium rotaxane **60**·2PF_6.

2.5.2 *Fluorescence Behaviour*

The fluorescence anion sensing potential of the acyclic receptors was studied using luminescence titration experiments. Similarly to the analogous absorption titrations above, a solution of the receptor was titrated with TBA·Cl in CH_3CN, with an excitation wavelength of λ_{ex} = 320 nm.

In contrast to the absorption behaviour observed for acyclic prototriazolium receptor $\mathbf{20}^{2+}$, its fluorescence emission intensity underwent significant quenching upon addition of TBA·Cl (**Figure 2-18a**). SpecFit analysis determined a 1:1 stoichiometric association constant of K_a = 488(1) M^{-1} (**Figure 2-18b**), which is of similar magnitude to the value obtained *via* the ^{1}H NMR titration experiment.

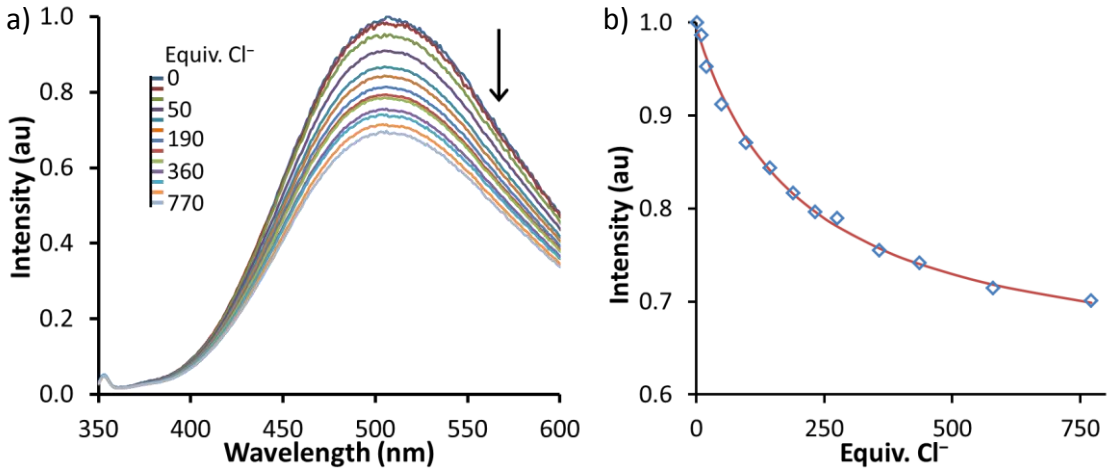


Figure 2-18: a) Fluorescence emission spectra of **20**·2BF_4 upon addition of Cl^-; and **b)** experimental titration intensity data (points) and the fitted binding model (line) at 510 nm (λ_{ex} = 320 nm, 10 μM host, CH_3CN, 293 K).

An analogous fluorescence titration experiment was conducted on iodotriazolium receptor **22**$^{2+}$, however, addition of TBA·Cl did not give a quantifiable response.

A luminescent anion titration experiment was also conducted on rotaxane **60**·2PF_6. The emission spectrum of the rotaxane in 10% H_2O/CH_3CN showed a broad peak centered at $\lambda_{em} \approx 485$ nm (λ_{ex} = 334 nm). Addition of TBA·Cl resulted in an increase in the intensity of this peak (**Figure 2-19a**), which may be attributed to rigidification of the receptor upon anion binding, which decreases the incidence of non-radiative relaxation pathways. Unfortunately, obtaining consistent, reproducible emission spectra proved challenging. It was possible to fit a 1:1 stoichiometric binding model to the titration data using SpecFit[34] (**Figure 2-19b**). However, the determined association constants varied widely; for example K_a = 5886(1) and 7110(1) M^{-1} for two analogous titration experiments.

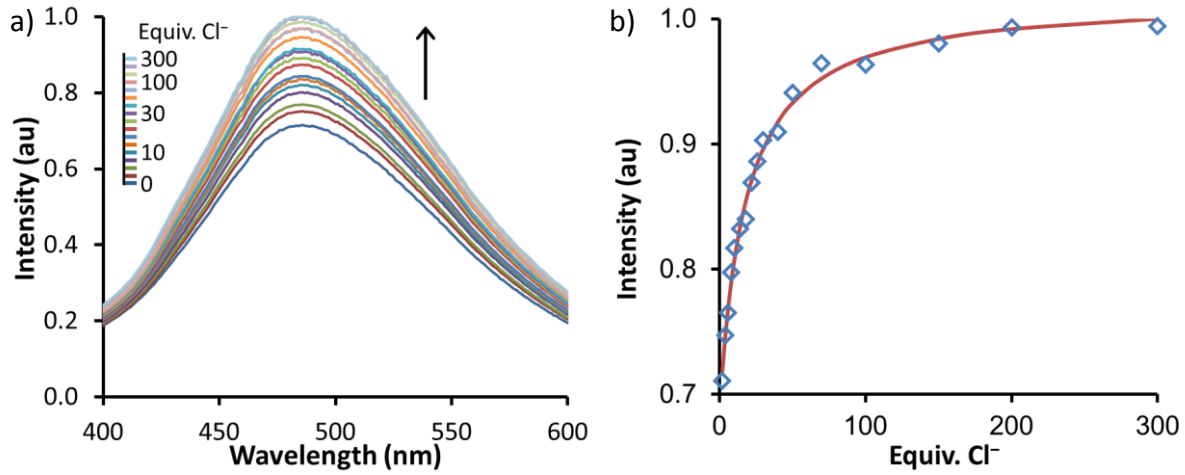


Figure 2-19: a) Luminescence emission spectra of rotaxane **60**·2PF$_6$ upon addition of TBA·Cl; and **b)** the experimental normalised emission values at λ = 485 nm (points), and the fitted binding isotherm (line) (K_a = 5886(1) M^{-1}, λ_{ex} = 334 nm, 10% H_2O/CH_3CN, 293 K).

As a consequence no further fluorescence binding studies were undertaken with rotaxane **60**·2PF$_6$.

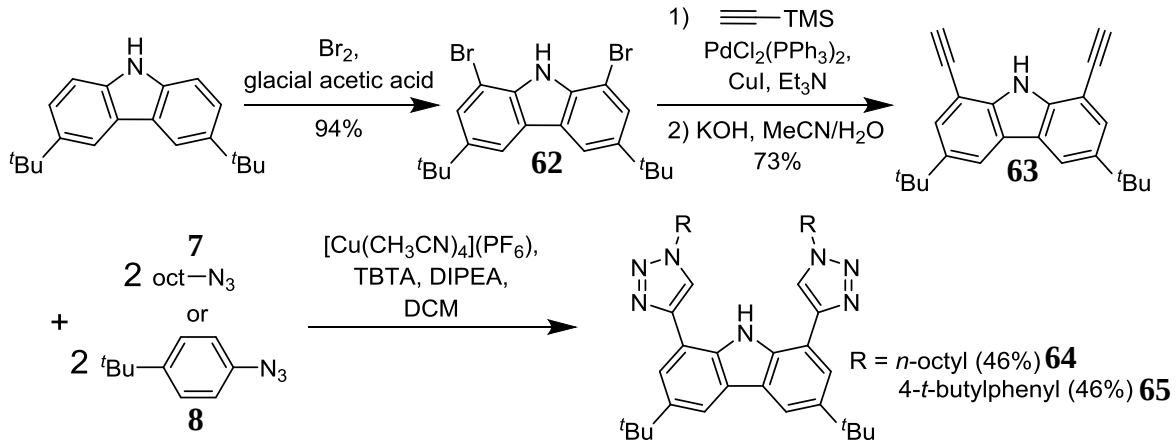
2.6 *Acyclic 1,8-Substituted Carbazole Systems*

Two acyclic systems were developed to study the 1,8-bis-triazole carbazole motif, which were substituted at the triazole N-terminus by either *n*-octyl (**64**) or 4-*tert*-butyl-benzene (**65**) groups. The carbazole was also functionalised at the 3,6-positions with *tert*-butyl groups for increased solubility.

2.6.1 *Synthesis of 1,8-Substituted Acyclic Carbazole Systems*

The synthetic procedure used to prepare acyclic receptors **64** and **65** is shown in **Scheme 2-19**. 3,6-Bis-*tert*-butylcarbazole was treated with bromine in glacial acetic acid to give 1,8-dibromocarbazole **62** in 94% yield.[36] This was reacted in a Sonogashira coupling[13] with TMS-acetylene in triethylamine, and after removal of the TMS groups using KOH in 6% H_2O/CH_3CN, the 1,8-diethynylcarbazole product **63** was isolated in 73% overall yield. A

CuAAC (click) reaction[19] with *n*-octyl azide **7** or 1-azido-4-*tert*-butyl-benzene **8** produced the target 1,8-bis-triazole carbazole acyclic receptors **64** and **65** respectively, both in 46% yield.



Scheme 2-19: Synthesis of 1,8-bis-triazole carbazole acyclic receptors **64** and **65**.

2.6.2 *Crystal Structures of Model Systems*

Crystals suitable for single crystal X-ray diffraction structural analysis were obtained for both acyclic receptors. Data were collected for full structure determination of **64** and **65** at 150 K, and data tables are given in **Appendix A**.

As shown in the crystal structures (**Figure 2-20**), the triazole units of both systems are oriented with the hydrogens pointing away from the prospective binding cavity. It is interesting to note that in both structures there are hydrogen bonding interactions between the pyrollic N–H of the carbazole, and the triazole units. The N–H···N distances lie within the range 2.203(2)–2.408(2) Å, which is 77–84% of the sum of the van der Waals radii, $\%vdW_{H,N}$.[37] It should be noted that the calculated errors for these values are underestimated due to the inherent limitations of X-ray diffraction in accurately locating and positioning hydrogen atoms.

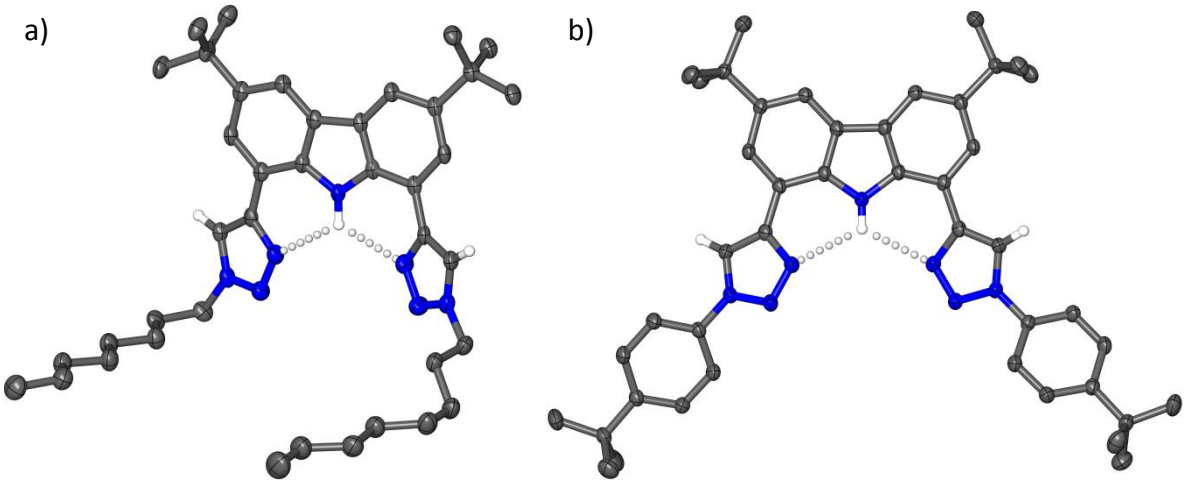


Figure 2-20: The structures of acyclic model systems **a) 64**; and **b) 65**, determined using single crystal X-ray diffraction. Non-acidic hydrogen atoms and solvent molecules are omitted for clarity, and thermal ellipsoids are shown at 50% probability.

2.6.3 *Anion Binding Studies*

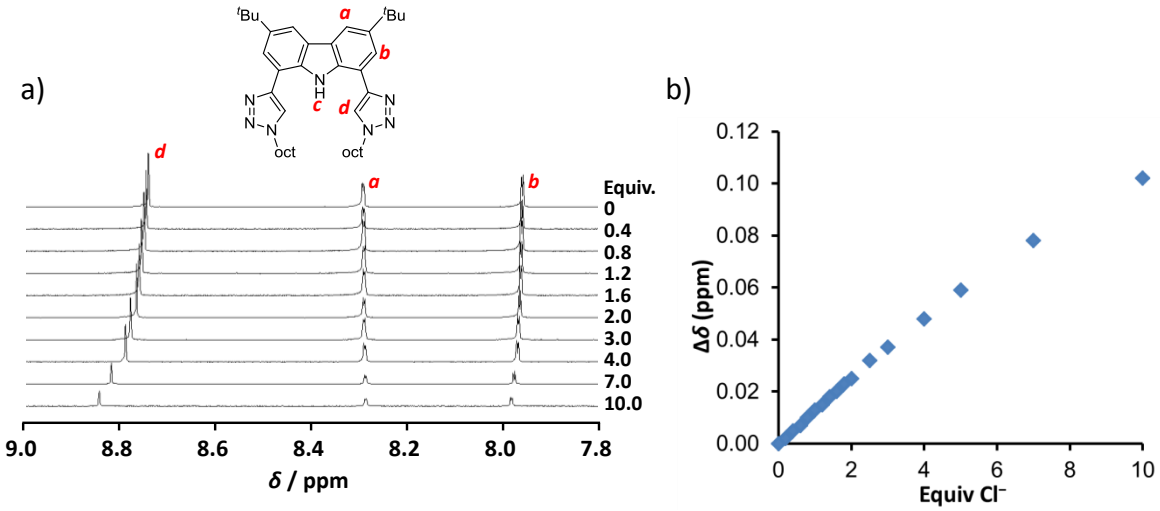


Figure 2-21: a) Truncated ^{1}H NMR spectra of **64** upon addition of TBA·Cl; and **b)** the experimental titration data, following triazole proton *d* (d_6-acetone, 293 K, 500 MHz).

A preliminary ^{1}H NMR titration study of receptor **64** with TBA·Cl was undertaken in d_6-acetone. Addition of the halide anion induced a minor shift in the triazole proton signal *d* (**Figure 2-21**), however the interaction was too weak to determine an accurate association constant, implying negligible binding. It is also noteworthy that there was no significant

change in the pyrollic N–H proton *c* shift, suggesting that the anion was not binding within the receptor cavity.

The crystal structures shown in **§2.6.2** provide a possible explanation for the low binding strength. As mentioned above, the structures exhibit multiple intramolecular hydrogen bonding interactions between the carbazole N–H, and triazole N atoms. In order for an anion to bind within the receptor cavity, these hydrogen bonds must be broken, creating an enthalpic barrier to the binding event. Anion binding within the cavity is thus thermodynamically disfavoured, resulting in the weak association with Cl^-.

An additional factor may be that the binding cavity is too small to accommodate anions of similar or greater size to Cl^-. Nevertheless, there was the possibility that the receptor might be selective for F^- which, as a smaller anion, could be of a complementary size to the host cavity. A ^1H NMR titration study with F^- in CD_3CN demonstrated that this basic anion in fact deprotonates the carbazole, resulting in a visible colour change from colourless to yellow, and a remarkable change in the fluorescence from dull purple to a brilliant blue. This deprotonation-induced colorimetric response is consistent with previously-reported behaviour of other carbazole-containing anion receptor systems interacting with basic anions such as fluoride.[38]

2.6.4 *Metal Complexation Studies*

During the course of this work, a report was published which described an analogous 1,8-bis-triazole carbazole ligand which was used to form a complex with Cu(II) (**Figure 2-22**).[39] This complex was demonstrated to be a highly selective and sensitive fluorescent sensor for cyanide, operating by the displacement approach (**§1.2.5.1**). Attention

was therefore turned to the possibility of using carbazole-based acyclic systems **64** and **65** to form metal complexes, in the hope that the Lewis acidic metal centre in the resulting complexes could be exploited for anion coordination and anion-templated interpenetrative assemblies.

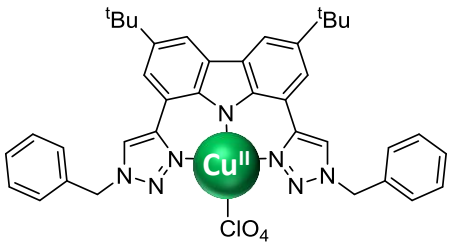


Figure 2-22: Jang's 1,8-bis-triazole carbazole copper(II) complex for cyanide sensing.[39]

As an initial study into the metal complexation properties of the 1,8-bis-triazole carbazole motif, attempts were made to investigate the binding stoichiometry and coordination behaviour using single crystal X-ray diffraction. A series of liquid/liquid diffusion crystallisations were setup, combining aryl-appended acyclic model **65** and the acetate salt of a range of transition metal cations. It was hoped that the basic acetate anion would deprotonate the carbazole, facilitating coordination of the ligand to the metal.

The crystallisation with nickel(II) acetate successfully produced diffraction-quality single crystals, and data were collected for structure determination at 150 K. Data tables are given in **Appendix A**. While a structure solution could be obtained, the data were not of sufficient quality to allow anisotropic refinement, hence the atoms of the structure (**Figure 2-23**) were modelled isotropically, and without hydrogen atoms. It should be noted that this structure is given by way of illustration only, and as the poor quality of the data precluded a full refinement, the atomic parameters should be not be treated as absolute. The crystal structure shows that the complex has a 2:1 ligand:metal binding stoichiometry, with the Ni(II) adopting

a distorted octahedral coordination geometry. The ligands bind in a tridentate fashion, with the deprotonated carbazole nitrogen, and two triazole nitrogen donors coordinating to the metal.

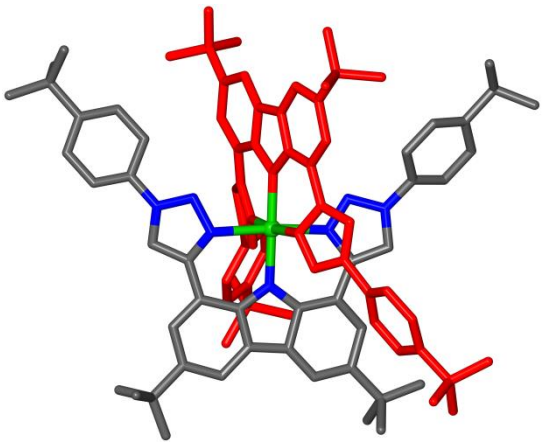
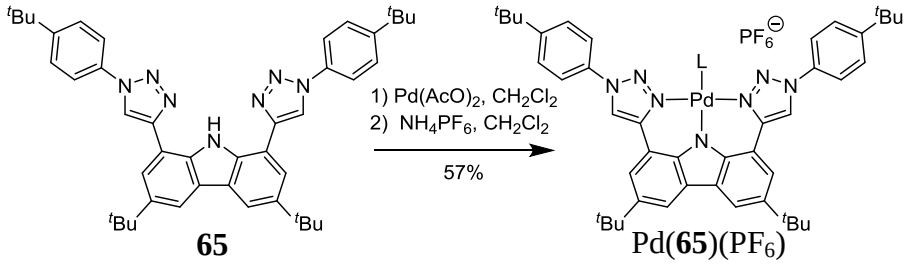


Figure 2-23: The structure of the Ni(**65**)$_2$ complex, as determined by single crystal X-ray diffraction. The atoms were modelled isotropically, and without hydrogen atoms.

The tridentate nature of the ligand makes it attractive to use in conjunction with a metal that adopts a square planar coordination geometry, as the fourth coordination site could be used to template the formation of an interpenetrated assembly. Palladium(II) complexes are known to preferentially adopt the desired square planar geometry, with the added benefit that the metal is diamagnetic, allowing study by NMR spectroscopy. A complexation reaction was therefore undertaken between aryl-appended ligand **65** and palladium(II) acetate, which successfully produced the acetate salt of the complex (**Figure 2-24**). Anion exchange converted the complex to the PF_6^- salt, but the aromatic signals in the ^{1}H NMR spectrum of the product suffered from extreme broadening, possibly due to aggregation effects. Nevertheless, the ^{19}F NMR spectrum displayed a diagnostic doublet peak for the PF_6^- anion, suggesting that anion exchange was successful.



Scheme 2-20: Synthesis of palladium(II) complex Pd(**65**)(PF_6).

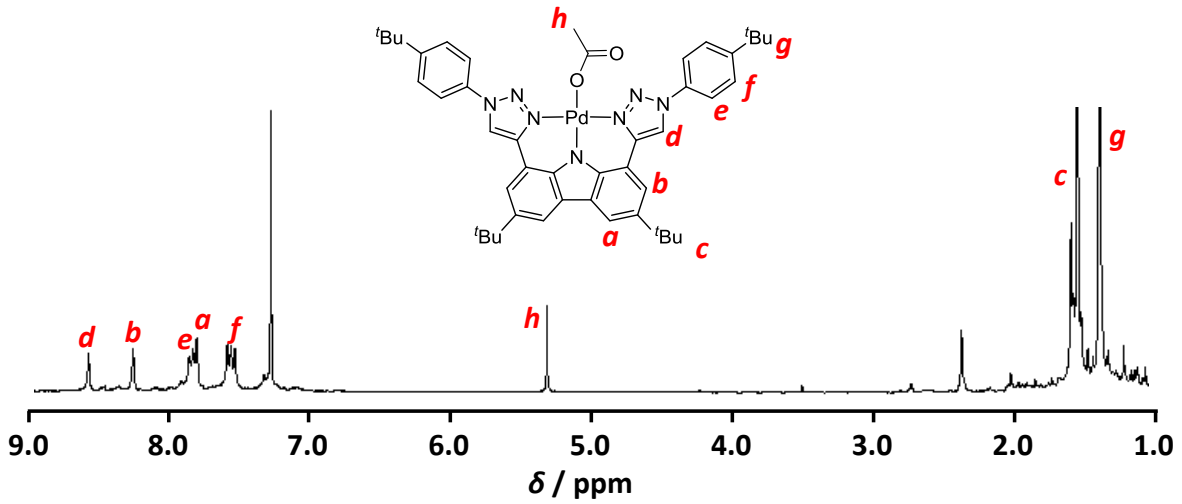


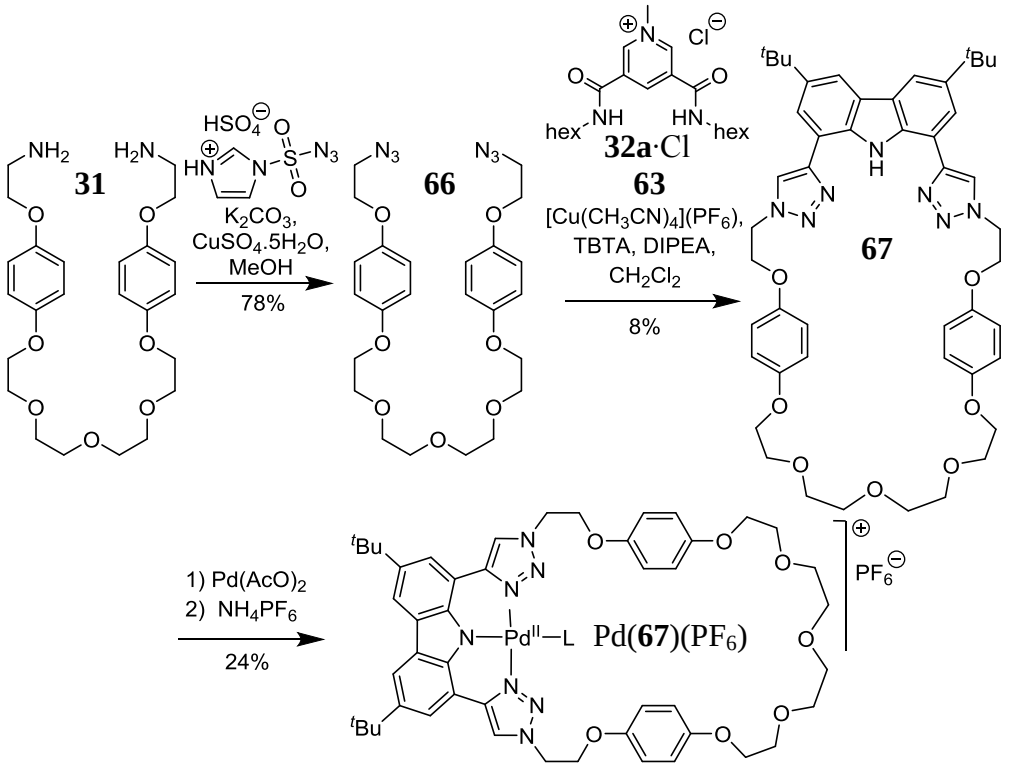
Figure 2-24: Assigned ^{1}H NMR spectrum of Pd(**65**)(AcO) ($CDCl_3$, 298 K, 300 MHz).

2.6.5 *Macrocycles and Pseudorotaxanes*

Given the successful formation of a Pd(II) complex with ligand **65**, an analogous cyclic derivative **67**, which incorporates a bis-hydroquinone polyether chain, was designed and synthesised for potential use in the formation of interpenetrated structures.

The synthesis of this new carbazole-containing macrocycle **67** is shown in **Scheme 2-21**. Reaction of bis-amine precursor **31** with the HSO_4^- salt of imidazolesulfonyl azide, in the presence of K_2CO_3 and $CuSO_4{\cdot}5H_2O$,[40] gave bis-azide compound **66**. Reaction under CuAAC (click) conditions with the diethynylcarbazole precursor **63,** in the presence of the pyridinium chloride thread template **32a**, afforded macrocycle **67** in 8% yield. Complexation with

$Pd(AcO)_2$, followed by anion exchange for PF_6^-, gave the macrocycle complex Pd(**67**)(PF_6) in 24% yield. In contrast to the behaviour of the acyclic complex Pd(**65**)(PF_6), peak broadening was not observed in the ^{1}H NMR spectrum of the macrocyclic complex Pd(**67**)(PF_6).



Scheme 2-21: Synthesis of carbazole-containing macrocycle complex Pd(**67**)(PF_6). The coordinating ligand 'L' represents a solvent molecule.

Qualitative ^{1}H NMR pseudorotaxane assembly experiments were carried out to determine the potential of neutral macrocycle **67** and the corresponding cyclic Pd complex Pd(**67**)(PF_6) for forming interpenetrated assemblies with bis-amide pyridinium chloride thread **32**·Cl in $CDCl_3$ solution. As shown in **Figure 2-25**, addition of one equivalent of thread **32a**·Cl to macrocycle **67** results in a minor upfield shift of the macrocycle hydroquinone proton peaks *5* and *6*. This behaviour is diagnostic of interpenetration, and is due to favourable aromatic donor–acceptor interactions between the electron-rich hydroquinone units of the macrocycle

and the electron-deficient pyridinium group of the thread. However, the small magnitude of the shift ($\Delta\delta \approx 0.05$ ppm) suggests that the pseudorotaxane assembly is of low stability.

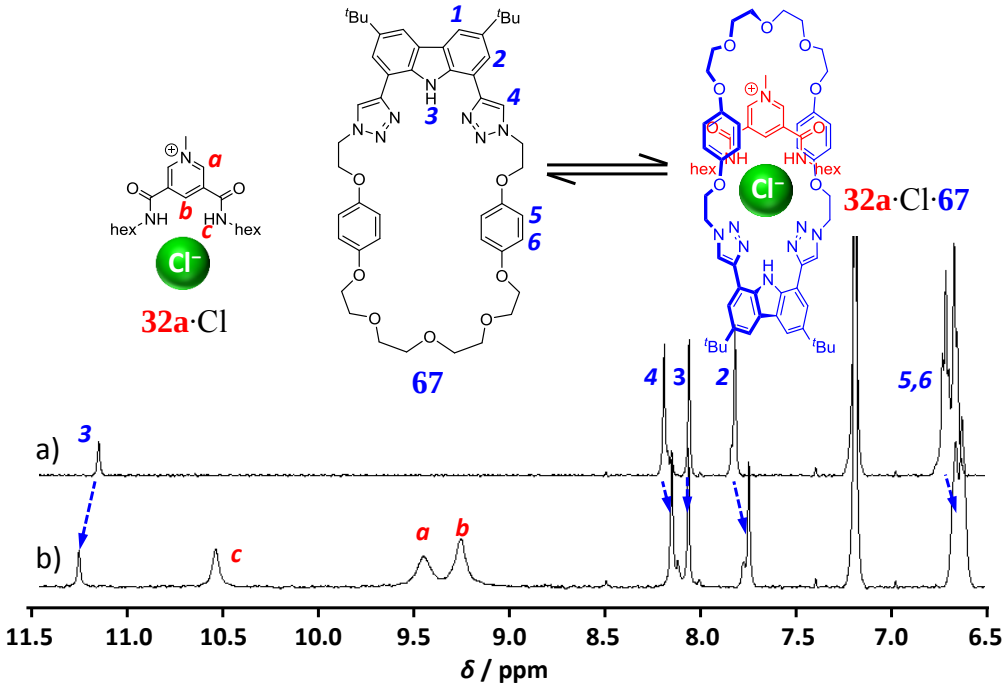


Figure 2-25: a) Carbazole-based macrocycle **67**; and **b)** after addition of bis-amide pyridinium chloride thread **32a**·Cl ($CDCl_3$, 293 K, 500 MHz).

While there is a small shift of carbazole pyrrolic proton *3* which may be due to anion coordination, the triazole proton *4* exhibits a minor upfield shift, which is contrary to the behaviour expected for anion coordination. The poor anion binding affinity of the 1,8-bis-triazole carbazole motif (**§2.6.3**) implies that there is a minimal contribution of the anion to template pseudorotaxane formation. The major interactions that stabilise the interpenetrated structure are likely to be the aforementioned aromatic donor–acceptor interactions, and possible weak hydrogen bonding interactions between the pyridinium methyl protons and the macrocycle's polyether oxygens.

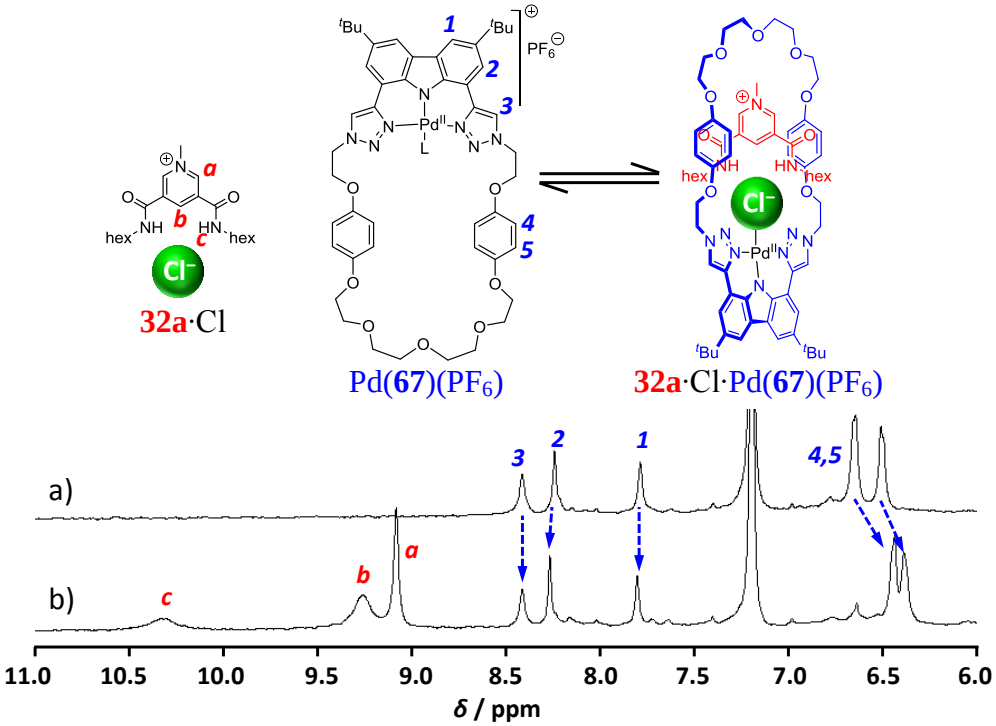
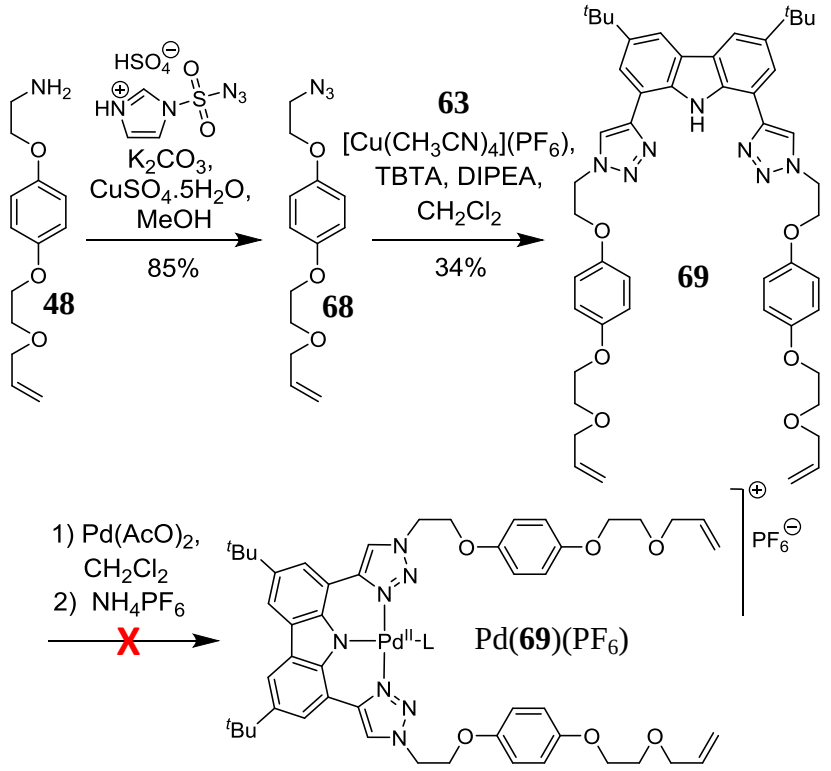


Figure 2-26: a) Pd(II) complex macrocycle Pd(**67**)(PF_6); and **b)** after addition of bis-amide pyridinium chloride thread **32a**·Cl ($CDCl_3$, 293 K, 500 MHz). The coordinating ligand 'L' represents a solvent molecule.

It was expected that complex macrocycle Pd(**67**)(PF_6) would be more effective at forming a pseudorotaxane with the pyridinium-based thread **32a**·Cl, due to the ability of the Cl^- template to coordinate to the Pd(II) metal centre. The square planar coordination geometry of the Pd(II) would result in the chloride being bound within the macrocycle cavity, thus the pyridinium thread would similarly reside within the macrocycle. As shown in **Figure 2-26**, addition of the pyridinium thread **32a**·Cl does indeed result in a significant upfield shift of the macrocycle hydroquinone protons ($\Delta\delta \approx 0.17$ ppm), suggesting the formation of a stable pseudorotaxane species.

While the low synthetic yield of macrocycle Pd(**67**)(PF_6) precluded its incorporation into an interlocked molecule, ^{1}H NMR evidence for formation of an anion-templated interpenetrated

species encouraged the development of an alternative macrocycle design. A bis-vinyl terminated macrocycle precursor was thus envisaged, which could undergo a ring-closing metathesis (RCM) reaction around a pyridinium-based axle to form a rotaxane.

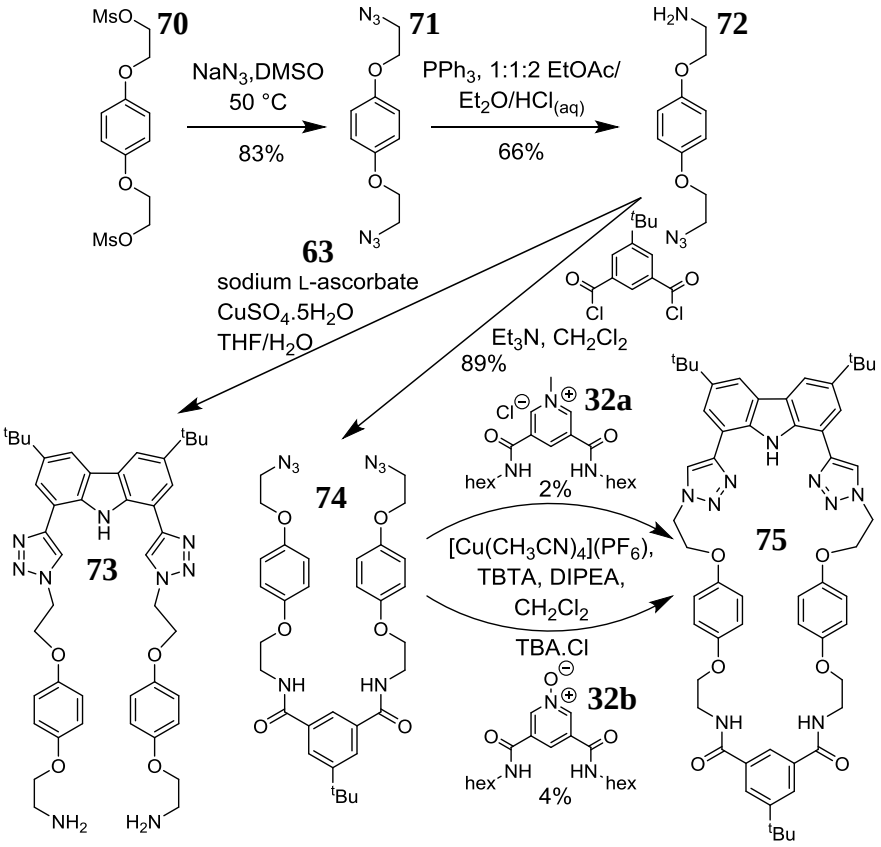


Scheme 2-22: Attempted synthesis of the Pd(II) complex of carbazole-based macrocycle precursor Pd(**69**)(PF_6). The coordinating ligand 'L' represents an expected solvent molecule.

Attempts to prepare macrocycle precursor complex Pd(**69**)(PF_6) were undertaken according to **Scheme 2-22**. Allyl-appended amine **48** was converted to the corresponding allyl-appended azide **68** in 85% yield.[41] Reaction of two equivalents of azide **68** with diethynylcarbazole **63** under CuAAC (click) conditions afforded bis-triazole precursor **69** (34%). Complexation with palladium(II) acetate, followed by an anion exchange to PF_6^-, resulted in a product with a ^{1}H NMR spectrum which displayed a number of unassignable proton signals. It is possible that this observation was a result of the palladium(II) also interacting with the allyl groups of the macrocycle precursor. In the hope of negating this

interaction, excess chloride was added, however, the ^{1}H NMR spectrum remained unassignable.

A bifunctional macrocycle was designed that incorporated an isophthalamide group in addition to the bis-triazole carbazole unit. Isophthalamide-based macrocycles are well-established macrocycle components of rotaxanes containing bis-amide pyridinium-based axle components (**§1.4.1.3**).



Scheme 2-23: Synthesis of bifunctional macrocycle **75**.

The synthetic procedure undertaken to obtain bifunctional macrocycle **75** is shown in **Scheme 2-23**. Bis-mesylate compound **70** was reacted with NaN_3 to form bis-azide intermediate **71** in 83% yield, and subsequent mono-reduction with PPh_3 afforded mono-amine **72** in 66% yield. There were then two different routes for preparing the macrocycle.

The first attempted method involved reaction of mono-amine **72** with diethynylcarbazole **63** under CuAAC (click) conditions to form bis-triazole intermediate **73**. Unfortunately, **73** was highly insoluble in all common organic solvents, thus further reaction to form a macrocycle was impossible. The other synthetic path involved condensation of 5-(*tert*-butyl)isophthaloyl dichloride with two equivalents of the mono-amine **72**, in the presence of triethylamine, which successfully formed bis-azide intermediate **74** in 89% yield.

Initially, bis-azide intermediate **74** was reacted with **63** under the CuAAC (click) conditions, in the presence of one equivalent of bis-amide pyridinium chloride template **32a**·Cl, and macrocycle **75** was isolated in only 2% yield due to challenging purification procedures. Given the bifunctional nature of the macrocycle, it was believed that bis-amide pyridine *N*-oxide-based thread **32b**, in conjunction with a Cl^- anion template, might provide a better template for macrocycle formation. However, only a modest improvement in macrocycle yield to 4% was achieved.

The very low yield of macrocycle **75** discouraged any further study into its incorporation into interlocked structures.

2.7 *Conclusions and Future Work*

A systematic anion binding study was carried out on eight different bis-triazolium carbazole-based acyclic receptors. The effects of varying three different structural properties of the receptor were studied: the carbazole was substituted with prototriazolium or iodotriazolium groups; these groups were connected to the carbazole by either the C- or N-terminus; and the triazolium motifs were further substituted by either alkyl or aryl substituents. Importantly, the XB receptors were found to be far superior halide complexants compared to the HB

receptors, although the aryl-appended HB receptors **21** and **25** bound SO_4^{2-} with the strongest affinity. The halide selectivity for all the XB receptors followed the trend $Cl^- > Br^- > I^-$, while there was no halide preference observed for the HB receptors. In general, the aryl-appended receptors displayed a minor increase in halide binding strength compared to the analogous alkyl-appended receptors, and no general differences in the binding behaviour of the C- and N-linked receptors were observed.

Attempts were made to synthesise rotaxane host systems incorporating a bis-iodotriazolium carbazole-containing axle component. The stoppering method was unsuccessful in forming a rotaxane, whereas the ring-closing method was successfully employed to synthesise rotaxane **60**·2PF_6. Through ^{1}H NMR titration experiments in 45:45:10 $CDCl_3/CD_3OD/D_2O$, this rotaxane demonstrated a strong preference for halides over the oxoanions, with a halide selectivity trend of $Br^- > Cl^- > I^-$.

Two neutral acyclic receptors based on the 1,8-bis-triazole carbazole motif were prepared, and shown to be ineffective at anion binding. However, this motif behaved as a tridentate ligand in the formation of metal complexes, and the possibility of forming interpenetrated and interlocked systems using a square planar Pd(II) complex was investigated. A macrocycle containing the Pd(II) complex of the 1,8-bis-triazole carbazole group was shown to form a pseudorotaxane assembly with a bis-amide pyridinium-based thread. However, the low yield of macrocycle formation prompted the development of other molecular components for incorporation in interlocked structures. An allyl-appended macrocycle precursor was synthesised with the intention of using ring-closing metathesis to form the macrocycle. Unfortunately, the PF_6^- salt of the corresponding Pd(II) complex appeared to result in undesired coordination products which could not be removed, so this avenue was abandoned.

A bifunctional macrocycle was also successfully synthesised, though low yields prevented further study into using this macrocycle in the formation of interpenetrated and interlocked structures.

Although a suitable synthetic procedure for 3,6-bis-bromotriazole carbazole systems has thus far proved elusive, future work might look at the activity of different catalysts to synthesise these systems. The receptor motifs integrated into XB rotaxane **60**·2PF_6 may also be suitable for incorporation into a catenane host system, and other macrocycles may be explored to create analogous XB rotaxanes with different host cavities. Indeed, this possibility is explored in Chapter 4, in which a XB macrocycle is used in conjunction with carbazole-based axle **56**$^{2+}$, to form an all-XB rotaxane.

2.8 *References*

(1) Chmielewski, M. J.; Charon, M.; Jurczak, J. *Org. Lett.* **2004**, *6*, 3501.
(2) Gale, P. A. *Chem. Commun.* **2008**, 4525.
(3) Gross, D. E.; Mikkilineni, V.; Lynch, V. M.; Sessler, J. L. *Supramol. Chem.* **2010**, *22*, 135.
(4) Curiel, D.; Sanchez, G.; Ramirez de Arellano, C.; Tarraga, A.; Molina, P. *Org. Biomol. Chem.* **2012**, *10*, 1896.
(5) Sanchez, G.; Espinosa, A.; Curiel, D.; Tarraga, A.; Molina, P. *J. Org. Chem.* **2013**, *78*, 9725.
(6) Piątek, P.; Lynch, V. M.; Sessler, J. L. *J. Am. Chem. Soc.* **2004**, *126*, 16073.
(7) Li, Y.; Flood, A. H. *J. Am. Chem. Soc.* **2008**, *130*, 12111.
(8) Schulze, B.; Friebe, C.; Hager, M. D.; Günther, W.; Köhn, U.; Jahn, B. O.; Görls, H.; Schubert, U. S. *Org. Lett.* **2010**, *12*, 2710.
(9) Serpell, C. J.; Kilah, N. L.; Costa, P. J.; Félix, V.; Beer, P. D. *Angew. Chem. Int. Ed.* **2010**, *49*, 5322.
(10) Kilah, N. L.; Wise, M. D.; Serpell, C. J.; Thompson, A. L.; White, N. G.; Christensen, K. E.; Beer, P. D. *J. Am. Chem. Soc.* **2010**, *132*, 11893.
(11) Smith, K.; James, D. M.; Mistry, A. G.; Bye, M. R.; Faulkner, D. J. *Tetrahedron* **1992**, *48*, 7479.
(12) Xu, H.; Yin, K.; Huang, W. *J. Phys. Chem. C* **2009**, *114*, 1674.
(13) Sonogashira, K.; Tohda, Y.; Hagihara, N. *Tetrahedron Lett.* **1975**, *16*, 4467.
(14) Zhu, W.; Ma, D. *Chem. Commun.* **2004**, 888.
(15) Zhao, T.; Liu, Z.; Song, Y.; Xu, W.; Zhang, D.; Zhu, D. *J. Org. Chem.* **2006**, *71*, 7422.

(16) Alami, M. d.; Ferri, F.; Linstrumelle, G. *Tetrahedron Lett.* **1993**, *34*, 6403.
(17) Alvarez, S. G. A., Mijo T. *Synthesis* **1997**, *4*, 413.
(18) Barr, L.; Lincoln, S. F.; Easton, C. J. *Supramol. Chem.* **2005**, *17*, 547.
(19) Rostovtsev, V. V.; Green, L. G.; Fokin, V. V.; Sharpless, K. B. *Angew. Chem. Int. Ed.* **2002**, *41*, 2596.
(20) Hofmeister, H.; Annen, K.; Laurent, H.; Wiechert, R. *Angew. Chem. Int. Ed. Eng.* **1984**, *23*, 727.
(21) Kuijpers, B. H. M.; Dijkmans, G. C. T.; Groothuys, S.; Quaedflieg, P. J. L. M.; Blaauw, R. H.; van Delft, F. L.; Rutjes, F. P. J. T. *Synlett* **2005**, *2005*, 3059.
(22) Hein, J. E.; Tripp, J. C.; Krasnova, L. B.; Sharpless, K. B.; Fokin, V. V. *Angew. Chem. Int. Ed.* **2009**, *48*, 8018.
(23) Meng, L. G.; Cai, P. J.; Guo, Q. X.; Xue, S. *Synth. Commun.* **2008**, *38*, 225.
(24) Brotherton, W. S.; Clark, R. J.; Zhu, L. *J. Org. Chem.* **2012**, *77*, 6443.
(25) Hynes, M. J. *J. Chem. Soc., Dalton Trans.* **1993**, 311.
(26) White, N. G.; Beer, P. D. *Supramol. Chem.* **2012**, *24*, 473.
(27) Ng, K.-Y.; Felix, V.; Santos, S. M.; Rees, N. H.; Beer, P. D. *Chem. Commun.* **2008**, 1281.
(28) Wisner, J. A.; Beer, P. D.; Drew, M. G. B. *Angew. Chem. Int. Ed.* **2001**, *40*, 3606.
(29) Gibson, H. W.; Lee, S. H.; Engen, P. T.; Lecavalier, P.; Sze, J.; Shen, Y. X.; Bheda, M. *J. Org. Chem.* **1993**, *58*, 3748.
(30) Aucagne, V.; Hänni, K. D.; Leigh, D. A.; Lusby, P. J.; Walker, D. B. *J. Am. Chem. Soc.* **2006**, *128*, 2186.
(31) Sambrook, M. R.; Beer, P. D.; Lankshear, M. D.; Ludlow, R. F.; Wisner, J. A. *Org. Biomol. Chem.* **2006**, *4*, 1529.
(32) Mullen, K. M.; Mercurio, J.; Serpell, C. J.; Beer, P. D. *Angew. Chem. Int. Ed.* **2009**, *48*, 4781.
(33) Wisner, J. A.; Beer, P. D.; Drew, M. G. B.; Sambrook, M. R. *J. Am. Chem. Soc.* **2002**, *124*, 12469.
(34) Specfit v. 2.02 ed., Spectrum Software Associates Chapel Hill, NC, USA: 1997.
(35) Insufficient data were obtained to enable accurate modelling of the association constant.
(36) Gibson, V. C.; Spitzmesser, S. K.; White, A. J. P.; Williams, D. J. *Dalton Trans.* **2003**, 2718.
(37) Alvarez, S. *Dalton Trans.* **2013**, *42*, 8617.
(38) Amendola, V.; Boiocchi, M.; Fabbrizzi, L.; Palchetti, A. *Chem. Eur. J.* **2005**, *11*, 5648.
(39) Gee, H.-C.; Lee, C.-H.; Jeong, Y.-H.; Jang, W.-D. *Chem. Commun.* **2011**, *47*, 11963.
(40) Fischer, N.; Goddard-Borger, E. D.; Greiner, R.; Klapötke, T. M.; Skelton, B. W.; Stierstorfer, J. *J. Org. Chem.* **2012**, *77*, 1760.
(41) White, N. G.; Beer, P. D. *Chem. Commun.* **2012**, *48*, 8499.

Chapter 3: Naphthalene-Based Anion Receptors

3.1 *Introduction*

The photo-active properties of naphthalene have been exploited in the development of colorimetric and fluorescent anion receptors.[1-5] For example, the receptor in **Figure 3-1a** was shown to exhibit a deprotonation-induced response to the basic anions AcO^-, F^- and $H_2PO_4^-$ in DMSO, resulting in a naked-eye detectable colour change from yellow to various shades of purple for the different anions.[1] The fluorescence properties of naphthalene were utilised in Kang's tetraimidazolium receptor, which was shown to selectively sense iodide in 10% DMSO/CH_3CN (**Figure 3-1b**).[6]

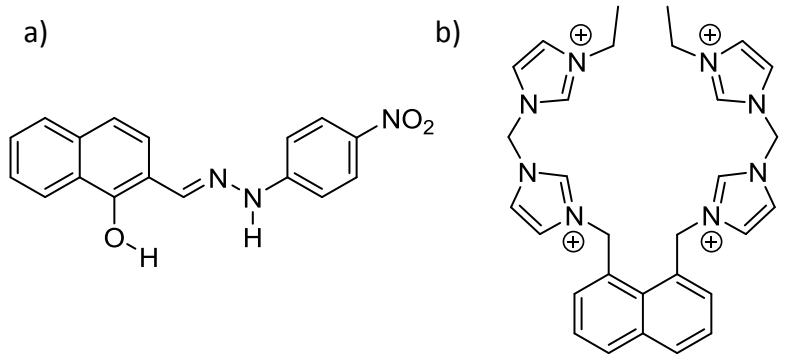


Figure 3-1: Naphthalene-based anion receptors, **a)** Lin's hydrazone-containing colorimetric sensor;[1] and **b)** Kang's tetraimidazolium fluorescence sensor.[7]

3.2 *Outline*

The optical and structural properties of naphthalene make it an attractive spacer unit on which to attach anion recognition motifs. Initially, a HB receptor motif was envisaged, in which naphthalene was substituted at the 2,7-positions by prototriazolium groups (**Figure 3-2a**). With the ultimate intention of incorporating this motif into an interlocked anion receptor, macrocycle derivatives were developed, and their ability to form anion-templated pseudorotaxane assemblies investigated.

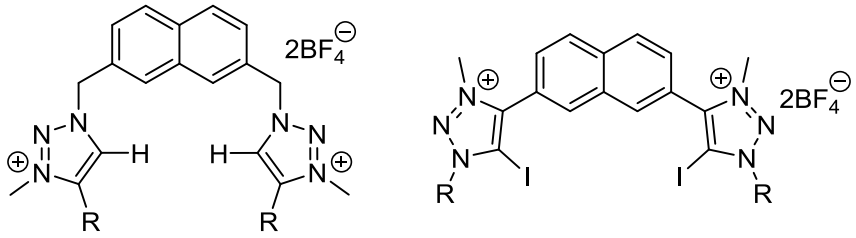


Figure 3-2: Naphthalene-containing anion receptors motifs, substituted by **a)** HB triazoliomethyl groups; and **b)** XB iodotriazolium groups.

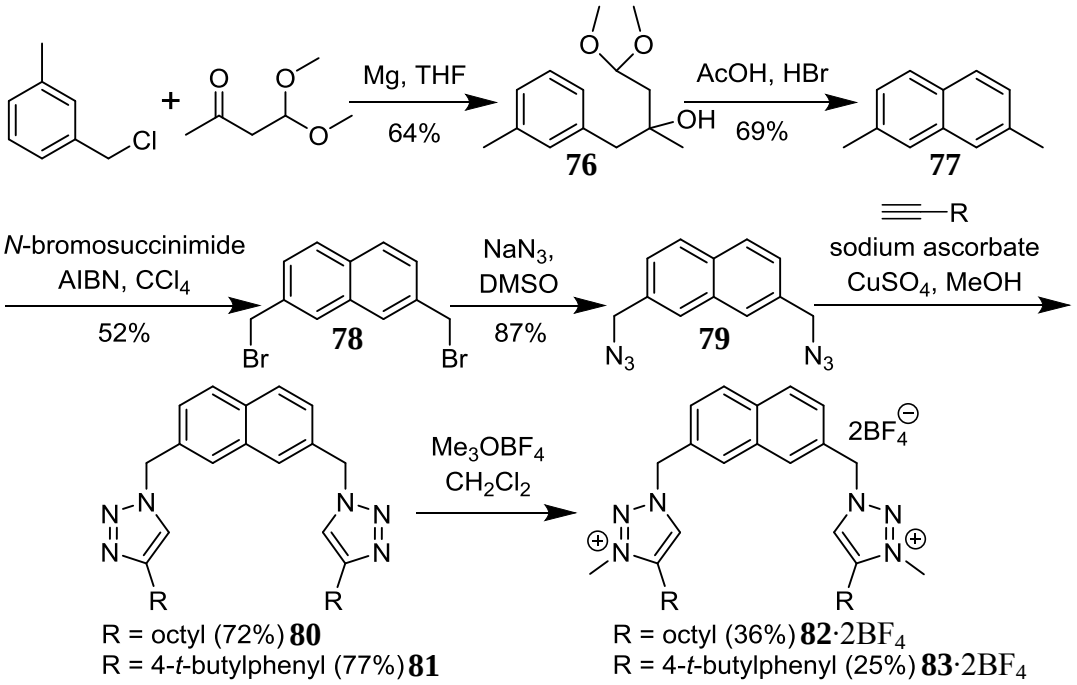
With the objective of increasing receptor preorganisation for stronger anion binding, a more rigid receptor was also devised in which XB functionalised triazolium groups were directly connected to the naphthalene. The resulting binding cavity is large enough to allow for convergent XB from iodine atoms substituted on the triazolium groups (**Figure 3-2b**). Following studies on acyclic systems, this 2,7-bis-iodotriazolium naphthalene motif was incorporated as an axle component into a rotaxane and the interlocked host's anion binding properties investigated.

3.3 *Naphthalene-Based Hydrogen Bonding Receptors*

3.3.1 *Synthesis of Acyclic Receptors*

The synthesis of naphthalene-based acyclic receptors **82**·$2BF_4$ and **83**·$2BF_4$ is shown in **Scheme 3-1**. Preparation of 2,7-bis(bromomethyl)naphthalene was performed according to a literature procedure.[8,9] A Grignard reaction was first undertaken between 3-methylbenzyl chloride and acetyl acetaldehyde dimethyl acetal, giving benzyl hydroxyacetal **76** in 64% yield. Treatment with glacial acetic acid and hydrobromic acid gave the ring-closed elimination product, 2,7-dimethylnapththalene **77** in 69% yield. A radical bromination reaction with *N*-bromosuccinimide in CCl_4, using AIBN as a radical initiator, afforded the 2,7-bis(bromomethyl)naphthalene product **78** (52%). Reaction with NaN_3 in DMSO gave the

corresponding bis-azide-substituted product **79** (87%), which upon a CuAAC (click) reaction with two equivalents of either 1-decyne or 1-ethynyl-4-*tert*-butylbenzene, in the presence of $CuSO_4$ and sodium ascorbate in MeOH, produced bis-triazole products **80** and **81** in 72% and 77% yield respectively. Methylation with $Me_3O{\cdot}BF_4$ gave bis-triazolium receptors **82**$\cdot 2BF_4$ and **83**$\cdot 2BF_4$ in 36% and 25% respective yields.



Scheme 3-1: Synthesis of bis-triazolium naphthalene receptors **82**$\cdot 2BF_4$ and **83**$\cdot 2BF_4$.

Crystals suitable for single crystal X-ray diffraction structural analysis were obtained for aryl-linked bis-triazole precursor **81**, and the corresponding bis-triazolium receptor **83**$\cdot 2BF_4$. Data were collected for full structure determination at 150 K, and data tables are given in **Appendix A**.

As shown in the crystal structures (**Figure 3-3**), both molecules adopt a relatively linear packing conformation in the solid state. The structure of **83**$\cdot 2BF_4$ exhibits weak hydrogen bonding interactions between the triazolium groups and the BF_4^- counterions, with C–H···F

distances in the range 2.305(3)–2.339(4) Å (%vdW$_{H,F}$ = 87–88%).[10]

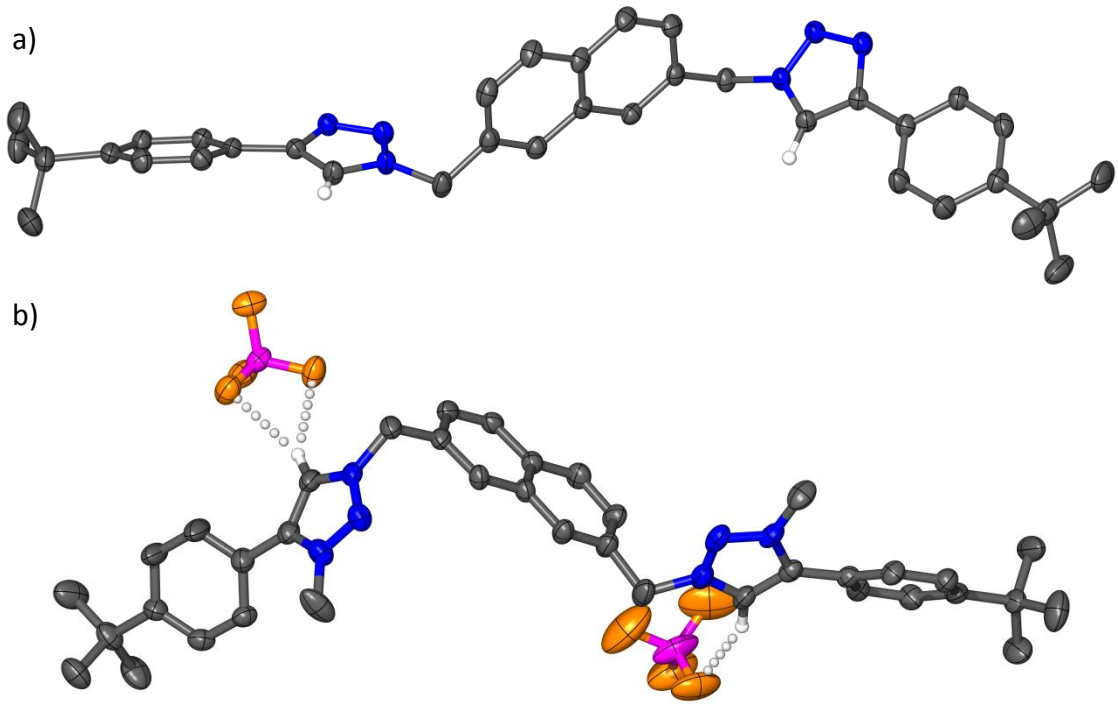


Figure 3-3: Single crystal structures of **a)** neutral bis-triazole precursor **81**; and **b)** the corresponding bis-triazolium receptor **83**·2BF$_4$. Disorder, non-acidic hydrogen and solvent atoms have been removed for clarity, and thermal ellipsoids are shown at 50% probability. The crystal structure of **81** contains two molecules in the asymmetric unit of similar conformation; only one is displayed in the figure.

3.3.2 *Anion Recognition Properties of HB Naphthalene-Based Receptors 82·2BF$_4$ and 83·2BF$_4$*

The anion binding properties of **82**·2BF$_4$ and **83**·2BF$_4$ were investigated using ^{1}H NMR titration experiments. The halide anions were studied in CD_3CN, while SO_4^{2-} binding required study in d_6-DMSO due to solubility constraints. Addition of the respective TBA salts to both receptors induced changes in the chemical shifts of the receptors' proton resonances, most notably those corresponding to the internal naphthalene proton *c* and the triazolium proton *d* (**Figure 3-4**). By monitoring the shifts of triazolium proton *d*, a 1:1 stoichiometric binding model was fitted to the data using WinEQNMR2[11] to determine

the association constants shown in **Table 3-1**.

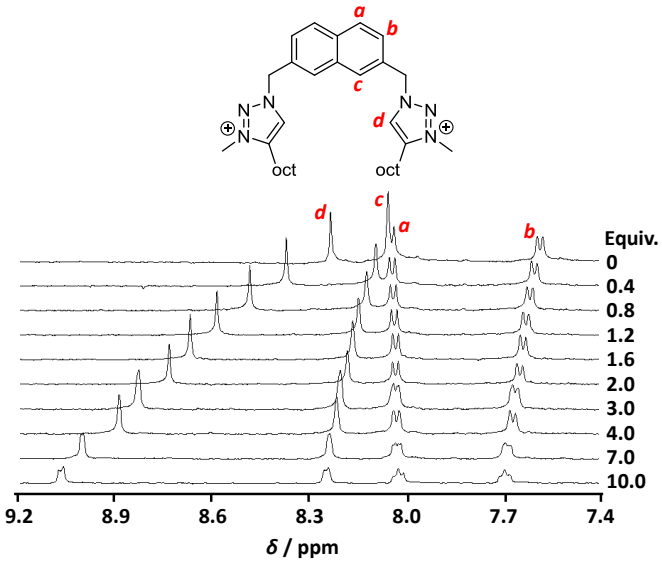


Figure 3-4: Truncated ^{1}H NMR spectra of **82**·2BF$_4$ upon addition of TBA·Cl (CD_3CN, 293 K, 500 MHz).

While oxoanion SO_4^{2-} was bound with the strongest affinity, which is expected due to its higher charge, the receptors exhibit a modest halide selectivity trend of $Cl^- > Br^- > I^-$. There also appears to be very little difference in the halide binding strength between alkyl- and aryl-appended receptors **82**$^{2+}$ and **83**$^{2+}$. Furthermore, with the exception of the association between **82**$^{2+}$ and Cl^-, all anions are bound more weakly than the analogous N-linked, HB carbazole-based receptors **24**$^{2+}$ and **25**$^{2+}$ (**§2.3.2.1**).

Table 3-1: Association constants, K_a (M^{-1}), obtained from ^{1}H NMR titrations, for acyclic receptors **82**$^{2+}$ and **83**$^{2+}$ with different anions. Errors are given in parentheses (CD_3CN, 293 K, 500 MHz).

	82^{2+}	**83**$^{2+}$
Cl^-	270(10)	231(6)
Br^-	101(1)	141(2)
I^-	90(2)	121(2)
SO_4^{2-} [a]	230(40)	400(40)

[a] Titration conducted in d_6-DMSO. K_a values were determined by monitoring the triazolium proton resonance.

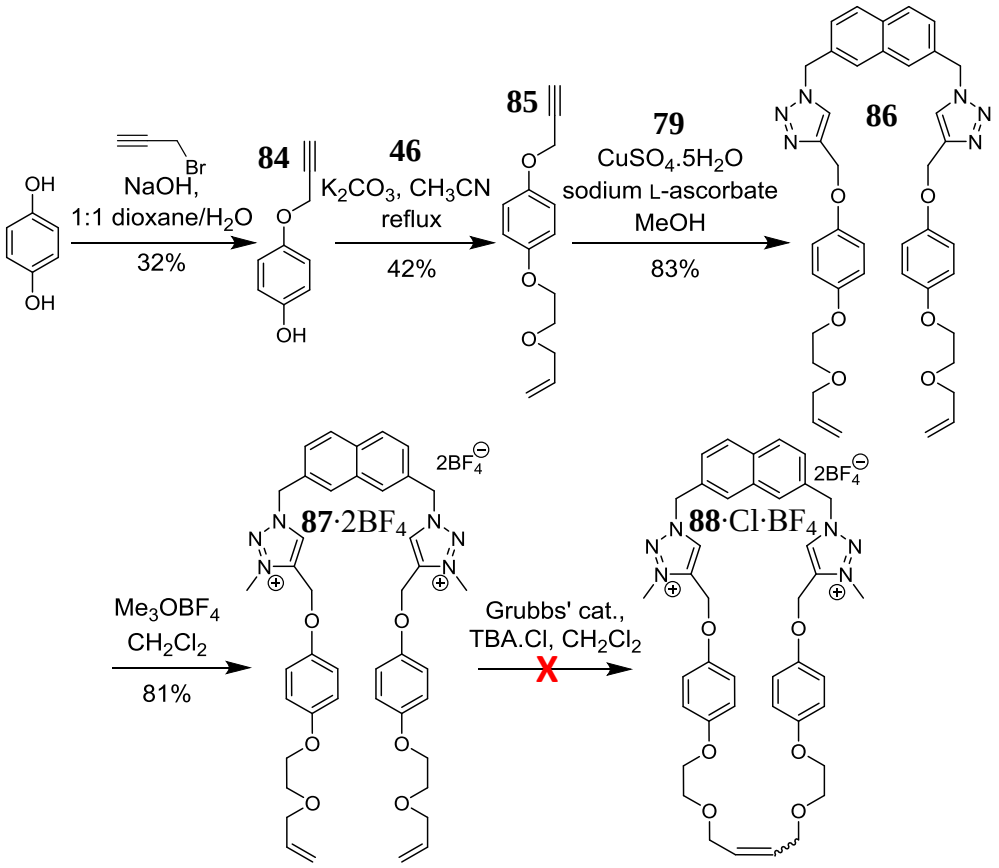
Consistent with the binding behaviour of carbazole-based receptors $\mathbf{24}^{2+}$ and $\mathbf{25}^{2+}$, SO_4^{2-} is bound more strongly by the aryl-appended receptor $\mathbf{83}^{2+}$. As discussed in **§2.3.2.1**, the strong affinity of the aryl-appended receptor is likely to be due to a highly complementary binding cavity for this anion. It is also noteworthy that the naphthalene-based receptors bind SO_4^{2-} with lower affinity than the carbazole-based receptors, which may be a consequence of the reduced preorganisation of naphthalene-based receptors $\mathbf{82}^{2+}$ and $\mathbf{83}^{2+}$ due to the presence of methylene spacer groups between the naphthalene and the triazolium motifs.

3.3.3 *Macrocycles and Pseudorotaxanes*

Following confirmation that the bis-triazole naphthalene motif was an effective anion receptor, attempts were then made to incorporate this functional group into macrocycles for potential use in the formation of interpenetrated assemblies.

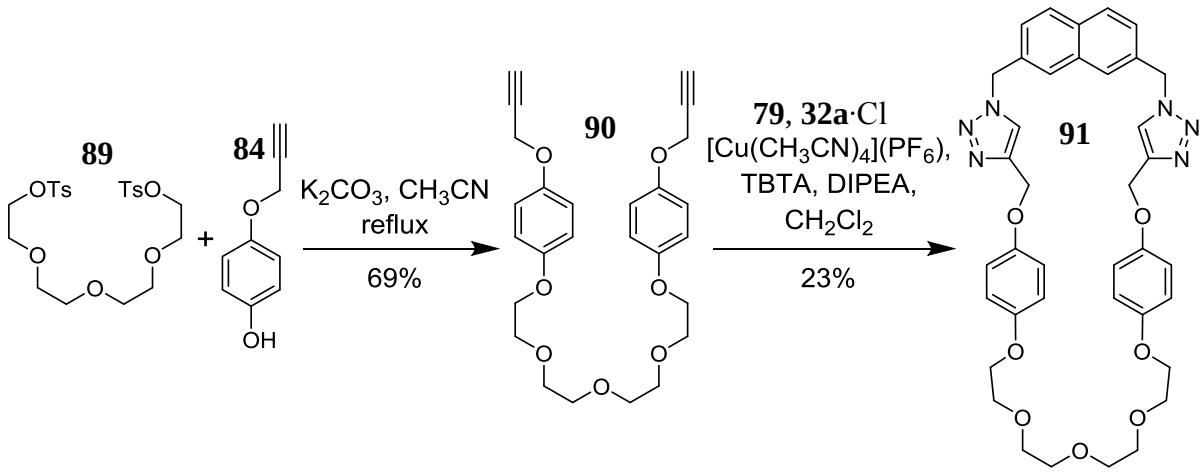
Initially, a bis-vinyl-appended macrocycle precursor containing the bis-triazole naphthalene motif was designed, which could undergo ring-closing metathesis (RCM) to form a macrocycle (**Scheme 3-2**). Hydroquinone was reacted with one equivalent of propargyl bromide in the presence of NaOH, affording mono-functionalised alkyne derivative **84** in 32% yield. Reaction with allyl-appended mesylate **46** in the presence of K_2CO_3 gave alkyne **85** in 42% yield. A CuAAC (click) reaction with bis-azide **79** produced the bis-triazole product **86** in 83% yield, and methylation afforded the corresponding bis-triazolium compound $\mathbf{87}\cdot 2BF_4$ (81%). Unfortunately, cyclisation attempts conducted in the presence of one equivalent of TBA·Cl as a potential template, using both 1st and 2nd generation Grubbs' catalysts, were not successful in forming macrocycle $\mathbf{88}^{2+}$. Only starting material was observed after an extended reaction period, which is difficult to rationalise considering Grubbs' catalyst has previously been successfully used in the presence of similar triazolium-

containing molecules.[12]



Scheme 3-2: Attempted synthesis of ring-closed bis-triazolium macrocycle **88**·Cl·BF_4.

Considering the clipping strategy *via* RCM was not suitable for forming interlocked structures with the naphthalene-based system, the stoppering approach was investigated as an alternative synthetic route to obtain a rotaxane. Naphthalene-based macrocycle **91** was prepared *via* a CuAAC (click) cyclisation reaction (**Scheme 3-3**). Bis-tosylate polyether **89** was reacted with mono-alkyne functionalised hydroquinone **84** in the presence of K_2CO_3, to afford bis-propargyl-appended precursor **90** in 69% yield. Reaction with one equivalent of bis-azide **79**, in the presence of bis-amide pyridinium chloride template **32a**·Cl under CuAAC (click) conditions, gave macrocycle **91** in 23% isolated yield.



Scheme 3-3: Synthesis of neutral macrocycle **91**.

A quantitative ^{1}H NMR pseudorotaxane titration experiment was conducted in CD_2Cl_2, to determine the stability of an interpenetrated assembly formed between macrocycle **91** and bis-amide pyridinium chloride thread **32**·Cl. Upon addition of thread, an upfield shift of the macrocycle hydroquinone proton peaks *5* and *6* was observed indicating interpenetration (**Figure 3-5**). Downfield shifts were also observed for the triazole proton *4* and the internal naphthalene proton *3*, due to chloride coordination. WinEQNMR2[11] analysis of the shift in the mean hydroquinone peak position determined an apparent 1:1 stoichiometric association constant for pseudorotaxane formation of K_a = 46(3) M^{-1}. This is significantly lower than the association constant of an analogous pseudorotaxane assembly between thread **32**·Cl and an isophthalamide-based macrocycle (*cf.* $K_a > 10^4$ M^{-1} in CD_2Cl_2).[13]

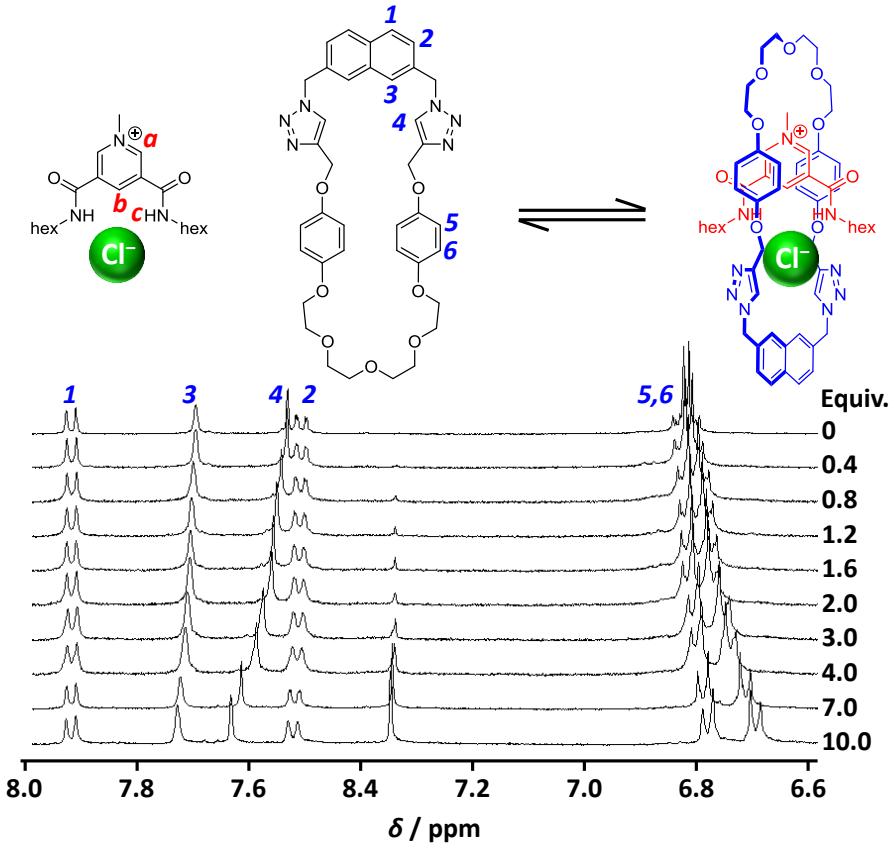
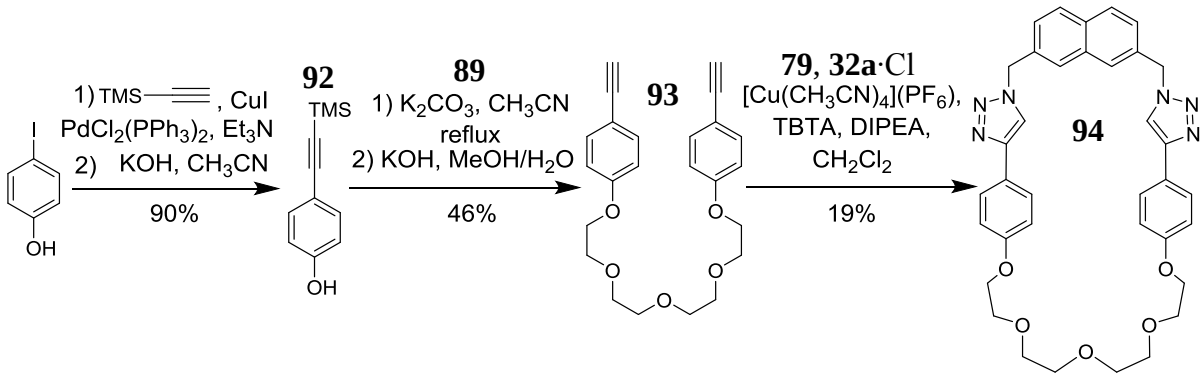


Figure 3-5: Truncated ^{1}H NMR spectra of macrocycle **91** upon addition of increasing equivalents of bis-amide pyridinium chloride thread **32a**·Cl (CD_2Cl_2, 293 K, 500 MHz).

In order to increase pseudorotaxane stability, a smaller, more preorganised macrocycle was prepared (**Scheme 3-4**). 4-Iodophenol was treated with TMS-acetylene under Sonogashira conditions, to afford 4-ethynylphenol **92** in 90% yield. Reaction with bis-tosylate **89** in the presence of K_2CO_3, followed by deprotection of the alkyne groups using KOH, gave bis-alkyne precursor **93** in 46% yield. A subsequent reaction with bis-azide compound **79** under CuAAC (click) conditions, in the presence of **32a**·Cl, produced macrocycle **94** in 19% yield.



Scheme 3-4: Synthesis of naphthalene-based macrocycle **94**.

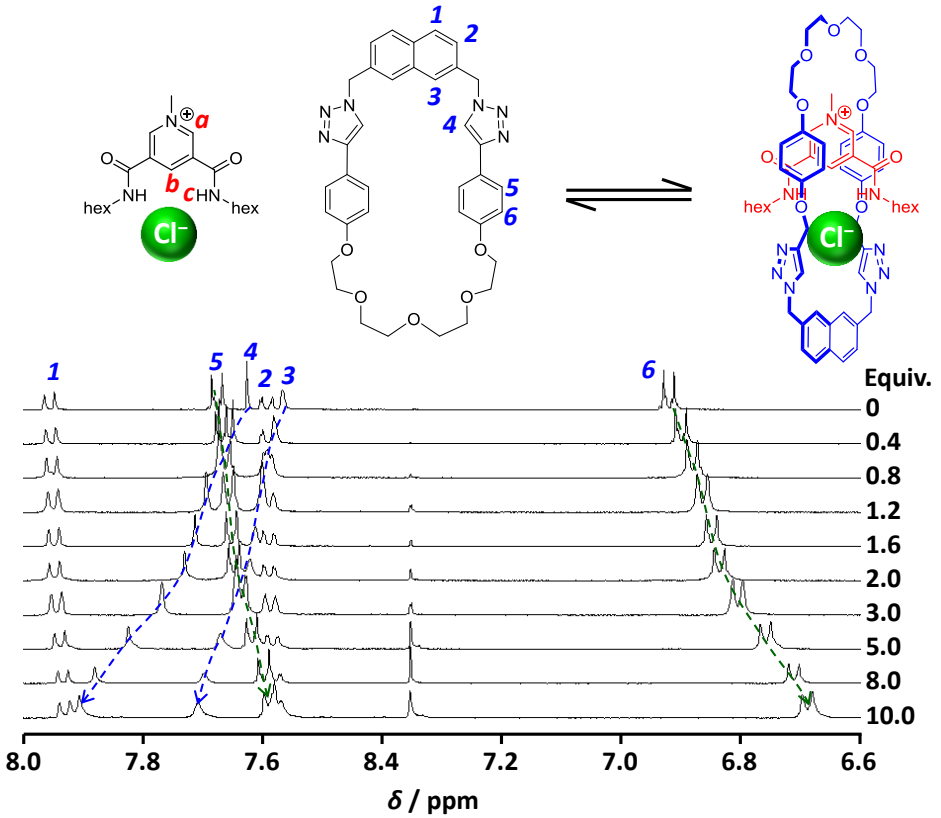


Figure 3-6: Truncated ^{1}H NMR spectra of macrocycle **94** upon addition of increasing equivalents of bis-amide pyridinium chloride thread **32a**·Cl (CD_2Cl_2, 293 K, 500 MHz).

An analogous ^{1}H NMR pseudorotaxane titration experiment was performed between macrocycle **94** and bis-amide pyridinium chloride thread **32a**·Cl in CD_2Cl_2. Upfield shifts in the phenylene protons *5* and *6* were noted indicating interpenetration (**Figure 3-6**), as well as

downfield shifts of the triazole proton *4* and the internal naphthalene proton *3*, due to binding of Cl^- within the macrocycle receptor cavity. WinEQNMR2[11] analysis of the mean value of the phenylene resonances *5* and *6* determined an apparent 1:1 stoichiometric association constant of $K_a = 50(1)$ M^{-1} which disappointingly again indicated a weak interpenetrative assembly.

Although the naphthalene-based macrocycles **91** and **94** were shown to form interpenetrated assemblies with bis-amide pyridinium chloride thread **32a**·Cl, the stabilities of these pseudorotaxane species were too weak to warrant attempts at forming analogous rotaxanes. Considering these results, the design of the naphthalene receptor system was modified to create a more rigid, preorganised anion recognition motif by removing the methylene units between the naphthalene and triazolium groups.

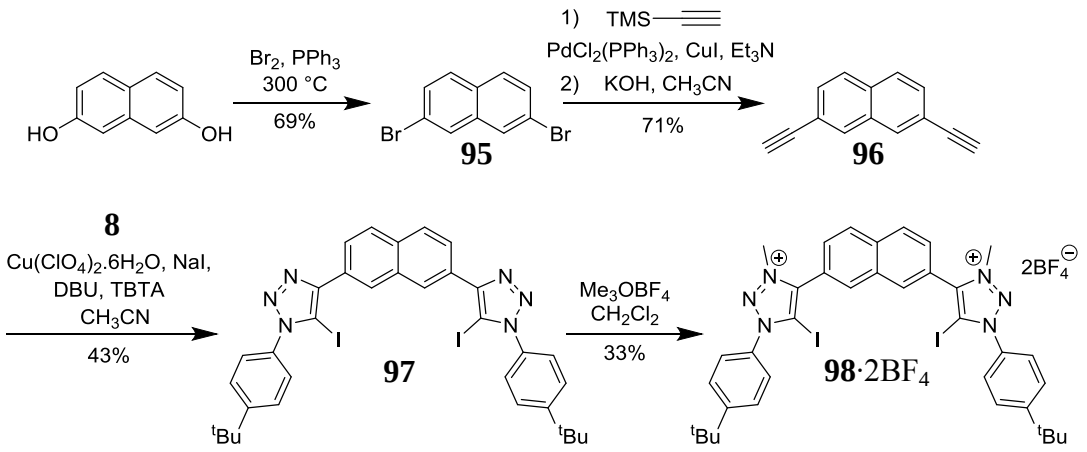
3.4 *Naphthalene-Based XB Receptor*

3.4.1 *Synthesis of Acyclic XB Bis-Iodotriazolium Naphthalene Receptor*

The most direct route to form both HB and XB receptors based on the 2,7-bis-triazolium naphthalene motif was *via* 2,7-diethynylnaphthalene **96**, which can be synthesised from 2,7-dibromonaphthalene **95** using a Sonogashira coupling reaction.[14]

The synthesis of the bis-iodotriazolium naphthalene acyclic receptor is shown in **Scheme 3-5**. Triphenylphosphine was reacted with bromine to form the activated brominating agent triphenylphosphine dibromide. Treatment with 2,7-dihydroxynaphthalene, followed by heating to ~300 °C for 2 h,[15] produced the desired product dibromonaphthalene **95** in 69% yield. Reaction with TMS-acetylene under Sonogashira conditions[14] afforded diethynylnaphthalene **96** in 71% yield, and treatment with azide **8** under the Brotherton one-

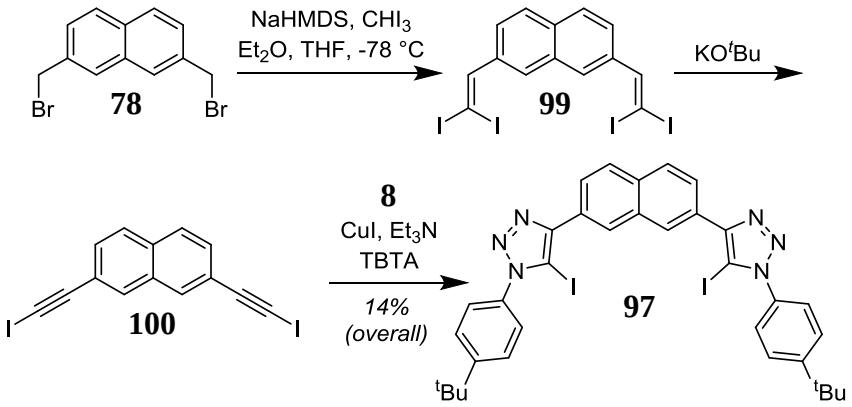
pot click conditions[16] (see **§2.3.1**) gave bis-iodotriazole **97** in 43% yield. Methylation gave the corresponding bis-iodotriazolium **98**·2BF_4 in 33% yield (**Scheme 3-5**).



Scheme 3-5: Synthesis of bis-iodotriazolium **98**·2BF_4.

A synthetic procedure was recently reported which converted benzylic bromide-based precursors to the corresponding aryl iodoalkyne in a one-pot reaction.[17] It was realised that it might be possible to use this reaction to synthesise 2,7-bis(iodoethynyl)naphthalene from 2,7-bis(bromomethyl)naphthalene **78**, providing an alternative route to form the iodotriazole intermediate **97**. The one-pot synthetic procedure is given in **Scheme 3-6**. A homologation reaction was performed by first reacting NaHMDS with CHI_3 to form a carbene, which was subsequently reacted with 2,7-bis(bromomethyl)naphthalene **78** to give the corresponding bis(*gem*-iodoalkene) intermediate **99**. Treatment with potassium *tert*-butoxide afforded bis(iodoethynyl)naphthalene **100**. Unfortunately, this compound was found to be highly light-sensitive, and isolation inevitably resulted in partial decomposition to the mono- and bis-protoalkyne forms. This gave an impure material for the iodotriazole reaction, thus resulting in a prohibitively difficult separation of the triazole products. As a result, the CuAAC (click) reagents were added directly to the reaction mixture without isolation of the

iodoalkyne intermediate **100**. The reaction was treated with CuI, Et_3N, TBTA and two equivalents of azide **8**, giving bis-iodotriazole **97** in 14% overall isolated yield.



Scheme 3-6: Synthesis of iodotriazole **97** *via* iodoalkyne.

Due to the low yields obtained *via* this reaction method, it was discarded in favour of the Sonogashira-coupling route described previously.

3.4.2 *Anion Recognition Properties of XB Naphthalene-Based Receptor 98·2BF$_4$*

^{1}H NMR anion titration experiments were conducted on **98**·2BF_4 in d_6-DMSO. Similarly to the XB carbazole-based systems (**§2.3.2.2**), the anion association properties were investigated indirectly by monitoring the signal of a proton proximal to the binding site. However, in contrast to the XB carbazole-based systems, the internal naphthalene proton signal did not shift significantly upon addition of anions. In fact, the proton resonance which gave the largest anion-induced perturbation was the iodotriazolium methyl group.

As shown in **Figure 3-7**, addition of halide anions resulted in a modest upfield shift of the iodotriazolium methyl proton resonance. However, these shifts were of insufficient magnitude to accurately determine association constants for receptor **98**$^{2+}$. Nevertheless, there is a clear anion-induced response, suggesting that this XB receptor is an effective anion host.

In contrast to the halide response, SO_4^{2-} addition caused the iodotriazolium methyl proton signal to shift significantly upfield until ~1 equivalent, after which a downfield perturbation was observed (**Figure 3-8a**). This behaviour indicates a strong 1:1 stoichiometric association followed by a 1:2 host:guest binding component, which could not be quantified.

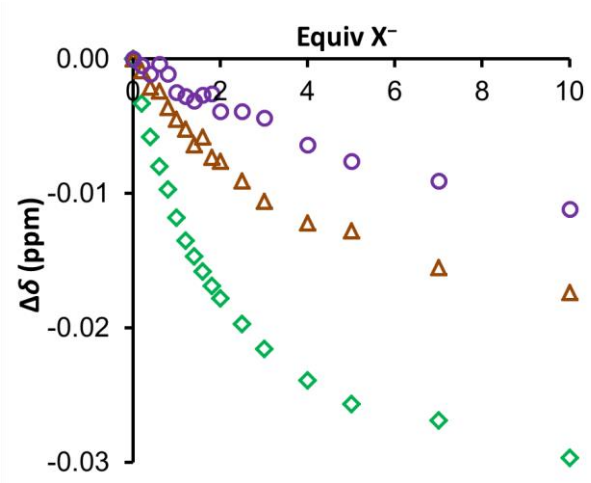


Figure 3-7: Experimental titration data for receptor **98**$^{2+}$ upon addition of ◇ Cl^-, △ Br^- and ○ I^-, following the iodotriazolium methyl proton (d_6-DMSO, 293 K, 500 MHz).

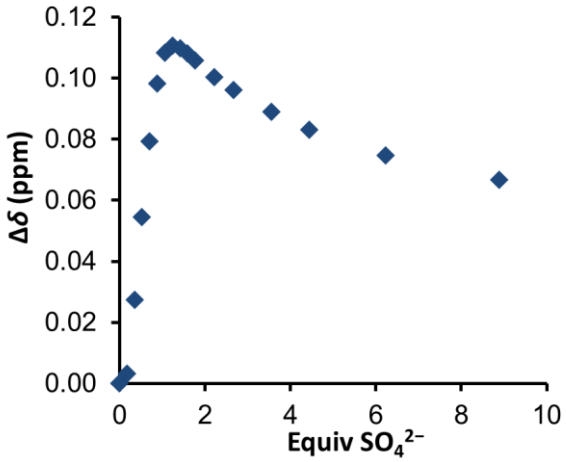


Figure 3-8: The ^{1}H NMR titration data for receptor **98**$^{2+}$ upon addition of $TBA_2{\cdot}SO_4$, following the iodotriazolium methyl proton (d_6-DMSO, 293 K, 500 MHz).

3.5 *XB Interpenetrated and Interlocked Molecules*

3.5.1 *Pseudorotaxane Assembly Investigations*

The feasibility of integration of the bis-iodotriazolium naphthalene motif into interlocked systems was investigated initially *via* a qualitative ^{1}H NMR titration pseudorotaxane assembly experiment, mixing equimolar amounts of thread **98**$^{2+}$, isophthalamide-based macrocycle **33** and TBA·Cl in d_6-acetone. As seen in **Figure 3-9**, a diagnostic upfield shift of macrocycle hydroquinone protons *5* and *6* is observed, which is indicative of interpenetration (**§2.4.1**). There are also significant downfield shifts of the macrocycle cavity protons *3* and *4*, due to interaction with the Cl^- anion template.

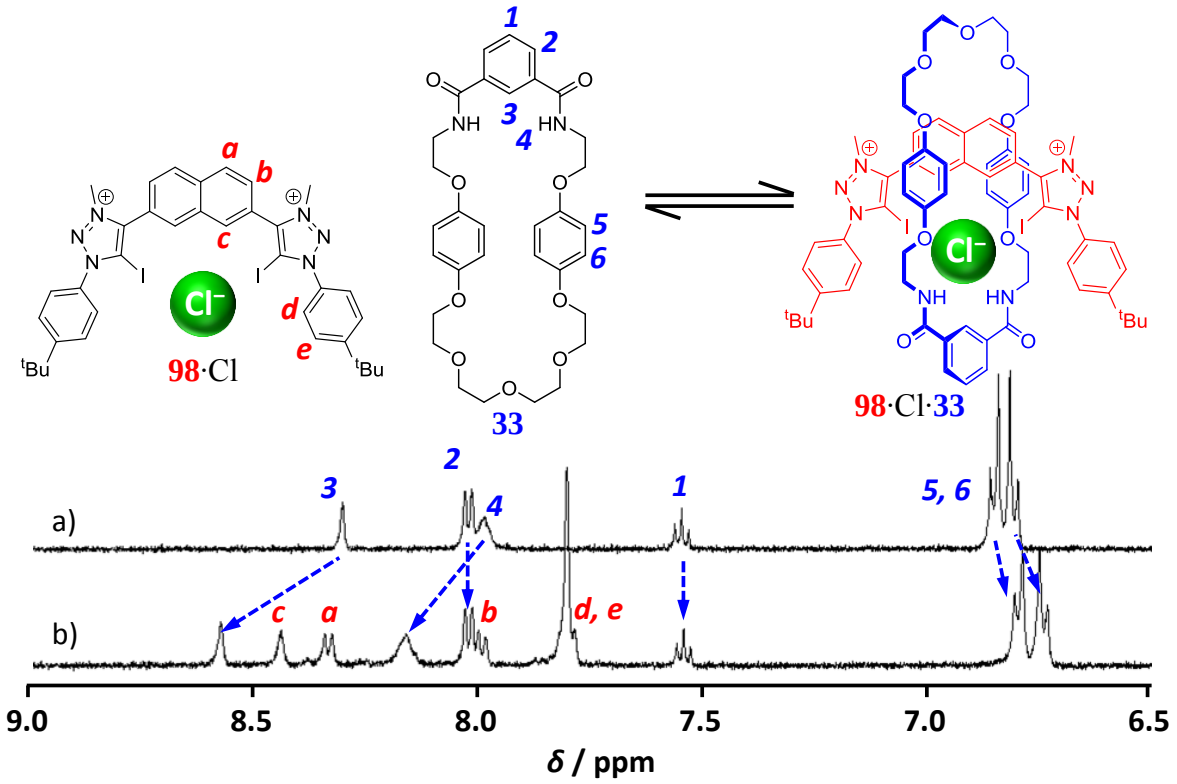
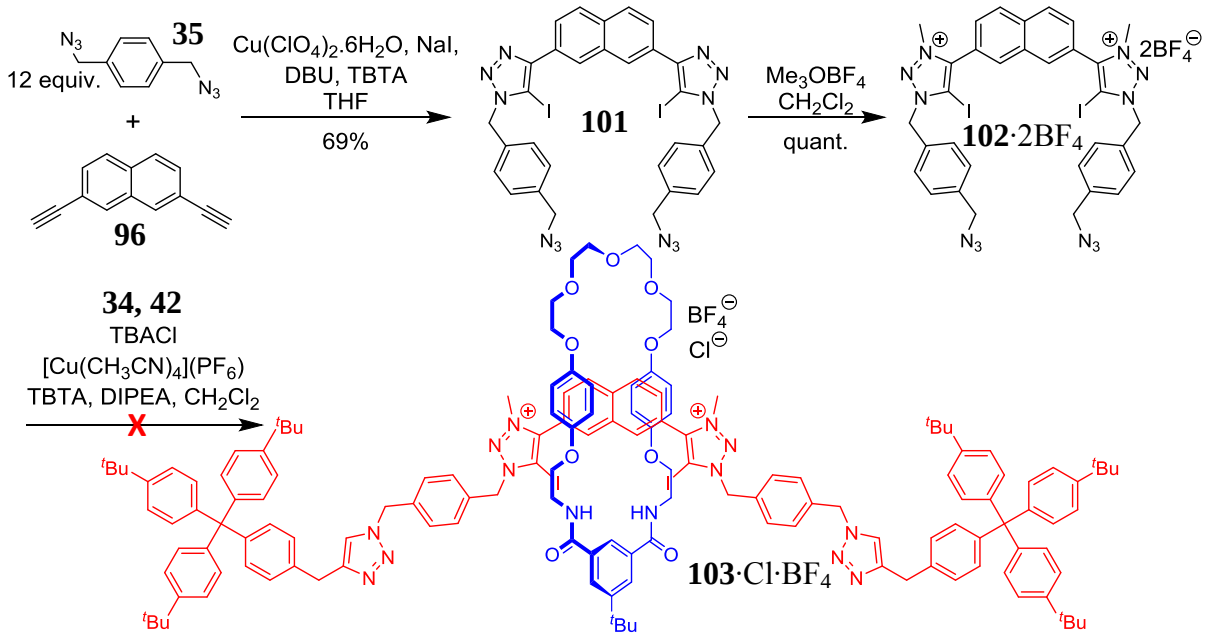


Figure 3-9: ^{1}H NMR spectra of **a)** naphthalene-based thread **98**·Cl; and **b)** after addition of isophthalamide-containing macrocycle **33** (d_6-acetone, 293 K, 500 MHz).

3.5.2 *Attempted Synthesis of Napthalene-Based Rotaxane by Stoppering Methodology*

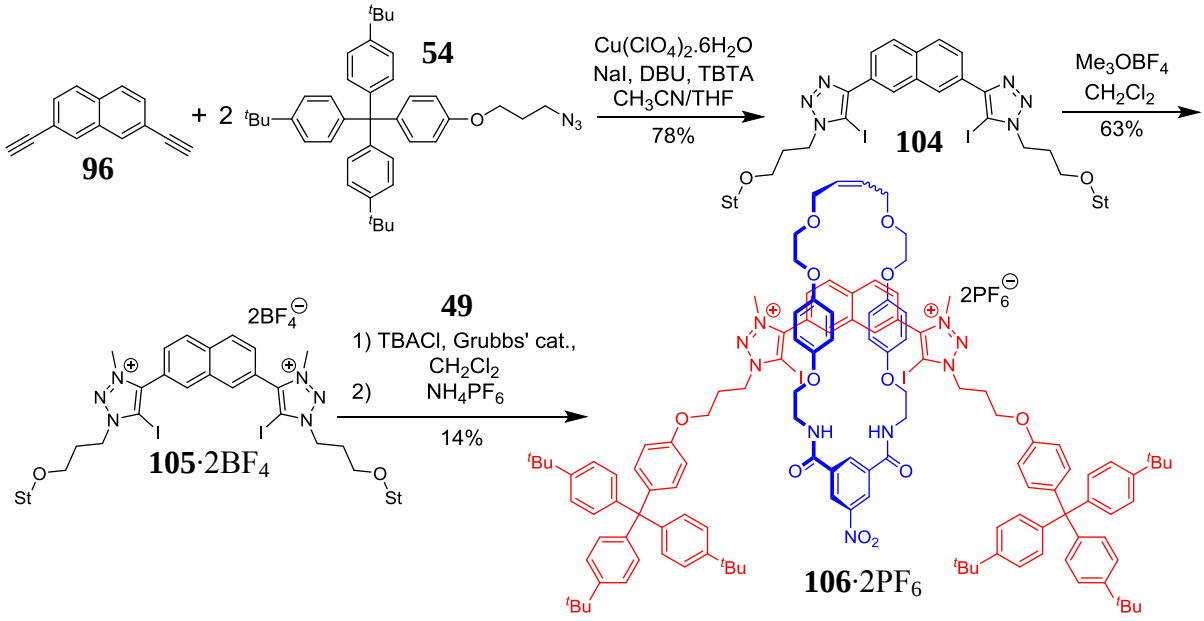
Attempts were made to synthesise a rotaxane containing bis-iodotriazolium naphthalene-based axle and isophthalamide macrocycle components using a CuAAC (click) stoppering synthetic approach (**Scheme 3-7**). 2,7-Diethynylnaphthalene **96** was reacted with an excess of bis-azide compound **35** in the presence of the Brotherton one-pot reagents,[16] to form bis-iodotriazole naphthalene **101** in 69% yield. Methylation produced the corresponding bis-iodotriazolium naphthalene **102**·2BF_4 in quantitative yield. This precursor was treated with isophthalamide-based macrocycle **34** and two equivalents of stopper alkyne **42**, TBA·Cl and [$Cu(CH_3CN)_4$](PF_6), TBTA and DIPEA to catalyse the CuAAC reaction. Unfortunately, while formation of the stoppered axle was observed, there was no evidence from mass spectrometry for rotaxane **103**$^{2+}$ being produced.



Scheme 3-7: Attempted synthesis of naphthalene-containing rotaxane **103**·Cl·BF_4 by stoppering methodology.

3.5.3 *Synthesis of Naphthalene-Based Rotaxane by Clipping Methodology*

Considering the stoppering approach was unsuccessful, an alternative ring-closing methodology was explored to prepare a rotaxane containing a bis-iodotriazolium naphthalene-based axle component. This approach had been successfully utilised in forming the analogous carbazole-based rotaxane **60**$^{2+}$ (**§2.4.3.2**).



Scheme 3-8: Synthesis of bis-iodotriazolium naphthalene-based rotaxane **106**·2PF_6.

The synthetic procedure undertaken to form the target rotaxane by the 'clipping' method is presented in **Scheme 3-8**. 2,7-Diethynylnaphthalene **96** is reacted with two equivalents of azide-appended stopper **54** under the Brotherton one-pot click conditions, to afford bis-iodotriazole axle precursor **104** in 78% yield. Methylation gave the bis-iodotriazolium axle component **105**·2BF_4 (36% yield), which was treated with an equimolar amount of bis-vinyl-appended macrocycle precursor **49** and TBA·Cl, in the presence of Stewart-Grubb's catalyst. Following chromatographic purification and anion exchange for the PF_6^- counteranion, naphthalene-based rotaxane **106**·2PF_6 was isolated in 14% yield and

characterised by ^{1}H NMR and ^{13}C NMR spectroscopy, high-resolution mass spectrometry and ^{1}H–^{1}H ROESY NMR spectroscopy.

As shown in the assigned ^{1}H NMR spectrum (**Figure 3-10**), proton signals for both macrocycle and axle are observed. Importantly, the hydroquinone protons *6* and *7* at ~6.5 ppm are split, which is a diagnostic feature that indicates the macrocycle is part of an interlocked molecule.

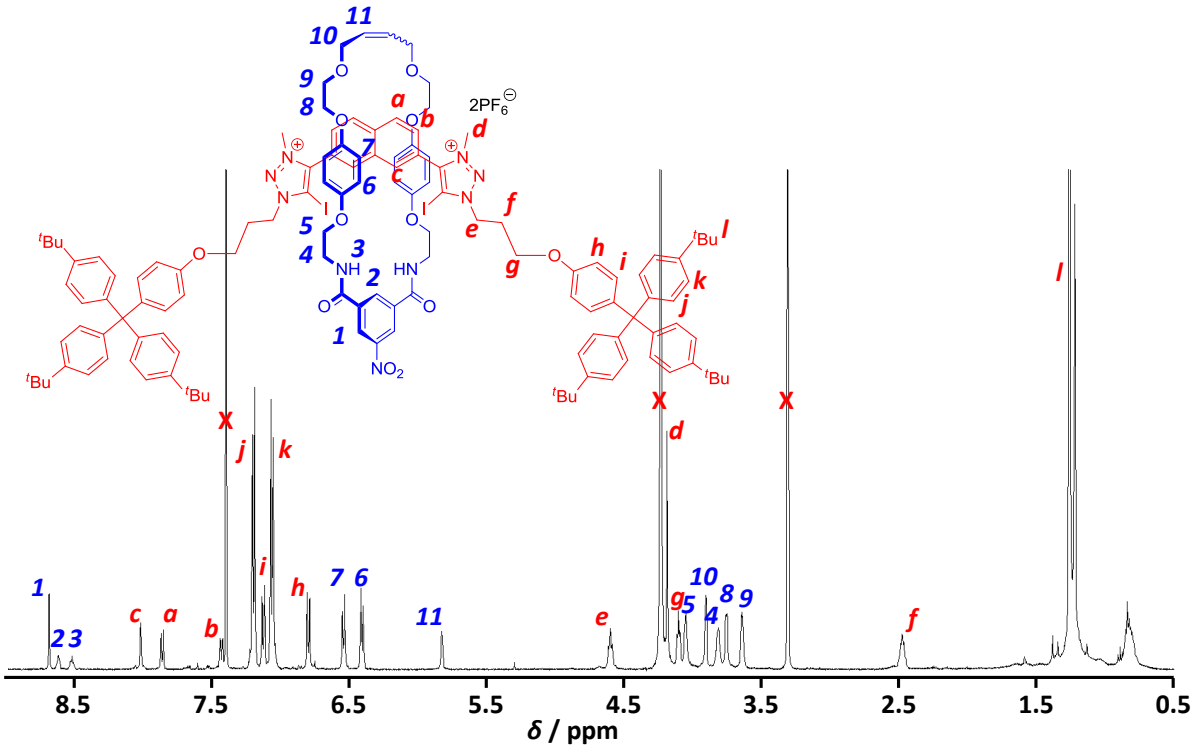


Figure 3-10: Assigned ^{1}H NMR spectrum of rotaxane **106**·2PF_6 (4:1 $CDCl_3$/MeOD, 298 K, 500 MHz). Red 'X's denote solvent peaks.

Additional evidence for the interlocked nature of rotaxane **106**·2PF_6 was obtained from ^{1}H–^{1}H ROESY NMR spectroscopy (**Figure 3-11**). Within the range shown, there are cross-component interactions observed between macrocycle alkene proton *11* and axle triazolium methyl proton *d* (cross-peak 1); macrocycle hydroquinone protons *6* and *7*, and axle

triazolium methyl proton *d* (cross-peak 2); and macrocycle hydroquinone protons *6* and *7*, and axle internal naphthalene proton *c* (cross-peak 3).

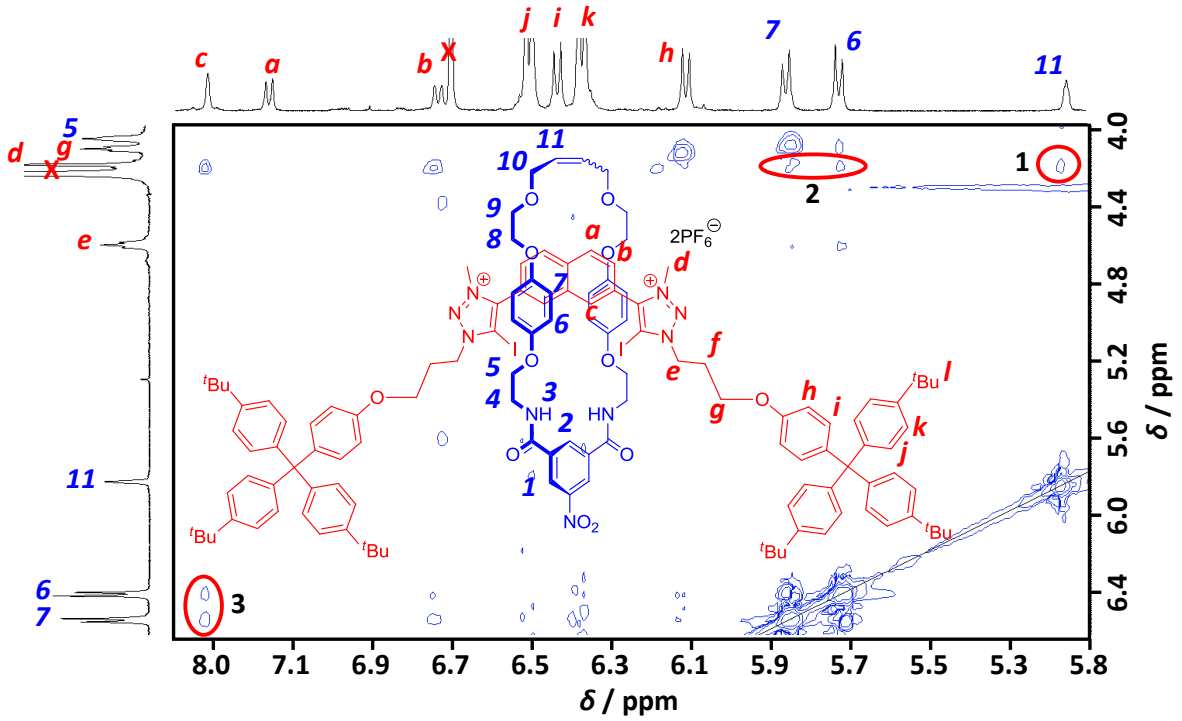


Figure 3-11: Expanded ^{1}H–^{1}H ROESY NMR spectrum of rotaxane **106**·2PF$_6$ (4:1 CDCl$_3$/MeOD, 298 K, 500 MHz). Red 'X's denote solvent peaks.

3.5.4 *Anion Recognition Properties of Rotaxane 106·2PF$_6$*

The anion binding properties of **106**·2PF$_6$ were studied using ^{1}H NMR anion titration experiments in 1:1 CDCl$_3$/CD$_3$OD. Upon addition of anions as their TBA salts, the most notable changes observed in the rotaxane proton signals were of the internal macrocycle proton *2*, which is directly involved in anion binding (**Figure 3-12**). In contrast to the acyclic receptor **98**$^{2+}$, *downfield* shifts were observed for the iodotriazolium methyl proton. The titration data were analysed using WinEQNMR2[11] by following the changes in the chemical shift of the macrocycle internal isophthalamide proton *2*, resulting in the binding isotherms shown in **Figure 3-13**, and determining the 1:1 association constants shown in **Table 3-2**.

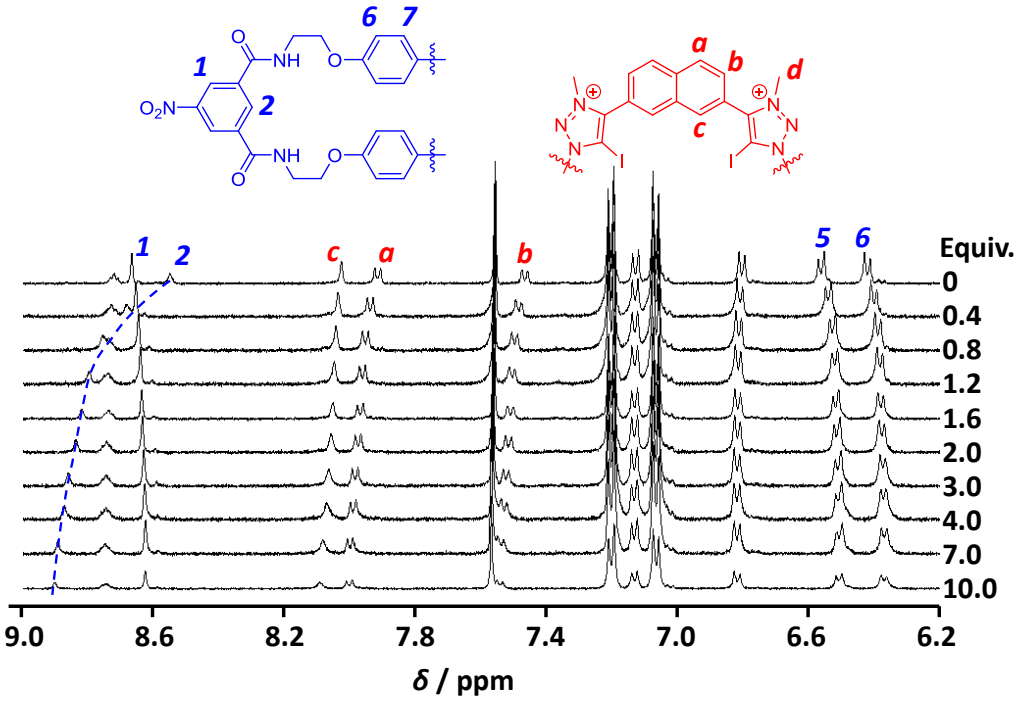


Figure 3-12: Truncated ^{1}H NMR spectra of **106**·2PF$_6$ upon addition of TBA·Cl (1:1 $CDCl_3$/CD_3OD, 293 K, 500 MHz).

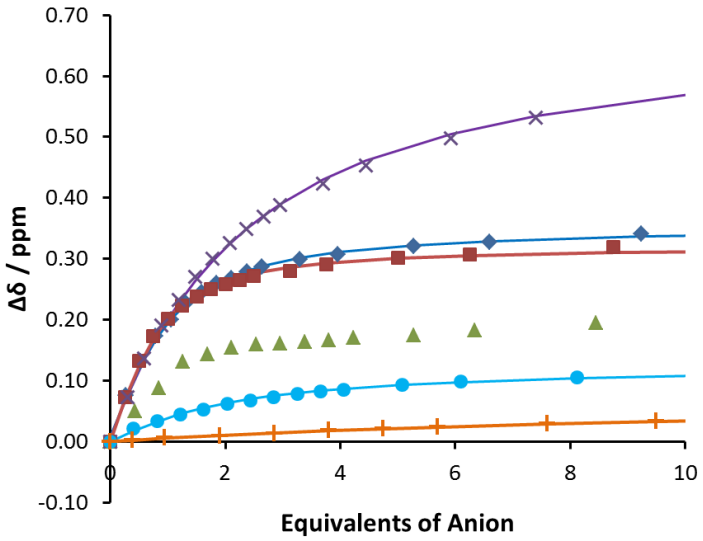


Figure 3-13: Experimental titration data (points) and fitted binding isotherms (lines) for the addition of ◆ Cl^-, ■ Br^-, ▲ I^-, ● AcO^-, ✕ $H_2PO_4^-$, and + NO_3^- anions to rotaxane **106**·2PF$_6$, monitoring the internal isophthalamide proton signal. Association with iodide was too strong for WinEQNMR2[11] to accurately quantify (1:1 $CDCl_3$/CD_3OD, 293 K, 500 MHz).

As shown in **Table 3-2**, in 1:1 $CDCl_3/CD_3OD$ there is a binding preference for the halides over the oxoanions, with a selectivity trend of $I^- >> Br^- > Cl^- > AcO^- > H_2PO_4^- > NO_3^-$. Iodide was bound with an association constant, $K_a > 10^4$ M^{-1} in 1:1 $CDCl_3/CD_3OD$, thus it was necessary to use the more competitive solvent mixture 45:45:10 $CDCl_3/CD_3OD/D_2O$ to determine a quantitative value. These results suggest that the rotaxane interlocked cavity is complementary for spherical halide guest species, with a particularly strong affinity for iodide, which required study in an aqueous solvent mixture.

Table 3-2: Association constants, K_a (M^{-1}), obtained from ^1H NMR titrations, for rotaxane **106**·$2PF_6$ with different anions. Errors are given in parentheses (1:1 $CDCl_3/CD_3OD$, 293 K, 500 MHz).

	106^{2+}
Cl^-	890(40)
Br^-	1450(30)
I^- [a]	205(20)
AcO^-	443(8)
$H_2PO_4^-$	213(8)
NO_3^-	33(1)

[a] Titration conducted in 45:45:10 $CDCl_3/CD_3OD/D_2O$. K_a values were determined by monitoring the internal isophthalamide proton resonance.

Comparison of naphthalene-based rotaxane **106^{2+}** with the analogous carbazole-based rotaxane **60^{2+}** (**§2.4.4**) demonstrates the importance of preorganisation and complementarity in determining the host anion binding behaviour. Carbazole-based rotaxane **60^{2+}** was a sufficiently potent anion receptor to warrant study in the highly competitive solvent medium of 45:45:10 $CDCl_3/CD_3OD/D_2O$, and generally bound anions more strongly than its naphthalene-based counterpart. Both rotaxanes bind the halides more strongly than the oxoanions, though the halide preference of the two rotaxanes is different: carbazole-based rotaxane **60^{2+}** exhibits selectivity for Br^-, while naphthalene-based rotaxane **106^{2+}** binds I^- with the strongest affinity. Nevertheless, it is interesting to note that the carbazole-based system is still a more potent receptor for I^- (*cf.* K_a = 750(60) M^{-1} in 45:45:10

$CDCl_3/CD_3OD/D_2O$). The reduced binding affinity of naphthalene-based rotaxane **106**$^{2+}$ may be partially due to decreased preorganisation resulting from its longer axle component. Furthermore, the binding 'bite' angle of the convergent XB iodotriazolium groups is also different between the two axle receptor units, which would alter the binding strength and selectivity.

3.6 *Fluorescence Properties of XB Napthalene-Based Receptors*

It was hoped that the fluorescence properties of the naphthalene motif incorporated into the acyclic and rotaxane receptors might be exploited to sense anions. A preliminary fluorescence anion titration experiment was carried out on acyclic receptor **98**$^{2+}$, adding aliquots of TBA·Cl in CH_3CN. While the receptor did produce fluorescence emission, there was only a minor response upon addition of chloride, which was of insufficient magnitude to determine quantitative anion binding behaviour (**Figure 3-14**).

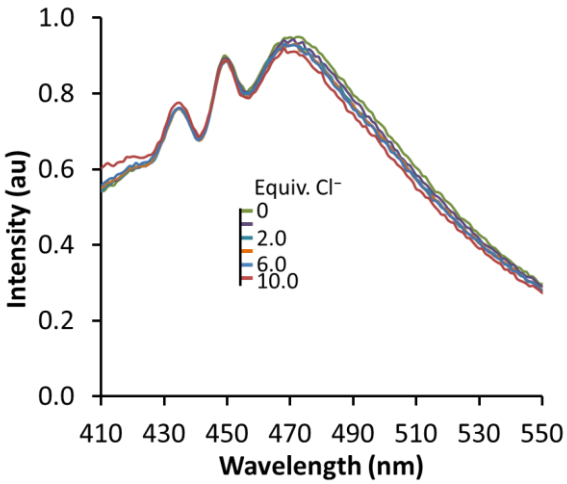


Figure 3-14: Fluorescence emission spectrum of receptor **98**·$2BF_4$ upon addition of TBA·Cl (λ_{ex} = 396 nm, CH_3CN, 293 K).

An analogous fluorescence titration experiment was also conducted on rotaxane **106**·$2PF_6$.

Once again, disappointingly there was no significant change in the fluorescence emission spectrum upon addition of the anion.

3.7 *Conclusions*

Two acyclic receptors based on the bis-triazolium naphthalene motif were synthesised, and shown to bind halide and sulfate anions in CD_3CN. With the intention of forming rotaxane interlocked molecules which incorporate this motif within a macrocycle component, a bis-vinyl-appended bis-triazolium macrocycle precursor was developed. However, RCM cyclisation attempts using Grubbs' catalysts were unsuccessful. Nevertheless, two neutral macrocycles were made and shown to form weak pseudorotaxane assemblies with a bis-amide pyridinium chloride thread.

A more rigid, preorganised acyclic receptor based on the XB 2,7-bis(iodotriazolium)-naphthalene motif demonstrated anion binding behaviour in d_6-DMSO. After establishing the formation of a chloride anion-templated pseudorotaxane assembly with an isophthalamide-based macrocycle, a novel XB rotaxane was synthesised *via* a ring-clipping methodology. This interlocked anion host was shown to be selective for I^- over halides and oxoanions, due to the size and shape complementarity of the rotaxane host's binding domain.

Disappointingly, the organic fluorophores naphthalene and carbazole proved to be inefficient anion sensing probes in the receptor systems studied. The integration of an anion responsive luminescent transition metal-based structural scaffold into XB receptors is discussed in the next chapter.

3.8 *References*

(1) Huang, W.; Su, H.; Yao, S.; Yang, Z.; Lin, H.; Lin, H. *J. Lumin.* **2011**, *131*, 1913.
(2) Langton, M. J.; Beer, P. D. *Chem. Eur. J.* **2012**, *18*, 14406.
(3) Zapata, F.; Caballero, A.; White, N. G.; Claridge, T. D. W.; Costa, P. J.; Félix, V. t.; Beer, P. D. *J. Am. Chem. Soc.* **2012**, *134*, 11533.
(4) Caballero, A.; Zapata, F.; White, N. G.; Costa, P. J.; Félix, V.; Beer, P. D. *Angew. Chem. Int. Ed.* **2012**, *51*, 1876.
(5) Sharma, D.; Sahoo, S.; Bera, R.; Kamal, R. *J. Fluoresc.* **2013**, *23*, 387.
(6) Kim, H.; Kang, J. *Tetrahedron Lett.* **2005**, *46*, 5443.
(7) Padilla-Tosta, M. E.; Fox, O. D.; Drew, M. G. B.; Beer, P. D. *Angew. Chem. Int. Ed.* **2001**, *40*, 4235.
(8) Wolinska-Mocydlarz, J.; Canonne, P.; Leitch, L. C. *Synthesis* **1974**, *1974*, 566.
(9) Katz, T. J.; Slusarek, W. *J. Am. Chem. Soc.* **1979**, *101*, 4259.
(10) Alvarez, S. *Dalton Trans.* **2013**, *42*, 8617.
(11) Hynes, M. J. *J. Chem. Soc., Dalton Trans.* **1993**, 311.
(12) White, N. G.; Costa, P. J.; Carvalho, S.; Félix, V.; Beer, P. D. *Chem. Eur. J.* **2013**, *19*, 17751.
(13) Hancock, L. M., *Anion-Templated Synthesis of Functional Interlocked Architectures*, DPhil Thesis, University of Oxford, 2011.
(14) Neenan, T. X.; Whitesides, G. M. *J. Org. Chem.* **1988**, *53*, 2489.
(15) Talele, H. R.; Chaudhary, A. R.; Patel, P. R.; Bedekar, A. V. *ARKIVOC* **2011**, *2011*, 15.
(16) Brotherton, W. S.; Clark, R. J.; Zhu, L. *J. Org. Chem.* **2012**, *77*, 6443.
(17) Pelletier, G.; Lie, S.; Mousseau, J. J.; Charette, A. B. *Org. Lett.* **2012**, *14*, 5464.

Chapter 4: Halogen Bonding Rhenium(I) Bipyridyl- and Diquat-Based Anion Receptors

4.1 *Introduction*

Transition metal complexes of hydrogen bond donor functionalised 2,2′-bipyridine derivatives have been previously exploited in the development of anion sensors (**§1.2.5.2**).[1] Acyclic,[2-4] macrocyclic,[5-8] and more recently, interlocked rotaxane receptor systems incorporating transition metal bipyridyl complexes have been shown to be capable of sensing anions in solution,[9,10] and with the latter class of receptor, also when immobilised on surfaces.[11] For example, the rotaxane in **Figure 4-1** was shown to be selective for Cl^- over oxoanions in 9:1 acetone/water, and sensed anions *via* an increase in the MLCT luminescence emission intensity of the rhenium(I) bipyridyl-based metal complex.[9]

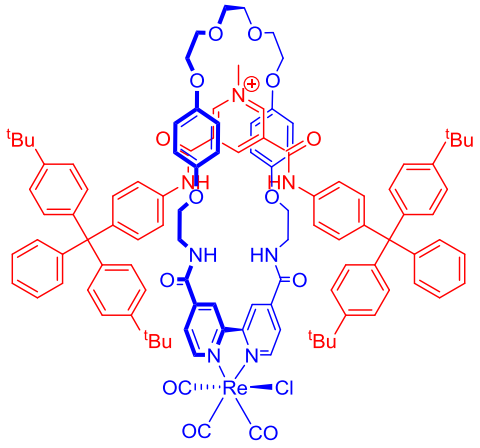


Figure 4-1: Structure of Beer's rhenium(I) bipyridine-containing rotaxane.

4.2 *Outline*

In this chapter the synthesis of a new XB receptor group that contains a photo-active rhenium(I) bipyridyl complex was investigated. The motif shown in **Figure 4-2a** was targeted, in which the bipyridyl ligand is substituted at the 4,4′-positions with XB iodotriazole groups. Acyclic XB and HB rhenium(I) bipyridyl receptors were prepared, and

their anion binding and sensing properties studied. Incorporating the XB rhenium(I) bipyridyl motif into the macrocyclic component of a rotaxane host enabled anions to be recognised and sensed in competitive aqueous solvent media purely through XB interactions.

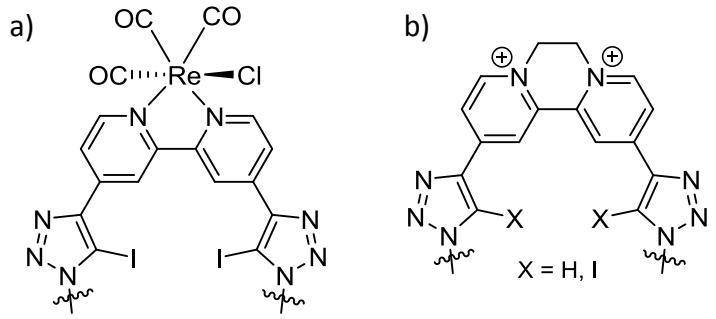


Figure 4-2: The 4,4′-bis-iodotriazole-2,2′-bipyridyl receptor motifs under investigation: **a)** rhenium(I) bipyridyl complex; and **b)** diquat.

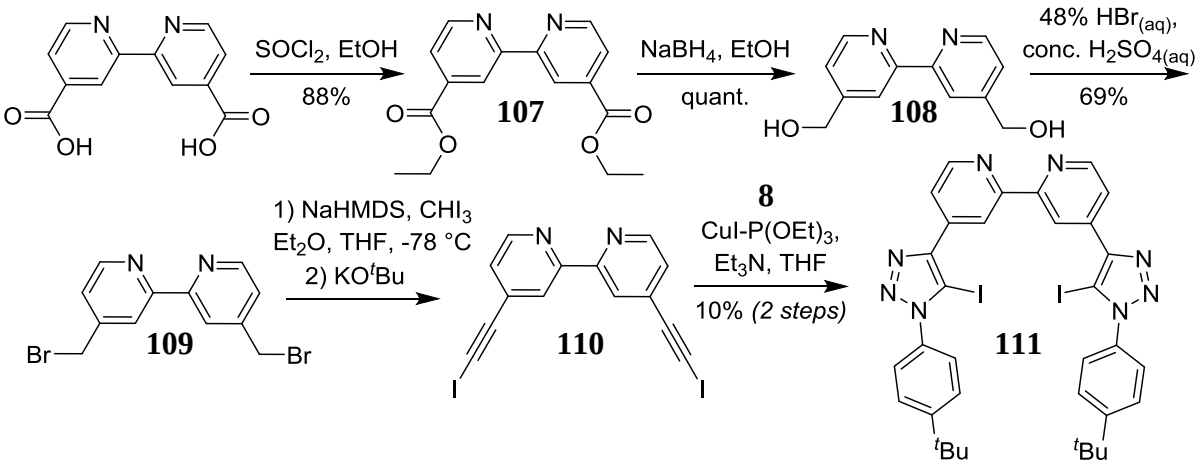
The dicationic, redox-active, preorganised diquat motif has surprisingly not been previously utilised as an anion receptor component. The synthesis of acyclic diquat-based XB and HB anion receptors (**Figure 4-2b**) was explored, including attempts to construct an all-XB rotaxane that contained a diquat-based axle.

4.3 *Acyclic Rhenium(I) Bipyridyl Receptors*

4.3.1 *Synthesis of Acyclic Receptors*

As mentioned in **§3.4.1**, the one-pot synthesis of iodoalkynes from the corresponding benzyl bromide species was recently reported.[12] It was hoped that this synthetic route could be adapted for the preparation of 4,4′-bis-iodoethynyl-2,2′-bipyridine **110**. The starting material, 4,4′-bis-bromomethyl-2,2′-bipyridine **109**, was synthesised as shown in **Scheme 4-1**. Esterification of 2,2′-bipyridine-4,4′-dicarboxylic acid with ethanol afforded bis-ethyl ester **107** in 88% yield. Reduction with $NaBH_4$ gave bis-hydroxymethyl-functionalised **108** in

quantitative yield, which was treated with 48% $HBr_{(aq.)}$ and concentrated H_2SO_4 to give the bis-bromo product **109** in 69% yield.



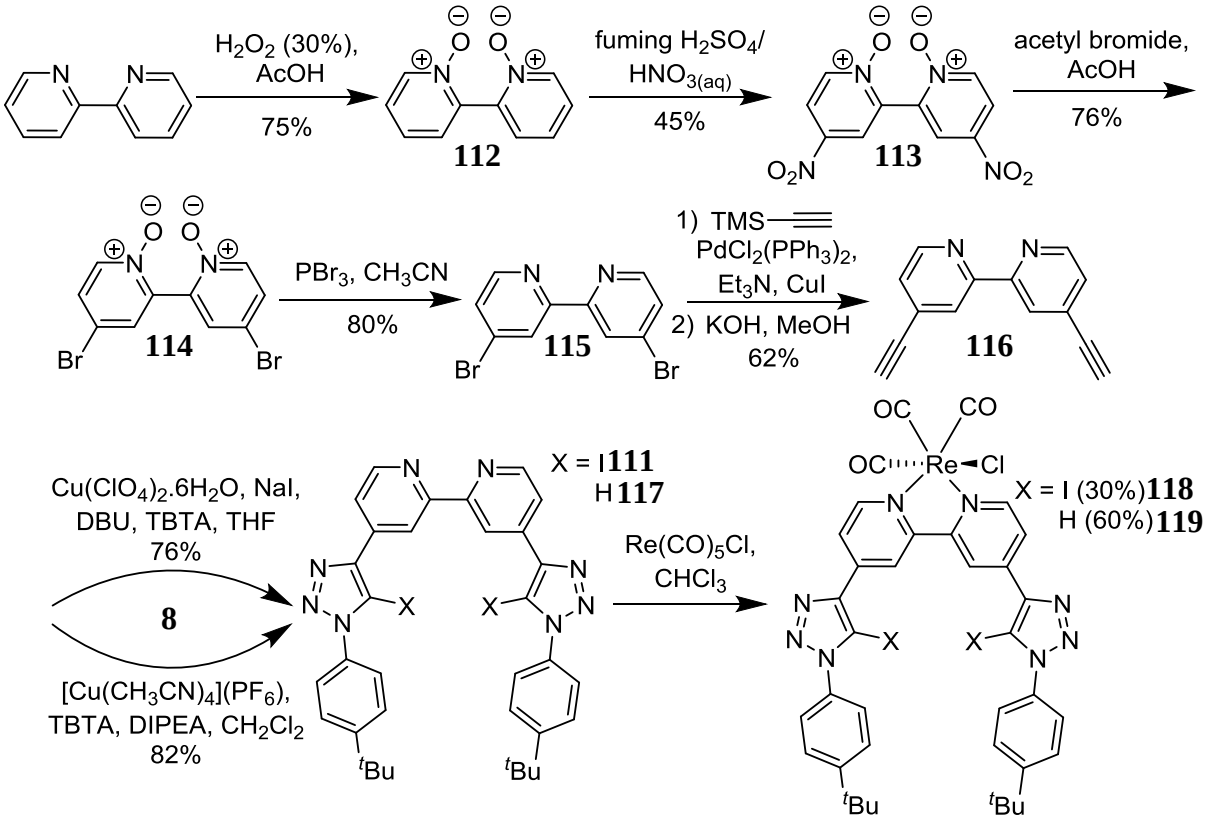
Scheme 4-1: Synthesis of bis-iodotriazole bipyridine precursor **111**.

Previously-described one-pot conditions[12] (**§3.4.1**) were employed to convert the bromomethyl precursor to bis-iodoalkyne compound **110**. Unfortunately this intermediate was highly unstable to light, so it was necessary to attempt the synthesis of bis-iodotriazole **111** without purification of the bis-iodoalkyne precursor. The CuAAC (click) reaction between **110** and two equivalents of azide **8** using CuI as a catalyst was unsuccessful. However, a recent report described the synthesis of triazole-substituted bipyridine molecules using the triethylphosphite complex of copper(I) iodide, $CuI–P(OEt)_3$,[13] which has a much higher solubility in organic solvents than CuI, enabling a higher catalyst loading. Addition of a slight molar excess of $CuI–P(OEt)_3$ to the reaction mixture gave the bis-iodotriazole product **111** in 10% isolated yield over two steps.

The low yield of **111** using the above synthetic procedure necessitated an alternative route to be sought. This involved the initial synthesis of diethynylbipyridine compound **116**, from which the desired bis-iodotriazole species could be prepared *via* the Brotherton one-pot

reaction conditions.[14]

Compound **116** was synthesised according to a literature procedure[13] (**Scheme 4-2**). Reaction of 2,2′-bipyridine with hydrogen peroxide in glacial acetic acid gave *N*-oxide **112** in 75% yield, and a subsequent nitration reaction afforded the 4,4′-bis-nitro derivative **113** (45%). Reaction with acetyl bromide in glacial acetic acid gave the corresponding bis-bromo compound **114** (76%), followed by deprotection of the *N*-oxide with PBr_3 to form 4,4′-dibromo-2,2′-bipyridine **115** (80%). Reaction with TMS-acetylene under Sonogashira conditions,[15] followed by deprotection, produced bis-alkyne **116** in 62% yield.



Scheme 4-2: Synthesis of rhenium(I) bipyridyl complex receptors **118** and **119**.

Reaction of bis-alkyne **116** with two equivalents of azide **8** under the Brotherton one-pot conditions[14] afforded the target bis-iodotriazole bipyridine compound **111** in 76% yield. The

prototriazole-functionalised analogue **117** was synthesised in 82% yield by reacting bis-alkyne **116** with two equivalents of azide **8** in the presence of $[Cu(CH_3CN)_4](PF_6)$, TBTA and DIPEA. Complexation reactions with $Re(CO)_5Cl$ afforded the rhenium(I) complexes **118** and **119** in 30% and 60% respective yields (**Scheme 4-2**).

4.3.2 *Anion Recognition Properties of Acyclic Complex Receptors*

Unfortunately, prototriazole receptor **119** was surprisingly highly insoluble in all common organic solvents, precluding study of its anion binding properties. However, iodotriazole-based receptor **118** was sufficiently soluble in halogenated solvents to enable ^{1}H NMR anion titration experiments to be undertaken. Addition of anions as their respective TBA salts to **118** in $CDCl_3$ induced perturbations of the aromatic proton signals. In particular, a downfield shift of the internal bipyridyl proton *3*, and upfield shifts of external bipyridyl proton *2* and upper phenyl proton *4*, were observed (**Figure 4-3a**).

WinEQNMR2[16] analysis of the titration data, monitoring the chemical shift change of upper phenyl proton *4*, determined 1:1 stoichiometric anion association constants (**Table 4-1**, **Figure 4-3b**). The receptor exhibits the selectivity trend $Cl^- > Br^- > AcO^- > I^- > NO_3^- > SO_4^{2-}$. Interestingly, the binding affinity with SO_4^{2-} is the weakest of the anions studied, despite possessing the greatest charge. This behaviour may be attributed to ion pairing effects, which are known to have a significant effect on the amount of free anion in highly non-competitive solvents such as $CDCl_3$.[17,18]

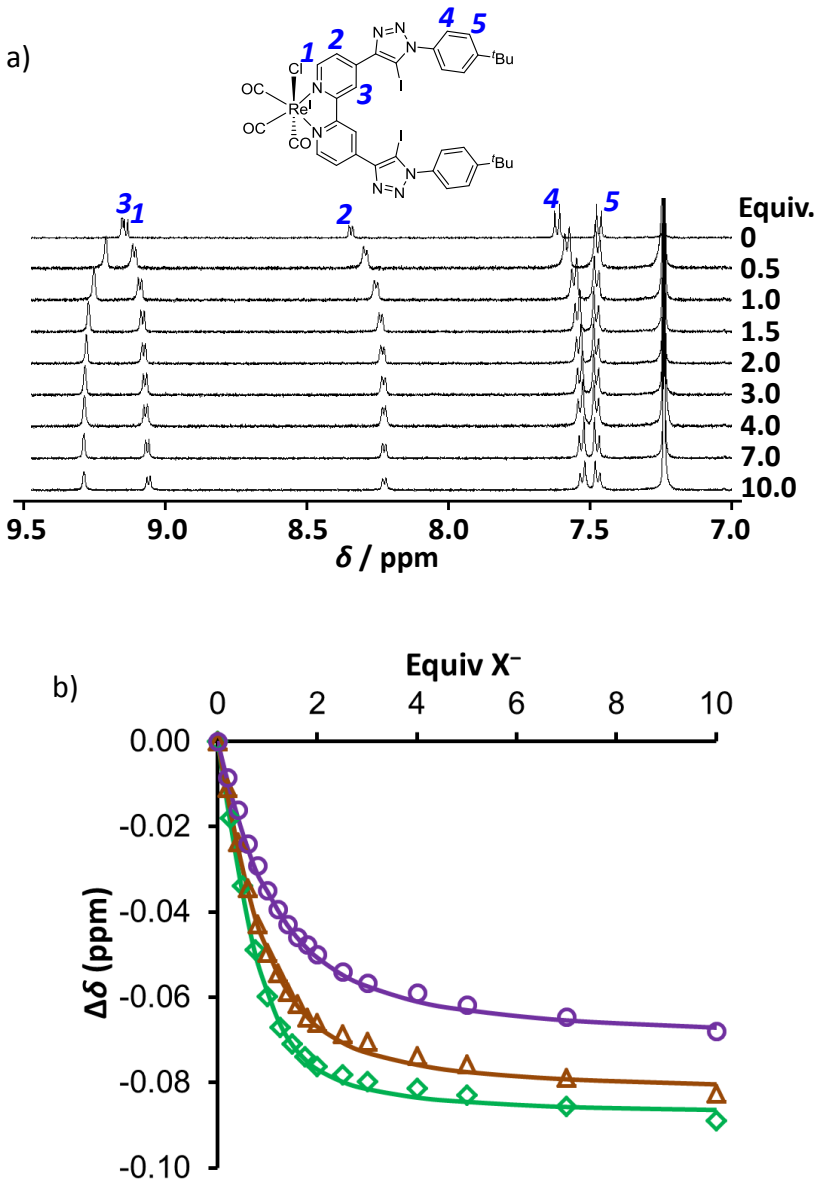


Figure 4-3: a) Truncated ^{1}H NMR spectra of iodotriazole receptor **118** upon addition of TBA·Cl; and **b)** experimental titration data (points) and fitted binding isotherms (lines) for receptor **118** upon addition of ◇ Cl^-, △ Br^- and ○ I^-, monitoring upper phenyl proton *4* ($CDCl_3$, 293 K, 500 MHz).

Table 4-1: Association constants, K_a (M^{-1}), obtained from ^1H NMR titrations, for receptor **118** with different anions. Errors are given in parentheses ($CDCl_3$, 293 K, 500 MHz).

	118
Cl^-	3100(200)
Br^-	2200(200)
I^-	990(50)
AcO^-	1500(200)
NO_3^-	590(100)
SO_4^{2-}	70(20)

K_a values were determined by monitoring the upper phenyl proton resonance.

The optical properties of rhenium(I) bipyridyl complexes provide the potential for anion sensing. Initially, a preliminary UV-vis titration experiment was conducted on receptor **118** with TBA·Cl in $CHCl_3$, however, the minor effect of the anion on the absorption properties was too small to determine an association constant.

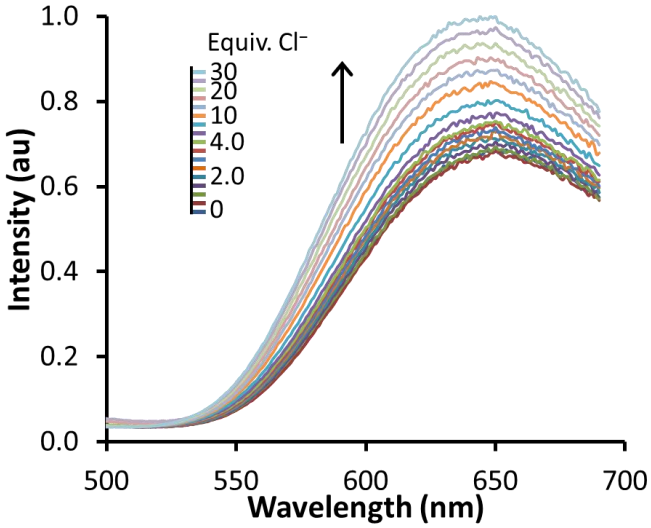


Figure 4-4: Luminescence emission spectra of iodotriazole receptor **118** upon addition of TBA·Cl (λ_{ex} = 405 nm, $CHCl_3$, 293 K).

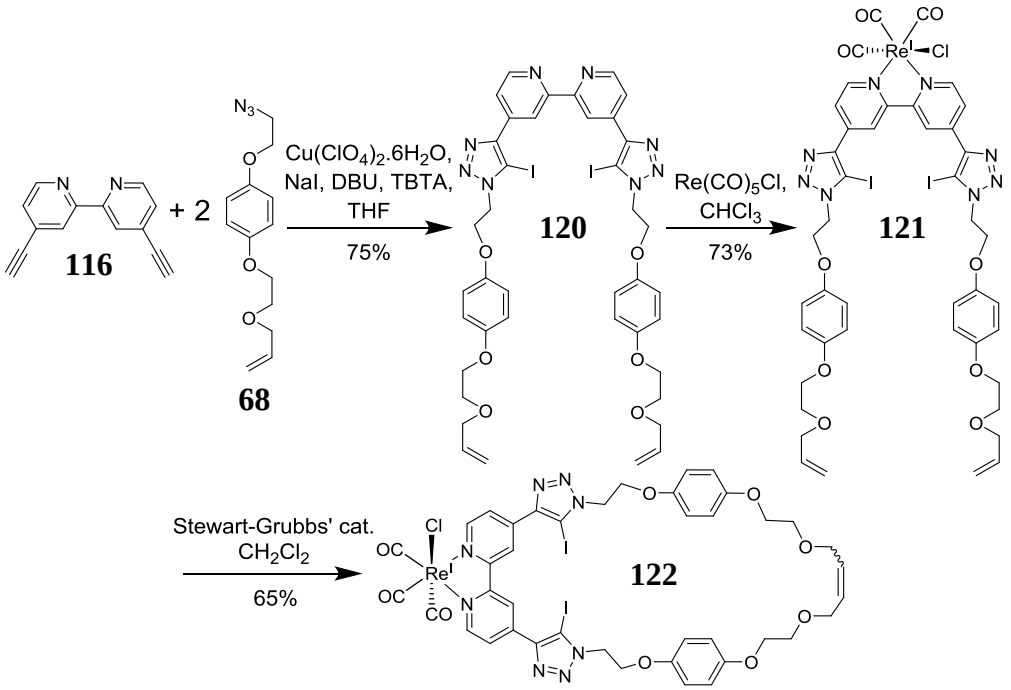
In contrast to the absorption results, the luminescence properties of **118** demonstrated a significant response upon addition of chloride in $CHCl_3$, with an increase in the intensity of the MLCT emission band, centered at ~645 nm (**Figure 4-4**).[19] This observation suggested

that the bis-iodotriazole rhenium(I) bipyridyl receptor motif was suitable for sensing anions by luminescence.

4.4 *XB Rhenium(I)-Containing Interpenetrated and Interlocked Structures*

4.4.1 *Pseudorotaxane Assembly Investigations*

Encouraged by the anion-binding results of XB acyclic receptor **118**, the XB rhenium(I) bipyridyl receptor motif was incorporated within a macrocycle for anion templated pseudorotaxane assembly investigations.



Scheme 4-3: Synthesis of XB rhenium(I) bipyridine macrocycle **122**.

The synthetic procedure to obtain XB macrocycle **122** is shown in **Scheme 4-3**. Reaction of bis-alkyne **116** with allyl-appended azide **68** under the Brotherton one-pot click conditions, gave bis-vinyl-appended intermediate **120** in 75% yield. Complexation with $Re(CO)_5Cl$ afforded the rhenium(I) bipyridine precursor **121** (73%), which was cyclised using Stewart–

Grubbs' RCM catalyst to give rhenium(I) bipyridine macrocycle **122** in 65% yield.

A qualititative ^{1}H NMR pseudorotaxane study was conducted by mixing equimolar amounts of macrocycle **122** and bis-amide pyridinium chloride thread **32a**·Cl in $CDCl_3$. Addition of the thread did not result in any significant shift in the macrocycle proton resonances, suggesting that these components were not forming an interpenetrated assembly.

An analogous ^{1}H NMR titration experiment was carried out with XB macrocycle **122**, XB carbazole-based thread **22** and TBA·Cl in $CDCl_3$ (**Figure 4-5**). Upfield shifts of the macrocycle hydroquinone signals *4* and *5* were observed, indicating formation of a pseudorotaxane.

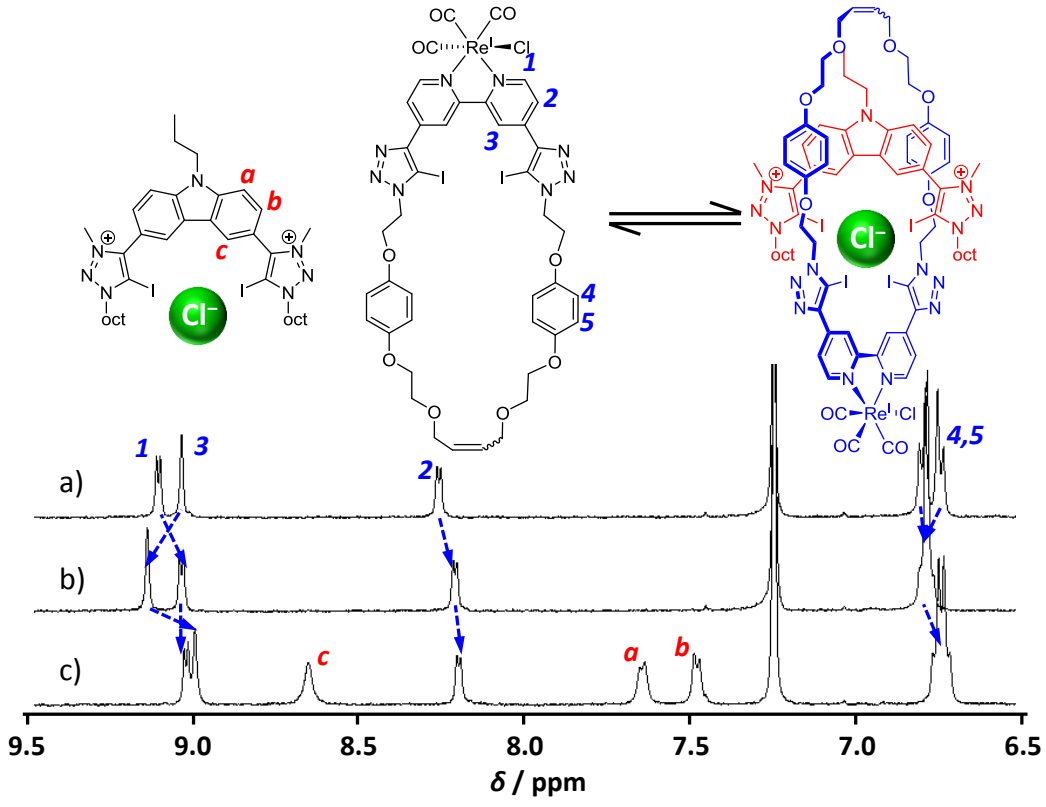
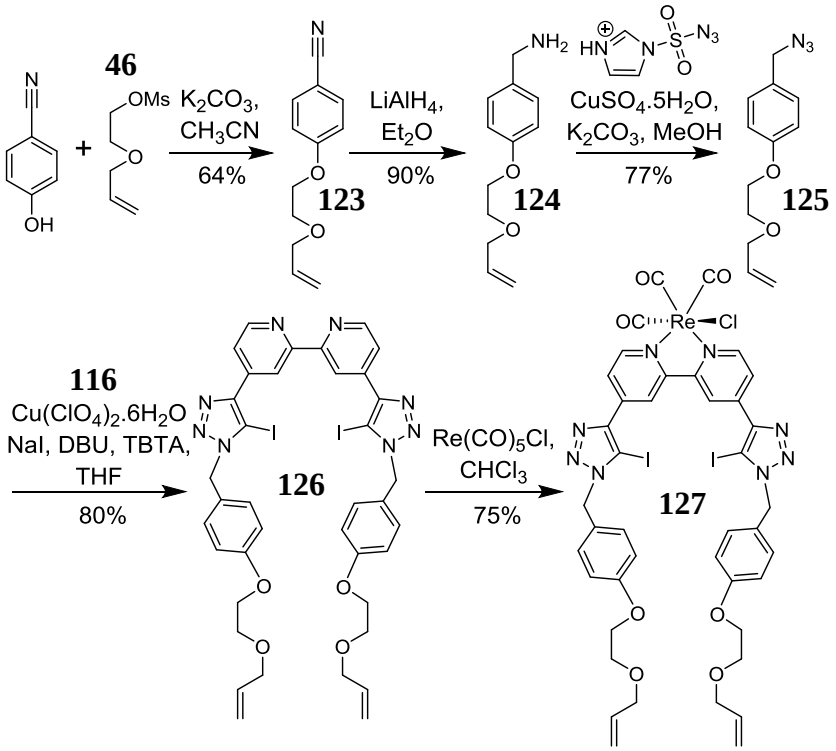


Figure 4-5: Truncated ^{1}H NMR spectra of **a)** XB rhenium(I) bipyridine macrocycle **122**; **b)** after addition of one equivalent of TBA·Cl; and **c)** after addition of one equivalent of XB carbazole-based thread **22**·2BF_4 ($CDCl_3$, 293 K, 500 MHz).

Although macrocycle **122** was shown to form an interpenetrated assembly with XB carbazole-based thread **22**·2BF_4, there was concern that the macrocycle was too large to form a stable rotaxane using a bis-terphenyl stoppered carbazole axle component. To test this, another ^{1}H NMR pseudorotaxane study was conducted with XB carbazole-based axle **51**·2BF_4. Addition of the axle to macrocycle **122** with TBA·Cl template in $CDCl_3$ resulted in the same upfield proton shift behaviour of the macrocycle hydroquinone resonances, as was observed in the analogous experiment with thread **22**. This observation implies that the axle is threading through the macrocycle, and the macrocycle is therefore too big to form a stable rotaxane.

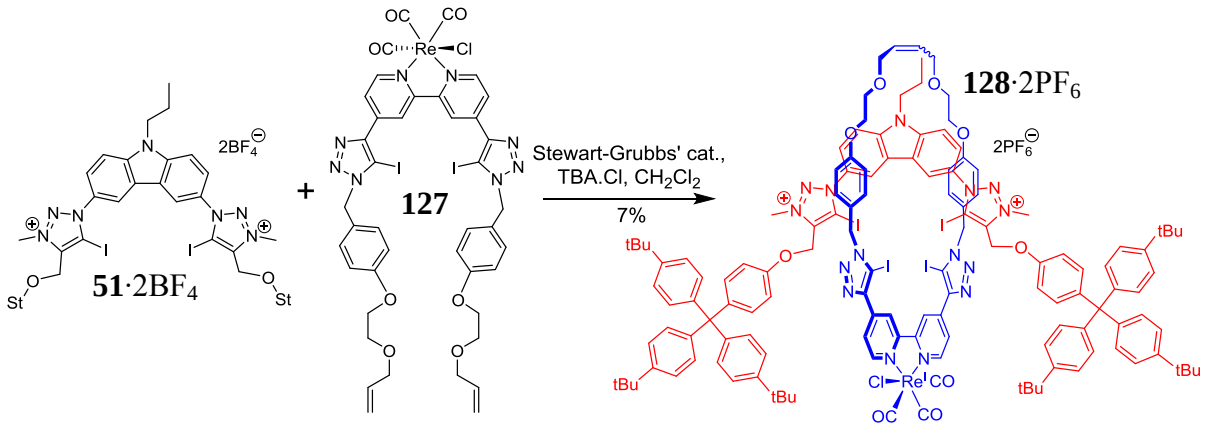
4.4.2 *Rhenium(I)-Based All-XB Rotaxane Synthesis*



Scheme 4-4: Synthesis of smaller rhenium(I) bipyridine macrocycle precursor **127**.

In order to decrease the size of the macrocycle, a precursor compound was envisaged in

which the allyl pendant arms were reduced in length by using a benzylic linker (**Scheme 4-4**). Reaction of 4-cyanophenol with mesylate **46** afforded allyl-appended nitrile compound **123** in 64% yield, which was reduced to form allyl-appended amine **124** (90%).[20] Reaction with the HSO_4^- salt of imidazole sulfonylazide in the presence of K_2CO_3 and a catalytic amount of $CuSO_4{\cdot}5H_2O$[21] gave the corresponding allyl-appended azide **125** in 77% yield. Reaction of two equivalents of **125** with 4,4′-diethynyl-2,2′-bipyridine **116** under the Brotherton one-pot reaction conditions[14] gave the bis-iodotriazole bipyridyl compound **126** in 80% yield. Complexation with $Re(CO)_5Cl$ afforded macrocycle precursor **127** in 75% yield.



Scheme 4-5: Synthesis of all-XB rotaxane **128**·$2PF_6$.

Following the successful synthesis of a smaller XB rhenium-based macrocycle precursor **127**, attempts were made to synthesise a rotaxane with XB carbazole-based axle $\mathbf{51}^{2+}$ (**Scheme 4-5**). An equimolar mixture of macrocycle precursor **127**, carbazole axle **51**·$2BF_4$ and TBA·Cl were reacted with Stewart–Grubbs' RCM catalyst. After purification by preparative TLC, followed by anion exchange using $NH_4PF_{6(aq.)}$, the rotaxane **128**·$2PF_6$ was isolated in 7% yield. It is noteworthy that repeating the synthesis in the absence of chloride gave only trace amounts of rotaxane, and the use of iodide as a potential templating anion resulted in a yield of 2%. Rotaxane **128**·$2PF_6$ was characterised by ^1H and ^{13}C NMR

spectroscopy, high resolution mass spectrometry, and ^{1}H–^{1}H ROESY NMR spectroscopy.

As shown in the ^{1}H NMR spectrum of rotaxane **128**·2PF$_6$ (**Figure 4-6**), many of the proton resonances have been split, due to asymmetrisation of the molecule. It is likely that this behaviour arises as a consequence of the carbazole *N*-propyl group of the axle, which may inhibit free movement of the macrocycle over the axle, restricting the macrocycle position to one side of the axle.

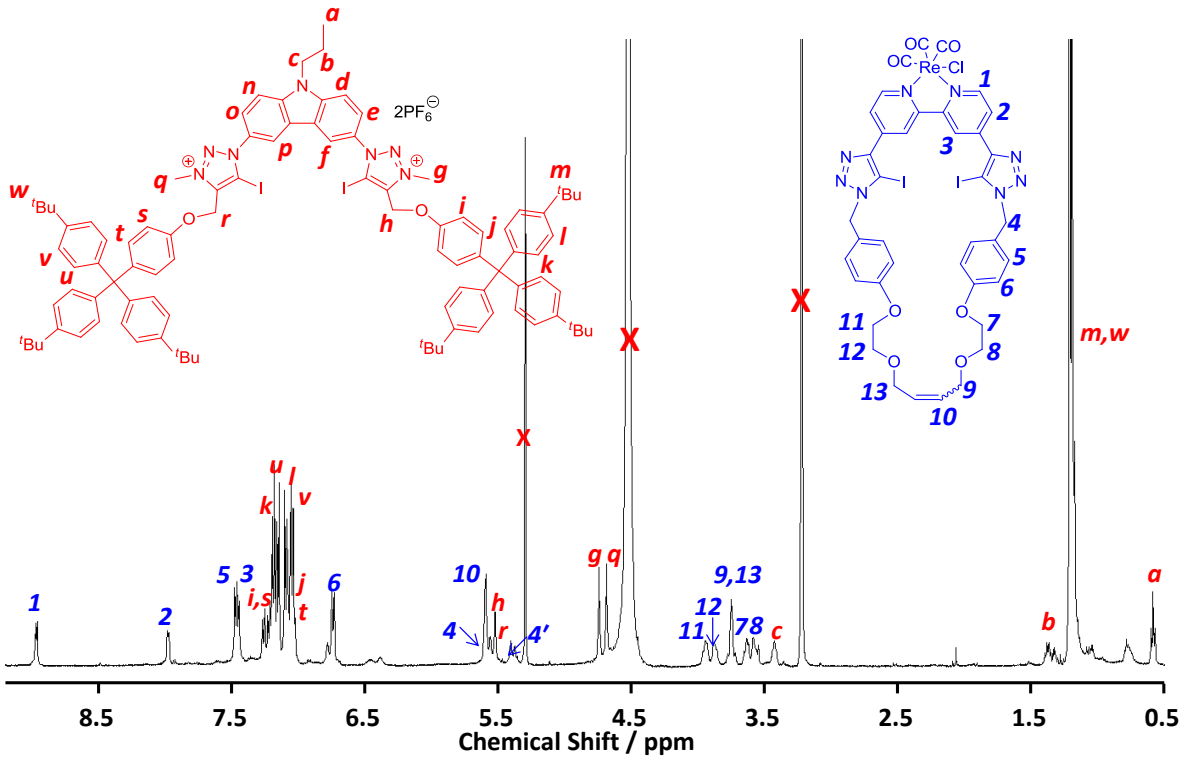


Figure 4-6: Assigned ^{1}H NMR spectrum of rotaxane **128**·2PF$_6$ (4:1 CD_2Cl_2/CD_3OD, 298 K, 500 MHz). Red 'X's denote solvent peaks.

^{1}H–^{1}H ROESY NMR spectroscopy provides additional evidence for the interlocked nature of rotaxane **128**·2PF$_6$ (**Figure 3-11**). There is a major intercomponent interaction between the axle triazolium methyl proton signal *g* and the macrocycle phenol proton *5*. Interestingly, no such intercomponent interaction exists with the other triazolium methyl resonance *q*,

supporting the asymmetric structural conformation of the rotaxane as described above.

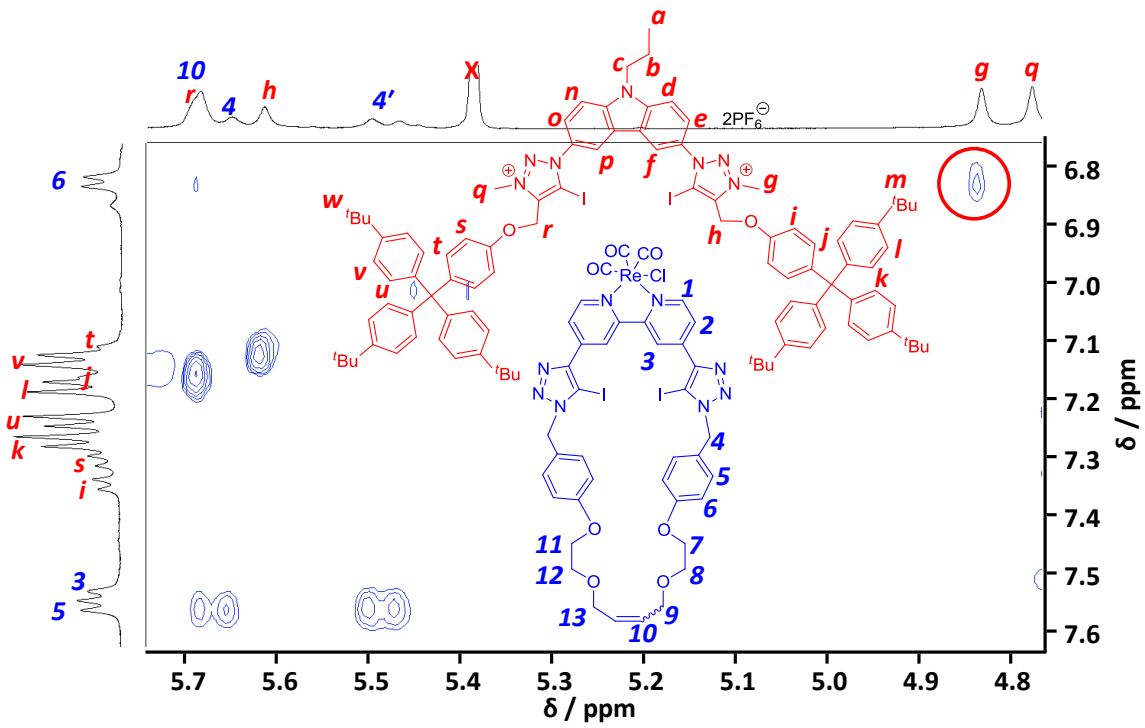


Figure 4-7: Truncated ^{1}H–^{1}H ROESY NMR spectrum of rotaxane **128**·2PF_6 (4:1 CD_2Cl_2/CD_3OD, 298 K, 500 MHz). Red 'X's denote solvent peaks.

Single crystal X-ray structural analysis provided final confirmation of the interlocked structure of rotaxane **128**$^{2+}$. Single crystals of the chloride salt of rotaxane **128**$^{2+}$ were obtained by slow evaporation of a 45:45:10 $CDCl_3$/CD_3OD/D_2O mixed solvent solution of the rotaxane with excess TBA·Cl. Data were collected for full structure determination at 100 K using synchrotron radiation (λ = 0.6889 Å), and data tables are given in **Appendix A**.

The crystal structure of **128**·2Cl clearly shows convergent halogen bonding between the iodotriazoles and iodotriazoliums, and the two Cl^- counterions (**Figure 4-8**). The macrocycle was modelled as being disordered over two positions with near-equal occupancy, and one of the axle triazolium units is disordered over two positions antiparallel to one another, pointing

either toward, or away from the cavity-bound Cl^-. One of the Cl^- anions is bound by three halogen bond donors in the rotaxane cavity, two from the macrocycle and one from the minor component of the disordered axle, while the other halide counterion is forming a halogen bond to the remaining axle iodotriazolium ($d_{I\cdots Cl}$ = 2.98–3.13(6) Å, **Figure 4-9**). The halogen bond distances are all significantly lower than the sum of the van der Waals radii,[22] with $\%vdW_{I,Cl}$ = 77–81%, giving further support for the strength of these halogen bonding interactions.

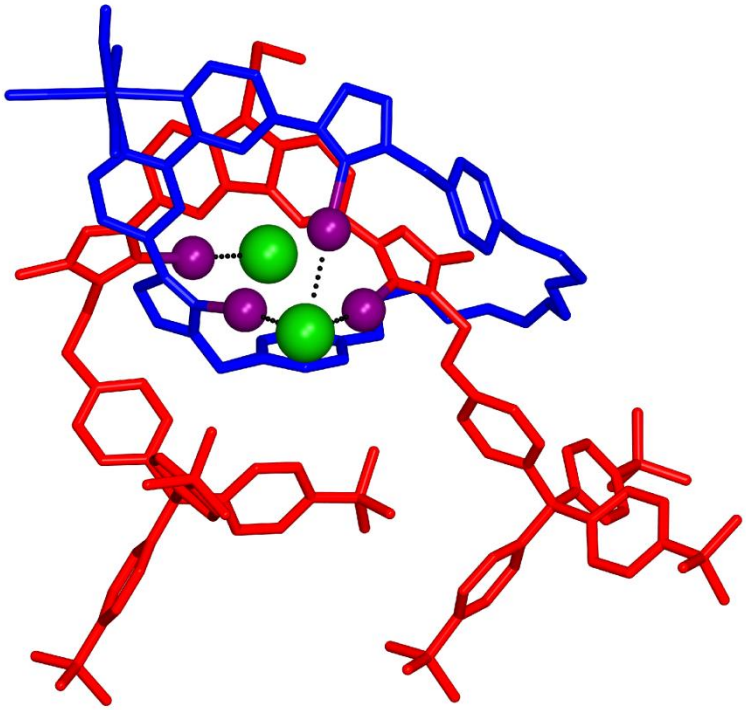


Figure 4-8: Single crystal structure of rotaxane **128**·2Cl, displaying the interlocked topology and halogen bonds. Green spheres represent chloride anions, purple spheres represent iodine atoms. Solvent molecules, hydrogen atoms and disorder have been omitted for clarity.

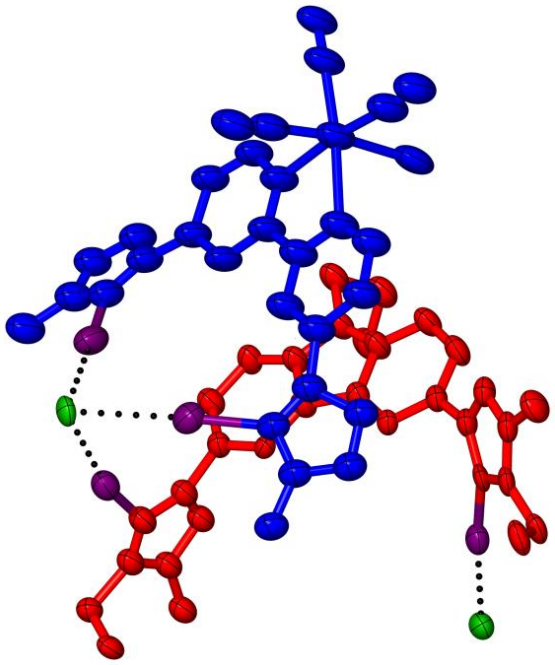


Figure 4-9: Close-up of the receptor portions of the single crystal structure of rotaxane **128**·2Cl. Thermal ellipsoids are displayed at 30% probability.

4.4.3 *Anion Binding Studies of All-XB Rotaxane 128*$^{2+}$

^{1}H NMR anion binding studies on rotaxane **128**·2PF_6 were initially undertaken with TBA·Cl in 45:45:10 $CDCl_3$/CD_3OD/D_2O (**Figure 4-10**). Importantly, significant perturbations were observed in the chemical shifts of the rotaxane's macrocycle component protons *3* and *5* proximal to the XB donor iodotriazole groups, which suggests that the halide anion is being bound within the interlocked cavity. Downfield shifts in the axle external carbazole protons *d* and *e* were also noted. Fitting the changes in the chemical shifts of macrocycle proton *5* to a 1:1 stoichiometric binding model using WinEQNMR2[16] determined an association constant of $K_a = 1030(30)$ M^{-1} (**Figure 4-11b**). For comparison, an analogous experiment was conducted with TBA·I, which gave an association constant for iodide of $K_a > 10^4$ M^{-1}, providing an early indication of the potency of this anion host system for the larger halide.

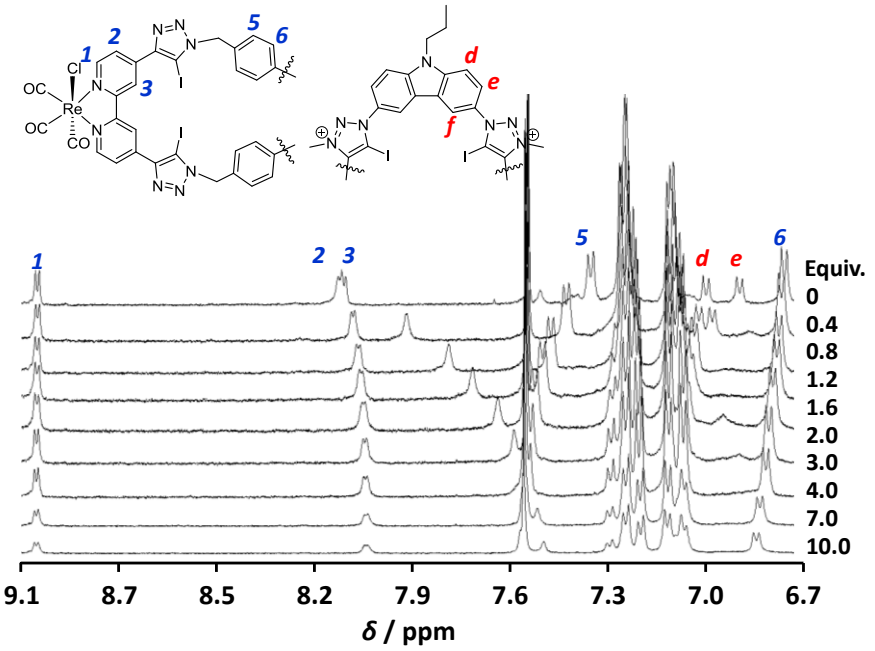


Figure 4-10: ^{1}H NMR spectral changes observed in **128**·2PF$_6$ upon addition TBA·Cl (45:45:10 $CDCl_3$/CD_3OD/D_2O, 293 K, 500 MHz).

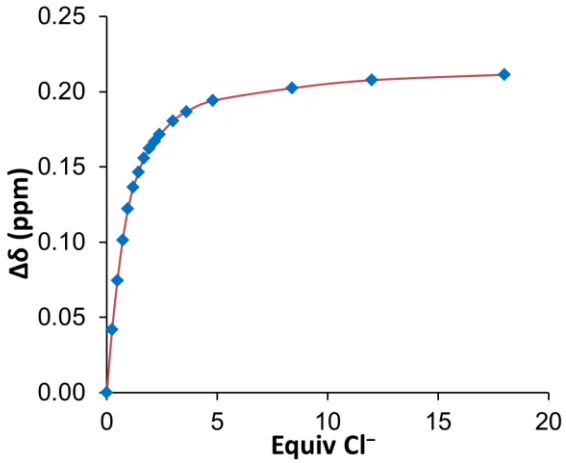


Figure 4-11: The experimental titration data (points) and the fitted binding isotherm (line) for **128**·2PF$_6$ upon addition of TBA·Cl, following the upper phenyl proton *5* of the macrocycle (45:45:10 $CDCl_3$/CD_3OD/D_2O, 293 K, 500 MHz).

Following the demonstration that the XB rhenium(I) bipyridyl acyclic receptor exhibited a luminescent response to anions (**§4.3.2**), luminescence spectroscopy was used to investigate the anion sensing potential of rotaxane **128**·2PF$_6$. Anion binding affinities of the rotaxane were determined in H_2O/CH_3CN solvent mixtures, monitoring the intensity of the rotaxane's

rhenium(I) bipyridyl macrocycle MLCT emission band upon the addition of a variety of anions.

Upon excitation at λ_{ex} = 400 nm the rotaxane exhibited the expected MLCT emission band of the integrated rhenium(I) bipyridyl centre at λ_{em} = 583 nm ($c = 1 \times 10^{-5}$ M in 10% H_2O/CH_3CN). In 10% H_2O/CH_3CN, the addition of Cl^- resulted in the intensity of the rotaxane's MLCT emission band initially increasing up to 20 equivalents of halide, followed by an intensity decrease (**Figure 4-12a**). Analogous behaviour was observed upon addition of Br^-. Addition of I^- gave the most notable optical response, producing significant fluorescence quenching of the rotaxane. In contrast, the oxoanions AcO^- and $H_2PO_4^-$ did not noticeably affect the emission properties of the rotaxane, suggesting no binding. The data were modelled using Specfit[23] to determine 1:1 and 1:2 stoichiometric association constants (**Figure 4-12b** and **Table 4-2**), which reveal strong binding of the halides with a selectivity preference of I^- > Br^- >> Cl^-.

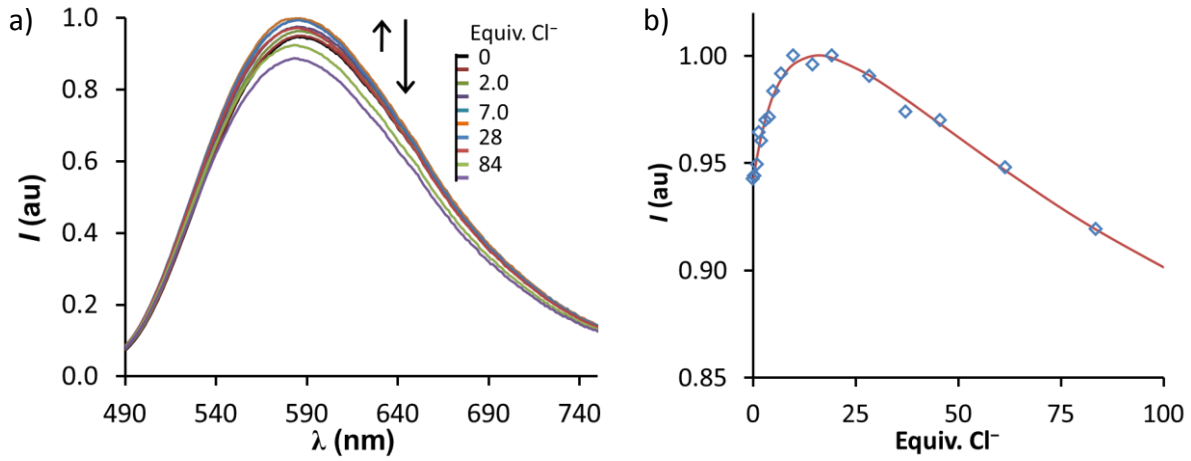


Figure 4-12: a) Changes in the luminescence emission spectra of rotaxane **128**·$2PF_6$ upon addition of increasing equivalents of Cl^-; **b)** Changes in the emission at 585 nm upon addition of Cl^- (points) and the fitted binding model (line) (λ_{ex} = 400 nm, 10% H_2O/CH_3CN, 298 K).

Considering the strong halide anion binding affinities exhibited by rotaxane **128**·2PF_6 in the 10% water solvent mixture, analogous titrations were undertaken with a wider range of anions in aqueous media containing higher water content of 20% and 50%. Similar luminescence sensing behaviour was observed upon addition of the halides (**Figure 4-13**, additional experimental spectra are given in **Appendix B**).

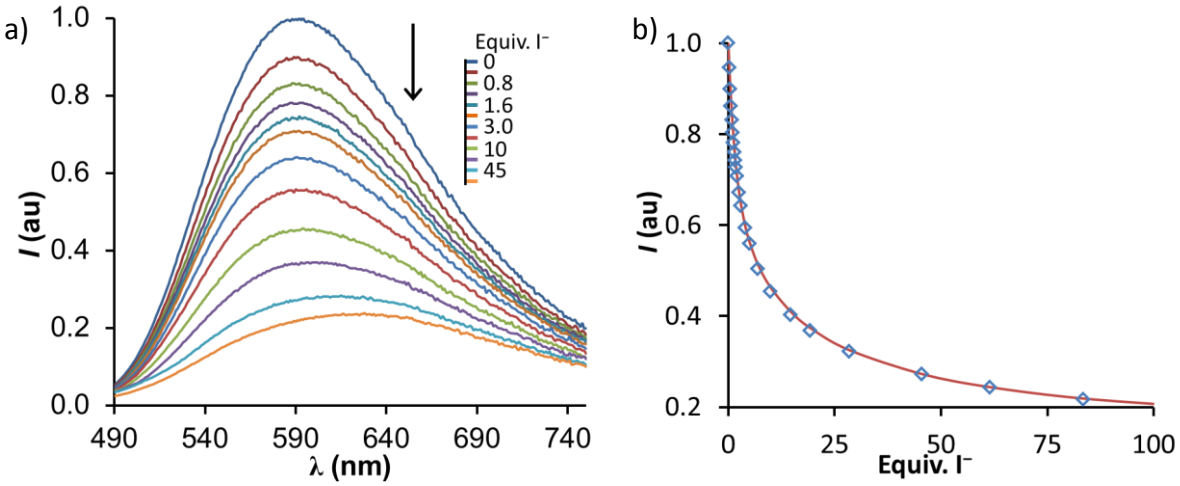


Figure 4-13: a) Changes in the luminescence emission spectra of rotaxane **128**·2PF_6 upon addition of increasing equivalents of TBA·I; **b)** Changes in the emission intensity at 585 nm upon addition of I^- (points) and the fitted binding model (line) (λ_{ex} = 400 nm, 20% H_2O/CH_3CN, 298 K).

Importantly, **Table 4-2** shows that despite the increased water content, the association constants for Cl^-, Br^- and I^- remain substantial in magnitude, especially for the heavier halides. Furthermore, it is noteworthy that the halides are bound preferentially over all the oxoanions and fluoride. Indeed, only HCO_3^- and SO_4^{2-} demonstrated any evidence of binding, which was much weaker than the aforementioned halides. This suggests the halogen bond donor cavity of the rotaxane is of complementary shape and size for the spherical halide guests, whereas oxoanions are too large and are of the wrong geometry to penetrate the interlocked host's binding domain.

Table 4-2: Anion association constants for rotaxane **128**·2PF_6 in H_2O/CH_3CN solvent mixtures at 298 K (λ_{ex} = 400 nm for 10% and 20% H_2O; 390 nm for 50% H_2O). Errors < 10%.

	10% H_2O		20% H_2O		50% H_2O
Anion	log(K_{11})	log(K_{12})	log(K_{11})	log(K_{12})	log(K_{11})[a]
F^-	-		NB		-
Cl^-	4.04	2.81	3.49	2.63	2.71
Br^-	5.02	3.42	4.49	2.87	3.76
I^-	5.14	3.74	4.95	3.61	4.38
AcO^-	NB		NB		-
$H_2PO_4^-$	NB		NB		-
HCO_3^-	-		< 2.0[b]		-
NO_3^-	-		NB		-
ClO_4^-	-		NB		-
SO_4^{2-}	-		< 1.0[b]		-

[a] No evidence of 1:2 binding for Cl^- or Br^-, K_{12} values not calculated for I^- due to precipitation problems above 16 equivalents; [b] The binding strength was too low to accurately determine an association constant.

In summary, rotaxane **128**·2PF_6 has been shown to exhibit a near-exclusive selectivity for the halides, with a particularly strong affinity for iodide. Indeed, the host–guest complex with iodide has a stability constant of log(K_a) > 4 in a highly competitive solvent mixture containing 50% water. **Table 4-2** shows that there is a relatively modest decrease in the association strength of the iodide complexed species with higher water content, which suggests that a water-soluble host analogue may be capable of binding iodide with exceptionally high affinity and selectivity in pure water. Furthermore, the ability of this all-XB host to sense anion binding through the integrated luminescent rhenium(I) bipyridyl complex represents a major step forward in the development of sensory XB interlocked anion receptors.

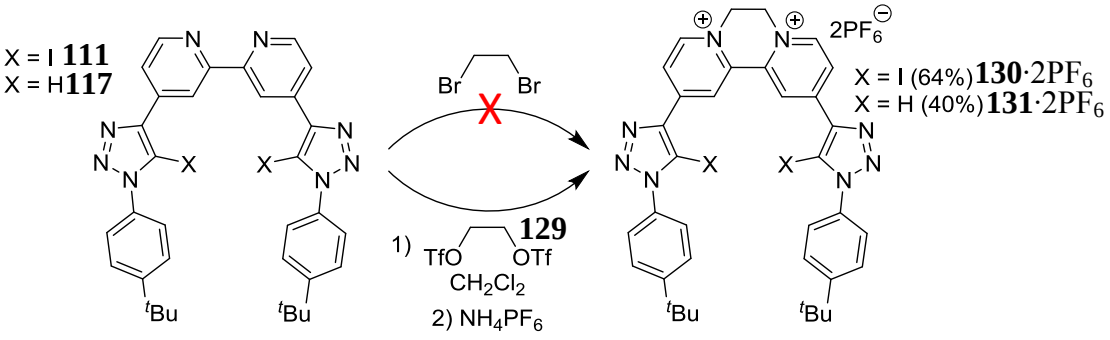
4.5 *Acyclic Diquat-Based Anion Receptors*

In addition to forming anion receptor complexes, the bis-iodotriazole bipyridyl moiety is also

suitable for alkylation of the bipyridyl nitrogens, generating a dicationic anion receptor. While diquat has been shown to form complexes with crown ether derivatives,[24,25] its incorporation into either interlocked architectures or anion receptor motifs has not been reported. The rigid diquat motif is particularly attractive as an anion sensing component due to its optical[26] and electrochemical[27] properties.

4.5.1 *Synthesis of Diquat-Based Acyclic Receptors*

Initial attempts to form an acyclic bis-triazole diquat-based receptor by reacting the bipyridyl precursor **117** with 1,2-dibromoethane[28] were unsuccessful (**Scheme 4-6**). However, a procedure was recently reported in which diquat was formed by the reaction of 1,2-bis(triflyl)ethane[29] **129** with a bipyridyl derivative under mild conditions.[30] This method was successfully employed to convert iodotriazole precursor **111** and prototriazole precursor **117** to the corresponding diquat-based receptors **130**·2PF_6 and **131**·2PF_6, respectively (**Scheme 4-6**).



Scheme 4-6: Synthesis of acyclic diquat-based receptors **130**·2PF_6 and **131**·2PF_6.

4.5.2 *Anion Recognition and Sensing Properties*

4.5.2.1 ^{1}H NMR Spectroscopic Studies

The anion binding behaviours of diquat-based receptors $\mathbf{130}^{2+}$ and $\mathbf{131}^{2+}$ were initially

studied by ^{1}H NMR titration experiments. Prototriazole receptor **131**$^{2+}$ was studied in d_6-DMSO, while iodotriazole receptor **130**$^{2+}$ proved to be a superior host, requiring the more competitive solvent mixture of 10% D_2O/d_6-DMSO to determine association constants. As shown in **Figure 4-14**, addition of bromide to prototriazole receptor **131**·2PF_6 resulted in significant perturbations of the receptor proton resonances. Specifically, the large downfield shifts of triazole proton *4* and internal diquat proton *3* suggest that the halide anion is binding within the receptor cavity. The change in the chemical shift of triazole proton *4* (**Figure 4-15a**) was monitored using WinEQNMR2[16] to determine anion association constants for prototriazole receptor **131**$^{2+}$ (**Table 4-3**). The anion binding properties of iodotriazole receptor **130**$^{2+}$ were studied by monitoring the internal diquat proton *3* (**Figure 4-15b**).

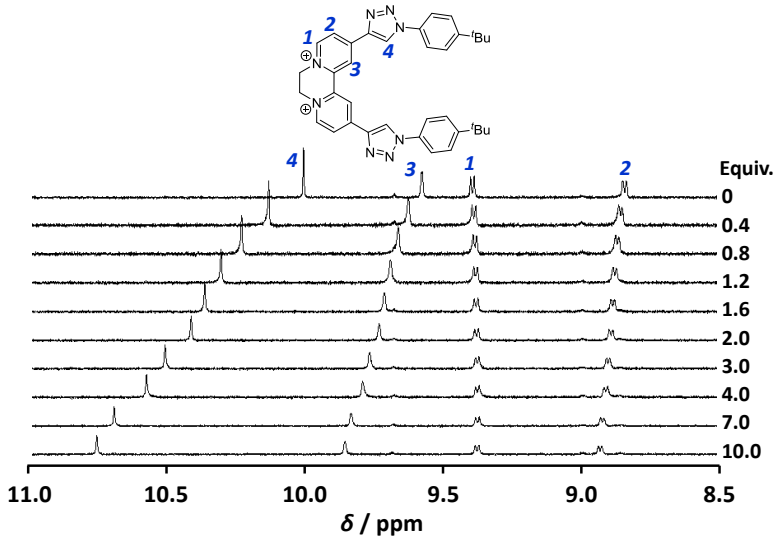


Figure 4-14: Truncated ^{1}H NMR spectra of prototriazole receptor **131**·2PF_6 upon addition of TBA·Br (d_6-DMSO, 293 K, 500 MHz).

Inspection of the anion-induced changes in the chemical shifts of iodotriazole receptor **131**·2PF_6 reveals an interesting feature: addition of Cl^- and Br^- resulted in a downfield shift of diquat proton *3*, while addition of I^- induced an upfield shift in this proton resonance

(**Figure 4-15b**). This behaviour may imply that the I^- anion is too large to reside within the receptor cavity, requiring a different geometrical conformation of the receptor.

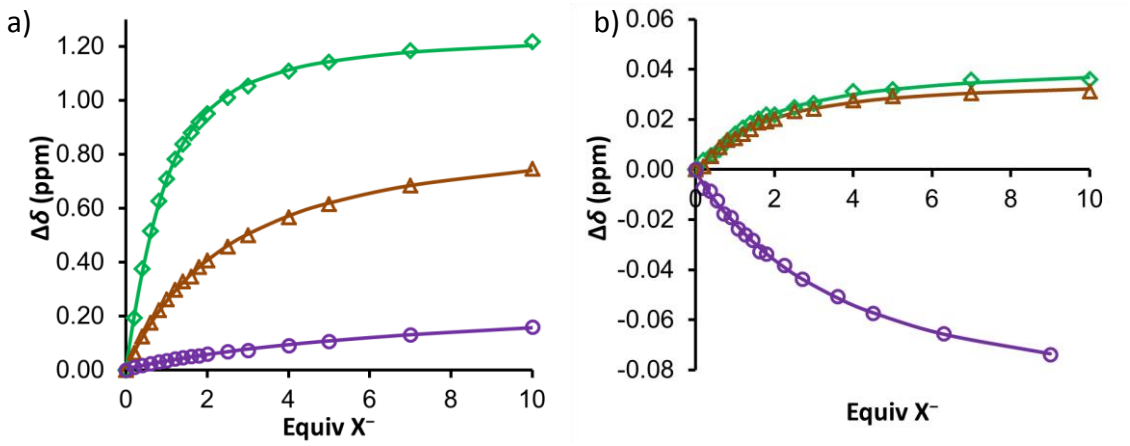


Figure 4-15: Experimental titration data (points) and fitted binding isotherms (lines) for receptors **a)** prototriazole **131**·2PF_6 monitoring triazole proton *4* (d_6-DMSO); and **b)** iodotriazole **130**·2PF_6 following internal diquat proton *3* (10% D_2O/d_6-DMSO), upon addition of ◇ Cl^-, △ Br^- and ○ I^- (293 K, 500 MHz).

As shown in **Table 4-3**, iodotriazole receptor $\mathbf{130}^{2+}$ exhibits a minor preference for Br^- over the other halides, while by contrast, prototriazole receptor $\mathbf{131}^{2+}$ displays a marked preference for Cl^-. Similarly to the carbazole-based receptors (**§2.3.2**), the bis-iodotriazole diquat-based receptor exhibits superior anion binding affinity, compared to its prototriazole analogue.

Table 4-3: Association constants, K_a (M^{-1}), obtained from ^1H NMR titrations, for receptors $\mathbf{130}^{2+}$ and $\mathbf{131}^{2+}$ with different anions. Iodotriazole receptor $\mathbf{130}^{2+}$ was studied in 10% D_2O/d_6-DMSO, and prototriazole receptor $\mathbf{131}^{2+}$ was studied in d_6-DMSO (293 K, 500 MHz). Errors < 10%.

	$\mathbf{130}^{2+}$	$\mathbf{131}^{2+}$
Cl^-	290	970
Br^-	340	201
I^-	128	44
NO_3^-	NB	36
SO_4^{2-}[a]	ppt	ppt

[a] Titration experiments with $TBA_2{\cdot}SO_4$ were attempted in up to 50% D_2O/d_6-DMSO, but addition of the anion invariably resulted in precipitation of the receptor.

4.5.2.2 Absorption Studies

To test the potential of exploiting the optical properties of diquat to probe anion binding behaviour, representative UV-visible spectroscopic absorption titration experiments were conducted on the iodotriazole **130**$^{2+}$ and prototriazole **131**$^{2+}$ receptors, adding aliquots of TBA·Cl in CH_3CN.

As shown in **Figure 4-16a**, addition of Cl^- to iodotriazole receptor **130**$^{2+}$ induced significant changes in the host absorption spectrum. The absorption intensity at 320 nm increased until ~1 equivalent, followed by an intensity decrease (**Figure 4-16b**). This behaviour is indicative of strong 1:1 stoichiometric host:guest association, with a significant 1:2 binding component as well. The spectral changes were analysed using the SpecFit program,[23] which determined a 1:1 association constant of $\log(K_a) > 6$.

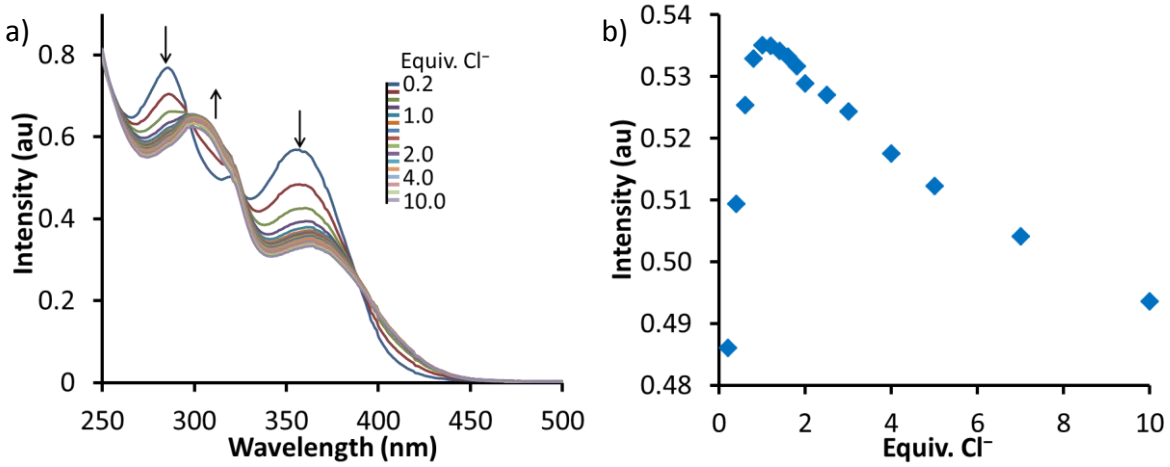


Figure 4-16: a) Changes in the absorption spectrum of diquat-based iodotriazole receptor **130**·2PF_6 upon addition of TBA·Cl; and **b)** changes in the absorption intensity at 320 nm ([host] = 20 μM, CH_3CN, 293 K).

An analogous absorption titration experiment was undertaken with prototriazole receptor **131**$^{2+}$. Addition of Cl^- induced a decrease in the intensity of the absorption band at ~355 nm.

Analysis of these changes using SpecFit determined a 1:1 stoichiometric association constant of $\log(K_a) = 5.0(1)$. These results are consistent with those obtained from the ^{1}H NMR titration experiments, confirming that the XB iodotriazole receptor **130**$^{2+}$ has a higher affinity for Cl^- than HB prototriazole receptor **131**$^{2+}$.

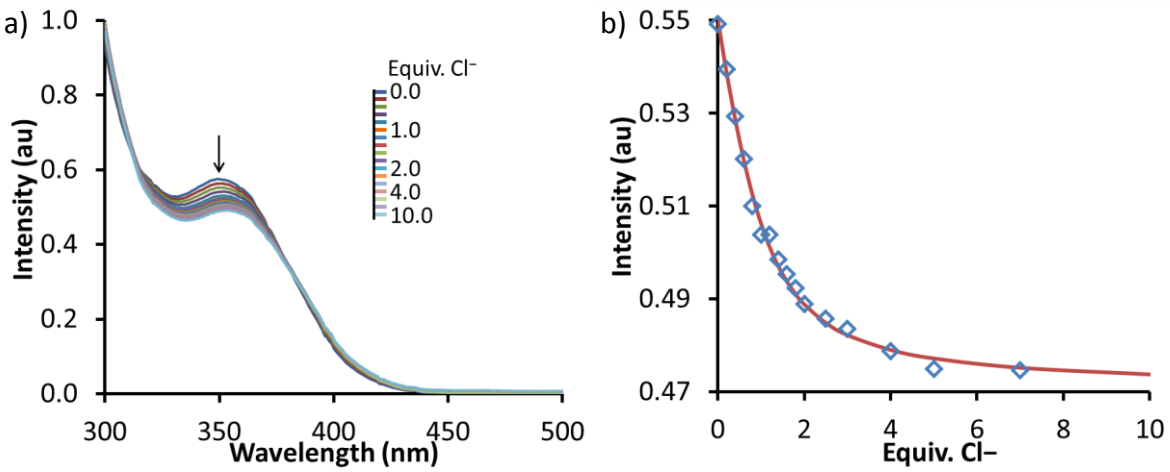


Figure 4-17: a) Changes in the absorption spectrum of diquat-based prototriazole receptor **131**·2PF_6 upon addition of TBA·Cl; and **b)** changes in the absorption intensity at 355 nm (points) and the fitted binding model (line) ([host] = 20 μM, CH_3CN, 293 K).

4.5.2.3 Electrochemical Studies

In addition to its optical properties, diquat is also known to be electrochemically active, providing another potential anion sensing method. Initially, cyclic voltammetry experiments were conducted in order to determine whether the diquat-based receptors were robust to electrochemical study. For an electrochemically reversible species, the current peak is proportional to the square root of the scan rate, $i \propto (\text{scan rate})^{1/2}$, and a plot of current *vs* $(\text{scan rate})^{1/2}$ is linear.[31] For comparison, the electrochemical data for diquat (DQ^{2+}), **130**·2PF_6 and **131**·2PF_6 are given in **Table 4-4**.

Table 4-4: Electrochemical data for DQ·2PF_6, **130**·2PF_6 and **131**·2PF_6, for both redox couples (mV).[a]

	E^1_{pa} [b]	E^1_{pc}	ΔE^1	$E^1_{1/2}$	E^2_{pa}	E^2_{pc}	ΔE^2	$E^2_{1/2}$
DQ·2PF_6	−370	−420	50	−400	−860	−910	50	−885
130·2PF_6	−270	−340	70	−305	-[c]	−755	-	-
131·2PF_6	−340	−390	50	−365	−770	−825	55	−800

[a] Conditions: 5×10^{-4} M solutions of compounds in 0.1 M TBA·PF_6 in CH_3CN, glassy carbon working electrode, Pt auxiliary electrode, Ag/AgCl reference electrode. CVs recorded with a scan rate of 100 mV s^{-1}; [b] Relative to the Ag/AgCl reference, errors ±5 mV; [c] peak value could not be determined.

Diquat displays two quasi-reversible sequential one-electron reduction redox processes, corresponding to the $DQ^{2+}/DQ^{+\bullet}$ (1) and $DQ^{+\bullet}/DQ$ (2) couples. Similar quasi-reversible behaviour was observed with bis-prototriazole-functionalised receptor **131**·2PF_6 (**Figure 4-18a**), where the reduction peak *vs* (scan rate)$^{1/2}$ plot displayed a linear relationship for both redox couples (**Figure 4-18b**).

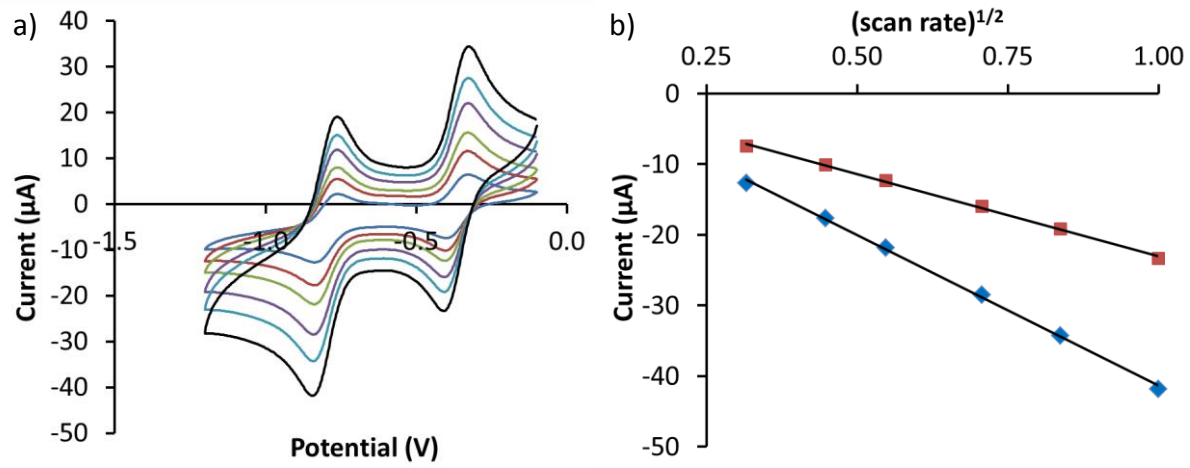


Figure 4-18: a) Cyclic voltammograms of prototriazole receptor **131**·2PF_6 with different scan rates; and **b)** plot of the reduction current *vs* (scan rate)$^{1/2}$ for both reduction peaks, with the lines of best fit (electrolyte: 0.1 M TBA·PF_6 in CH_3CN, 293 K, reference electrode: Ag/AgCl).

In contrast, the XB iodotriazole-based analogue **130**·2PF_6 exhibited quasi-reversible behaviour of the first reduction redox couple, and an irreversible second reduction redox

wave at a more cathodic potential, where the corresponding oxidation wave E^2_{pa} was absent (**Figure 4-19a**).

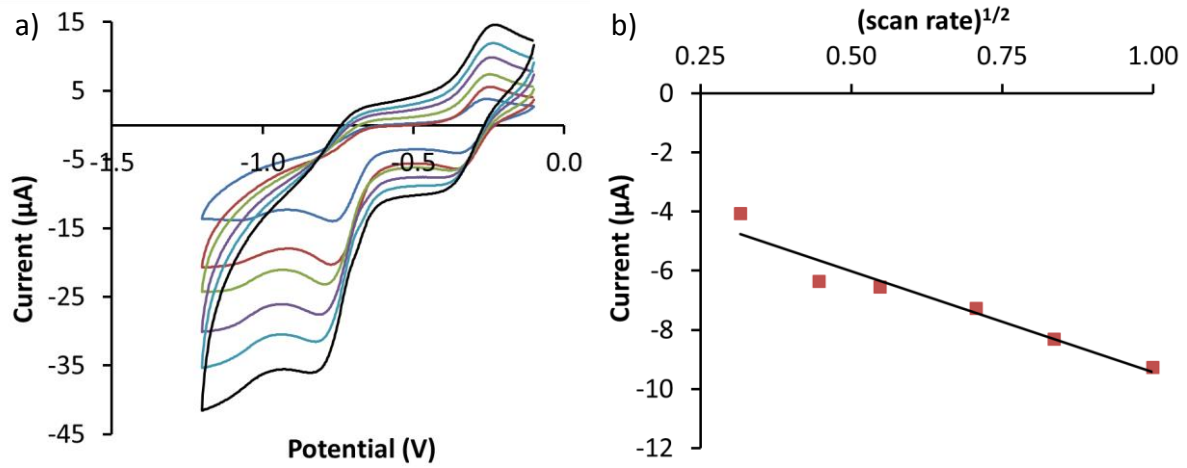


Figure 4-19: a) Cyclic voltammograms of iodotriazole receptor **130**·2PF_6 with different scan rates; and **b)** plot of the reduction current *vs* (scan rate)$^{1/2}$ for the E^1_{pc} reduction peak, with the line of best fit (electrolyte: 0.1 M TBA·PF_6 in CH_3CN, 293 K, reference electrode: Ag/AgCl).

The $E^1_{1/2}$ and $E^2_{1/2}$ values of receptor **131**·2PF_6 are shifted anodically by +35 mV and +85 mV, respectively, compared to DQ^{2+}. These shifts may be attributed to the electron-withdrawing triazole groups, which could favour diquat reduction, increasing the redox couples to more positive potentials. Similarly, the electronegative iodine substituents of bis-iodotriazole receptor **130**·2PF_6 enhance this effect, resulting in the $E^1_{1/2}$ and E^2_{pc} potentials being shifted anodically by +95 and +155 mV, respectively, in comparison to DQ^{2+}.

To investigate the electrochemical response of the diquat-based receptors to anions, the first reduction $E^1_{1/2}$ redox couple was monitored. Addition of halide anions induced notable cathodic shifts in the redox wave (**Figure 4-20a**, **Appendix C**), which increased in magnitude with increasing equivalents of anion (**Figure 4-20b**). The maximum observed halide-induced cathodic shifts are summarised in **Table 4-5**. Unfortunately, addition of $H_2PO_4^-$ and AcO^- resulted in immediate precipitation, precluding a comparative

electrochemical study with these oxoanions.

It is noteworthy that addition of chloride to the unsubstituted diquat molecule resulted in no significant shift in the E^1 redox couple. The observed cathodic shifts resulting from anion addition to electrochemical solutions of receptors **130**·2PF_6 and **131**·2PF_6 can therefore be attributed to anion binding in the receptor cavity. These anion-induced cathodic shifts arise from the proximal bound anion stabilising the cationic charged state of the host, which disfavours the reduction redox process.

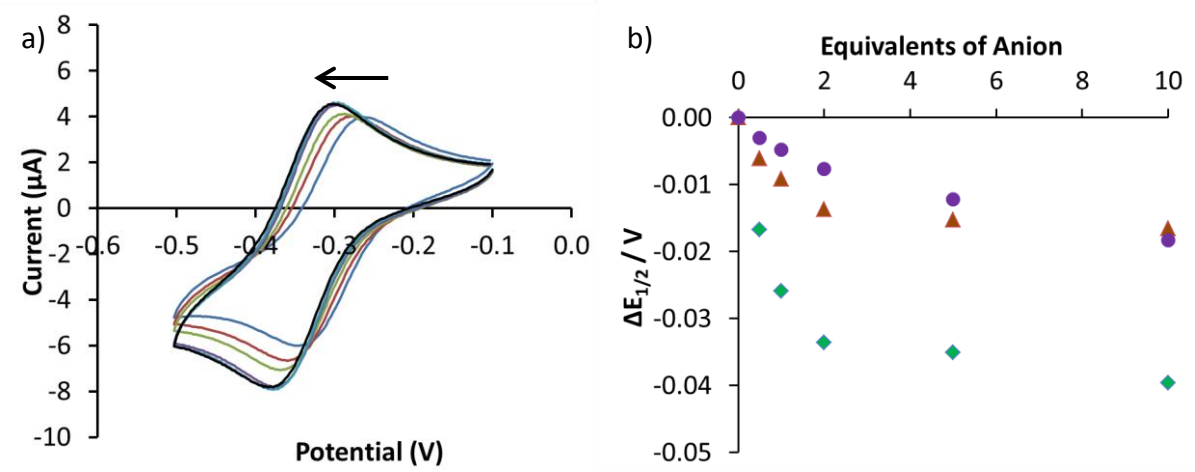


Figure 4-20: a) Cyclic voltammograms of iodotriazole receptor **130**·2PF_6 upon addition of Cl^- anions; and **b)** the difference in the $E^1_{1/2}$ values upon addition of ◆ Cl^-, ▲ Br^-, and ● I^- (electrolyte: 0.1 M TBA·PF_6 in CH_3CN, 293 K, reference electrode: Ag/AgCl).

Addition of anions to prototriazole receptor **131**·2PF_6 similarly resulted in a cathodic shift of the E^1 redox couple (**Figure 4-21a**). As for the iodotriazole analogue, $H_2PO_4^-$ and AcO^- could not be studied due to precipitation problems. However, the halide-induced shifts in the redox wave were monitored to produce electrochemical binding curves (**Figure 4-21b**).

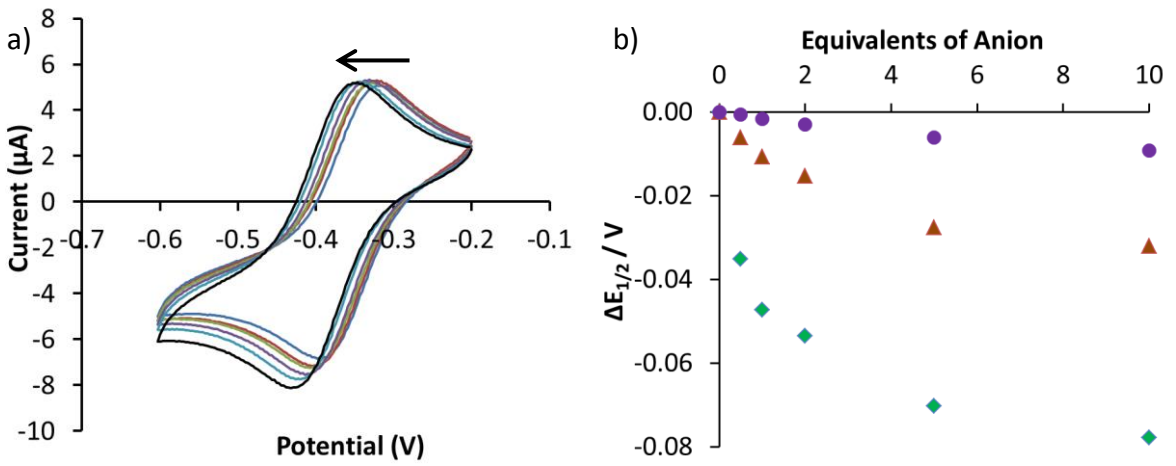


Figure 4-21: a) Cyclic voltammograms of iodotriazole receptor **131**·2PF_6 upon addition of Br^- anions; and **b)** the difference in the $E^1_{1/2}$ values upon addition of ◆ Cl^-, ▲ Br^-, and ● I^- (electrolyte: 0.1 M TBA·PF_6 in CH_3CN, 293 K, reference electrode: Ag/AgCl).

As shown in **Table 4-5**, addition of Cl^- resulted in the largest magnitudes of cathodic shifts for both diquat-based receptors. Notably, addition of Cl^- and Br^- to prototriazole receptor **131**·2PF_6 results in shifts that are approximately double the magnitude of the response from iodotriazole **130**·2PF_6.

Table 4-5: Cathodic shifts in the diquat^{2+}/diquat$^{+\bullet}$ redox couple $E^1_{1/2}$ (mV) of iodotriazole **130**·2PF_6 and prototriazole **131**·2PF_6 receptors upon addition of 10 equivalents of halide anions (electrolyte: 0.1 M TBA·PF_6 in CH_3CN, 293 K, reference electrode: Ag/AgCl). Values are reported to the nearest 5 mV.

	130·2PF_6	**131**·2PF_6
Cl^-	−40	−80
Br^-	−15	−30
I^-	−20	−10

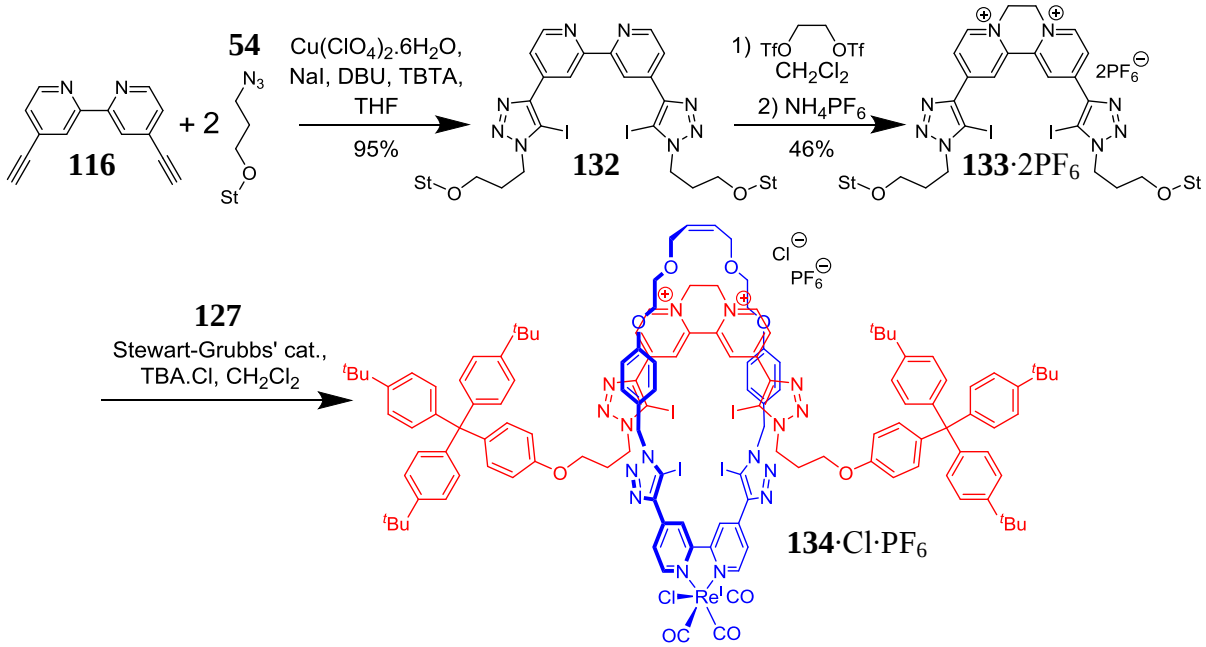
The prototriazole receptor **131**$^{2+}$ displays the largest magnitude of cathodic shift with Cl^-, followed by Br^- > I^-, which correlates with the ^{1}H NMR determined association constant selectivity trend. Iodotriazole receptor **130**$^{2+}$ exhibits the shift trend Cl^- > I^- > Br^-, which is different to the halide selectivity order determined *via* ^{1}H NMR studies. It is important to note however, that the ^{1}H NMR and electrochemistry anion binding experiments were undertaken

under different solvent conditions.

Both XB and HB diquat-based receptors exhibited strong halide binding affinities, and demonstrated their ability to sense anions through optical and electrochemical means. Attempts were then made to incorporate the XB diquat-based receptor motif into the axle component of a rotaxane.

4.6 *Attempted Synthesis of a Diquat-Containing All-XB Rotaxane*

The synthetic procedure undertaken to form the target rotaxane is shown in **Scheme 4-7**. Reaction of bis-alkyne **116** with two equivalents of stopper azide **54** under the Brotherton one-pot click conditions gave axle precursor **132** in 95% yield. Alkylation with 1,2-bis(triflyl)ethane afforded axle **133**·2PF_6 (46% yield), which was treated with equimolar amounts of macrocycle precursor **127** and TBA·Cl, and Stewart–Grubbs' catalyst, with the exclusion of light, to give rotaxane **134**·Cl·PF_6.



Scheme 4-7: Synthesis of diquat-containing rotaxane **134**·Cl·PF_6.

Although mass spectrometry provided evidence for rotaxane formation (**Figure 4-22a**), attempted purification using size-exclusion column chromatography failed to isolate any pure product. Furthermore, the relative intensity of the rotaxane mass peak had significantly decreased (**Figure 4-22b**). Fearing that the rotaxane was light-sensitive, a small sample of the crude reaction mixture was left exposed to light for 3 days. After this time, there was no longer evidence of the rotaxane by mass spectrometry.

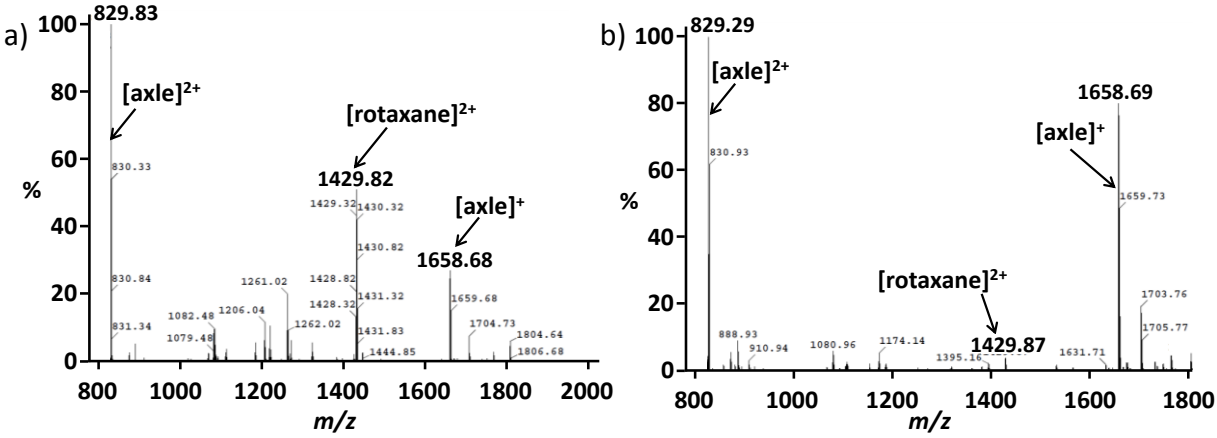


Figure 4-22: ESI+ mass spectra of **a)** crude **134**$^{2+}$ reaction mixture; and **b)** after purification by size exclusion chromatography.

Considering the apparent light-sensitive nature of the diquat-based all-XB rotaxane, and due to time constraints, further efforts to synthesise diquat-containing interlocked molecules were not undertaken.

4.7 *Conclusions and Future Work*

Two new anion receptor motifs have been developed, based on a rhenium(I) bipyridyl complex, and the diquat functional group.

A neutral acyclic receptor containing a XB rhenium(I) bipyridyl motif was shown by ^{1}H NMR spectroscopy to bind anions strongly in $CDCl_3$. This motif was successfully

incorporated into an allyl-appended macrocycle precursor, which was used in conjunction with a XB carbazole-based axle to form an all-XB rotaxane. This interlocked host system demonstrated strong and highly selective binding of halides in aqueous solvent mixtures, and was able to sense anions *via* luminescence spectroscopy. Importantly, halide anion binding behaviour remained strong in highly competitive aqueous solvent mixtures, with an association constant for I^- in 50% H_2O/CH_3CN of $\log(K_a) > 4$, making this XB rotaxane the most potent halide interlocked receptor reported to date.[32]

Acyclic HB and XB receptors based on the dicationic diquat motif also demonstrated potent anion binding affinities, with the XB iodotriazole-containing receptor exhibiting superior anion recognition behaviour. Both systems displayed an optical response upon addition of chloride, and they were also shown to exhibit an anion-induced electrochemical response, with cathodic shifts of the diquat redox couples. A XB diquat-based axle was then developed, and an attempt made to incorporate this component into an axle, in order to form an interlocked structure with the XB rhenium(I) bipyridyl-based macrocycle. Although there was mass spectrometry evidence for rotaxane formation, the interlocked molecule appeared to be unstable to light, and could not be isolated.

The neutral XB rhenium(I) bipyridyl-based macrocycle has been shown to effectively sense anions, and is certain to be incorporated into other interlocked structures in the future. While the target diquat-containing rotaxane could not be isolated, its electrochemical anion sensing properties encourage further efforts to integrate this redox-active receptor motif into other interlocked host molecular frameworks.

References

(1) Martínez-Máñez, R.; Sancenón, F. *Chem. Rev.* **2003**, *103*, 4419.
(2) Uppadine, L. H.; Redman, J. E.; Dent, S. W.; Drew, M. G. B.; Beer, P. D. *Inorg. Chem.* **2001**, *40*, 2860.
(3) Duff, T.; Grüßing, A.; Thomas, J.-L.; Duati, M.; Vos, J. G. *Polyhedron* **2003**, *22*, 775.
(4) Vickers, M. S.; Martindale, K. S.; Beer, P. D. *J. Mater. Chem.* **2005**, *15*, 2784.
(5) Watanabe, S.; Higashi, N.; Kobayashi, M.; Hamanaka, K.; Takata, Y.; Yoshida, K. *Tetrahedron Lett.* **2000**, *41*, 4583.
(6) Pratt, M. D.; Beer, P. D. *Tetrahedron* **2004**, *60*, 11227.
(7) Curiel, D.; Beer, P. D.; Paul, R. L.; Cowley, A.; Sambrook, M. R.; Szemes, F. *Chem. Commun.* **2004**, 1162.
(8) Curiel, D.; Beer, P. D.; Tárraga, A.; Molina, P. *Chem. Eur. J.* **2009**, *15*, 7534.
(9) Curiel, D.; Beer, P. D. *Chem. Commun.* **2005**, 1909.
(10) Hancock, L. M.; Marchi, E.; Ceroni, P.; Beer, P. D. *Chem. Eur. J.* **2012**, *18*, 11277.
(11) Lehr, J.; Lang, T.; Blackburn, O. A.; Barendt, T. A.; Faulkner, S.; Davis, J. J.; Beer, P. D. *Chem. Eur. J.* **2013**, *19*, 15898.
(12) Pelletier, G.; Lie, S.; Mousseau, J. J.; Charette, A. B. *Org. Lett.* **2012**, *14*, 5464.
(13) Fabbrizzi, P.; Cecconi, B.; Cicchi, S. *Synlett* **2011**, *2011*, 223.
(14) Brotherton, W. S.; Clark, R. J.; Zhu, L. *J. Org. Chem.* **2012**, *77*, 6443.
(15) Sonogashira, K.; Tohda, Y.; Hagihara, N. *Tetrahedron Lett.* **1975**, *16*, 4467.
(16) Hynes, M. J. *J. Chem. Soc., Dalton Trans.* **1993**, 311.
(17) Alunni, S.; Pero, A.; Reichenbach, G. *J. Chem. Soc., Perkin Trans. 2* **1998**, 1747.
(18) Hua, Y.; Ramabhadran, R. O.; Uduehi, E. O.; Karty, J. A.; Raghavachari, K.; Flood, A. H. *Chem. Eur. J.* **2011**, *17*, 312.
(19) Insufficient data were collected for accurate determination of an association constant.
(20) White, N. G.; Costa, P. J.; Carvalho, S.; Félix, V.; Beer, P. D. *Chem. Eur. J.* **2013**, *19*, 17751.
(21) Goddard-Borger, E. D.; Stick, R. V. *Org. Lett.* **2007**, *9*, 3797.
(22) Alvarez, S. *Dalton Trans.* **2013**, *42*, 8617.
(23) Specfit v. 2.02 ed., Spectrum Software Associates Chapel Hill, NC, USA: 1997.
(24) H. Kohnke, F.; Fraser Stoddart, J.; Allwood, B. L.; Williams, D. J. *Tetrahedron Lett* **1985**, *26*, 1681.
(25) Allwood, B. L.; Shahriari-Zavareh, H.; Stoddart, J. F.; Williams, D. J. *J. Chem. Soc., Chem. Commun.* **1987**, 1058.
(26) Coe, B. J.; Harris, J. A.; Brunschwig, B. S.; Garín, J.; Orduna, J. *J. Am. Chem. Soc.* **2005**, *127*, 3284.
(27) Summers, L. A. *Tetrahedron* **1968**, *24*, 2697.
(28) Schmalzl, K.; Summers, L. *Aust. J. Chem.* **1977**, *30*, 657.
(29) Lindner, E.; von Au, G.; Eberle, H.-J. *Chem. Ber.* **1981**, *114*, 810.
(30) Coe, B. J.; Fielden, J.; Foxon, S. P.; Asselberghs, I.; Clays, K.; Van Cleuvenbergen, S.; Brunschwig, B. S. *Organometallics* **2011**, *30*, 5731.
(31) Bard, A. J.; Faulkner, L. R. *Electrochemical Methods - Fundamentals and Applications, 2nd Ed.*; John Wiley & Sons, Inc.: New York, USA, 2001.
(32) Hancock, L. M.; Gilday, L. C.; Carvalho, S.; Costa, P. J.; Félix, V.; Serpell, C. J.; Kilah, N. L.; Beer, P. D. *Chem. Eur. J.* **2010**, *16*, 13082.

Chapter 5: Conclusions

Conclusions

The theme of this thesis was to explore the anion recognition behaviour of halogen bonding (XB) motifs, which were constructed around host structural scaffold units with potential sensing properties.

The systematic study of acyclic carbazole-based anion receptors, in conjunction with the diquat-based receptors, demonstrated the superior halide binding affinity of XB systems over hydrogen bonding (HB) analogues. Furthermore, almost all the acyclic XB receptors exhibited the halide binding trend $Cl^- > Br^- > I^-$. The exception to this order of binding was the diquat-based system, which displayed a minor preference for Br^- and was the most potent XB acyclic halide complexant, capable of recognising halides in a 10% water solvent mixture.

Integration of XB motifs into interlocked rotaxane host systems significantly augments halide binding affinity, requiring competitive aqueous solvent mixtures to quantify the binding behaviour. The observed selectivity for the larger halides Br^- and I^- under these aqueous conditions is consistent with the Hofmeister series bias, which favours the heavier halides on the basis of ease of desolvation. Future work will involve determining thermodynamic data, to establish whether enthalpy and/or entropy are favourable contributions to the overall recognition process.

These studies also highlight the importance of the precise nature of the rotaxane's three-dimensional binding cavity, for determining anion binding strength and selectivity. A carbazole-based mixed XB and HB rotaxane was found to be selective for Br^-, while a similar rotaxane integrating a XB naphthalene motif demonstrated a preference for I^-. An

all-XB rotaxane incorporating a rhenium(I) bipyridyl unit in the macrocycle component was shown to optically sense halide anions by luminescence, maintaining a high binding affinity in up to 50% water solvent mixtures, with a strong preference for I^-. This observation serves as compelling evidence that combining XB in an interlocked host design with an optical probe leads to a potent anion sensory system.

The strong anion binding affinities, and the optical and electrochemical properties of the XB rhenium(I) bipyridyl complex and diquat groups, make these receptor motifs worthy of future exploitation and development in anion receptor design.

As observed in the all-XB rhenium(I) bipyridyl-based rotaxane, increasing the water content appears to only have a minor effect on the binding strength of the halides, especially I^-. This bodes well for developing XB interlocked host systems which can function in pure water, with the opportunity for sensing a wide range of target biological anion analytes.

Chapter 6: Experimental Methods

6.1 *Titration Protocols*

6.1.1 *NMR Titrations*

Spectra for ^{1}H NMR titration experiments were recorded at 293 K on either a Varian Unity Plus 500 spectrometer, or a Bruker AVIII 500 spectrometer, both operating at 500 MHz. $CDCl_3$ was filtered through alumina immediately before use, to remove acidic impurities. The initial samples contained 0.5 mL of a 2.0 mmol L^{-1} solution of host. A solution of the anion as the tetrabutylammonium salt (100 mmol L^{-1}) was added in aliquots, the samples shaken thoroughly and spectra recorded. The spectra were generally recorded after 0, 0.2, 0.4, 0.6, 0.8, 1.0, 1.2, 1.4, 1.6, 1.8, 2.0, 2.5, 3.0, 4.0, 5.0, 7.0 and 10.0 equivalents of anion were added. Association constants were obtained by analysis of the resulting data using the WinEQNMR2[1] software. Where applicable, errors for these association constants are given, but it should be noted that these errors are only calculated from the least squares residuals, and do not take into consideration any experimental error, such as accuracy of the mass of receptor and guest, or volume of solvent. While every care was taken with the measurements, the association constant errors given should be taken as a guide, and not treated as absolute – they are most likely to have been underestimated.

6.1.2 *UV-vis Titrations*

UV-vis absorption titration experiments were performed on a T60U (PG Instruments Ltd) spectrophotometer at 293 K. The sample volume was 2.5 mL, and the anion was dissolved in a solution of the receptor at the same concentration as was being studied. Association constants were calculated from the absorption data using Specfit®.[2]

6.1.3 *Luminescence Titrations*

Luminescence titrations were undertaken using a HORIBA Fluorolog, and the data were processed using FluorEssence and Origin. For each luminescence titration experiment, 2.5 mL of a 0.010 mmol L^{-1} solution of host was used initially. A solution of the anion as the tetrabutylammonium salt (except HCO_3^-, which was used as the tetraethylammonium salt) was added in aliquots, the samples shaken thoroughly and the emission spectra recorded. The anion was dissolved in a 0.010 mmol L^{-1} solution of host in order to maintain a constant concentration of host throughout the titration. The concentration of anion and the aliquots added depended on the expected anion binding strength. For the titrations conducted on rotaxane **128**·$2PF_6$ in 10% or 20% H_2O/CH_3CN, an excitation wavelength of λ_{ex} = 400 nm was used; in 50% H_2O/CH_3CN, a wavelength of λ_{ex} = 390 nm was used as it gave a better luminescence response in this solvent mix. Association constants were calculated from the luminescence data using Specfit®.[2]

6.2 *X-ray Crystallography*

Single crystals were obtained by either slow evaporation of a solution of the compound (**64** from CH_3CN; **81** and **83**·$2BF_4$ from $CHCl_3$; **128**·$2PF_6$ from 45:45:10 $CDCl_3/CD_3OD/D_2O$), or liquid/liquid diffusion (**65** and Ni(**65**)$_2$ from CH_2Cl_2/MeOH).

Single crystal X-ray diffraction data were collected for **64**, Ni(**65**)$_2$ and **83**·$2BF_4$ using graphite monochromated Cu Kα radiation (λ = 1.5418 Å) on an Oxford Diffraction/Agilent Technologies SuperNova diffractometer. For **65** and **81**, data were collected on a Nonius Kappa-CCD using Mo-Kα (0.71073 Å) radiation. For **128**·$2PF_6$, data were collected using silicon double crystal monochromated synchrotron radiation (λ = 0.6889 Å) at Diamond

Light Source beamline I19[3] on a custom built Rigaku diffractometer. The diffractometer was equipped with a Cryostream N_2 open-flow cooling device,[4] and the data were collected at 100(2) K.

Series of ω-scans were performed to a maximum resolution of 0.77 Å. Cell refinement, data reduction, and scaling were performed using CrysAlisPro (Agilent Technologies, 2011).

The structures were generally solved by charge flipping using Superflip.[5] The structures were refined using full-matrix least-squares on F^2 within the CRYSTALS suite.[6] Other than Ni(**65**)$_2$ which was refined isotropically, all non-hydrogen atoms were refined with anisotropic displacement parameters. Disordered portions were modelled using refined partial occupancies. Geometric and vibrational restraints were applied where appropriate to ensure physically reasonable models. The H atoms were usually located in the difference map, but those attached to carbon atoms were repositioned geometrically. H atoms which could not be located in the difference map were positioned to satisfy chemical and geometric requirements. The H atoms were initially refined with soft restraints on the bond lengths and angles to regularise their geometry, after which the positions were refined with riding constraints.

The structure of rotaxane **128**·2PF_6 contained significant void space, which contained diffuse electron density that could not be resolved in the difference map, and PLATON SQUEEZE[7,8] was used to account for this residual electron density in the refinement.

After the construction of a stable, physically reasonable, and complete model, the weights were optimised,[9-11] anomalous reflections were omitted, and absent high-angle data were pruned using the Wilson plot. This generally led to convergence of the refinement, giving the

final structure.

IUCr CheckCIF/PLATON was used to validate the structure, and warnings were dealt with as appropriate or justified using validation reply forms.

Molecular graphics were produced using X-Seed[12] and POV-RAY.[13]

Complete data, including particular refinement details where appropriate, are presented in CIF format on the attached CD.

6.3 *Synthesis and Characterisation*

6.3.1 *Reactants and Reagents*

Dry solvents were obtained by purging with nitrogen and then passing through an MBraun MPSP-800 column. H_2O was deionised and microfiltered using a Milli-Q® Millipore machine. All tetrabutylammonium salts, Grubbs' catalysts, $[Cu(CH_3CN)_4](PF_6)$ and TBTA were stored in a vacuum desiccator over phosphorus pentoxide before use. $Cu(ClO_4)_2 \cdot 6H_2O$ was carefully dried *in vacuo* before use. All other solvents and commercial reagents were used without further purification. Column chromatography was performed on silica gel (particle size: 40-63 μm) and preparative TLC was performed on 20 × 20 cm plates, with a silica layer of thickness 1 mm. Et_3N was distilled from, and stored over, KOH pellets. TBTA (tris(benzyltriazolemethyl)amine)[14] and imidazolesulfonyl azide hydrogensulfate[15,16] were prepared according to literature procedures. 3,6-Bis-*tert*-butylcarbazole was kindly donated by Michael Kelly.

6.3.2 *Characterisation*

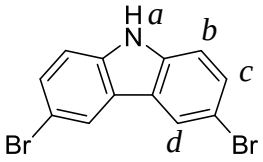
Routine NMR spectra were recorded on either a Varian Mercury 300 spectrometer, with ^1H

operating at 300 MHz, ^{13}C at 75.5 MHz and ^{19}F at 283 MHz, or a Bruker AVIII 400 nanobay instrument, with ^{1}H operating at 400 MHz and ^{13}C at 101 MHz. Where there was insufficient compound to characterise properly on this instrument, ^{1}H data were recorded on a Bruker AVIII 500 MHz spectrometer, and ^{13}C data were recorded on a Bruker AVII 500 spectrometer with a 5 mm $^{13}C(^{1}H)$ dual cryoprobe operating at 126 MHz. Low resolution mass spectrometry was conducted on a Waters LCT premier spectrometer, and high resolution mass spectra were recorded on a Bruker microTOF spectrometer.

All ^{1}H NMR spectra were referenced to the residual solvent peak, and where mixed solvents were used, the spectra were referenced to the solvent with the most deuterium atoms (e.g.: a 4:1 CD_2Cl_2/CD_3OD mixture would be referenced to the residual methanol signal). All reactions were conducted under a nitrogen atmosphere and exposed to ambient light, unless otherwise stated.

6.4 *Synthesis of Compounds from Chapter 2*

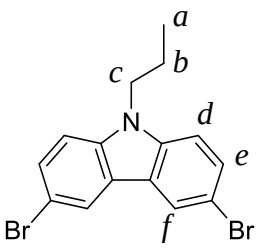
3,6-Dibromocarbazole, 1



Based on a literature procedure.[17] Carbazole (1.67 g, 10.0 mmol) and silica (40 g) were stirred in CH_2Cl_2 (200 mL), with the exclusion of light. A solution of *N*-bromosuccinimide (3.56 g, 20.0 mmol) dissolved in CH_2Cl_2 (250 mL) was added dropwise, then stirred at RT for 5 h. The green mixture was filtered and the silica washed with CH_2Cl_2 (3 × 60 mL), then the combined extracts were washed with water (400 mL), dried ($MgSO_4$) and the solvent removed *in vacuo*. The residue was recrystallised from ethanol, giving the product as a green/grey solid (1.28 g, 39%); **^{1}H NMR** (400 MHz, $CDCl_3$) δ ppm 8.14 (s, 2H, 2 × H_d), 8.10

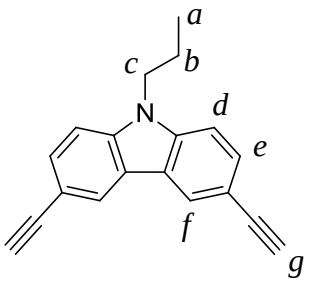
(s, 1H, 2 × H_a), 7.53 (d, ^3J = 8.56 Hz, 2H, 2 × H_c), 7.31 (d, ^3J = 8.56 Hz, 2H, 2 × H_b); **^{13}C NMR** (101 MHz, $CDCl_3$) δ ppm 138.35, 129.32, 124.11, 123.28, 112.65, 112.22; **HRMS (FI+)** *m/z*: 324.8876 ($[M]^+$, calc. for $[C_{12}H_7Br_2N]^+$ = 324.8925).

***N*-Propyl dibromocarbazole, 2**



Based on a literature procedure.[18] 3,6-Dibromocarbazole **1** (3.25 g, 10.0 mmol) and TBA·Cl (0.322 g, 1.16 mmol) were dissolved in DMSO (50 mL). $NaOH_{(aq.)}$ (50% w/w, 2.25 mL) and 1-bromopropane (1.4 mL, 1.8 g, 15 mmol) were added, and the mixture stirred at 60 °C for 12 h. The reaction was then quenched with water (100 mL), and extracted into CH_2Cl_2 (3 × 40 mL). The organic extracts were combined and washed with water (4 × 40 mL), dried ($MgSO_4$) and the solvent removed *in vacuo*. The residue was then purified by column chromatography (20% CH_2Cl_2/pet. ether), giving the product as white crystals (3.14 g, 85%); **^{1}H NMR** (300 MHz, $CDCl_3$) δ ppm 8.15 (s, 2H, 2 × H_f), 7.56 (dd, ^3J = 8.80 Hz, ^4J = 1.76 Hz, 2H, 2 × H_e), 7.29 (d, ^3J = 9.39 Hz, 2H, 2 × H_d), 4.23 (t, ^3J = 7.00 Hz, 2H, 2 × H_c), 1.89 (sxt, ^3J = 7.16 Hz, 2H, 2 × H_b), 0.95 (t, ^3J = 7.33 Hz, 3H, 2 × H_a).

Diethynylcarbazole, 3

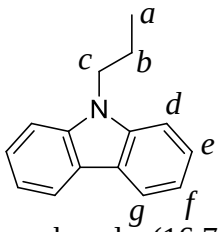


Method 1: To a degassed solution of dibromocarbazole **2** (1.0 g, 2.1 mmol) and TMS-acetylene (1.87 mL, 1.3 g, 13 mmol) in dry triethylamine (20 mL) were added copper(I) iodide (13 mg, 0.068 mmol) and $Pd(PPh_3)_2Cl_2$ (95 mg, 0.13 mmol). The mixture was stirred for 5 d at 85 °C in a closed vial. The reaction mixture was allowed to cool to RT, whereupon

it was flushed through a silica pad with CH_2Cl_2 (150 mL). The solvent was removed *in vacuo*. To the resultant residue was added CH_3CN (40 mL), water (2 mL) and KOH (0.60 g, 11 mmol), and the mixture was stirred for 1 h. The organic solvent was removed *in vacuo*. $NH_4Cl_{(aq.)}$ (1 M, 40 mL) was added, and the mixture was extracted into $CHCl_3$ (3 × 30 mL). The combined organics were washed with $NH_4Cl_{(aq.)}$ (1 M, 30 mL) and water (2 × 30 mL), dried ($MgSO_4$), filtered and concentrated to dryness *in vacuo*. The residue was purified by column chromatography (30% CH_2Cl_2 in pet. ether) to give the desired product **3** as a light brown solid (0.424 mg, 61%).

Method 2: To a degassed solution of diiodocarbazole **5** (1.0 g, 2.1 mmol) and trimethylsilyl-acetylene (1.5 mL, 11 mmol) in dry triethylamine (20 mL) were added copper(I) iodide (10 mg, 0.050 mmol) and $Pd(PPh_3)_2Cl_2$ (75 mg, 0.11 mmol). The mixture was stirred for 72 h at 85 °C in a closed vial. The reaction mixture was allowed to cool to RT, after which it was purified according to the same procedure as described in Method 1, giving the desired product **3** (0.470 g, 84%) as a light brown solid; **^{1}H NMR** (300 MHz, $CDCl_3$) δ ppm 8.23 (d, ^4J = 1.76 Hz, 2H, 2 × H_f), 7.62 (dd, ^3J = 8.21, ^4J = 1.76 Hz, 2H, 2 × H_e), 7.36 (d, ^3J = 8.21 Hz, 2H, 2 × H_d), 4.27 (t, ^3J = 7.04 Hz, 2H, 2 × H_c), 3.09 (s, 2H, 2 × H_g), 1.91 (sxt, ^3J = 7.27 Hz, 2H, 2 × H_b), 0.97 (t, ^3J = 7.33 Hz, 3H, 3 × H_a); **^{13}C NMR** (76 MHz, $CDCl_3$): δ ppm 140.70, 130.10, 124.74, 122.20, 112.65, 108.98, 84.70, 75.45, 44.83, 22.27, 11.73; **HRMS (FI+)** *m/z*: 257.1210 ($[M]^+$, calc. for $[C_{19}H_{15}N]^+$ = 257.1205).

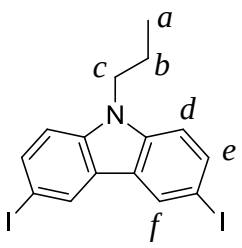
_N_-Propylcarbazole, 4



Based on a literature procedure.[19] To carbazole (16.7 g, 100 mmol) dissolved in toluene (20 mL) was added TBA·I (1.11 g, 3.0 mmol) as a phase transfer catalyst, 1-bromopropane (15.4 g, 11.4 mL, 125 mmol) and $NaOH_{(aq.)}$ (50% w/v, 120 mL). The reaction mixture was heated to 80 °C and stirred for 2 h. The solvent was then removed *in vacuo*, then the residue extracted with CH_2Cl_2 (3 × 20 mL) from H_2O (40 mL). The organic layer was dried ($MgSO_4$), the solvent removed *in vacuo* and the crude recrystallised from ethanol to give pure

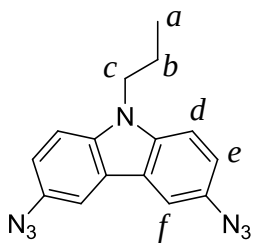
product **4** as a brown crystalline solid (16.7 g, 80%); **^{1}H NMR** (300 MHz, $CDCl_3$) δ ppm 8.12 (d, ^3J = 8.21 Hz, 2H, 2 × H_g), 7.38–7.53 (m, 4H, 2 × H_d, 2 × H_e), 7.19–7.29 (m, 2H, 2 × H_f), 4.30 (t, ^3J = 7.04 Hz, 2H, 2 × H_c), 1.93 (sxt, ^3J = 7.27 Hz, 2H, 2 × H_b), 0.99 (t, ^3J = 7.33 Hz, 2H, 3 × H_a); **^{13}C NMR** (76 MHz, $CDCl_3$): δ ppm 140.48, 125.52, 122.78, 120.29, 118.67, 108.66, 44.58, 22.28, 11.79**; HRMS (FI+)** *m/z*: 209.1202 ($[M]^+$, calc. for $[C_{15}H_{15}N]^+$ = 209.1205).

Diiodocarbazole, 5



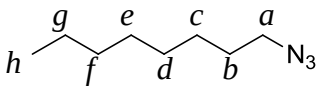
Based on a literature procedure.[19] *N*-propyl carbazole **9** (2.09 g, 10 mmol) and *N*-iodosuccinimide (5.40 g, 24 mmol) were stirred in $CHCl_3$ (100 mL) and acetic acid (30 mL) for 6 h at RT. The solvent was evaporated *in vacuo* and the residue poured into water (200 mL). The mixture was extracted into CH_2Cl_2 (4 × 50 mL) and the combined organics dried ($MgSO_4$) and the solvent removed *in vacuo*. The residue was purified by column chromatography (silica; 0–15% CH_2Cl_2 in pet. ether) to give the desired product **5** (3.74 g, 81%) as a white crystalline solid; **^{1}H NMR** (300 MHz, $CDCl_3$) δ ppm 8.34 (d, ^4J = 1.17 Hz, 2H, 2 × H_f), 7.72 (dd, ^3J = 8.80, 1.76 Hz, 2H, 2 × H_e), 7.19 (d, ^3J = 8.80 Hz, 2H, 2 × H_d), 4.21 (t, ^3J = 7.04 Hz, 2H, 2 × H_c), 1.87 (sxt, ^3J = 7.27 Hz, 2H, 2 × H_b), 0.94 (t, ^3J = 7.33 Hz, 3H, 3 × H_a); **^{13}C NMR** (76 MHz, $CDCl_3$): δ ppm 139.54, 134.46, 129.32, 110.92, 81.64, 44.74, 22.18, 11.73; **HRMS (FI+)** *m/z*: 460.9142 ($[M]^+$, calc. for $[C_{15}H_{13}I_2N]^+$ = 460.9138).

Diazidocarbazole, 6



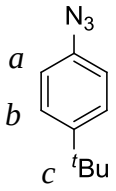
Diiodocarbazole **5** (500 mg, 1.1 mmol), sodium azide (210 mg, 3.2 mmol), copper(I) iodide (41 mg, 0.21 mmol), L-proline (50 mg, 0.43 mmol), NaOH (17 mg, 0.43 mmol) and sodium ascorbate (130 mg, 0.65 mmol) were stirred in DMSO (4 mL) in a sealed tube for 36 h at 60 °C. The reaction mixture was allowed to cool to RT, whereupon it was partitioned between diethyl ether (50 mL) and water (100 mL). $HCl_{(aq.)}$ (1 M, 20 mL) was added and the mixture extracted into diethyl ether (4 × 50 mL). The combined organics were washed with $HCl_{(aq.)}$ (1 M, 25 mL), $NaOH_{(aq.)}$ (10%, 25 mL), water (50 mL) and brine (50 mL), dried ($MgSO_4$), filtered and concentrated to dryness *in vacuo* to give the desired product **12** (180 mg, 55%) as an orange solid; **^{1}H NMR** (300 MHz, $CDCl_3$): δ ppm 7.71 (d, ^4J = 1.76 Hz, 2H, 2 × H_f), 7.38 (d, ^3J = 8.80 Hz, 2H, 2 × H_d), 7.16 (dd, ^3J = 8.51, ^4J = 2.05 Hz, 2H, 2 × H_e), 4.25 (t, ^3J = 7.63 Hz, 2H, 2 × H_c), 1.90 (sxt, ^3J = 7.04 Hz, 2H, 2 × H_b), 0.96 (t, ^3J = 7.33 Hz, 3H, 2 × H_a); **^{13}C NMR** (126 MHz, $CDCl_3$): δ ppm 138.65, 131.33, 122.87, 117.92, 110.44, 110.05, 44.94, 22.33, 11.74; **HRMS (FI+)** *m/z*: 291.1240 ($[M]^+$, calc. for $[C_{15}H_{13}N_7]^+$ = 291.1232).

***n*-Octyl azide, 7**



Based on a literature procedure.[20] 1-Bromooctane (1.93 g, 10.0 mmol) was dissolved in DMSO (40 mL). Sodium azide (0.98 g, 15 mmol) was added and the resultant mixture stirred overnight at RT. The mixture was diluted with water (50 mL) and extracted into diethyl ether (2 × 80 mL). The combined organics were washed with water (2 × 80 mL) and brine (80 mL), dried ($MgSO_4$), filtered and concentrated to dryness *in vacuo* to give the desired product **14** (1.4 g, 92%) as a colourless oil; **^{1}H NMR** (300 MHz, $CDCl_3$) δ ppm 3.25 (t, ^3J = 6.89 Hz, 2H, 2 × H_a), 1.69–1.50 (m, 2H, 2 × H_b), 1.45–1.17 (m, 10H, 2 × $H_{c–g}$), 0.89 (t, ^3J = 6.75 Hz, 3H, 3 × H_h).

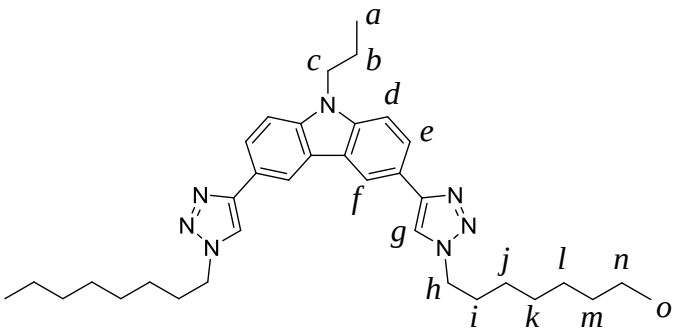
1-Azido-4-(*tert*-butyl)benzene, 8



Based on a literature procedure.[21] 4-(*Tert*-butyl)aniline (1.0 g, 6.7 mmol) was added to $HCl_{(aq.)}$ (17%, 40 mL), followed by ethanol (10 mL). The mixture was carefully heated until the aniline had dissolved and then cooled to −5 °C, whereupon sodium nitrite (0.690 g, 10.0 mmol) was added portionwise. The mixture was stirred for 10 min, and then sodium azide (0.650 g, 10.0 mmol) was added portionwise. The resultant mixture was allowed to warm to RT, whereupon it was stirred overnight. The mixture was diluted with water (40 mL) and extracted into diethyl ether (3 × 40 mL). The combined organics were washed with $NaHCO_{3(aq.)}$ (3 × 20 mL) and brine (20 mL), dried ($MgSO_4$), filtered and concentrated to dryness *in vacuo* to give the desired product **13** (820 mg, 70%) as a dark red oil; **^{1}H NMR** (300 MHz, $CDCl_3$) δ ppm 7.38 (d, ^3J = 8.80 Hz, 2H, 2 × H_b), 6.97 (d, ^3J = 8.80 Hz, 2H, 2 × H_a), 1.32 (s, 9H, 9 × H_c).

General Procedure 1: To a solution of diethynylcarbazole **3** (59 mg, 0.23 mmol, 1.0 eq.) and azide (2.2 eq.) in CH_2Cl_2 (25 mL) were added TBTA (27 mg, 0.050 mmol) and $[Cu(CH_3CN)_4](PF_6)$ (19 mg, 0.050 mmol), followed by DIPEA (26 mg, 0.20 mmol). The resultant mixture was stirred for 72 h at RT. The reaction mixture was concentrated to dryness *in vacuo* and the residue purified by column chromatography (1% MeOH/CH_2Cl_2) to give the desired product.

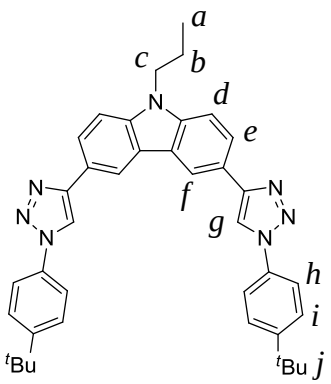
C-linked alkyl-appended bis-prototriazole receptor precursor, 9



n-Octyl azide **7** (79 mg, 0.51 mmol) was reacted by *General Procedure 1* to give the desired

product **9** (121 mg, 93%); **^{1}H NMR** (300 MHz, $CDCl_3$): δ ppm 8.60 (d, ^4J = 1.8 Hz, 2H, 2 × H_f), 7.99 (dd, ^3J = 8.8, ^4J = 1.8 Hz, 2H, 2 × H_e), 7.81 (s, 2H, 2 × H_g), 7.46 (d, ^3J = 8.2 Hz, 2H, 2 × H_d), 4.44 (t, ^3J = 7.0 Hz, 4H, 4 × H_h), 4.31 (t, ^3J = 7.0 Hz, 2H, 2 × H_c), 2.06–1.88 (m, 6H, 2 × H_b, 4 × H_i), 1.46–1.24 (m, 20H, 20 × $H_{j–n}$), 1.00 (t, ^3J = 7.6 Hz, 3H, 2 × H_a), 0.93–0.84 (m, 6H, 6 × H_o); **^{13}C NMR** (76 MHz, $CDCl_3$): δ ppm 140.77, 123.89, 123.15, 117.84, 109.24, 50.64, 44.83, 31.73, 30.37, 29.08, 26.60, 22.62, 22.36, 14.13, 11.80; **HRMS (ESI+)** *m/z*: 568.4113 ($[M + H]^+$, calc. for $[C_{35}H_{50}N_7]^+$ = 568.4122).

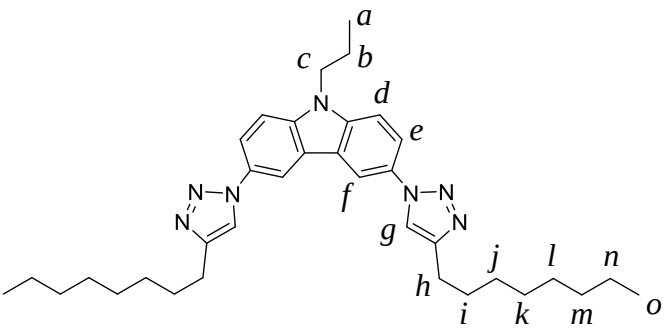
C-linked aryl-appended bis-prototriazole receptor precursor, 10



1-Azido-4-(tert-butyl)benzene **8** (89 mg, 0.51 mmol) was reacted by *General Procedure 1* to give the desired product **10** (125 mg, 90%); **^{1}H NMR** (300 MHz, $CDCl_3$) δ ppm 8.65 (s, 2H, 2 × H_f), 8.23 (s, 2H, 2 × H_g), 8.04 (dd, ^3J = 8.8, ^4J = 1.2 Hz, 2H, 2 × H_e), 7.75 (d, ^3J = 8.2 Hz, 4H, 4 × H_h), 7.56 (d, ^3J = 8.8 Hz, 4H, 4 × H_i), 7.44 (d, ^3J = 8.8 Hz, 2H, 2 × H_d), 4.25 (t, ^3J = 7.0 Hz, 2H, 2 × H_c), 1.93 (sxt, ^3J = 7.3 Hz, 2H, 2 × H_b), 1.39 (s, 18H, 18 × H_j), 0.99 (t, ^3J = 7.3 Hz, 3H, 2 × H_a); **^{13}C NMR** (76 MHz, $CDCl_3$): δ ppm 151.88, 149.15, 140.88, 134.75, 126.61, 124.04, 123.13, 121.50, 120.11, 117.99, 116.81, 109.27, 44.81, 34.79, 31.29, 22.37, 11.81; **HRMS (ESI+)** *m/z*: 608.3482 ($[M + H]^+$, calc. for $[C_{39}H_{42}N_7]^+$ = 608.3496).

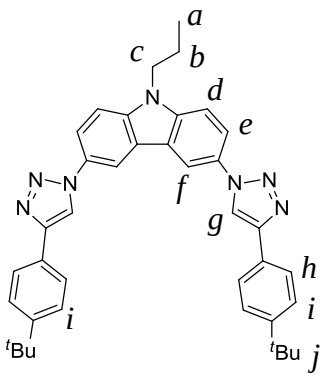
General Procedure 2: To a solution of diazidocarbazole **6** (23 mg, 0.078 mmol, 1.0 eq.) and alkyne (2.6 eq.) in CH_2Cl_2 (12 mL) were added TBTA (27 mg, 0.050 mmol) and $[Cu(CH_3CN)_4](PF_6)$ (19 mg, 0.050 mmol), followed by DIPEA (30 mg, 0.25 mmol). The resultant mixture was stirred for 72 h at RT. The reaction mixture was washed with $HCl_{(aq.)}$ (1 M, 2 × 10 mL) and $NaHCO_{3(aq.)}$ (2 × 10 mL), dried ($MgSO_4$), filtered and concentrated to dryness *in vacuo*. The residue was purified by column chromatography (1% MeOH/CH_2Cl_2) to give the desired product.

N-linked alkyl-appended bis-prototriazole receptor precursor, 11



1-Decyne (28 mg, 0.20 mmol) was reacted by *General Procedure 2* to give the desired product **11** (31 mg, 70%) as a brown oil; **^{1}H NMR** (300 MHz, $CDCl_3$): δ ppm 8.35 (d, ^{4}J = 2.1 Hz, 2H, 2 × H_f), 7.84 (dd, ^{3}J = 8.8, ^{4}J = 2.0 Hz, 2H, 2 × H_e), 7.79 (s, 2H, 2 × H_g), 7.51 (d, ^{3}J = 8.7 Hz, 2H, 2 × H_d), 4.33 (t, ^{3}J = 7.1 Hz, 2H, 2 × H_c), 2.82 (t, ^{3}J = 7.7 Hz, 4H, 4 × H_h), 1.94 (sxt, ^{3}J = 7.3 Hz, 2H, 2 × H_b), 1.83–1.66 (m, 4H, 4 × H_i), 1.51–1.18 (m, 20H, 20 × $H_{j–n}$), 0.98 (t, ^{3}J = 7.4 Hz, 3H, 3 × H_a), 0.93–0.82 (m, 6H, 6 × H_o); **^{13}C NMR** (76 MHz, $CDCl_3$): δ ppm 149.12, 140.66, 130.17, 122.68, 119.82, 119.46, 113.10, 109.99, 45.10, 31.88, 29.50, 29.39, 29.33, 29.25, 25.77, 22.68, 22.35, 14.13, 11.76; **HRMS (ESI+)** *m/z*: 568.4119 ($[M + H]^+$, calc. for $[C_{35}H_{50}N_7]^+$ = 568.4122).

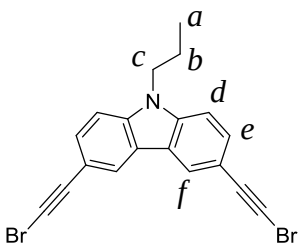
N-linked aryl-appended bis-prototriazole receptor precursor, 12



1-(*Tert*-butyl)-4-ethynylbenzene (126 mg, 0.20 mmol) was reacted by *General Procedure 2* to give the desired product **12** (140 mg, 74%) as a brown solid; **^{1}H NMR** (300 MHz, $CDCl_3$): δ ppm 8.39 (d, ^{4}J = 2.0 Hz, 2H, 2 × H_f), 8.25 (s, 2H, 2 × H_g), 7.97–7.82 (m, 6H, 2 × H_e, 4 × H_h), 7.55–7.40 (m, 6H, 2 × H_d, 4 × H_i), 4.30 (t, ^{3}J = 7.1 Hz, 2H, 2 × H_c), 1.95 (sxt, ^{3}J = 7.2 Hz, 2H, 2 × H_b), 1.36 (s, 18H, 18 × H_j), 0.98 (t, ^{3}J = 7.4 Hz, 3H, 3 × H_a); **^{13}C NMR** (76 MHz, $CDCl_3$): δ ppm 151.44, 148.31, 140.74, 129.92, 127.55, 122.65, 119.81, 117.94,

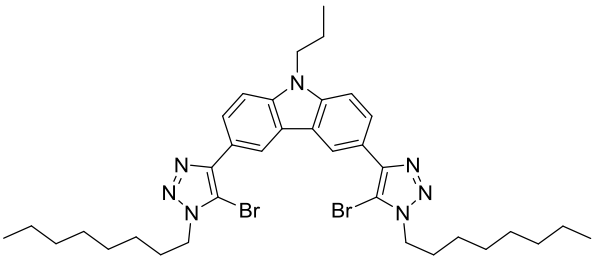
113.11, 109.98, 45.09, 34.71, 22.35, 11.76; **HRMS (ESI+)** *m/z*: 630.3336 ($[M + Na]^+$, calc. for $[C_{39}H_{41}N_7Na]^+$ = 630.3316).

Bis(bromoethynyl)carbazole, 13



Diethynylcarbazole **3** (100 mg, 0.38 mmol) was dissolved in acetone (12 mL) and excluded from light. *N*-bromosuccinimide (0.17 g, 0.94 mmol) and $AgNO_3$ (16 mg, 0.094 mmol) were added and the reaction mixture stirred at RT in the dark for 2 h, after which a suspension was formed. The solvent was removed *in vacuo*, then the residue was dissolved in CH_2Cl_2 and washed with water (2 × 10 mL), then dried ($MgSO_4$) and the solvent removed *in vacuo*. The residue was purified by column chromatography (15% CH_2Cl_2/ pet. ether), giving a yellow oil that solidified on standing (53 mg, 34%); **^{1}H NMR** (300 MHz, $CDCl_3$) δ ppm 8.17 (d, ^4J = 1.17 Hz, 2H, 2 × H_f), 7.56 (dd, ^3J = 8.21, ^4J = 1.76 Hz, 2H, 2 × H_e), 7.34 (d, ^3J = 8.80 Hz, 2H, 2 × H_d), 4.25 (t, ^3J = 7.00 Hz, 2H, 2 × H_c), 1.90 (sxt, ^3J = 7.20 Hz, 2H, 2 × H_b), 0.97 (t, ^3J = 7.60 Hz, 3H, 2 × H_a). **HRMS (FI+)** *m/z*: 416.9384 ($[M]^+$, calc. for $[C_{19}H_{13}Br_2N]^+$ = 416.9377).

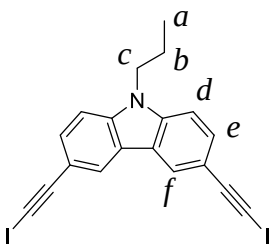
Attempted Synthesis of bis-bromotriazole carbazole, 14



CuI (28 mg, 0.15 mmol) and $Cu(AcO)_2$ (22.4 mg, 0.15 mmol) were dissolved in dry THF (10 mL) and stirred for 30 min. This solution was then added to a solution of bis(bromoethynyl)carbazole **3** (30 mg, 0.073 mmol) and *n*-octyl azide **7** (23 mg, 0.15 mmol) dissolved in dry THF (10 mL). The mixture was heated at 50 °C for 14 d, then cooled to RT,

then $NH_4OH_{(aq.)}$ (10% w/w, 5 mL) was added, and the THF removed *in vacuo*. The residue was extracted with CH_2Cl_2 (3 × 20 mL), then the combined organic extracts were washed with water (20 mL), dried ($MgSO_4$) and the solvent removed *in vacuo*. The residue was purified by preparative TLC plate (silica, 1% MeOH/CH_2Cl_2), giving the product as a mixture of bromotriazole- and iodotriazole-substituted carbazole, which could not be purified further. NB: An initial attempt to form the product using CuBr instead of CuI did not result in any detectable reaction.

Bis(iodoethynyl)carbazole, 15



Method 1: This procedure was not successful in producing the desired product. Diethynylcarbazole **3** (50 mg, 0.19 mmol) was dissolved in acetone (12 mL) and excluded from light. *N*-iodosuccinimide (225 mg, 1.0 mmol) and $AgNO_3$ (17 mg, 0.1 mmol) were added and the reaction mixture stirred at RT in the dark for 2 h.

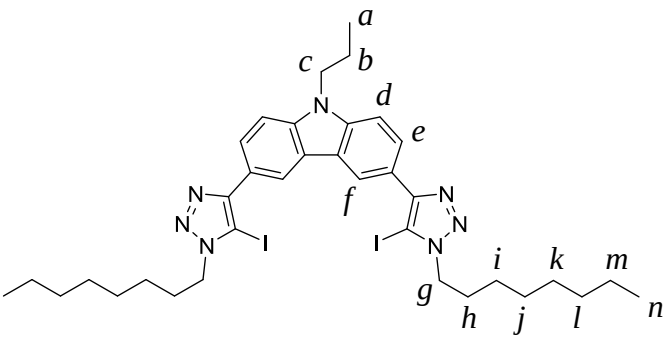
Method 2: Diethynylcarbazole **3** (59 mg, 0.23 mmol) was added to a solution of DMAP (120 mg, 0.98 mmol) and iodine (124 mg, 0.98 mmol) in dry CH_2Cl_2 (4 mL), and the mixture heated at reflux for 6 h (NB: extended heating reduces yield due to product decomposition). The reaction was cooled to RT, washed with a saturated aqueous sodium thiosulfate solution (5 mL), and the aqueous phase was extracted with diethyl ether (3 × 20 mL). The organics were combined, washed with brine (10 mL), dried ($MgSO_4$) and the solvent removed *in vacuo*. The residue was purified by column chromatography (5% EtOAc/pet. ether) in the dark, giving the product as a yellow oil (48 mg, 41%).

Method 3: Diethynylcarbazole **3** (100 mg, 0.39 mmol) was dissolved in THF (2 mL), and treated with CuI (8 mg, 0.045 mmol) and *N*-iodomorpholine (290 mg, 0.86 mmol). The reaction mixture was stirred at RT for 2 h, after which a white precipitate had formed. The suspension was poured onto a pad of neutral alumina, which had been packed with CH_2Cl_2, and the filtrate collected under vacuum. The solid phase was washed with CH_2Cl_2

(4 × 10 mL), and the organic fractions were combined, washed with a saturated aqueous solution of sodium thiosulfate (20 mL), dried ($MgSO_4$) and the solvent removed. The residue was then filtered through a silica pad, eluting with 10% EtOAc/hexane, and the filtrate solvent was removed *in vacuo*. The residue was recrystallised from hexane, giving the product as a yellow solid (77 mg, 39%). Note that this product is highly unstable to light, rapidly decomposing to the protoalkyne form, and must be used immediately; **^{1}H NMR** (300 MHz, $CDCl_3$) δ ppm 8.15 (s, 2H, 2 × H_f) 7.55 (dd, ^3J = 8.80 Hz, ^4J = 1.76 Hz, 2H, 2 × H_e) 7.33 (d, ^3J = 8.80 Hz, 2H, 2 × H_d) 4.24 (t, ^3J = 7.60 Hz, 2H, 2 × H_c) 1.90 (sxt, ^3J = 7.40 Hz, 2H, 2 × H_b) 0.96 (t, ^3J = 7.33 Hz, 3H, 3 × H_a).

General Procedure 3: Based on a recently reported procedure.[22] To a solution of azide (2.3 eq.) in CH_3CN (2 mL) were added sodium iodide (240 mg, 1.6 mmol) and $Cu(ClO_4)_2 \cdot 6H_2O$ (300 mg, 0.80 mmol). The resultant mixture was stirred for 5 min at RT. To the mixture was then added TBTA (21 mg, 0.040 mmol) and DBU (61 mg, 0.40 mmol), followed by diethynylcarbazole **3** (51 mg, 0.20 mmol, 1.0 eq.) and THF (1 mL) for solubility. The solution was then stirred overnight at RT in the dark. The reaction mixture was diluted with CH_2Cl_2 (50 mL), washed with $NH_4OH_{(aq.)}$ (25 mL) and brine (2 × 25 mL), dried ($MgSO_4$), filtered and concentrated to dryness *in vacuo*. The residue was purified by preparative TLC (0.5% MeOH/CH_2Cl_2) to give the desired product.

C-linked alkyl-appended bis-iodotriazole receptor precursor, 16

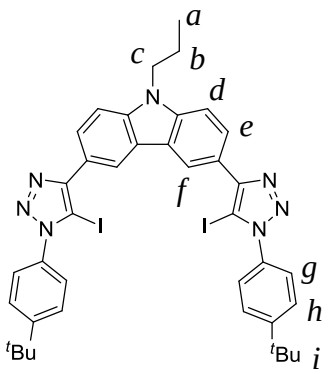


Method 1: Diethynylcarbazole **3** (86 mg, 0.17 mmol) and *n*-octyl azide **7** (58 mg, 0.37 mmol) were dissolved in dry THF (2 mL). Concurrently, CuI (16 mg, 0.084 mmol) and triethylamine (0.07 mL, 5.1 mg, 0.050 mmol) were stirred together in dry THF (2 mL) for 20 min at RT. The CuI solution was then added to the carbazole solution. The reaction mixture was stirred for 3 d, then quenched with $NH_4OH_{(aq.)}$ (10%, 2 mL) and the THF removed *in vacuo*. Water

(5 mL) was added and the aqueous phase extracted with CH_2Cl_2 (3 × 10 mL). The combined organic fractions were dried ($MgSO_4$) and the solvent removed *in vacuo*. The residue was purified by preparative TLC plate (1% MeOH/CH_2Cl_2), giving the product as an off-white solid (2.2 mg, 2%).

Method 2: *n*-Octyl azide **7** (70 mg, 0.45 mmol) was reacted by *General Procedure 3* to give the desired product **16** (68 mg, 54%); **^{1}H NMR** (300 MHz, $CDCl_3$): δ ppm 8.72 (d, ^4J = 1.8 Hz, 2H, 2 × H_f), 8.06 (dd, ^3J = 8.8, ^4J = 1.8 Hz, 2H, 2 × H_e), 7.53 (d, ^3J = 8.8 Hz, 2H, 2 × H_d), 4.49 (t, ^3J = 7.3 Hz, 4H, 4 × H_g), 4.35 (t, ^3J = 7.3 Hz, 2H, 2 × H_c), 2.06–1.88 (m, 6H, 2 × H_b, 4 × H_h), 1.50–1.24 (m, 20H, 20 × $H_{i–m}$), 1.03 (t, ^3J = 7.3 Hz, 3H, 2 × H_a), 0.95–0.85 (m, 6H, 6 × H_n); **^{13}C NMR** (76 MHz, $CDCl_3$): δ ppm 150.63, 140.89, 125.76, 122.92, 121.36, 119.88, 108.95, 75.83, 51.02, 44.90, 31.74, 30.02, 29.02, 26.47, 22.63, 22.40, 14.11, 11.84; **HRMS (ESI+)** *m/z*: 842.1867 ($[M + Na]^+$, calc. for $[C_{35}H_{47}I_2N_7Na]^+$ = 842.1875).

C-linked aryl-appended bis-iodotriazole receptor precursor, 17

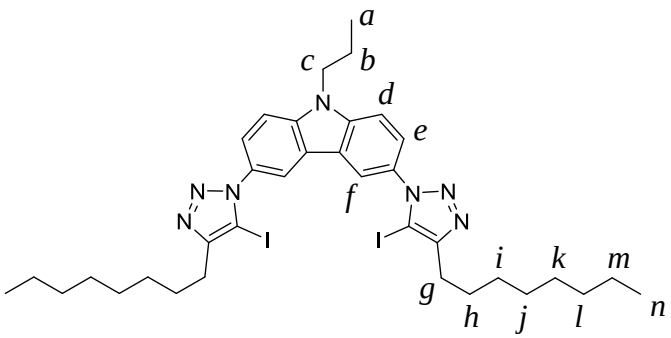


1-Azido-4-(tert-butyl)benzene (79 mg, 0.45 mmol) was reacted by *General Procedure 3* to give the desired product **17** (127 mg, 74%); **^{1}H NMR** (300 MHz, $CDCl_3$): δ ppm 8.81 (d, ^4J = 1.6 Hz, 2H, 2 × H_f), 8.14 (dd, ^3J = 8.6, ^4J = 1.7 Hz, 2H, 2 × H_e), 7.63–7.49 (m, 10H, 2 × H_d, 4 × H_g, 4 × H_h), 4.36 (t, ^3J = 7.2 Hz, 2H, 2 × H_c), 2.00 (spt, ^3J = 6.9 Hz, 2H, 2 × H_b), 1.40 (s, 18H, 18 × H_i), 1.05 (t, ^3J = 7.3 Hz, 3H, 3 × H_a); **^{13}C NMR** (76 MHz, $CDCl_3$): δ ppm 153.42, 151.20, 141.03, 134.56, 126.26, 125.99, 122.98, 121.18, 120.16, 109.03, 44.96, 34.99, 31.30, 22.44, 11.89; **HRMS (ESI+)** *m/z*: 882.1223 ($[M + Na]^+$, calc. for $[C_{39}H_{39}I_2N_7Na]^+$ = 882.1249).

General Procedure 4: Based on a recently reported procedure.[22] To a solution of diazidocarbazole **6** (64 mg, 0.22 mmol, 1.0 eq.) in CH_3CN (10 mL) was added sodium iodide

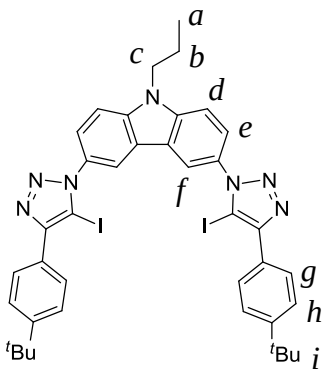
(240 mg, 1.6 mmol) and $Cu(ClO_4)_2 \cdot 6H_2O$ (300 mg, 0.80 mmol). The resultant mixture was stirred for 5 min at RT. To the mixture was then added TBTA (22 mg, 0.040 mmol), DBU (67 mg, 0.44 mmol) and THF (1 mL) for solubility, followed by alkyne (2.8 eq.). The resultant mixture was stirred overnight at RT. The reaction mixture was concentrated to dryness *in vacuo*, diluted with CH_2Cl_2 (50 mL), washed with $NH_4OH_{(aq.)}$ (25 mL), $HCl_{(aq.)}$ (1 M, 25 mL), $NaHCO_{3(aq.)}$ (25 mL), water (25 mL) and brine (25 mL), dried ($MgSO_4$), filtered and concentrated to dryness *in vacuo*. The residue was purified by preparative TLC (1% $MeOH/CH_2Cl_2$) to give the desired product.

N-linked alkyl-appended bis-iodotriazole receptor precursor, 18



1-Decyne (83 mg, 0.60 mmol) was reacted by *General Procedure 4* to give the desired product **18** (41 mg, 23%); **^{1}H NMR** (300 MHz, $CDCl_3$): δ ppm 8.22 (d, ^4J = 1.8 Hz, 2H, 2 × H_f), 7.64 (dd, ^3J = 8.8, ^4J = 2.4 Hz, 2H, 2 × H_e), 7.59 (d, ^3J = 8.8 Hz, 2H, 2 × H_d), 4.41 (t, ^3J = 7.0 Hz, 2H, 2 × H_c), 2.78 (t, ^3J = 7.6, 4H, 4 × H_g), 2.02 (sxt, ^3J = 7.2 Hz, 2H, 2 × H_b), 1.80 (quin, ^3J = 7.6, 4H, 4 × H_h), 1.52–1.22 (m, 20H, 20 × $H_{i–m}$), 1.05 (t, ^3J = 7.3 Hz, 3H, 3 × H_a), 0.95–0.84 (m, 6H, 6 × H_n); **^{13}C NMR** (76 MHz, $CDCl_3$): δ ppm 152.43, 141.41, 129.51, 124.64, 122.44, 118.80, 109.56, 80.39, 45.28, 31.87, 29.32, 29.29, 29.22, 29.06, 26.38, 22.67, 22.36, 14.11, 11.79; **MS (ESI+)** *m/z*: 820.24 ($[M + H]^+$, calc. for $[C_{35}H_{48}I_2N_7]^+$ = 820.21); **HRMS (ESI+)** *m/z*: 842.1865 ($[M + Na]^+$, calc. for $[C_{35}H_{47}I_2N_7Na]^+$ = 842.1880).

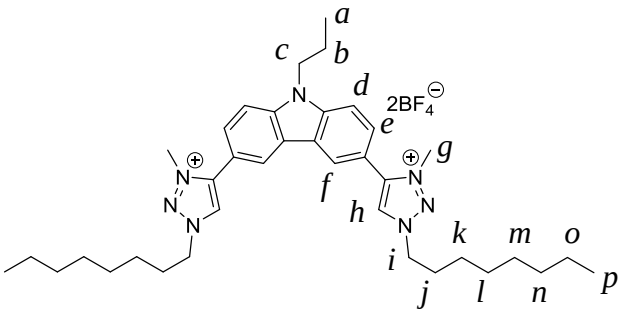
N-linked aryl-appended bis-iodotriazole receptor precursor, 19



1-(*Tert*-butyl)-4-ethynylbenzene (95 mg, 0.60 mmol) was reacted by *General Procedure 4* to give the desired product **19** (58 mg, 31%); **^{1}H NMR** (300 MHz, $CDCl_3$): δ ppm 8.30 (d, ^4J = 1.8 Hz, 2H, 2 × H_f), 8.02–7.98 (m, 4H, 4 × H_g), 7.70 (dd, ^3J = 8.8, ^4J = 2.4 Hz, 2H, 2 × H_e), 7.65 (d, ^3J = 8.8, 2H, 2 × H_d), 7.58–7.52 (m, 4H, 4 × H_h), 4.45 (t, ^3J = 7.0 Hz, 2H, 2 × H_c), 2.05 (sxt, ^3J = 7.2 Hz, 2H, 2 × H_b), 1.39 (s, 18H, 18 × H_i), 1.08 (t, ^3J = 7.6 Hz, 3H, 3 × H_a); **^{13}C NMR** (76 MHz, $CDCl_3$): δ ppm 151.74, 150.08, 141.56, 129.38, 127.31, 125.86, 125.60, 125.11, 122.46, 119.37, 109.67, 78.81, 45.34, 34.77, 31.48, 22.42, 11.86; **HRMS (ESI+)** *m/z*: 882.1216 ($[M + Na]^+$, calc. for $[C_{39}H_{39}I_2N_7Na]^+$ = 882.1249).

General Procedure 5: To a solution of bis-triazole receptor precursor (1.0 eq.) in dry CH_2Cl_2 was added $Me_3O{\cdot}BF_4$ (3.0 eq.). The solution was stirred overnight under N_2 at RT. The reaction was quenched with MeOH (one drop) and stirred for 5 min, before the organic solvent was removed *in vacuo*. The residue was purified either by column chromatography (silica) or by preparative TLC (silica) to give the desired product.

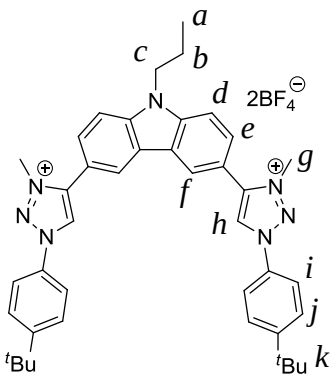
C-linked alkyl-appended bis-prototriazolium receptor, 20·2BF$_4$



Receptor precursor **9** (120 mg, 0.22 mmol) was reacted by *General Procedure 5* in dry CH_2Cl_2 (25 mL). Purification by column chromatography (75:20:5 CH_2Cl_2/acetone/MeOH)

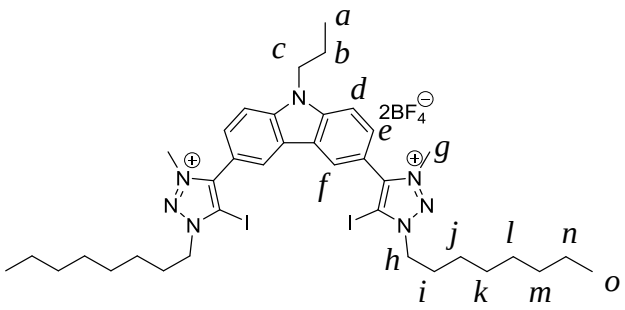
gave the desired product **20**·2BF_4 (84 mg, 50%) as a white solid; **^{1}H NMR** (300 MHz, CD_3CN): δ ppm 8.55–8.51 (m, 4H, 2 × H_h, 2 × H_f), 7.87 (d, ^3J = 8.2 Hz, 2H, 2 × H_d), 7.77 (dd, ^3J = 8.8, ^4J = 1.8 Hz, 2H, 2 × H_e), 4.61 (t, ^3J = 7.3 Hz, 4H, 4 × H_i), 4.49 (t, ^3J = 7.0 Hz, 2H, 2 × H_c), 4.29 (s, 6H, 6 × H_g), 2.11–1.95 (m, 6H, 2 × H_b, 4 × H_j), 1.50–1.23 (m, 20H, 20 × $H_{k–o}$), 0.98 (t, ^3J = 7.3 Hz, 3H, 3 × H_a), 0.93–0.84 (m, 6H, 6 × H_p); **^{13}C NMR** (76 MHz, CD_3CN): δ ppm 144.02, 142.46, 127.92, 127.52, 122.59, 122.40, 113.63, 111.00, 53.87, 44.76, 38.47, 31.48, 28.98, 28.77, 28.55, 25.66, 22.36, 22.05, 13.41, 10.76; **HRMS (ESI+)** *m/z*: 298.7244 $[M – 2(BF_4)]^{2+}$, calc. for $[C_{37}H_{55}N_9]^{2+}$ = 298.7254).

C-linked aryl-appended bis-prototriazolium receptor, 21·2BF_4



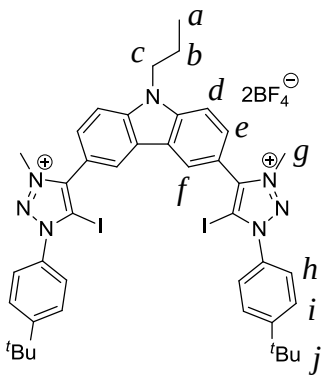
Receptor precursor **10** (105 mg, 0.170 mmol) was reacted by *General Procedure 5* in dry CH_2Cl_2 (25 mL). Purification by column chromatography (75:20:5 CH_2Cl_2/acetone/MeOH) gave the desired product **21**·2BF_4 (81 mg, 58%) as a white solid; **^{1}H NMR** (300 MHz, CD_3CN): δ ppm 9.01 (s, 2H, 2 × H_h), 8.66 (d, ^4J = 1.2 Hz, 2H, 2 × H_f), 7.96–7.75 (m, 12H, 2 × H_d, 2 × H_e, 4 × H_i, 4 × H_j), 4.52 (t, ^3J = 7.0 Hz, 2H, 2 × H_c), 4.43 (s, 6H, 6 × H_g), 1.99 (sxt, J = 7.0 Hz, 2H, 2 × H_b), 1.40 (s, 18H, 18 × H_k), 1.00 (t, ^3J = 7.3 Hz, 3H, 3 × H_a); **^{13}C NMR** (76 MHz, CD_3CN): δ ppm 155.77, 144.69, 142.64, 132.68, 127.58, 126.30, 122.71, 121.08, 113.40, 111.20, 44.83, 38.90, 34.88, 30.30, 22.06, 10.77; **HRMS (ESI+)** *m/z*: 318.6927 $([M − 2(BF_4)]^{2+}$, calc. for $[C_{41}H_{47}N_7]^+$ = 318.6941).

C-linked alkyl-appended bis-iodotriazolium receptor, 22·2BF$_4$



Receptor precursor **16** (95 mg, 0.12 mmol) was reacted by *General Procedure 5* in dry CH_2Cl_2 (20 mL). Purification by preparative TLC (10% MeOH/CH_2Cl_2) gave the desired product **22**·2BF$_4$ (39 mg, 33%); **^{1}H NMR** (300 MHz, CD_3CN): δ ppm 8.41 (s, 2H, 2 × H_f), 7.92 (d, ^3J = 8.8 Hz, 2H, 2 × H_d), 7.69 (dd, ^3J = 8.2, ^4J = 1.2 Hz, 2H, 2 × H_e), 4.63 (t, ^3J = 7.3 Hz, 4H, 4 × H_h), 4.52 (t, ^3J = 7.0 Hz, 2H, 2 × H_c), 4.19 (s, 6H, 6 × H_g), 2.09–1.97 (m, 6H, 2 × H_b, 4 × H_i), 1.54–1.25 (m, 20H, 20 × $H_{j–n}$), 1.01 (t, ^3J = 7.3 Hz, 3H, 3 × H_a), 0.95–0.86 (m, 6H, 6 × H_o); **^{13}C NMR** (76 MHz, CD_3CN): δ ppm 147.62, 142.59, 128.08, 123.26, 122.48, 113.63, 111.07, 89.78, 54.83, 48.93, 44.84, 38.93, 31.49, 28.55, 25.64, 22.37, 13.43, 10.81; **HRMS (ESI+)** *m/z*: 424.6211 ($[M - 2(BF_4)]^{2+}$, calc. for $[C_{37}H_{53}I_2N_7]^{2+}$ = 424.6220).

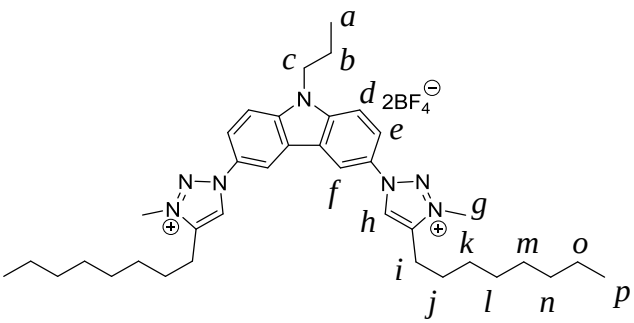
C-linked aryl-appended bis-iodotriazolium receptor, 23·2BF$_4$



Receptor precursor **17** (57 mg, 0.066 mmol) was reacted by *General Procedure 5* in dry CH_2Cl_2 (20 mL). Purification by preparative TLC (10% MeOH/CH_2Cl_2) gave the desired product **23**·2BF$_4$ (14 mg, 20%); **^{1}H NMR** (300 MHz, CD_3CN): δ ppm 8.55 (d, ^4J = 1.2, 2H, 2 × H_f), 7.96 (d, ^3J = 8.8 Hz, 2H, 2 × H_d), 7.84–7.75 (m, 6H, 2 × H_e, 4 × H_h), 7.71–7.65 (m, 4H, 4 × H_i), 4.54 (t, ^3J = 7.0 Hz, 2H, 2 × H_c), 4.30 (s, 6H, 2 × H_g), 2.01 (sxt, ^3J = 7.3 Hz, 2H, 2 × H_b), 1.41 (s, 18H, 18 × H_j), 1.03 (t, ^3J = 7.3 Hz, 3H, 3 × H_a); **^{13}C NMR** (76 MHz, CD_3CN) δ ppm 156.31, 147.89, 142.72, 132.98, 128.07, 127.29, 125.76, 123.41, 122.55,

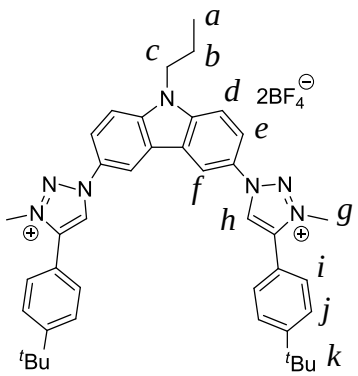
113.59, 111.24, 109.98, 39.14, 34.98, 30.33; **HRMS (ESI+)** *m/z*: 444.5899 $[M - 2(BF_4)]^{2+}$, calc. for $[C_{41}H_{45}I_2N_7]^{2+}$ = 444.5907).

N-linked alkyl-appended bis-prototriazolium receptor, 24·2BF$_4$



Receptor precursor **11** (94 mg, 0.17 mmol) was reacted by *General Procedure 1* in dry CH_2Cl_2 (25 mL). Purification by preparative TLC (10% MeOH/CH_2Cl_2) gave the desired product **24**·2BF_4 (23 mg, 38%); **^{1}H NMR** (300 MHz, CD_3CN): δ ppm 8.79–8.66 (m, 4H, 2 × H_f, 2 × H_h), 8.02 (d, ^3J = 8.8 Hz, 2H, 2 × H_e), 7.91 (d, ^3J = 9.2 Hz, 2H, 2 × H_d), 4.50 (t, ^3J = 7.0 Hz, 2H, 2 × H_c), 4.26 (s, 6H, 6 × H_g), 2.91 (t, ^3J = 7.6 Hz, 4H, 4 × H_i), 1.96 (sxt, ^3J = 7.3 Hz, 2H, 2 × H_b), 1.82 (quin, ^3J = 7.0 Hz, 4H, 4 × H_j), 1.57–1.23 (m, 20H, 20 × $H_{k–o}$), 0.97 (t, ^3J = 7.3 Hz, 3H, 3 × H_a), 0.93–0.86 (m, 6H, 6 × H_p); **^{13}C NMR** (126 MHz, CD_3CN): δ ppm 146.26, 143.15, 128.55, 126.76, 123.06, 120.87, 115.33, 112.24, 45.64, 38.19, 32.16, 29.44, 29.15, 27.15, 23.54, 22.97, 22.60, 13.99, 11.28; **^{19}F NMR** (283 MHz, CD_3CN): δ ppm −151.53, −151.68; **HRMS (ESI+)** *m/z*: 298.7246 ($[M - 2(BF_4)]^{2+}$, calc. for $[C_{37}H_{55}N_7]^{2+}$ = 298.7254).

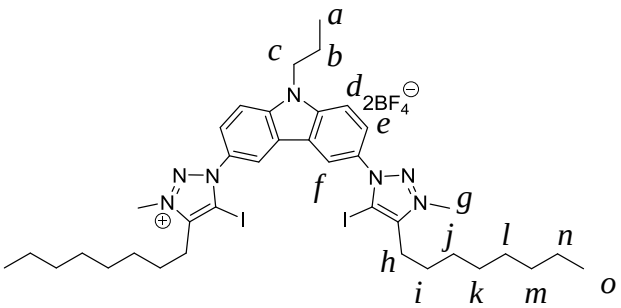
N-linked aryl-appended bis-prototriazolium receptor, 25·2BF$_4$



Receptor precursor **12** (34 mg, 0.056 mmol) was reacted by *General Procedure 5* in dry CH_2Cl_2 (10 mL). Purification by column chromatography (75:20:5 CH_2Cl_2/acetone/MeOH)

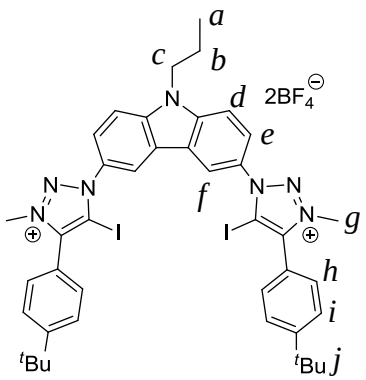
gave the desired product **25**·2BF_4 (25 mg, 56%) as a brown solid; **^{1}H NMR** (300 MHz, CD_3CN): δ ppm 9.03 (s, 2H, 2 × H_h), 8.83 (d, ^4J = 2.4 Hz, 2H, 2 × H_f), 8.08 (dd, ^3J = 8.8 Hz, ^4J = 2.4 Hz, 2H, 2 × H_e), 7.91 (d, ^3J = 8.8 Hz, 2H, 2 × H_d), 7.79–7.67 (m, 8H, 4 × H_i, 4 × H_j), 4.49 (t, ^3J = 7.0 Hz, 2H, 2 × H_c), 4.35 (s, 6H, 6 × H_g), 1.96 (sxt, ^3J = 7.6 Hz, 2H, 2 × H_b), 1.40 (s, 18H, 18 × H_k), 0.98 (t, ^3J = 7.3 Hz, 3H, 3 × H_a); **^{13}C NMR** (76 MHz, CD_3CN): δ ppm 155.59, 143.97, 142.62, 129.08, 127.84, 126.76, 126.48, 122.52, 120.18, 119.56, 114.71, 111.77, 45.07, 38.88, 34.83, 30.30, 22.05, 10.73; **HRMS (ESI+)** *m/z*: 318.6932 ($[M - 2(BF_4)]^{2+}$, calc. for $[C_{41}H_{47}N_7]^{2+}$ = 318.6941).

N-linked alkyl-appended bis-iodotriazolium receptor, 26·2BF_4



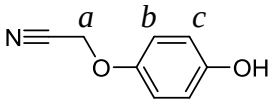
Receptor precursor **18** (41 mg, 0.050 mmol) was reacted by *General Procedure 5* in dry CH_2Cl_2 (20 mL). Purification by preparative TLC (10% MeOH/CH_2Cl_2) gave the desired product **26**·2BF_4 (21 mg, 44%); **^{1}H NMR** (300 MHz, CD_3CN): δ ppm 8.48 (d, ^4J = 2.4 Hz, 2H, 2 × H_f), 7.94 (d, ^3J = 8.8 Hz, 2H, 2 × H_d), 7.77 (dd, ^3J = 8.8, ^4J = 2.4 Hz, 2H, 2 × H_e), 4.54 (t, ^3J = 7.0 Hz, 2H, 2 × H_c), 4.32 (s, 6H, 6 × H_g), 3.01–2.91 (m, 4H, 4 × H_h), 1.99 (sxt, ^3J = 7.3 Hz, 2H, 2 × H_b), 1.72 (quin, ^3J = 7.6 Hz, 4H, 4 × H_i), 1.55–1.26 (m, 20H, 20 × $H_{j–n}$), 1.01 (t, ^3J = 7.6 Hz, 3H, 3 × H_a), 0.94–0.87 (m, 6H, 6 × H_o); **^{13}C NMR** (126 MHz, CD_3CN): δ ppm 149.01, 143.42, 128.12, 125.07, 122.60, 119.96, 112.07, 45.75, 38.99, 29.44, 27.53, 24.79, 22.97, 13.98, 11.28; **HRMS (ESI+)** *m/z*: 424.6208 ($[M - 2(BF_4)]^{2+}$, calc. for $[C_{37}H_{53}I_2N_7]^{2+}$ = 424.6220).

N-linked aryl-appended bis-iodotriazolium receptor, 27·2BF$_4$



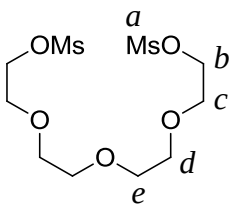
Receptor precursor **19** (32 mg, 0.037 mmol) was reacted by *General Procedure 5* in dry CH_2Cl_2 (15 mL). Purification by preparative TLC (10% MeOH/CH_2Cl_2) gave the desired product **27**·2BF$_4$ (21 mg, 55%); **^{1}H NMR** (300 MHz, CD_3CN): δ ppm 8.63 (d, ^4J = 2.4 Hz, 2H, 2 × H_f), 7.98 (d, ^3J = 8.8 Hz, 2H, 2 × H_d), 7.88 (dd, ^3J = 8.8 Hz, ^4J = 2.4 Hz, 2H, 2 × H_e), 7.81–7.75 (m, 4H, 4 × H_h), 7.64–7.57 (m, 4H, 4 × H_i), 4.57 (t, ^3J = 7.3 Hz, 2H, 2 × H_c), 4.25 (s, 6H, 6 × H_g), 2.02 (sxt, ^3J = 7.3 Hz, 2H, 2 × H_b), 1.41 (s, 18H, 18 × H_j), 1.04 (t, ^3J = 7.6 Hz, 3H, 3 × H_a); **^{13}C NMR** (126 MHz, CD_3CN): δ ppm 156.40, 147.79, 143.51, 130.42, 128.25, 127.33, 125.15, 122.69, 120.49, 120.13, 112.19, 45.79, 39.72, 35.47, 22.62, 11.36; **HRMS (ESI+)** *m/z*: 444.5891 ($[M - 2(BF_4)]^{2+}$, calc. for $[C_{41}H_{45}I_2N_7]^{2+}$ = 444.5907).

Mono-substituted hydroquinone, 28



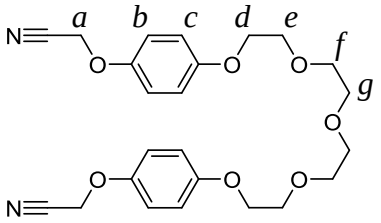
Based on a literature procedure.[23] To a degassed solution of NaOH (8.4 g, 0.21 mol) and hydroquinone (11.6g, 0.105 mol) in dioxane and water (1:1, 300 mL) was added dropwise a solution of bromoacetonitrile (7.3 mL, 0.11 mol) in degassed dioxane (50 mL). The resultant mixture was stirred for 1 h, degassing throughout. $HCl_{(aq.)}$ (1 M, 250 mL) was added and the mixture extracted into CH_2Cl_2 (3 × 200 mL). The combined organics were washed with brine (200 mL), dried ($MgSO_4$), filtered and concentrated to dryness *in vacuo*. The residue was purified by column chromatography (2% MeOH/CH_2Cl_2) to give the desired product **28** (9.3 g, 60%) as a green oil; **^{1}H NMR** (300 MHz, $CDCl_3$) δ ppm 6.98–6.73 (m, 4H, 2 × H_b, 2 × H_c), 4.71 (s, 2H, 2 × H_a).

Mesylated polyether, 29



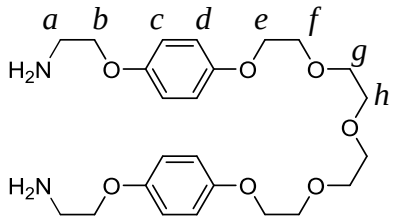
Based on literature procedure.[24] A solution of tetraethylene glycol (2.0 mL, 12 mmol) and triethylamine (7.9 mL, 57 mmol) in dry CH_2Cl_2 (100 mL) was cooled to 0 °C, whereupon a solution of methanesulfonyl chloride (3.9 mL, 50 mmol) in dry CH_2Cl_2 (50 mL) was added dropwise. The mixture was allowed to warm to RT whereupon it was stirred for 1 h. The solution was washed with water (2 × 75 mL), $HCl_{(aq.)}$ (1 M, 3 × 50 mL) and brine (3 × 75 mL), dried ($MgSO_4$), filtered and concentrated to dryness *in vacuo* to give the desired product **29** (3.9 g, 98%) as a yellow oil; **^{1}H NMR** (300 MHz, $CDCl_3$) δ ppm 4.40–4.37 (m, 4H, 4 × H_b), 3.79–3.69 (m, 4H, 4 × H_c), 3.67–3.56 (m, 8H, 4 × H_d, 4 × H_e), 3.08 (s, 6H, 6 × H_a); **MS (ESI+)** *m/z*: 351.09 ($[M + H]^+$, calc. for $[C_{10}H_{22}O_9S_2]^+$ = 351.07).

Bis-nitrile polyether, 30



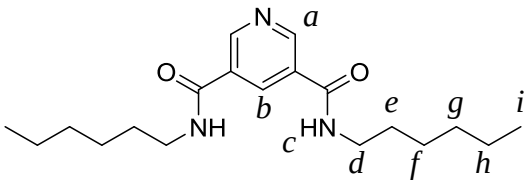
Based on literature procedure.[23] Mono-substituted hydroquinone **28** (1.8 g, 12 mmol) and mesylated polyether **29** (1.8 g, 5.0 mmol) were dissolved in dry CH_3CN (100 mL). K_2CO_3 (6.9 g, 50 mmol) was added and the resultant mixture heated at reflux for 72 h. The reaction was allowed to cool to RT, whereupon it was filtered and concentrated to dryness *in vacuo*. The residue was redissolved in $CHCl_3$ (75 mL), filtered and the solvent removed *in vacuo*. The residue was purified by column chromatography (3% MeOH/CH_2Cl_2) to give the desired product **30** (1.1 g, 20%) as a yellow solid; **^{1}H NMR** (300 MHz, $CDCl_3$): δ ppm 6.94–6.82 (m, 8H, 4 × H_b, 4 × H_c), 4.68 (s, 4H, 4 × H_a), 4.10–4.02 (m, 4H, 4 × H_d), 3.86–3.77 (m, 4H, 4 × H_e), 3.74–3.63 (m, 8H, 4 × H_f, 4 × H_g); **MS (ESI+)** *m/z*: 479.11 ($[M + Na]^+$, calc. for $[C_{24}H_{28}N_2NaO_7]^+$ = 479.18).

Bis-amine polyether, 31



Based on a literature procedure.[23] A solution of bis-nitrile polyether **30** (800 mg, 1.8 mmol) in dry THF (40 mL) was added dropwise to a solution of borane (1 M in THF, 16 mL, 70 °C). The resultant solution was heated for 4 h at reflux and then allowed to cool to RT. MeOH (~50 mL) was added to quench the reductant, after which the solution was reduced to 20 mL *in vacuo*. $HCl_{(aq.)}$ (6 M, 40 mL) was added and the mixture stirred for 15 min at RT, then the organic solvent was removed *in vacuo*. To the remaining aqueous solution was added CH_2Cl_2 (30 mL) and $NaOH_{(aq.)}$ (10%) until the pH of the mixture was 9, whereupon the mixture was stirred for 30 min. The organic layer was separated, washed with water (50 mL), dried ($MgSO_4$), filtered and concentrated to dryness *in vacuo* to afford the desired product **31** (650 mg, 79%) as a white solid; **^{1}H NMR** (300 MHz, $CDCl_3$): δ ppm 6.83 (s, 8H, 4 × H_c, 4 × H_d), 4.07 (dd, ^3J = 5.8, 3.9 Hz, 4H, 4 × H_e), 3.92 (t, ^3J = 5.1 Hz, 4H, 4 × H_b), 3.83 (dd, ^3J = 5.8, 4.0 Hz, 4H, 4 × H_f), 3.75–3.65 (m, 8H, 4 × H_g, 4 × H_h), 3.14–2.96 (m, 4H, 4 × H_a); **MS (ESI+)** *m/z*: 465.3 ($[M + H]^+$, calc. for $[C_{24}H_{37}N_2O_7]^+$ = 465.3).

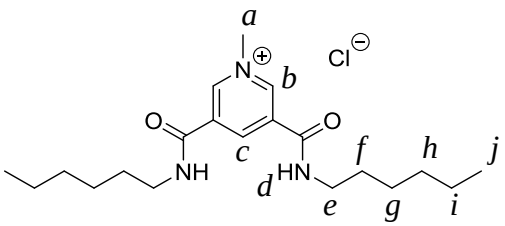
Bis-amide pyridine thread, 32



Based on a literature procedure.[25] Pyridine-3,5-dicarboxylic acid (0.86 g, 4.99 mmol) was suspended in thionyl chloride (5 mL) with a catalytic drop of DMF, and heated at reflux (79 °C) for 16 h, after which the solid had dissolved. Excess thionyl chloride was cautiously removed *in vacuo*, and the bis-acid chloride product used immediately, assuming quantitative yield of formation. The solid was dissolved in dry CH_2Cl_2 (10 mL) and added dropwise to a solution of *n*-hexylamine (0.91 g, 1.18 mL, 9.0 mmol) and triethylamine (1.5 mL) in dry CH_2Cl_2 (40 mL) at 0 °C. The reaction mixture was stirred for 2 h at RT under a N_2

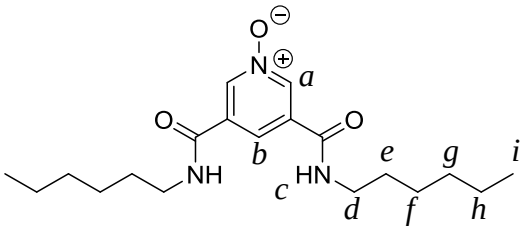
atmosphere, then subsequently washed with citric acid (10% w/w, 4 × 60 mL). The organic layer was dried ($MgSO_4$), and the solvent removed *in vacuo* to give the product **32** as an off-white solid (1.37 g, 91%); **^{1}H NMR** (neutral precursor, 300 MHz, $CDCl_3$) δ ppm 9.10 (br. s., 2H, 2 × H_c), 8.52 (s, 1H, 1 × H_b), 7.09 (t, ^3J = 5.57 Hz, 2H, 2 × H_a), 3.46 (q, ^3J = 6.50 Hz, 4H, 4 × H_d), 1.63 (quin, ^3J = 7.00 Hz, 4H, 4 × H_e), 1.23–1.45 (m, 12H, 12 × $H_{f–h}$), 0.84–0.93 (m, 6H, 6 × H_i).

Bis-amide pyridinium thread, 32a



Based on a literature procedure.[25] The bis-amide pyridine precursor **32** (1.37 g, 4.10 mmol) and methyl iodide (2 mL) were dissolved in $CHCl_3$ (50 mL) and heated at reflux for 2 d. The solvent was removed *in vacuo*, then the residue redissolved in $CHCl_3$ (25 mL) and washed with $NH_4Cl_{(aq.)}$ (9 × 40 mL) and H_2O (2 × 25 mL), dried ($MgSO_4$) and the solvent removed *in vacuo*, giving the product **32a**·Cl as a yellow solid (1.4 g, 89%); **^{1}H NMR** (300 MHz, $CDCl_3$) δ ppm 10.43 (s, 1H, 1 × H_c), 9.39 (s, 2H, 2 × H_d), 9.35 (t, ^3J = 5.28 Hz, 2H, 2 × H_b), 4.57 (s, 3H, 3 × H_a), 3.44 (q, ^3J = 7.00 Hz, 4H, 4 × H_e), 1.64–1.77 (m, 4H, 4 × H_f), 1.26–1.45 (m, 12H, 12 × $H_{g–i}$), 0.88 (t, ^3J = 6.50 Hz, 6H, 6 × H_j).

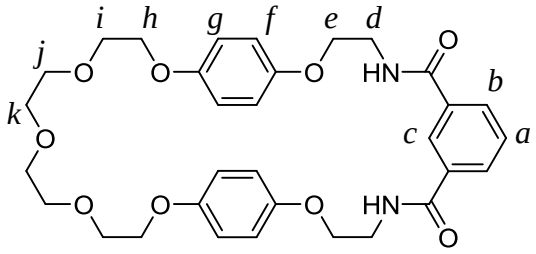
Bis-amide pyridine *N*-oxide thread, 32b



Bis-amide pyridine thread **32** (0.50 g, 1.5 mmol) and $NaHCO_3$ (3.8 g, 45 mmol) were dissolved in 1:1 H_2O/2-butanone (35 mL). A solution of oxone (0.675 g, 1.13 mmol) in H_2O (20 mL) was added dropwise, and the mixture stirred at RT for 3 h. Sodium chloride (12 g) was added, and the product extracted in $CHCl_3$ (3 × 25 mL), dried ($MgSO_4$) and the solvent removed *in vacuo*. The crude was purified by column chromatography (4% MeOH/CH_2Cl_2),

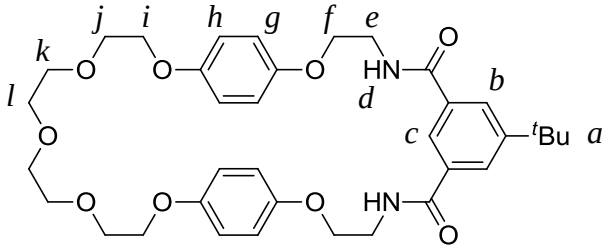
giving the product **32b** as an off-white solid (0.156 g, 30%); **^{1}H NMR** (300 MHz, $CDCl_3$) δ ppm 8.96 (br. s., 2H, 2 × H_c), 8.34 (br. s, 1H, 1 × H_b), 7.80 (br. s., 2H, 2 × H_a), 3.44 (br. s., 4H, 4 × H_d), 1.65 (br. s., 4H, 4 × H_f), 1.20–1.47 (m, 12H, 4 × $H_{f–h}$), 0.89 (br. s., 6H, 6 × H_i).

Isophthalamide macrocycle, 33



Based on a literature procedure.[23] Isophthaloyl dichloride (87 mg, 0.43 mmol) in dry CH_2Cl_2 (10 mL) was added dropwise to a solution of bis-amine compound **31** (200 mg, 0.43 mmol), triethylamine (0.70 mL, 5.0 mmol) and bis-amide pyridinium chloride template **32a**·Cl (165 mg, 0.43 mmol) in dry CH_2Cl_2 (20 mL). The resultant solution was stirred for 1 h at RT, then washed with $HCl_{(aq.)}$ (10%, 2 × 25 mL) and water (2 × 25 mL), dried ($MgSO_4$), filtered and concentrated to dryness *in vacuo*. The residue was purified by column chromatography (5% MeOH/$CHCl_3$), giving the product **33** as a white solid (116 mg, 46%); **^{1}H NMR** (300 MHz, $CDCl_3$): δ ppm 8.05 (dd, ^3J = 7.92 Hz, ^4J = 1.5 Hz, 2H, 2 × H_b), 7.98 (s, 1H, 2 × H_c), 7.56 (t, ^3J = 7.63 Hz, 1H, 1 × H_a), 6.79 (s, 8H, 4 × H_f, 4 × H_g), 4.13–4.07 (m, 4H, 4 × H_h), 4.06–4.01 (m, 4H, 4 × H_e), 3.90–3.67 (m, 16H, 4 × H_d, 4 × H_i, 4 × H_j, 4 × H_k).

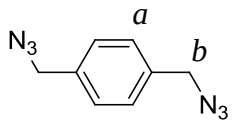
***Tert*-butyl isophthalamide macrocycle, 34**



Based on a literature procedure.[23] DMF (one drop) was added to a suspension of 5-*tert*-butylisophthalic acid (1.0 g, 4.5 mmol) in thionyl chloride (5 mL), and the resultant mixture stirred for 16 h at reflux. Excess thionyl chloride was removed *in vacuo* (with a dry ice/acetone condenser), and the desired acid chloride product used immediately in the synthesis of macrocycle **20**, assuming quantitative yield. The bis-acid chloride (170 mg,

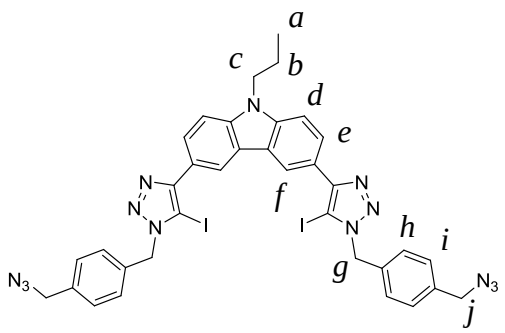
0.65 mmol) in dry CH_2Cl_2 (30 mL) was added dropwise to a solution of bis-amine compound **31** (300 mg, 0.65 mmol), bis-amide pyridinium chloride template **32a**·Cl (250 mg, 0.65 mmol) and triethylamine (0.70 mL, 5.0 mmol) in dry CH_2Cl_2 (20 mL). The resultant solution was stirred for 2 h at RT. The solution was then washed with $HCl_{(aq.)}$ (10%, 2 × 40 mL) and water (2 × 40 mL), dried ($MgSO_4$), filtered and concentrated to dryness *in vacuo*. The residue was purified by column chromatography (5% MeOH/$CHCl_3$) to afford a yellow solid, which was washed with cold MeOH (3 × 10 mL) to give the desired product **34** (230 mg, 56%) as a white solid; **^{1}H NMR** (300 MHz, $CDCl_3$): δ ppm 8.08 (d, ^4J = 1.5 Hz, 2H, 2 × H_b), 7.94 (s, 2H, 2 × H_d), 7.73–7.69 (m, 1H, 1 × H_c), 6.78 (s, 8H, 4 × H_g, 4 × H_h), 4.10 (t, ^3J = 4.9 Hz, 4H, 4 × H_i), 4.03 (dd, ^3J = 5.8, 3.7 Hz, 4H, 4 × H_f), 3.90–3.65 (m, 16H, 4 × H_e, 12 × $H_{j–l}$), 1.37 (s, 9H, 9 × H_a); **MS (ESI+)** *m/z*: 651.35 ($[M + H]^+$, calc. for $[C_{36}H_{47}N_2O_9]^+$ = 651.33).

Bis-azide compound, 35



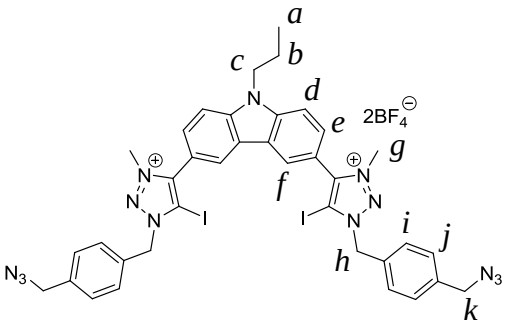
Based on a literature procedure.[26] To a solution of 1,4-bis(bromomethyl)benzene (2.0 g, 7.6 mmol) in DMSO (40 mL) was added sodium azide (1.5 g, 23 mmol). The solution was stirred overnight at RT, then diluted with water (240 mL) and extracted with diethyl ether (3 × 80 mL). The combined organics were washed with water (3 × 80 mL) and brine (80 mL), dried ($MgSO_4$), filtered and concentrated to dryness *in vacuo* to afford product **35** (1.4 g, 95%) as a colourless oil; **^{1}H NMR** (300 MHz, $CDCl_3$): δ ppm 7.34 (s, 4H, 4 × H_a), 4.36 (s, 4H, 4 × H_b).

Bis-iodotriazole axle precursor, 36



To a degassed solution of bis-azide **35** (870 mg, 4.8 mmol) in THF (15 mL) was added sodium iodide (480 mg, 3.2 mmol) and $Cu(ClO_4)_2 \cdot 6H_2O$ (590 mg, 1.6 mmol). The resultant mixture was stirred for 5 min at RT. To the mixture was then added TBTA (42 mg, 0.080 mmol) and DBU (120 mg, 0.80 mmol), followed by bis-alkyne carbazole **3** (100 mg, 0.20 mmol). The mixture was stirred overnight at RT in the dark, after which it was diluted with CH_2Cl_2 (50 mL), washed with $NH_4OH_{(aq.)}$ (30 mL) and brine (2 × 30 mL), dried ($MgSO_4$), filtered and concentrated to dryness *in vacuo*. The residue was purified by preparative TLC (1% MeOH/CH_2Cl_2) to give the desired product **36** (300 mg, 85%); **^{1}H NMR** (300 MHz, $CDCl_3$): δ ppm 8.71 (s, 2H, 2 × H_f), 8.07 (d, ^3J = 8.8 Hz, 2H, 2 × H_e), 7.50 (d, ^3J = 8.2 Hz, 2H, 2 × H_d), 7.41–7.31 (m, 8H, 4 × H_h, 4 × H_i), 5.72 (s, 4H, 4 × H_g), 4.40–4.29 (m, 6H, 2 × H_c, 4 × H_j), 1.97 (sxt, ^3J = 7.6 Hz, 2H, 2 × H_b), 1.01 (t, ^3J = 7.3 Hz, 3H, 3 × H_a); **^{13}C NMR** (76 MHz, $CDCl_3$): δ ppm 151.21, 140.95, 135.75, 134.56, 128.68, 128.32, 125.70, 122.89, 121.15, 119.82, 109.02, 54.31, 54.06, 44.90, 22.38, 11.83; **HRMS (ESI+)** *m/z*: 908.0617 ($[M + Na]^+$, calc. for $[C_{35}H_{29}I_2N_{13}Na]^+$ = 908.0650).

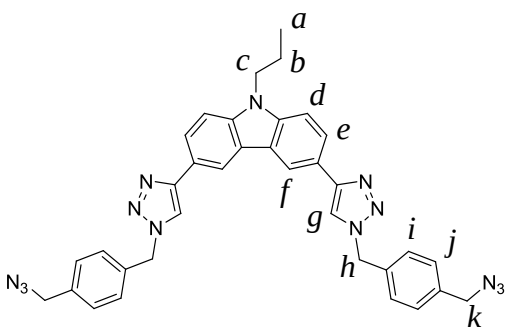
Bis-iodotriazolium axle precursor, 37·2BF$_4$



To a solution of axle precursor **36** (300 mg, 0.34 mmol) in dry CH_2Cl_2 (40 mL) was added $Me_3O \cdot BF_4$ (120 mg, 0.81 mmol). The solution was stirred overnight at RT, then the reaction

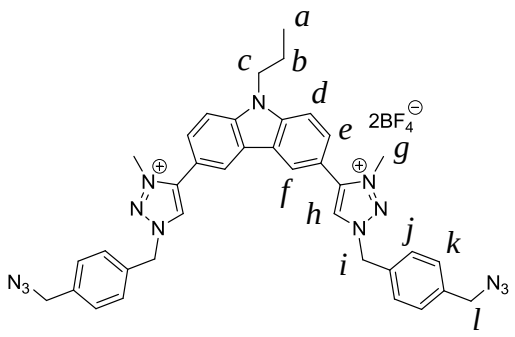
was quenched with MeOH (one drop) and stirred for 5 min, before the organic solvent was removed *in vacuo*. The residue was purified by preparative TLC (10% MeOH/CH_2Cl_2) to give the desired product **37·2BF$_4$** (170 mg, 46%); **^{1}H NMR** (300 MHz, CD_3CN): δ ppm 8.43 (d, ^4J = 1.8 Hz, 2H, 2 × H_f), 7.90 (d, ^3J = 8.2 Hz, 2H, 2 × H_d), 7.69 (dd, ^3J = 8.8 Hz, ^4J = 1.8 Hz, 2H, 2 × H_e), 7.57–7.45 (m, 8H, 4 × H_i, 4 × H_j), 5.87 (s, 4H, 4 × H_h), 4.51 (t, ^3J = 7.0 Hz, 2H, 2 × H_c), 4.49 (s, 4H, 4 × H_k), 4.21 (s, 6H, 6 × H_g), 2.00–1.92 (m, 2H, 2 × H_b), 1.00 (t, ^3J = 7.3 Hz, 3H, 2 × H_a); **^{13}C NMR** (76 MHz, CD_3CN): δ ppm 148.05, 142.62, 137.49, 131.61, 129.39, 129.02, 128.00, 123.40, 122.44, 113.46, 111.09, 57.55, 53.61, 39.15, 22.06, 10.79; **HRMS (ESI+)** *m/z*: 457.5611 ([M – 2(BF_4)]$^{2+}$, calc. for [$C_{37}H_{35}I_2N_{13}$]$^{2+}$ = 457.5608).

Bis-prototriazole axle precursor, 38



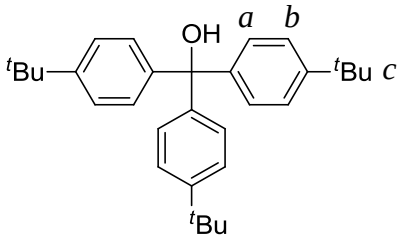
To a solution of diethynylcarbazole **3** (32 mg, 0.13 mmol) and diazide **21** (270 mg, 1.5 mmol) in dry CH_2Cl_2 (20 mL) were added TBTA (16 mg, 0.030 mmol) and [Cu(CH_3CN)$_4$](PF_6) (11 mg, 0.030 mmol), followed by DIPEA (14 mg, 0.11 mmol). The resultant mixture was stirred for 72 h at RT. The reaction mixture was concentrated to dryness *in vacuo* and the residue purified by column chromatography (1% MeOH/CH_2Cl_2) to give the desired product **38** (63 mg, 79%); **^{1}H NMR** (300 MHz, $CDCl_3$): δ ppm 8.47 (d, ^4J = 1.2 Hz, 2H, 2 × H_f), 7.92 (dd, ^3J = 8.2, ^4J = 1.8 Hz, 2H, 2 × H_e), 7.72 (s, 2H, 2 × H_g), 7.39–7.29 (m, 10H, 2 × H_d, 4 × H_i, 4 × H_j), 5.58 (s, 4H, 4 × H_h), 4.35 (s, 4H, 4 × H_k), 4.20 (t, ^3J = 7.0 Hz, 2H, 2 × H_c), 1.87 (sxt, ^3J = 7.3, 2H, 2 × H_b), 0.93 (t, ^3J = 7.6 Hz, 3H, 3 × H_a); **^{13}C NMR** (76 MHz, $CDCl_3$): δ ppm 149.15, 140.75, 136.04, 134.95, 128.87, 128.53, 123.86, 123.03, 121.63, 118.84, 117.79, 109.20, 54.26, 53.77, 44.75, 22.31, 11.75.

Bis-prototriazolium axle precursor, 39·2BF$_4$



To a solution of axle precursor **38** (63 mg, 0.10 mmol) in dry CH_2Cl_2 (25 mL) was added $Me_3O{\cdot}BF_4$ (35 mg, 0.24 mmol). The solution was stirred overnight at RT. The reaction was quenched with MeOH (one drop) and stirred for 5 min, before the organic solvent was removed *in vacuo*. The residue was purified by preparative TLC (10% MeOH/CH_2Cl_2) to give the desired product **39·2BF$_4$** (37 mg, 45%); **^{1}H NMR** (300 MHz, CD_3CN): δ ppm 8.57 (s, 2H, 2 × H_h), 8.48 (d, ^4J = 1.8 Hz, 2H, 2 × H_f), 7.84 (d, ^3J = 8.8 Hz, 2H, 2 × H_d), 7.73 (dd, ^3J = 8.8, ^4J = 1.8 Hz, 2H, 2 × H_e), 7.61–7.44 (m, 8H, 4 × H_j, 4 × H_k), 5.80 (s, 4H, 4 × H_i), 4.50–4.42 (m, 6H, 2 × H_c and 4 × H_l), 4.27 (s, 6H, 2 × H_g), 1.98–1.88 (m, 2H, 2 × H_b), 0.95 (t, ^3J = 7.3 Hz, 3H, 3 × H_a); ^{13}C NMR (76 MHz, CD_3CN) δ ppm 144.37, 142.46, 137.63, 132.09, 129.69, 129.10, 128.09, 127.53, 122.48, 113.45, 110.96, 56.68, 53.61, 44.74, 38.64, 30.30, 22.03, 10.74; **MS (ESI+)** *m/z*: 331.7 ($[M - 2(BF_4)]^{2+}$, calc. for $[C_{37}H_{37}N_{13}]^{2+}$ = 331.7).

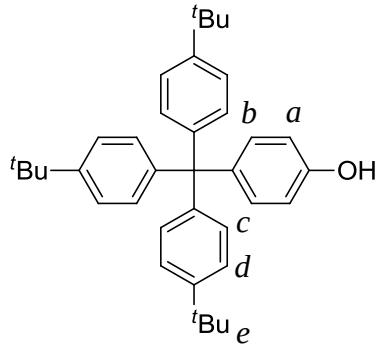
Terphenyl alcohol, 40



Based on a literature procedure.[27] A three-necked flask fitted with a pressure-equalising dropping funnel and reflux condenser was thoroughly dried. The flask was charged with magnesium turnings (1.0 g, 41 mmol), then dry THF (10 mL) was added, followed by iodine (two crystals) and 5 mL of a solution of 1-bromo-4-(*tert*-butyl)benzene (6.1 mL, 35 mmol) in dry THF (20 mL). The remainder of this solution was added dropwise to the magnesium, after which the mixture was cautiously heated to reflux, whereupon it was stirred for 1 h. A

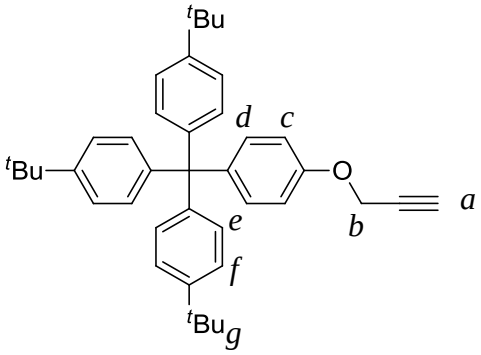
solution of diethyl carbonate (1.4 mL, 12 mmol) in dry THF (10 mL) was added dropwise and the reaction stirred at reflux for a further 1 h. The mixture was allowed to cool to RT, whereupon it was poured onto a mixture of ice (40 g) and sulfuric acid (conc. aq., 4 mL). THF was removed *in vacuo*, and the resultant aqueous solution extracted with CH_2Cl_2 (3 × 40 mL). The combined organics were washed with $Na_2CO_{3(aq.)}$ (5%, 40 mL), water (40 mL) and brine (40 mL), dried ($MgSO_4$), filtered and concentrated *in vacuo* to afford a pale yellow solid. This solid was recrystallized from boiling cyclohexane (20 mL) giving the product **40** as a pale yellow solid (2.5 g, 50%); **^{1}H NMR** (300 MHz, $CDCl_3$): δ ppm 7.35–7.28 (m, 6H, 6 × H_b), 7.22–7.14 (m, 6H, 6 × H_a), 1.34–1.29 (m, 27H, 27 × H_c); **MS (ESI+)** *m/z*: 411.34 ($[M - OH]^+$, calc. for $[C_{31}H_{39}]^+$ = 411.30).

Trityl alcohol, 41



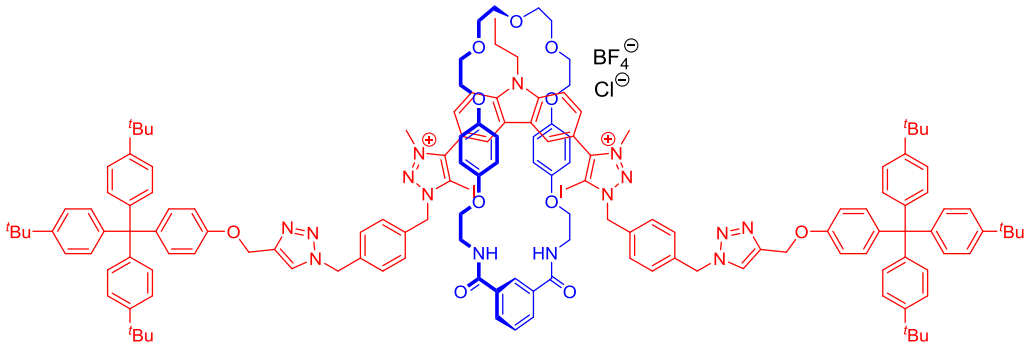
Based on a literature procedure.[28] To a suspension of terphenyl alcohol **40** (1.3 g, 3.0 mmol) in molten phenol (10.0 g, 106 mmol) was added $HCl_{(aq.)}$ (35%, 0.5 mL). The resultant mixture was heated at 120 °C for 15 h before being allowed to cool to RT, whereupon $KOH_{(aq.)}$ (7 M, 30 mL) was added. The mixture was filtered and the resultant pale yellow precipitate washed with water (50 mL), acetic acid (20% aq., 50 mL) and water (50 mL) before being dissolved in $CHCl_3$ (100 mL). The solution was dried ($MgSO_4$), filtered and concentrated to dryness *in vacuo*. The resulting white solid was suspended in pet. ether (25 mL) and heated at reflux for 30 min. Filtration of the suspension afforded **41** (660 mg, 43%) as an off-white solid; **^{1}H NMR** (300 MHz, $CDCl_3$): δ ppm 7.34–7.14 (m, 6H, 6 × H_d), 7.14–6.98 (m, 8H, 6 × H_c, 2 × H_b), 6.78–6.57 (m, 2H, 2 × H_a), 1.30 (s, 27H, 27 × H_e).

Stopper alkyne, 42



Based on a literature procedure.[29] To a suspension of trityl alcohol **41** (380 mg, 0.75 mmol) and K_2CO_3 (520 mg, 3.7 mmol) in dry DMF (8 mL) was added propargyl bromide (80% solution in toluene, 0.10 mL, 1.1 mmol). The mixture was heated overnight at 80 °C. The resultant brown suspension was filtered to remove base and then concentrated to dryness *in vacuo*. The resultant brown residue was dissolved in ethyl acetate (30 mL) and water (25 mL), and washed with lithium chloride solution (sat. aq., 8 × 20 mL). The organic solvent was dried ($MgSO_4$), filtered and concentrated to dryness *in vacuo* to give **42** (300 mg, 74%) as a white solid; **^{1}H NMR** (300 MHz, $CDCl_3$): δ ppm 7.25–7.19 (m, 6H, 6 × H_f), 7.13–7.03 (m, 8H, 6 × H_e, 2 × H_d), 6.87–6.80 (m, 2H, 2 × H_c), 4.68–4.63 (m, 2H, 2 × H_b), 2.51 (s, 1H, 1 × H_a), 1.29 (s, 27H, 27 × H_g).

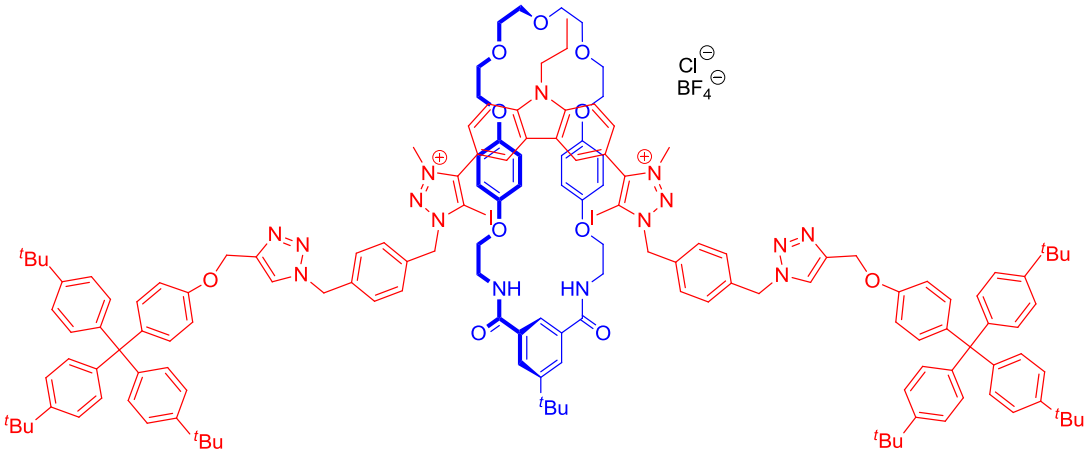
Stoppered bis-iodotriazolium [2]rotaxane, 43·BF_4·Cl



A solution of macrocycle **33** (21 mg, 0.034 mmol) and TBA·Cl (10 mg, 0.034 mmol) in dry acetone (10 mL) was stirred at RT for 30 min. Axle precursor **37**·2BF_4 (25 mg, 0.023 mmol), stopper alkyne **42** (27 mg, 0.050 mmol) and TBTA (2.4 mg, 0.0046 mmol) were added and the solution stirred for 1 h. [Cu(CH_3CN)$_4$](PF_6) (1.7 mg, 0.0046 mmol) was added and the

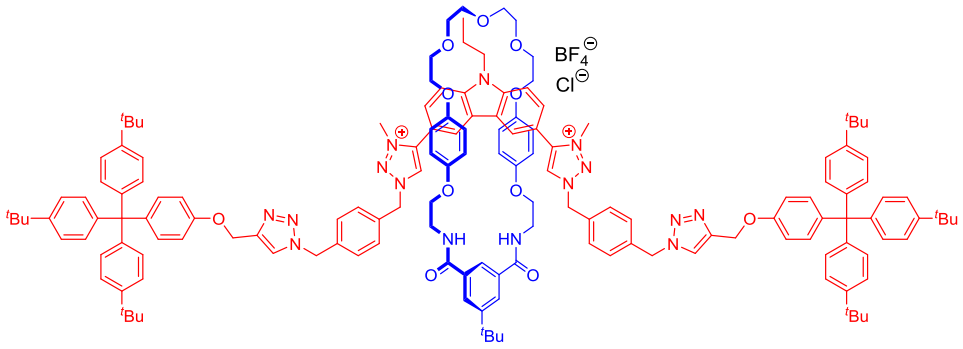
solution stirred for 72 h at RT. Crude MS analysis indicated no presence of desired product **43**·BF_4·Cl.

Stoppered bis-iodotriazolium [2]rotaxane, 44·BF_4·Cl



To a solution of axle precursor **37**·2BF_4 (55 mg, 0.050 mmol) and macrocycle **34** (49 mg, 0.075 mmol) in dry CH_2Cl_2 (50 mL) was added TBA·Cl (21 mg, 0.075 mmol), followed by stopper alkyne **42** (60 mg, 0.11 mg), TBTA (5.3 mg, 0.010 mmol), [Cu(CH_3CN)$_4$](PF_6) (3.7 mg, 0.010 mmol) and DIPEA (13 mg, 0.10 mmol). The resultant mixture was stirred for 6 d at RT, then concentrated to dryness *in vacuo* and the residue purified by preparative TLC (10% MeOH/CH_2Cl_2) to afford trace amounts of impure product **44**·BF_4·Cl; **MS (ESI+)** *m/z*: 1325.69 ([M − BF_4 − Cl]$^{2+}$, calc. for [$C_{153}H_{173}I_2N_{15}O_{11}$]$^+$ = 1325.98).

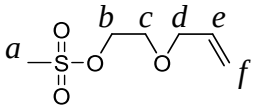
Stoppered bis-prototriazolium [2]rotaxane, 45·BF_4·Cl



To a solution of axle precursor **41**·2BF_4 (37 mg, 0.044 mmol) and macrocycle **34** (43 mg, 0.067 mmol) in dry CH_2Cl_2 (50 mL) was added TBA·Cl (19 mg, 0.067 mmol), followed by stopper alkyne **42** (53 mg, 0.098 mg), TBTA (4.7 mg, 0.0089 mmol), [Cu(CH_3CN)$_4$](PF_6)

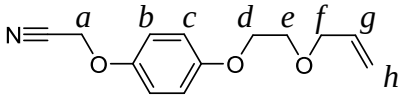
(3.3 mg, 0.0089 mmol) and DIPEA (11 mg, 0.089 mmol). The resultant mixture was stirred for 6 d at RT, then concentrated to dryness *in vacuo* and the residue purified by preparative TLC (10% MeOH/CH_2Cl_2) to afford a trace amount of impure product **45**·BF_4·Cl; **HRMS (ESI+)** *m/z*: 1199.6777 ($[M - BF_4 - Cl]^{2+}$, calc. for $[C_{153}H_{175}N_{15}O_{11}]^+$ = 1199.6808).

Mesylate, 46



Based on literature procedure.[30] A solution of mesyl chloride (5.0 mL, 65 mmol) in dry CH_2Cl_2 (100 mL) was added dropwise to a solution of 2-(allyloxy)ethan-1-ol (5.9 mL, 55 mmol) and triethylamine (16 mL, 115 mmol) in dry CH_2Cl_2 (100 mL) at 0 °C. The mixture was allowed to warm to RT, whereupon it was stirred for 1 h. The solution was washed with water (2 × 75 mL), $HCl_{(aq.)}$ (1 M, 2 × 20 mL) and brine (75 mL), dried ($MgSO_4$), filtered and concentrated to dryness *in vacuo*. Traces of residual solvent were removed by placing the resultant oil under high vacuum for 48 h to give the desired product **46** (9.0 g, 91%) as a red oil; **^{1}H NMR** (300 MHz, $CDCl_3$): δ ppm 5.96–5.80 (m, 1H, 1 × H_e), 5.33–5.17 (m, 2H, 2 × H_f), 4.37 (dd, ^3J = 3.8, 2.1 Hz, 2H, H_d), 4.03 (dt, ^3J = 5.6, 1.6 Hz, 2H, 2 × H_b), 3.72–3.68 (m, 2H, 2 × H_c), 3.05 (s, 3H, 3 × H_a).

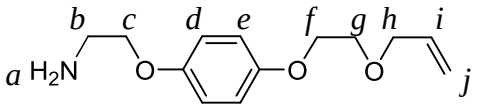
Nitrile-appended vinyl compound, 47



This compound has been previously reported in the literature.[31] A suspension of mono-substituted hydroquinone **28** (1.0 g, 6.8 mmol), mesylate **46** (1.2 g, 6.8 mmol) and K_2CO_3 (4.7 g, 34 mmol) in dry CH_3CN (75 mL) was heated at 95 °C for 72 h. The mixture was allowed to cool to RT whereupon it was filtered and concentrated to dryness *in vacuo*. The resultant residue was dissolved in CH_2Cl_2 (20 mL), washed with $HCl_{(aq.)}$ (1 M, 2 × 20 mL), water (2 × 20 mL), $NaOH_{(aq.)}$ (10%, 2 × 20 mL), water (2 × 20 mL) and brine (20 mL), dried ($MgSO_4$), filtered and concentrated to dryness *in vacuo*. The residue was purified by column chromatography (70:30 hexane/ethyl acetate) to afford the desired product **47** (660 mg, 42%); **^{1}H NMR** (300 MHz, $CDCl_3$): δ ppm 7.01–6.82 (m, 4H, 2 × H_b, 2 × H_c), 6.04–5.83 (m, 1H,

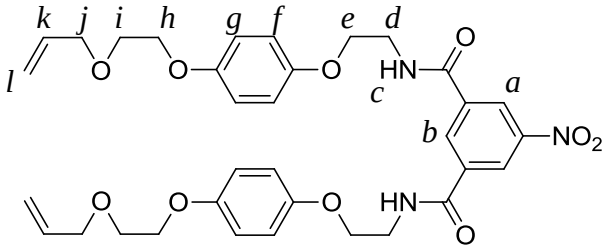
1 × H_g), 5.36–5.18 (m, 2H, 2 × H_h), 4.71 (s, 2H, 2 × H_a), 4.18–4.03 (m, 4H, 2 × H_d, 2 × H_f), 3.88–3.72 (m, 2H, 2 × H_e). **MS (ESI+)** *m/z*: 256.07 ($[M + Na]^+$, calc. for $[C_{13}H_{15}NNaO_3]^+$ = 256.10).

Amine-appended vinyl compound, 48



Based on a literature procedure.[31] A solution of nitrile-appended vinyl compound **47** (660 mg, 2.8 mmol) in dry diethyl ether (25 mL) was added dropwise to a solution of lithium aluminium hydride (330 mg, 8.70 mmol) in dry diethyl ether (25 mL). The mixture was heated at reflux for 3 h, allowed to cool to RT and quenched dropwise with water (0.2 mL), $NaOH_{(aq.)}$ (15%, 0.2 mL) and more water (until effervescence subsided). The mixture was filtered and washed with diethyl ether, then the filtrate was separated and the organic layer dried ($MgSO_4$), filtered and concentrated to dryness *in vacuo* to afford desired product **48** (350 mg, 53%); **^{1}H NMR** (300 MHz, $CDCl_3$): δ ppm 6.93–6.75 (m, 4H, 2 × H_d, 2 × H_e), 6.04–5.85 (m, 1H, 1 × H_i), 5.37–5.17 (m, 2H, 2 × H_j), 4.14–4.04 (m, 4H, 2 × H_f, 2 × H_h), 3.94 (t, ^3J = 5.1 Hz, 2H, 2 × H_c), 3.79 (t, ^3J = 4.9 Hz, 2H, 2 × H_g), 3.05 (t, ^3J = 5.1 Hz, 2H, 2 × H_b), 1.54 (br. s, 2H, 2 × H_a). **MS (ESI+)** *m/z*: 238.11 ($[M + H]^+$, calc. for $[C_{13}H_{20}NO_3]^+$ = 238.14).

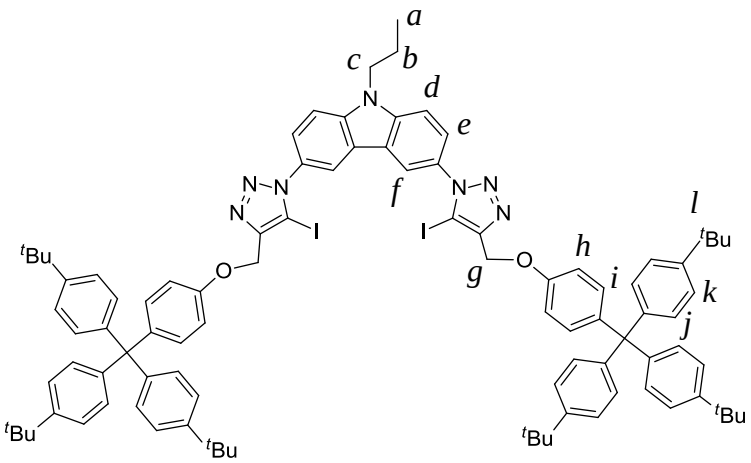
Bis-vinyl macrocycle precursor, 49



Based on a literature procedure.[32] A suspension of 5-nitroisophthalic acid (300 mg, 1.4 mmol) and DMF (one drop) in thionyl dichloride (1.5 mL) was heated at reflux for 16 h. Excess solvent was removed *in vacuo* and the crude acid dichloride dissolved in dry CH_2Cl_2 (40 mL), then 19 mL of this solution was added dropwise to a solution of amine-appended vinyl compound **48** (350 mg, 1.5 mmol) and triethylamine (2.8 mL, 25 mmol) in dry CH_2Cl_2 (25 mL) at 0 °C. The resultant solution was stirred at 0 °C for 2 h. The solution was washed

with $HCl_{(aq.)}$ (10%, 3 × 40 mL) and water (3 × 40 mL), dried ($MgSO_4$), filtered and concentrated to dryness *in vacuo*. The residue was purified by column chromatography (7:3 ethyl acetate/CH_2Cl_2) to afford **49** (320 mg, 72%) as a pale yellow solid; **^{1}H NMR** (300 MHz, CD_3CN): δ ppm 8.72 (d, ^4J = 1.5 Hz, 2H, 2 × H_a), 8.60 (t, ^4J = 1.6 Hz, 1H, 1 × H_b), 7.60 (t, ^3J = 5.5 Hz, 2H, 2 × H_c), 6.84 (s, 8H, 4 × H_f, 4 × H_g), 6.04–5.85 (m, 2H, 2 × H_k), 5.37–5.15 (m, 4H, 4 × H_l), 4.19–4.02 (m, 12H, 4 × H_h, 4 × H_j, 4 × H_e), 3.94–3.84 (m, 4H, 4 × H_i), 3.78 (dd, ^3J = 5.3, 4.1 Hz, 4H, 4 × H_d); **MS (ESI+)** *m/z*: 650.23 ($[M + H]^+$, calc. for $[C_{34}H_{40}N_3O_{10}]^+$ = 650.27).

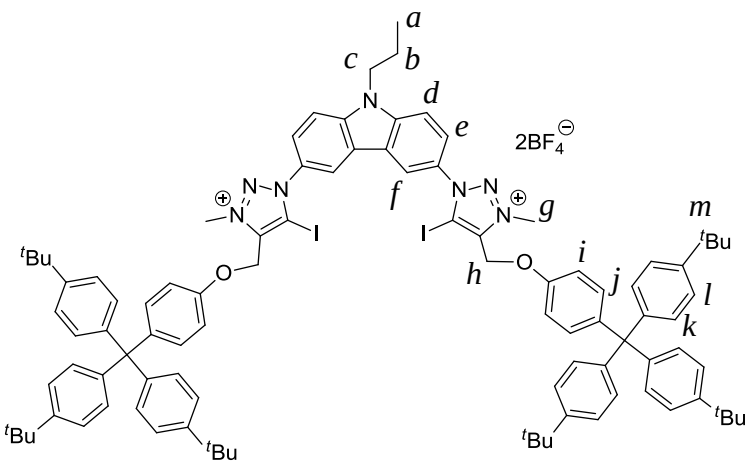
N-linked bis-iodotriazole axle precursor, 50



To a solution of diazidocarbazole **6** (190 mg, 0.66 mmol) in dry THF (10 mL) was added sodium iodide (720 mg, 4.8 mmol) and $Cu(ClO_4)_2{\cdot}6H_2O$ (890 mg, 2.4 mmol). The resultant mixture was stirred for 5 min at RT. To the mixture was then added TBTA (69 mg, 0.13 mmol) and DBU (200 mg, 1.3 mmol), followed by stopper alkyne **42** (810 mg, 1.5 mmol). The resultant mixture was stirred overnight at RT in the dark, then diluted with CH_2Cl_2 (100 mL), washed with $NH_4OH_{(aq.)}$ (100 mL), water (50 mL) and brine (50 mL), dried ($MgSO_4$), filtered and the solvent removed *in vacuo*. The residue was purified by column chromatography (0.5% to 1% MeOH/CH_2Cl_2) to give the desired product **50** (870 mg, 80%); **^{1}H NMR** (300 MHz, $CDCl_3$): δ ppm 8.26 (d, ^4J = 1.76 Hz, 2H, 2 × H_f), 7.70–7.62 (m, 4H, 2 × H_d, 2 × H_e), 7.25 (d, ^3J = 9.38 Hz, 12H, 12 × H_j), 7.15 (d, ^3J = 8.80 Hz, 4H, 4 × H_h), 7.11 (d, ^3J = 6.45 Hz, 12 H, 12 × H_k), 6.98 (d, ^3J = 8.80 Hz, 4H, 4 × H_i), 5.23 (s, 4H, 4 × H_g), 4.44 (t, ^3J = 7.04 Hz, 2 H, 2 × H_c), 2.04 (sxt, ^3J = 7.04 Hz, 2 H, 2 × H_b), 1.31 (s, 54H, 54 × H_l), 1.07 (t, ^3J = 7.33 Hz, 3 H, 3 × H_a); **^{13}C NMR** (75 MHz, $CDCl_3$): δ ppm

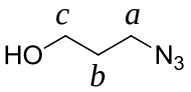
156.30, 148.32, 147.80, 144.06, 141.56, 140.31, 132.32, 130.73, 129.14, 124.73, 124.07, 122.43, 118.91, 113.50, 109.78, 83.19, 63.08, 61.91, 34.30, 31.40, 22.41, 11.86; **HRMS (ESI+)** m/z: 1651.6191 ($[M+Na]^+$, calc. for $[C_{95}H_{103}I_2N_7NaO_2]^+$ = 1651.6187).

N-linked bis-iodotriazolium axle, 51·2BF$_4$



To a solution of axle precursor **50** (360 mg, 0.22 mmol) in dry CH_2Cl_2 (55 mL) was added $Me_3O{\cdot}BF_4$ (78 mg, 0.53 mmol). The solution was stirred overnight at RT. The reaction was quenched with MeOH (one drop) and stirred for 5 min, before the organic solvent was removed *in vacuo*. The residue was purified by column chromatography (5% MeOH/CH_2Cl_2) to give the desired product **51**·2BF$_4$ (350 mg, 87%); **^{1}H NMR** (300 MHz, CD_3CN): δ ppm 8.52 (d, ^4J = 2.1 Hz, 2H, 2 × H_f), 7.98 (d, ^3J = 8.9 Hz, 2H, 2 × H_d), 7.81 (dd, ^3J = 8.9, ^4J = 2.2 Hz, 2H, 2 × H_e), 7.36 (d, ^3J = 8.2 Hz, 12H, 12 × H_k), 7.30 (d, ^3J = 8.8 Hz, 4H, 4 × H_i), 7.21 (d, ^3J = 8.2 Hz, 12H, 12 × H_l), 7.05 (d, ^3J = 8.8 Hz, 4H, 4 × H_j), 5.40 (s, 4H, 4 × H_h), 4.57 (t, ^3J = 7.4 Hz, 2H, 2 × H_c), 4.47 (s, 6H, 6 × H_g), 1.99 (m, 2H, 2 × H_b), 1.30 (s, 54H, 54 × H_m), 1.04 (t, ^3J = 7.4 Hz, 3H, 3 × H_a); **^{13}C NMR** (75 MHz, CD_3CN): δ ppm 155.15, 148.63, 144.37, 143.28, 142.94, 141.85, 131.99, 130.17, 127.28, 124.60, 117.34, 114.28, 109.99, 63.14, 33.98, 30.56 *(seven resonances not distinguishable)*; **HRMS (ESI+)** *m/z*: 828.8379 ($[M - 2(BF_4)]^{2+}$, calc. for $[C_{97}H_{109}I_2N_7O_2]^{2+}$ = 828.8361).

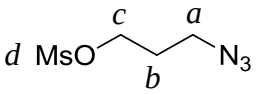
3-Azido-1-propanol, 52



Based on a literature procedure.[29] 3-Bromo-1-propanol (3.00 g, 14.4 mmol) and NaN_3

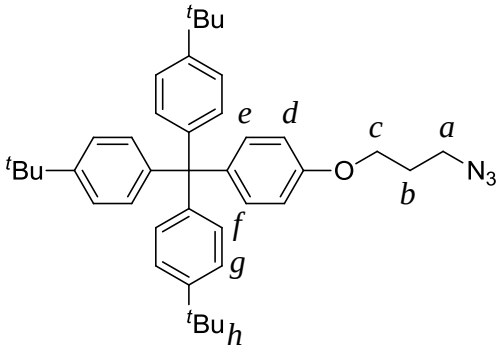
(1.87 g, 28.8 mmol) were dissolved in water (40 mL) and heated at 80 °C overnight. The solution was then cooled to RT and extracted with ethyl acetate (5 × 40 mL), then the combined organics were washed with brine (30 mL) and dried over $MgSO_4$, before the solvent was removed *in vacuo* to give the product **52** as a colourless oil (1.38 g, 95%); **^{1}H NMR** (400 MHz, $CDCl_3$) δ ppm 3.76 (t, ^3J = 5.90 Hz, 2H, 2 × H_c), 3.46 (t, ^3J = 6.60 Hz, 2H, 2 × H_a), 1.84 (quin, ^3J = 6.27 Hz, 2H, 2 × H_b).

3-Azidopropyl mesylate, 53



This compound has been previously reported in the literature.[33] 3-Azido-1-propanol **52** (1.32 g, 13.1 mmol) and triethylamine (2.61 g, 3.6 mL, 25.8 mmol) were dissolved in dry THF (200 mL), and the solution cooled to 0 °C. Mesyl chloride (2.24 g, 1.51 mL, 19.6 mmol) was added and the solution stirred at RT overnight under N_2. The solvent was then removed *in vacuo*, and the solid residue dissolved in CH_2Cl_2 (100 mL). The solution was washed with water (3 × 100 mL), $NaHCO_{3(aq.)}$ (5% w/w, 3 × 100 mL), dried over $MgSO_4$ and the solvent removed *in vacuo* to give the product **53** as a red oil (2.35 g, quant.); **^{1}H NMR** (300 MHz, $CDCl_3$) δ ppm 4.33 (t, ^3J = 5.90 Hz, 2H, 2 × H_c), 3.49 (t, ^3J = 6.74 Hz, 2H, 2 × H_a), 3.04 (s, 3H, 2 × H_d), 2.02 (quin, ^3J = 6.16 Hz, 2H, 2 × H_b).

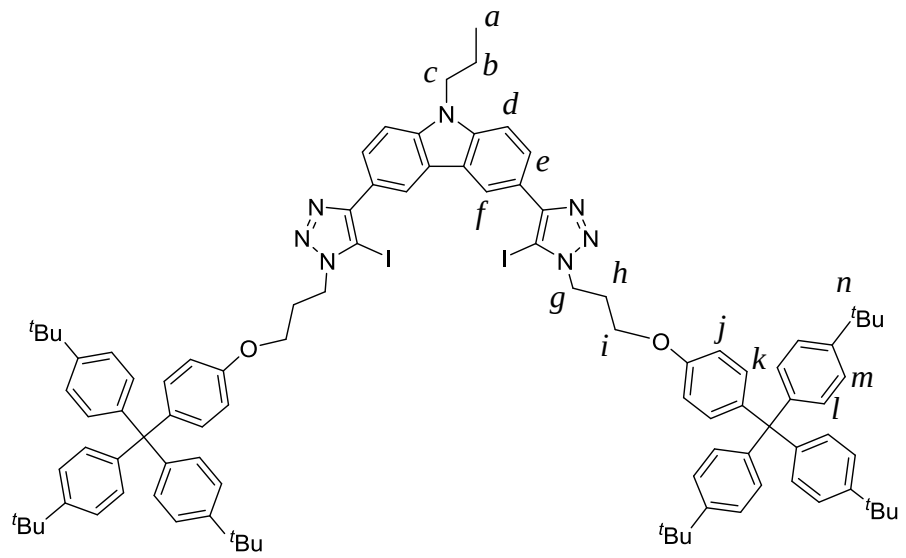
Azidopropyl stopper, 54



Based on a literature procedure.[29] Stopper alcohol **41** (0.526 g, 1.98 mmol) and azide **53** (0.388 g, 2.17 mmol) were dissolved in 2-butanone (25 mL). K_2CO_3 (1.35 g, 9.77 mmol) was added and the mixture heated at 80 °C overnight under N_2, then the reaction was cooled to RT, the solid filtered off and the solvent removed. The residue was purified by column

chromatography (7:3 hexane/CH_2Cl_2) to give the product **54** as a white powder (0.526 g, 45%); **^{1}H NMR** (300 MHz, $CDCl_3$) δ ppm 7.26–7.21 (m, 6H, 6 × H_f), 7.12–7.04 (m, 8H, 2 × H_e, 6 × H_g), 6.77 (d, ^3J = 8.80 Hz, 2H, 2 × H_d), 4.03 (t, ^3J = 5.90 Hz, 2H, 2 × H_c), 3.52 (t, ^3J = 6.50 Hz, 2H, 2 × H_a), 2.05 (quin, ^3J = 6.50 Hz, 2H, 2 × H_b).

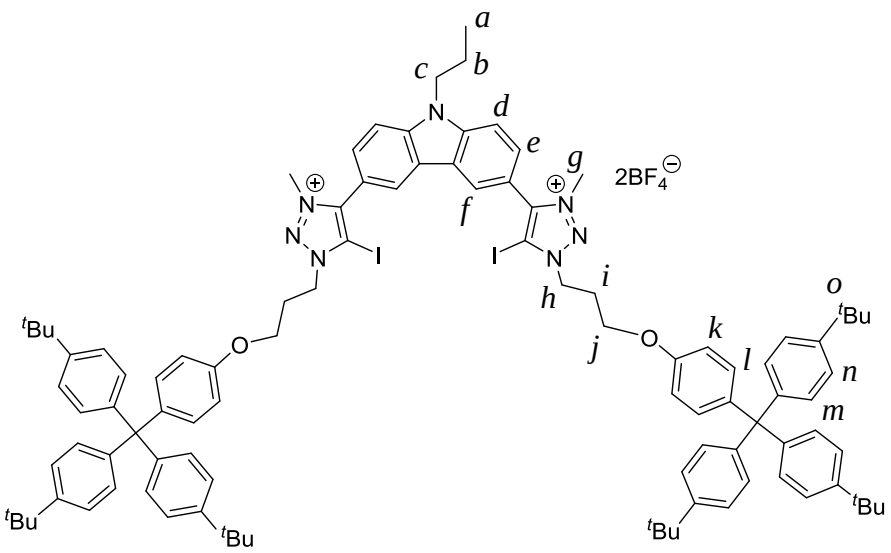
C-linked alkyl bis-iodotriazole axle precursor, 55



To a solution of azide stopper **54** (186 mg, 0.32 mmol) in THF (1.5 mL) was added sodium iodide (0.15 g, 1.0 mmol) and $Cu(ClO_4)_2{\cdot}6H_2O$ (0.19 g, 0.51 mmol). The resultant mixture was stirred for 5 min at RT. To the mixture was then added TBTA (13 mg, 0.02 mmol) and DBU (39 mg, 0.26 mmol), followed by 3,6-diethynylcarbazole **3** (32 mg, 0.13 mmol). The resultant mixture was stirred overnight at RT in the dark, then diluted with CH_2Cl_2 (100 mL), washed with $NH_4OH_{(aq.)}$ (100 mL), water (50 mL) and brine (50 mL), dried ($MgSO_4$), filtered and the solvent removed *in vacuo*. The residue was purified by column chromatography (0.75% MeOH/CH_2Cl_2) to give the desired product **55** (0.19 g, 88%); **^{1}H NMR** (500 MHz, $CDCl_3$) δ ppm 8.73 (d, ^4J = 0.92 Hz, 2H, 2 × H_f), 8.04 (dd, ^3J = 8.24, ^4J = 1.53 Hz, 2H, 2 × H_e), 7.47 (d, ^3J = 8.85 Hz, 2H, 2 × H_d), 7.23 (d, ^3J = 8.54 Hz, 12H, 12 × H_l), 7.11 (d, ^3J = 8.85 Hz, 4H, 4 × H_j), 7.10 (d, ^3J = 8.54 Hz, 12H, 12 × H_m), 6.78 (d, ^3J = 8.85 Hz, 4H, 4 × H_k), 4.67 (t, ^3J = 6.70 Hz, 4H, 4 × H_g), 4.29 (t, ^3J = 6.70 Hz, 2H, 2 × H_c), 4.05 (t, ^3J = 5.30 Hz, 4H, 4 × H_i), 2.46 (quin, ^3J = 6.10 Hz, 4H, 4 × H_h), 1.94 (sxt, ^3J = 7.00 Hz, 2H, 2 × H_b), 1.30 (s, 54H), 0.99 (t, ^3J = 7.30 Hz, 3H, 3 × H_a); **^{13}C NMR** (126 MHz, $CDCl_3$) δ ppm 156.22, 150.65, 148.23, 144.06, 140.86, 139.92, 132.24, 130.67, 125.72, 124.00, 122.89,

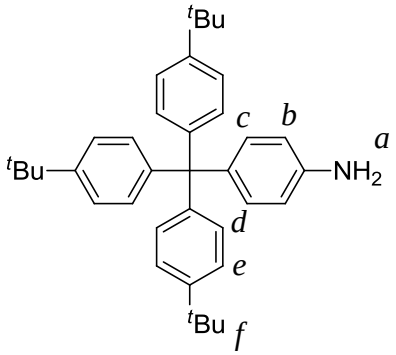
121.28, 119.82, 113.06, 108.93, 76.26, 64.05, 63.01, 47.98, 44.81, 34.22, 31.34, 29.68, 22.31, 11.77.

C-linked bis-iodotriazole axle, 56·2BF$_4$



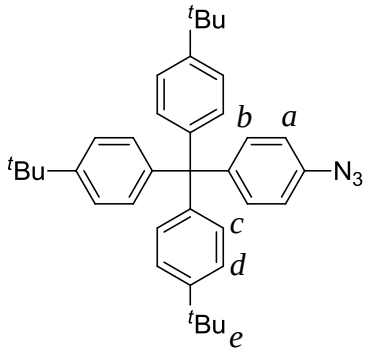
To a solution of axle precursor **55** (190 mg, 0.11 mmol) in dry CH_2Cl_2 (25 mL) was added $Me_3O{\cdot}BF_4$ (41 mg, 0.28 mmol). The solution was stirred at RT for 16 h, then the reaction was quenched with MeOH (one drop) and stirred for 5 min, before the organic solvent was removed *in vacuo*. The residue was purified by column chromatography (5% MeOH/CH_2Cl_2) to give the desired product **56**·2BF$_4$ as a white solid (0.127 g, 60%); **^{1}H NMR** (300 MHz, $CDCl_3$) δ ppm 8.61 (s, 2H, 2 × H_f), 7.66 (d, ^3J = 8.80 Hz, 2H, 2 × H_e), 7.50 (d, ^3J = 8.80 Hz, 2H, 2 × H_d), 7.22 (d, ^3J = 8.21 Hz, 12H, 12 × H_m), 7.05–7.14 (m, 16H, 4 × H_k, 12 × H_n), 6.73 (d, ^3J = 8.80 Hz, 4H, 2 × H_l), 4.79 (t, ^3J = 7.00 Hz, 4H, 4 × H_h), 4.20 (s, 6H, 6 × H_g), 4.17 (br. s., 2H, 2 × H_c), 4.09 (t, ^3J = 4.70 Hz, 4H, 4 × H_j), 2.53 (br. s., 4H, 4 × H_i), 1.84 (br. s., 2H, 2 × H_b), 1.29 (s, 54H, 54 × H_o), 0.91 (t, ^3J = 7.33 Hz, 3H, 3 × H_a)**; ^{13}C NMR** (76 MHz, $CDCl_3$) δ ppm 155.90, 148.27, 147.57, 144.00, 142.28, 140.11, 132.32, 130.61, 128.05, 124.04, 123.85, 122.73, 113.12, 112.95, 110.43, 89.03, 63.59, 63.00, 52.38, 44.96, 39.17, 34.22, 31.32, 28.48, 22.23, 11.66.

Stopper amine, 57



Based on a literature procedure.[27] A suspension of terphenyl alcohol **40** (1.0 g, 2.3 mmol) in acetyl chloride (5.0 mL, 70 mmol) was heated overnight at 60 °C. Residual solvent was removed *in vacuo* and the resultant residue dissolved immediately in aniline (7.0 mL, 77 mmol). The mixture was stirred overnight at 130 °C, then allowed to cool to RT before being poured into $HCl_{(aq.)}$ (10%, 25 mL) and stirred for 20 min. The mixture was extracted into CH_2Cl_2 (3 × 20 mL) and the combined organics washed with $HCl_{(aq.)}$ (10%, 25 mL), $Na_2CO_{3(sat.\ aq.)}$ (2 × 25 mL) and water (2 × 25 mL), dried ($MgSO_4$), filtered and concentrated to dryness *in vacuo*. The residue was purified by column chromatography (CH_2Cl_2) to afford the desired product **57** (490 mg, 41%); **^{1}H NMR** (300 MHz, $CDCl_3$): δ ppm 7.25–7.19 (m, 6H, 6 × H_d), 7.11–7.05 (m, 6H, 6 × H_e), 7.03–6.97 (m, 2H, 2 × H_c), 6.69 (d, ^3J = 8.5 Hz, 2H, 2 × H_b), 3.49 (br. s, 2H, 2 × H_a), 1.29 (s, 27H, 27 × H_f).

Stopper azide, 58



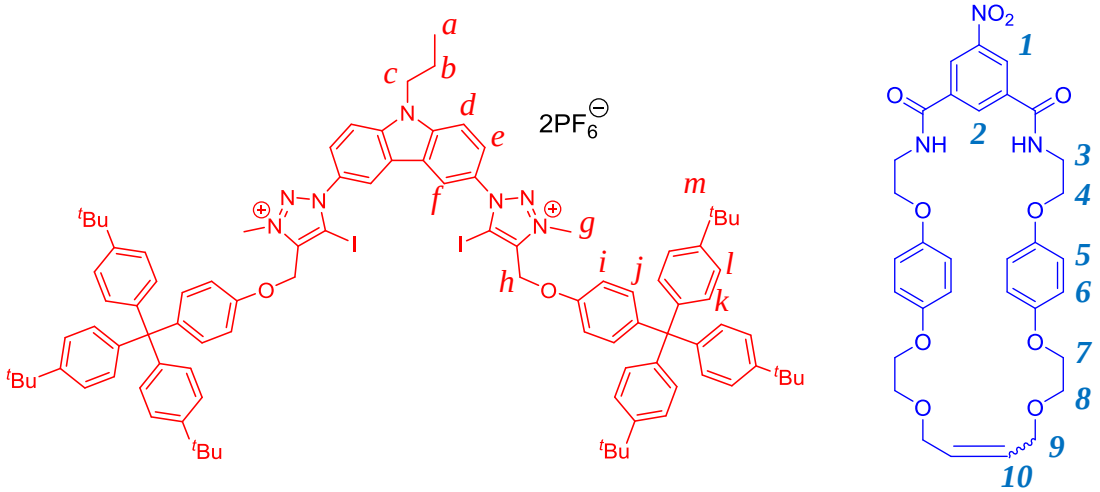
Based on a literature procedure.[34] A suspension of stopper amine **57** (310 mg, 0.61 mmol) in a mixture of ethanol and $HCl_{(conc.\ aq.)}$ (9:1, 250 mL) was cooled to 0 °C, whereupon sodium nitrite (84 mg, 1.2 mmol) was added. After stirring for 2 min, sodium azide (79 mg,

1.2 mmol) was added and the resultant mixture stirred for 2 h at 0 °C. The mixture was diluted with water (200 mL) and extracted with diethyl ether (450 mL), then the organic layer was washed with $Na_2CO_{3(sat.\ aq.)}$ (2 × 200 mL) and brine (200 mL), dried ($MgSO_4$), filtered and concentrated to dryness *in vacuo*. The residue was dissolved in a mixture of pet. ether and CH_2Cl_2 (1:1, 75 mL) and filtered through a silica pad, which was washed with pet. ether/CH_2Cl_2 (1:1, 75 mL). The filtrate was concentrated to dryness *in vacuo* to afford **58** (290 mg, 88%); **^{1}H NMR** (300 MHz, $CDCl_3$): δ ppm 7.28–7.14 (m, 8H, 2 × H_b, 6 × H_c), 7.10–7.01 (m, 6H, 2 × H_d), 6.94–6.86 (m, 2H, 2 × H_a), 1.30 (s, 27H, 27 × H_e).

Attempted synthesis of C-linked aryl axle precursor, 59

To a solution of stopper azide **58** (290 mg, 0.54 mmol) in degassed THF (5 mL) was added sodium iodide (290 mg, 2.0 mmol) and $Cu(ClO_4)_2{\cdot}6H_2O$ (360 mg, 1.0 mmol). The resultant mixture was stirred for 5 min at RT, then TBTA (26 mg, 0.050 mmol) and DBU (75 mg, 0.49 mmol) were added, followed by 3,6-diethynylcarbazole **3** (63 mg, 0.25 mmol). The resultant mixture was stirred overnight at RT in the dark, then diluted with CH_2Cl_2 (50 mL), washed with $NH_4OH_{(aq.)}$ (25 mL) and brine (2 × 25 mL), dried ($MgSO_4$), filtered and the solvent removed *in vacuo*. Crude MS analysis indicated no presence of desired product **59**.

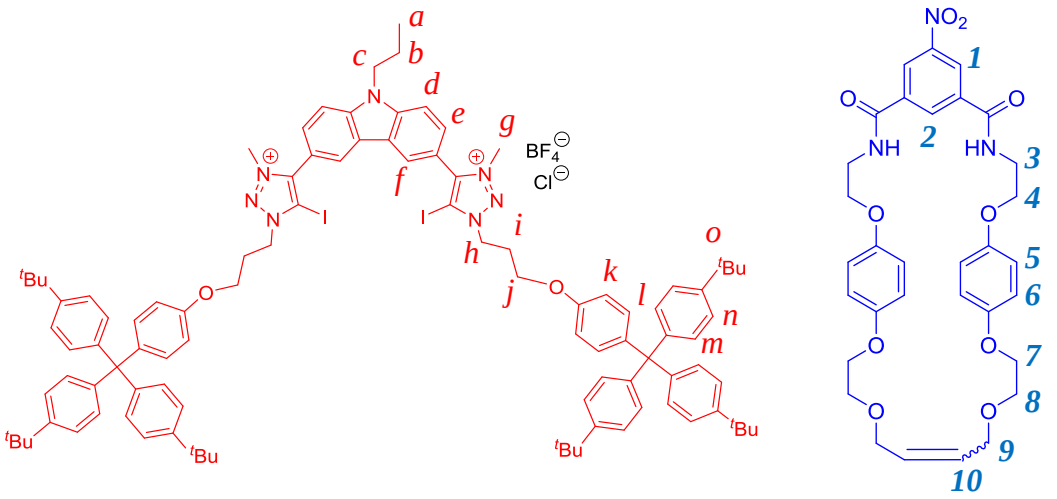
Bis-iodotriazolium [2]rotaxane, 60·2PF$_6$



A solution of axle **51**·2BF$_4$ (250 mg, 0.14 mmol), TBA·Cl (38 mg, 0.14 mmol) and macrocycle precursor **49** (133 mg, 0.20 mmol) in dry CH_2Cl_2 (20 mL) was stirred for 30 min at RT. Stewart–Grubbs' catalyst (13 mg, 10% w/w cat.) was added and the solution stirred for

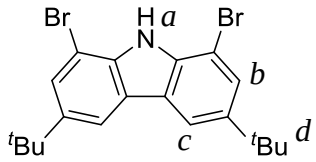
4 d. The solvent was removed *in vacuo* and the residue purified, first using iterative preparative TLC (3 × 2% MeOH/CH_2Cl_2), then using a second preparative TLC plate (EtOAc). After running a third preparative TLC plate (10% MeOH/CH_2Cl_2), the near-pure rotaxane was anion-exchanged for PF_6^- by taking up the solid in CH_2Cl_2 (10 mL) and stirring vigorously with $NH_4PF_{6(aq.)}$ (0.1 M, 10 mL) for 30 min. The organic layer was separated and washed with further $NH_4PF_{6(aq.)}$ (0.1 M, 6 × 10 mL) and H_2O (3 × 10 mL), then dried thoroughly *in vacuo*. The white powder was then recrystallised twice from MeOH, giving the pure rotaxane **60**·$2PF_6$ as an off-white powder (15 mg, 4%): **^{1}H NMR** (500 MHz, 4:1 CD_2Cl_2/CD_3OD) δ ppm 8.39 (s, 2H, 2 × H_1), 8.34 (s, 1H, 1 × H_2), 8.05 (s, 2H, 2 × H_f), 7.55 (d, ^3J = 9.00 Hz, 2H, 2 × H_e), 7.43 (d, ^3J = 7.78 Hz, 2H, 2 × H_d), 7.35 (d, ^3J = 8.85 Hz, 4H, 4 × H_j), 7.29 (d, ^3J = 8.54 Hz, 12H, 12 × H_k), 7.20 (d, ^3J = 8.70 Hz, 12H, 12 × H_l), 7.07 (d, ^3J = 8.85 Hz, 4H, 4 × H_i), 6.72 (d, ^3J = 9.16 Hz, 4H, 4 × H_6), 6.62 (d, ^3J = 9.00 Hz, 4H, 4 × H_7), 5.57 (s, 2H, 2 × H_{11}), 5.18 (s, 4H, 4 × H_h), 4.50 (s, 6H, 6 × H_g), 4.32 (t, ^3J = 7.25 Hz, 2H, 2 × H_c), 4.00–4.06 (m, 4H, 4 × H_5), 3.91 (d, ^3J = 4.88 Hz, 4H, 4 × H_8), 3.81 (br. s., 4H, 4 × H_{10}), 3.76 (br. s., 4H, 4 × H_4), 3.71 (br. s., 4H, 4 × H_9), 1.89 (sxt, ^3J = 7.14 Hz, 2H, 2 × H_b), 1.30 (s, 54H, 54 × H_m), 0.99 (t, ^3J = 7.40 Hz, 3H, 3 × H_a); **^{13}C NMR** (126 MHz, 4:1 CD_2Cl_2/CD_3OD) δ ppm 165.55, 155.66, 153.34, 153.29, 149.26, 148.39, 144.87, 142.86, 136.00, 132.96, 131.00, 130.66, 130.13, 127.65, 125.76, 125.48, 125.02, 124.77, 122.21, 119.42, 115.52, 115.42, 114.28, 111.31, 71.41, 69.96, 68.72, 67.44, 63.88, 59.62, 40.52, 40.37, 34.78, 32.50, 30.24, 23.25, 22.69, 11.81; **HRMS (ESI+)** *m/z*: 1139.9550 ($[M - 2(PF_6)]^{2+}$, calc. for $[C_{129}H_{144}I_2N_{10}O_{12}]^{2+}$ = 1139.9538).

C-linked bis-iodotriazole rotaxane, 61·Cl·BF_4



A solution of axle **56**·2BF_4 (250 mg, 0.14 mmol), TBA·Cl (38 mg, 0.14 mmol) and macrocycle precursor **49** (133 mg, 0.20 mmol) in dry CH_2Cl_2 (20 mL) was stirred for 30 min at RT. Grubbs' II catalyst (13 mg, 10% w/w cat.) was added and the solution stirred for 4 d. The solvent was removed *in vacuo* and the residue purified, first using iterative preparative TLC 3 × 1% MeOH/CH_2Cl_2), then using a second preparative TLC plate (EtOAc). Unfortunately during the last purification step, all trace of the rotaxane was lost, although an near-pure ^{1}H NMR was obtained beforehand; **HRMS (ESI+)** m/z: 1168.4821 ([M – Cl – BF_4]$^{2+}$, calc. for [$C_{133}H_{152}I_2N_{10}O_{12}$]$^{2+}$ = 1168.4851).

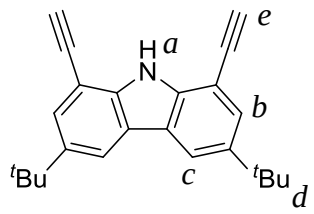
1,8-Dibromocarbazole, 62



Based on a literature procedure.[35] 3,6-Di-*tert*-butylcarbazole (5.00 g, 18.0 mmol) was dissolved in glacial acetic acid (250 mL). Bromine (6.4 g, 2.0 mL, 40.0 mmol) dissolved in glacial acetic acid (125 mL) was added to the carbazole solution over 30 min at RT, with the exclusion of light. The mixture was left to stir at RT for a further 45 min, after which the acetic acid was removed *in vacuo*, leaving a yellow crude powder. The residue was dissolved in EtOAc (175 mL), then the solution was washed with $NaOH_{(aq.)}$ (1 M, 3 × 60 mL), $NaHCO_{3(sat.\ aq.)}$ (60 mL), water (40 mL) and brine (40 mL), before being dried ($MgSO_4$) and

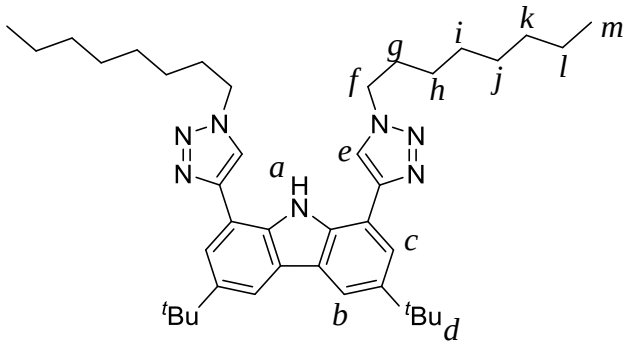
the solvent removed *in vacuo* giving a sticky residue. The product was redissolved into CH_2Cl_2 (20 mL) and the solvent removed *in vacuo*, giving the product as a light-yellow powder (7.42 g, 94%); **^{1}H NMR** (400 MHz, $CDCl_3$) δ ppm 8.15 (br. s, 1H, 1 × H_a) 7.99 (s, 2H, 2 × H_b) 7.65 (d, ^4J = 0.98 Hz, 2H, 2 × H_c) 1.45 (s, 18H, 18 × H_d); **^{13}C NMR** (101 MHz, $CDCl_3$) δ ppm 144.76, 136.30, 126.62, 124.80, 115.94, 103.99, 34.91, 31.89; **HRMS (FI+)** *m/z*: 437.0038 ($[M]^+$, calc. for $[C_{20}H_{23}Br_2N]^+$ = 437.0178).

1,8-Diethynyl carbazole, 63



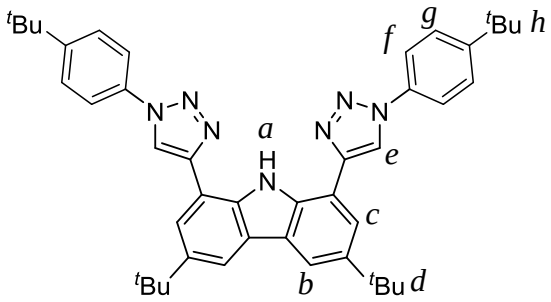
Based on a literature procedure.[36] To a degassed solution of dibromocarbazole **62** (0.60 g, 1.4 mmol) and TMS-acetylene (1.0 mL, 0.68 g, 6.9 mmol) in dry triethylamine (30 mL) were added copper(I) iodide (12 mg, 0.063 mmol) and $Pd(PPh_3)_2Cl_2$ (80 mg, 0.11 mmol). The mixture was stirred for 5 d at 85 °C in a closed vial. The reaction mixture was allowed to cool to RT, whereupon it was flushed through a silica pad with CH_2Cl_2 (150 mL). The solvent was removed *in vacuo*. To the resultant residue was added CH_3CN (30 mL), water (2 mL) and potassium hydroxide (0.40 g, 8.5 mmol), and the mixture was stirred for 1 h. The organic solvent was removed *in vacuo*. $NH_4Cl_{(aq.)}$ (1 M, 30 mL) was added, and the mixture was extracted into $CHCl_3$ (3 × 20 mL). The combined organics were washed with $NH_4Cl_{(aq.)}$ (1 M, 10 mL) and water (2 × 20 mL), dried ($MgSO_4$), and concentrated to dryness *in vacuo*. The residue was purified by column chromatography (10% EtOAc/pet. ether) to give the desired product **63** as a light brown powder (0.33 g, 72%); **^{1}H NMR** (400 MHz, $CDCl_3$) δ ppm 8.47 (br. s, 1H, 1 × H_a), 8.10 (s, 2H, 2 × H_b), 7.66 (d, ^4J = 1.47 Hz, 2H, 2 × H_c), 3.48 (s, 2H, 2 × H_e), 1.46 (s, 18H, 18 × H_d); **^{13}C NMR** (101 MHz, $CDCl_3$) δ ppm 142.76, 139.17, 127.50, 123.23, 117.97, 103.87, 81.34, 80.42, 34.72, 31.88; **HRMS (FI+)** *m/z*: 327.1996 ($[M]^+$, calc. for $[C_{20}H_{23}Br_2N]^+$ = 327.1987).

1,8-Bis-triazole alkyl carbazole, 64



To a solution of diethynylcarbazole **63** (100 mg, 0.31 mmol) and *n*-octyl azide **8** (100 mg, 0.64 mmol) in dry CH_2Cl_2 (50 mL) were added TBTA (170 mg, 0.32 mmol) and $[Cu(CH_3CN)_4](PF_6)$ (120 mg, 0.32 mmol), followed by DIPEA (120 mg, 0.93 mmol). The resultant solution was stirred for 72 h at RT. The reaction mixture was washed with $HCl_{(aq.)}$ (2 × 50 mL), $NaHCO_{3(sat.\ aq.)}$ (50 mL) and water (50 mL), dried ($MgSO_4$) and the solvent removed *in vacuo*. The residue was purified by column chromatography (2.5% MeOH/$CHCl_3$) to give the desired product as a yellow solid (0.15 g, 76%); **^{1}H NMR** (400 MHz, $CDCl_3$) δ ppm 11.64 (s, 1 H, 1 × H_a) 8.13 (s, 2H, 2 × H_c) 8.02 (s, 2H, 2 × H_e) 7.76 (d, ^4J = 0.98 Hz, 2H, 2 × H_b) 4.48 (t, ^3J = 7.21 Hz, 4H, 4 × H_f) 2.02 (quin, ^3J = 7.00 Hz, 4H, 4 × H_g), 1.52 (s, 18H, 18 × H_d) 1.45–1.21 (m, 20H, 20 × $H_{i–l}$) 0.88 (t, ^3J = 6.72 Hz, 6H, 6 × H_m); **^{13}C NMR** (101 MHz, $CDCl_3$) δ ppm 141.76, 135.73, 123.87, 120.22, 119.09, 116.23, 112.94, 50.52, 34.72, 32.11, 31.72, 30.75, 30.41, 29.03, 29.00, 26.55, 22.58, 14.03; **HRMS (ESI+)** *m/z*: 638.4893 ($[M + H]^+$, calc. for $[C_{40}H_{60}N_7]^+$ = 638.4905).

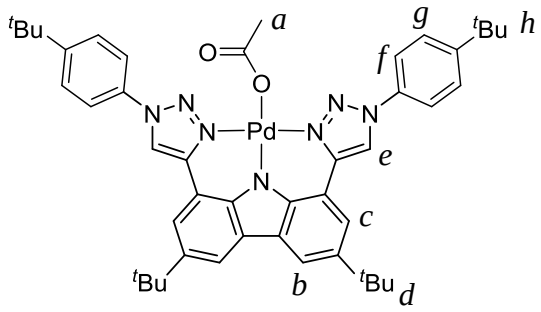
1,8-Bis-triazole aryl carbazole, 65



To a solution of diethynylcarbazole **63** (50 mg, 0.15 mmol) and 1-azido-4-(*tert*-butyl)benzene **7** (60 mg, 0.34 mmol) in dry CH_2Cl_2 (20 mL) were added TBTA (85 mg, 0.16 mmol) and

$[Cu(CH_3CN)_4](PF_6)$ (60 mg, 0.16 mmol), followed by DIPEA (0.06 mL, 0.045 mg, 0.35 mmol). The resultant solution was stirred for 3 d at RT. The reaction mixture was washed with $HCl_{(aq.)}$ (2 × 20 mL), $NaHCO_{3(sat.\ aq.)}$ (20 mL) and brine (20 mL), dried ($MgSO_4$) and the solvent removed *in vacuo*. The residue was purified by column chromatography (40% hexanes/CH_2Cl_2) to give the desired product **65** as a yellow solid (47 mg, 46%); **^{1}H NMR** (300 MHz, $CDCl_3$) δ ppm 11.98 (s, 1H, 1 × H_a), 8.43 (s, 2H, 2 × H_c), 8.15 (s, 2H, 2 × H_e), 7.82 (d, ^3J = 8.21 Hz, 4H, 4 × H_f), 7.77 (s, 2H, 2 × H_b), 7.61 (d, ^3J = 8.21 Hz, 4H, 4 × H_g), 1.53 (s., 9H, 9 × H_d), 1.42 (s, 9H, 9 × H_h).

Palladium(II) complex of acyclic carbazole compound, Pd(65)(AcO)

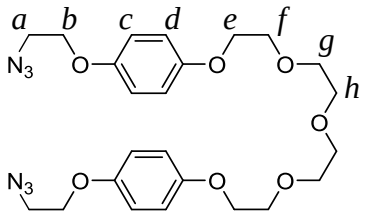


Acyclic carbazole-based compound **65** (20 mg, 0.030 mmol) and palladium(II) acetate (8 mg, 0.036 mmol) were dissolved in CH_2Cl_2, and stirred for 16 h under N_2 at RT. The solvent was removed *in vacuo*, and the residue purified by column chromatography (5% ethanol/CH_2Cl_2), to give the acetate salt of the complex product, Pd(**65**)(AcO), as an orange solid. **^{1}H NMR** (300 MHz, $CDCl_3$) δ ppm 8.57 (s, 2H, 2 × H_e), 8.25 (d, ^4J = 1.76 Hz, 2H, 2 × H_c), 7.84 (d, ^3J = 8.21 Hz, 4H, 4 × H_f), 7.80 (d, ^4J = 1.76 Hz, 2H, 2 × H_b), 7.57 (d, ^3J = 8.21 Hz, 4H, 4 × H_g), 7.53 (s, 2H, *unassigned*), 5.31 (s, 3H, 3 × H_a), 1.54 (s, 18H, 18 × H_d), 1.38 (s, 18H, 18 × H_h).

To convert the complex to the PF_6^- salt, the acetate product was dissolved in CH_2Cl_2 (10 mL), and stirred vigorously with $NH_4PF_{6(sat.\ aq.)}$ (10 mL) for 16 h. The aqueous layer was removed, and the organic layer washed with H_2O (2 × 10 mL), and the solvent removed *in vacuo* to give the PF_6^- salt of the product, Pd(**65**)(PF_6), as an orange solid (14.5 mg, 57% overall). Unfortunately, the ^{1}H NMR spectrum suffered from severe peak broadening and could not be properly analysed, but the ^{19}F NMR gave a diagnostic doublet for PF_6^-, suggesting that the anion exchange had worked; **^{19}F NMR** (283 MHz, CD_3CN) δ ppm −72.95

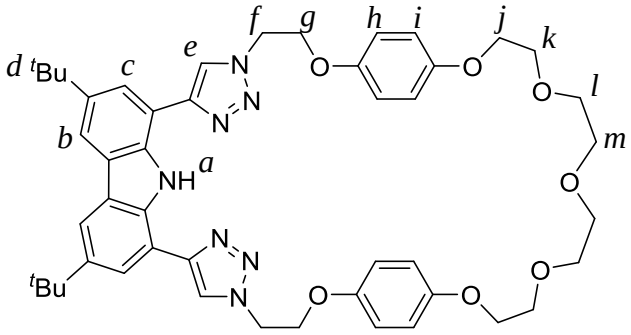
(d, $J_{F,P}$ = 706.47 Hz).

Bis-azide polyether, 66



Bis(amino) polyether **31** (316 mg, 0.687 mmol) was dissolved in MeOH (50 mL). The HSO_4^- salt of imidazolesulfonyl azide (344 mg, 1.64 mmol), K_2CO_3 (430 mg, 3.07 mmol) and $CuSO_4 \cdot 5H_2O$ (37 mg, 0.15 mmol) were added and the suspension was stirred at RT under a N_2 atmosphere for 3 d. It was cautiously concentrated to ~10 mL under reduced pressure, diluted with $HCl_{(aq.)}$ (1 M, 100 mL) and extracted with EtOAc (3 × 30 mL). The combined organic fractions were washed with brine (50 mL) and dried ($MgSO_4$), then taken to dryness under reduced pressure. The residue was purified by column chromatography (2% MeOH/CH_2Cl_2) to give the product **66** (0.278 g, 79%); **^{1}H NMR** (300 MHz, $CDCl_3$) δ ppm 6.85 (s, 8H, 4 × H_c, 4 × H_d), 4.03–4.13 (m, 8H, 4 × H_b, 4 × H_e), 3.80–3.87 (m, 4H, 4 × H_f), 3.66–3.76 (m, 8H, 4 × H_g, 4 × H_h), 3.57 (t, ^3J = 4.99 Hz, 4H, 4 × H_a); **MS (ESI+)** *m/z*: 517.22 ($[M + H]^+$, calc. for $[C_{24}H_{33}N_6O_7]^+$ = 517.23).

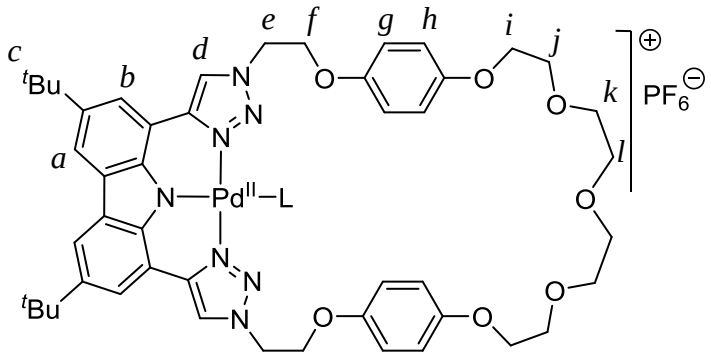
Carbazole-containing macrocycle, 67



To a solution of diethynylcarbazole **63** (20 mg, 0.061 mmol), bis-azide **66** (31 mg, 0.061 mmol) and bis-amide pyridinium chloride thread **32a**·Cl (25 mg, 0.061 mmol) in dry CH_2Cl_2 (100 mL) were added TBTA (39 mg, 0.073 mmol) and $[Cu(CH_3CN)_4](PF_6)$ (27 mg, 0.072 mmol), followed by DIPEA (0.030 mL, 0.022 mg, 0.17 mmol). The resultant solution was stirred for 14 d at RT, then the solvent was removed *in vacuo*, and the residue was

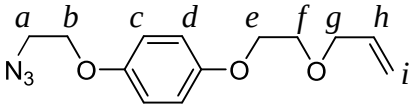
redissolved in $CHCl_3$, washed with $HCl_{(aq.)}$ (10%, 2 × 20 mL), $NaHCO_{3(sat.\ aq.)}$ (2 × 20 mL) and H_2O (20 mL), dried ($MgSO_4$) and the solvent removed *in vacuo*. The residue was purified by preparative silica TLC plate (3% MeOH/CH_2Cl_2) to give the desired product **67** as a brown solid (8 mg, 16%); **^{1}H NMR** (300 MHz, $CDCl_3$) δ ppm 11.27 (s, 1H, 1 × H_a), 8.26 (s, 2H, 2 × H_e), 8.14 (s, 2H, 2 × H_c), 7.88 (d, ^4J = 1.17 Hz, 2H, 2 × H_b), 6.69–6.84 (m, 8H, 4 × H_h, 4 × H_i), 4.87 (t, ^3J = 4.69 Hz, 4H, 4 × H_f), 4.42 (t, ^3J = 4.69 Hz, 4H, 4 × H_g), 3.90–3.99 (m, 4H, 2 × H_j), 3.72–3.80 (m, 4H, 4 × H_k), 3.61–3.70 (m, 8H, 4 × H_l, 4 × H_m), 1.52 (s, 18H, 18 × H_d); **^{13}C NMR** (126 MHz, $CDCl_3$) δ ppm 153.60, 152.25, 147.02, 142.12, 135.64, 123.96, 120.89, 120.52, 116.46, 115.82, 115.68, 112.76, 77.20, 70.77, 70.74, 69.66, 68.05, 67.50, 50.16, 34.79, 32.11; **HRMS (ESI+)** *m/z*: 844.4381 ($[M + H]^+$, calc. for $[C_{48}H_{58}N_7O_7]^+$ = 844.4392).

Pd complex of Carbazole-containing macrocycle, Pd(67)(PF_6)



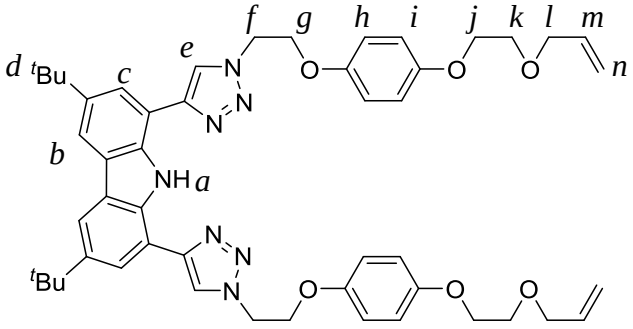
Carbazole-containing macrocycle **67** (8 mg, 0.0095 mg) and palladium(II) acetate (2.2 mg, 0.010 mmol) were dissolved in dry CH_2Cl_2 (10 mL) and stirred at RT for 16 h. The solvent was removed *in vacuo*, and the residue columned (5% ethanol/CH_2Cl_2) to give the acetate salt of the product. This was ion-exchanged for the PF_6^- anion by dissolving the complex in CH_2Cl_2 (10 mL) and stirring vigorously with $NH_4PF_{6(sat.\ aq.)}$ (10 mL), then removing the aqueous layer and washing the organic layer with H_2O (2 × 10 mL). The solvent was then removed *in vacuo*, and the solid thoroughly dried under reduced pressure, giving the product Pd(**67**)(PF_6) as an orange solid (2.5 mg, 24%); **^{1}H NMR** (300 MHz, $CDCl_3$) δ ppm 8.49 (s, 2H, 2 × H_b), 8.31 (s, 2H, 2 × H_d), 7.86 (s, 2H, 2 × H_a), 6.72 (d, ^3J = 9.39 Hz, 4H, 4 × H_g), 6.58 (d, ^3J = 8.80 Hz, 4H, 4 × H_h), 4.21 (s, 4H, 4 × H_e), 3.91–3.99 (m, 4H, 4 × H_f), 3.75–3.64 (m, 8H, 4 × H_i, 4 × H_j), 3.60 (s, 8H, 4 × H_k, 4 × H_l), 1.59 (s, 18H, 18 × H_c).

Vinyl-appended azide, 68



Based on a literature procedure.[37] Vinyl-appended amine **48** (578 mg, 2.44 mmol) was dissolved in MeOH (15 mL). The HSO_4^- salt of imidazolesulfonyl azide (814 mg, 3.00 mmol), K_2CO_3 (829 mg, 6.00 mmol) and $CuSO_4 \cdot 5H_2O$ (7.5 mg, 0.03 mmol) were added and the suspension was stirred at RT under a N_2 atmosphere for 3 d. It was cautiously concentrated to ~5 mL under reduced pressure, diluted with $HCl_{(aq.)}$ (10%, 100 mL) and extracted with EtOAc (3 × 100 mL). The combined organic fractions were washed with brine (100 mL) and dried ($MgSO_4$) then taken to dryness under reduced pressure. The residue was purified by column chromatography (2:1 petrol:EtOAc) to give the product **68** as a colourless oil (0.5485 g, 85%). **^{1}H NMR** (300 MHz, $CDCl_3$): δ ppm 6.84 (s, 4H, Ar*H*, 2 × H_c, 2 × H_d), 5.99–5.86 (m, 1H, 2 × H_h), 5.35–5.17 (m, 2H, 2 × H_i), 4.10–4.05 (m, 6H, 2 × H_a, 2 × H_e, 2 × H_g), 3.78–3.75 (m, 2H, 2 × H_b), 3.55 (t, ^3J = 4.7 Hz, 2H, 2 × H_f).

Allyl-appended carbazole-containing macrocycle, 69



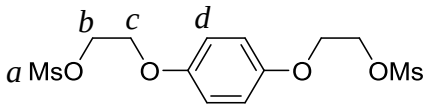
Diethynylcarbazole **63** (94 mg, 0.29 mmol), allyl-appended azide **68** (178 mg, 0.68 mmol), TBTA (190 mg, 0.35 mmol), $[Cu(CH_3CN)_4](PF_6)$ (150 mg, 0.40 mmol), then DIPEA (0.060 mL, 0.044 mg, 0.34 mmol) were dissolved in dry CH_2Cl_2 (20 mL), and stirred at RT for 5 d. The solution was then washed with $HCl_{(aq.)}$ (10%, 4 × 20 mL), $NaHCO_{3(sat.\ aq.)}$ (2 × 20 mL) and brine (20 mL), dried ($MgSO_4$) and the solvent removed *in vacuo*. The residue was purified by column chromatography (1% MeOH/CH_2Cl_2) to give the desired product **69** as an off-white solid (82 mg, 34%); **^{1}H NMR** (300 MHz, $CDCl_3$) δ ppm 11.81 (s, 1H, 1 × H_a), 8.22 (s, 2H, 2 × H_e), 8.14 (d, ^4J = 1.76 Hz, 2H, 2 × H_c), 7.73 (d, ^4J = 1.76 Hz, 2H, 2 × H_b), 6.80 (s, 8H, 4 × H_h, 4 × H_i), 5.85–6.00 (m, 2H, 2 × H_m), 5.17–5.34 (m, 4H,

4 × H_n), 4.83 (t, ^3J = 4.98 Hz, 4H, 4 × H_f), 4.36 (t, ^3J = 4.98 Hz, 4H, 4 × H_g), 4.04–4.08 (m, 4H, 4 × H_j), 3.98–4.04 (m, 4H, 4 × H_l), 3.70–3.76 (m, 4H, 4 × H_k), 1.51 (s, 18H, 18 × H_d); **^{13}C NMR** (76 MHz, $CDCl_3$) δ ppm 153.44, 152.13, 147.45, 141.70, 135.64, 134.47, 123.78, 120.41, 120.21, 117.23, 116.24, 115.60, 115.56, 112.75, 72.23, 68.46, 67.86, 67.15, 49.96, 34.66, 32.04; **HRMS (ESI+)** *m/z*: 854.4595 ($[M + H]^+$, calc. for $[C_{50}H_{60}N_6O_7]^+$ = 854.4600).

Attempted Synthesis of Pd complex of macrocycle precursor, Pd(69)(PF_6)

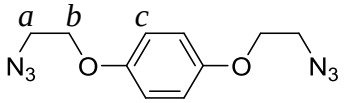
Carbazole-containing macrocycle precursor **69** (20 mg, 0.023 mg) and palladium(II) acetate (5.5 mg, 0.025 mmol) were dissolved in dry CH_2Cl_2 (5 mL) and stirred at RT for 16 h. The solvent was removed *in vacuo*, and the residue was ion-exchanged for the PF_6^- anion by dissolving the complex in CH_2Cl_2 (10 mL) and stirring vigorously with $NH_4PF_{6(sat.\ aq.)}$ (10 mL) for 16 h. The aqueous layer was then removed, and the organics washed with H_2O (2 × 10 mL) and the solvent removed *in vacuo*. The residue was then purified by preparative silica TLC (5% MeOH/$CHCl_3$). The NMR of the Pd(II) complex displayed a vast number of peaks, implying a mixture of complex species, and confirmation of the structure could not be made.

Bis-mesylate hydroquinone, 70



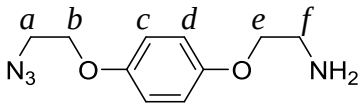
Based on a literature procedure.[38] To a solution of 2,2′-(1,4-phenylenebis(oxy))bis(ethan-1-ol) (4.96 g, 25.0 mmol) and triethylamine (7.6 g, 10.4 mL, 75.0 mmol) dissolved in dry CH_2Cl_2 at 0 °C was added mesyl chloride (8.6 g, 5.8 mL, 75.0 mmol) dropwise. The reaction was then warmed to RT, and stirred for 2 h. The solution was washed with $HCl_{(aq.)}$ (1 M, 2 × 50 mL) and brine (2 × 50 mL), dried ($MgSO_4$) and the solvent removed *in vacuo* to give the product **70** as a white solid (8.0g, 90%); **^{1}H NMR** (400 MHz, $CDCl_3$) δ ppm 6.86 (s, 4H, 4 × H_d), 4.50–4.61 (m, 4H, 4 × H_c), 4.16–4.26 (m, 4H, 4 × H_b), 3.10 (s, 6H, 6 × H_a).

Bis-azide hydroquinone, 71



Based on a literature procedure.[38] Bis-mesylate hydroquinone **70** (3.0 g, 8.5 mmol) and sodium azide (1.38 g, 21 mmol) were dissolved in DMSO (30 mL) and heated at 50 °C under N_2 for 3 d. The solution was cooled to RT, then after addition of H_2O (30 mL), was extracted with diethyl ether (2 × 30 mL). The organic extracts were combined, and washed with H_2O (2 × 30 mL) and brine (30 mL), dried ($MgSO_4$) and the solvent removed *in vacuo*, to give the product **71** (1.75 g, 83%); **^{1}H NMR** (300 MHz, $CDCl_3$) δ ppm 6.88 (s, 4H, 4 × H_c), 4.12 (t, ^3J = 5.00 Hz, 4H, 4 × H_a), 3.58 (t, ^3J = 4.99 Hz, 4H, 4 × H_b).

Monoreduced hydroquinone, 72



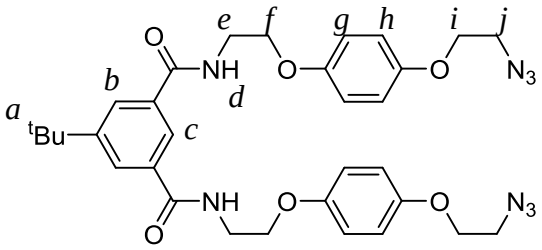
Based on a literature procedure.[38] Bis-azide hydroquinone **71** (1.0 g, 4.0 mmol) was dissolved in a 1:1:2 ethyl acetate/diethyl ether/5% $HCl_{(aq.)}$ (10 mL) solvent mixture, which was cooled to 0 °C. A solution of triphenylphosphine (1.05 g, 4.2 mmol) in 1:1:2 ethyl acetate/diethyl ether/5% $HCl_{(aq.)}$ (10 mL) was added to the first solution dropwise over the course of 1 h. The reaction mixture was then stirred for 16 h, allowing the solution to warm to RT. The solution was poured into a separating funnel, $HCl_{(aq.)}$ (5%, 10 mL) was added, the mixture shaken well, and the organics removed. The aqueous layer was further washed with CH_2Cl_2 (3 × 15 mL), and the organic washings discarded. The aqueous solution was then basified to pH 12 with 10% $NaOH_{(aq.)}$, and extracted with CH_2Cl_2 (3 × 25 mL). The organic extracts were combined, dried ($MgSO_4$) and the solvent removed *in vacuo* to give the mono-reduced product **72** as a colourless oil which solidified on standing (0.58 g, 66%); **^{1}H NMR** (300 MHz, $CDCl_3$) δ ppm 6.79–6.93 (m, 4H, 2 × H_c, 2 × H_d), 4.07–4.14 (m, 2H, 2 × H_a), 3.94 (t, ^3J = 5.28 Hz, 2H, 2 × H_f), 3.57 (t, ^3J = 4.99 Hz, 2H, 2 × H_b), 3.06 (t, ^3J = 5.28 Hz, 2H, 2 × H_e).

Attempted Synthesis of bis-amine-appended carbazole compound, 73

Diethynylcarbazole **63** (50 mg, 0.15 mmol) and mono-reduced azide **72** (85 mg, 0.38 mmol)

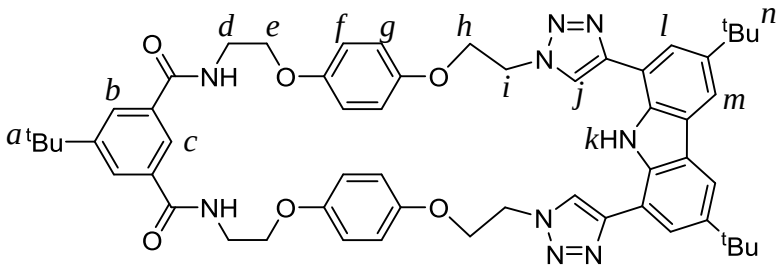
were dissolved in 1:1 THF/H_2O (10 mL). $CuSO_4$ (40 mg, 0.16 mmol) dissolved in H_2O (0.1 mL) and sodium L-ascorbate (60 mg, 0.30 mmol) were added, then the reaction was stirred vigorously at 50 °C for 3 d, after which a brown suspension had formed. Unfortunately, any product that may have formed appeared to be highly insoluble in all solvents tested, thus isolation and characterisation proved prohibitively difficult.

Bis-azide-appended isophthalamide compound, 74



Based on a literature procedure.[39] *t*-Butyl-3,5-dicarboxylic acid (0.10 g, 0.43 mmol) was suspended in thionyl chloride (2 mL) with a catalytic drop of DMF, and heated at reflux (79 °C) for 16 h, after which the solid had dissolved. Excess thionyl chloride was cautiously and thoroughly removed *in vacuo*, and the bis-acid chloride product used immediately, assuming quantitative yield of formation. The solid was dissolved in dry CH_2Cl_2 (5 mL) and added dropwise to a solution of the mono-reduced precursor **72** (0.20 g, 0.90 mmol) and dry triethylamine (0.25 mL) in dry CH_2Cl_2 (5 mL) at 0 °C. The reaction mixture was stirred for 2 h at RT under a N_2 atmosphere, then subsequently washed with aqueous citric acid (10% w/w, 4 × 12 mL). The organic layer was dried ($MgSO_4$), and the solvent removed *in vacuo* to give the product **74** as an off-white solid (0.24 g, 89%); **^{1}H NMR** (300 MHz, $CDCl_3$) δ ppm 7.96 (s, 2H, 2 × H_b), 7.93 (t, ^3J = 5.30 Hz, 1H, 1 × H_c), 6.87 (s, 8H, 4 × H_g, 4 × H_h), 6.67 (br. s., 2H, 2 × H_d), 4.06–4.16 (m, 8H, 4 × H_e, 4 × H_j), 3.87 (quin, ^3J = 5.30 Hz, 4H, 4 × H_f), 3.58 (t, ^3J = 4.99 Hz, 4H, 4 × H_i), 1.37 (s, 9H, 9 × H_a).

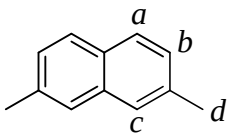
Bifunctional carbazole/isophthalamide macrocycle, 75



Bis-azide-appended precursor **74** (55 mg, 0.087 mmol), diethynylcarbazole **63** (29 mg, 0.087 mmol) and bis-amide pyridinium chloride template **32a**·Cl (33 mg, 0.087 mmol) were dissolved in dry CH_2Cl_2 (75 mL). $[Cu(CH_3CN)_4](PF_6)$ (36 mg, 0.096 mmol), TBTA (4.6 mg, 0.0087 mmol) and DIPEA (56 mg, 0.060 mL, 0.22 mmol) were added and the reaction stirred at RT for 7 d. The solvent was then removed *in vacuo*, and the residue dissolved in $CHCl_3$ (30 mL) and washed with $HCl_{(aq.)}$ (10%, 2 × 20 mL), $NaHCO_{3(sat.\ aq.)}$ (2 × 20 mL), $KCN_{(aq.)}$ (0.04 M, 2 × 20 mL) and H_2O (25 mL), then dried ($MgSO_4$) and the solvent removed *in vacuo*. The residue was then purified by preparative silica TLC plate (9% MeOH/CH_2Cl_2) to give the product **75** as a brown solid (1.5 mg, 2%); **^{1}H NMR** (300 MHz, $CDCl_3$) δ ppm 11.64 (s, 1H, 1 × H_k), 8.17 (s, 2H, 2 × H_j), 8.12 (d, ^4J = 1.76 Hz, 2H, 2 × H_l), 7.97 (s, 2H, 2 × H_b), 7.86 (s, 1H, 1 × H_c), 7.75 (d, ^4J = 1.76 Hz, 2H, 2 × H_m), 6.71 (s, 8H, 4 × H_f, 4 × H_g), 4.83 (t, ^3J = 4.10 Hz, 4H, 4 × H_i), 4.39 (t, ^3J = 4.70 Hz, 4H, 4 × H_h), 4.01 (br. s., 4H, 4 × H_d), 3.81 (br. s., 4H, 4 × H_e), 1.51 (s, 18H, 18 × H_n), 1.32 (s, 9H, 9 × H_a); **^{13}C NMR** (126 MHz, $CDCl_3$) δ ppm 167.36, 153.12, 152.63, 152.38, 141.87, 135.74, 134.52, 132.13, 128.79, 127.62, 123.93, 120.28, 116.44, 115.76, 115.29, 112.70, 77.20, 67.31, 67.20, 50.13, 39.68, 38.71, 35.05, 34.75, 32.11, 31.14; **HRMS (ESI+)** *m/z*: 958.4959 ($[M + H]^+$, calc. for $[C_{56}H_{64}O_6N_9]^+$ = 958.4974).

6.5 *Synthesis of Compounds from Chapter 3*

2,7-Dimethylnaphthalene, 77

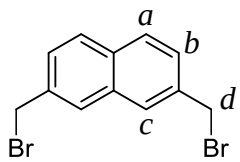


Based on a literature procedure.[40] 3-Methylbenzyl chloride (10.8 g, 10.15 mL, 77 mmol) was

added dropwise to a mixture of magnesium turnings (2.32 g, 95.6 mmol) in dry THF (50 mL), stirring under N_2 at 0 °C. Acetyl acetaldehyde dimethyl acetal (10.4 g, 10.4 mL, 79 mmol) in dry THF (30 mL) was then added dropwise, and the solution heated under reflux for 30 min, after which time the reaction mixture colour becomes burnt orange. The mixture was stirred at RT for a further 12 h. Water (4 mL) was added to quench the reaction, and the THF removed *in vacuo*. Et_2O (100 mL) was added to the concentrated residue, then the mixture was poured onto ice cold saturated NH_4Cl (160 mL), and left to settle for 12 h. The ether layer was separated, washed with water (3 × 20 mL), dried ($MgSO_4$) and the solvent removed *in vacuo* to give benzyl hydroxyacetal **76** as a red oil (11.6 g, 64%).

To synthesise 2,7-dimethylnaphthalene **77**, the intermediate benzyl hydroxyacetal **76** (11.6 g) was heated at 100 °C in glacial acetic acid (50 mL) and hydrobromic acid (48%, 40 mL) for 1 h. The reaction mixture was neutralised to ~pH 7 with $NaOH_{(aq.)}$ (1 M, ~50 mL), then the product was extracted with hexane (3 × 60 mL). The hexane extracts were washed with H_2O (3 × 50 mL), dried ($MgSO_4$) then flushed through a silica pad, washing with hexane (3 × 20 mL). The filtrate solvent was removed *in vacuo*, then placed under high vacuum to remove xylene impurity, leaving the product **77** as a white crystalline powder (5.23 g, 69%); **^{1}H NMR** (300 MHz, $CDCl_3$) δ ppm 7.71 (d, ^3J = 8.21 Hz, 2H, 2 × H_a), 7.53 (s, 2H, 2 × H_c), 7.25 (dd, ^3J = 7.63 Hz, ^4J = 1.76 Hz, 2H, 2 × H_b), 2.51 (s, 6H, 6 × H_d).

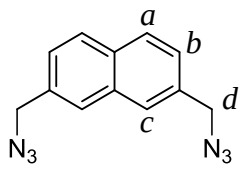
2,7-bis(bromomethyl)naphthalene, 78



Based on a literature procedure.[41] 2,7-dimethylnaphthalene **77** (1.8 g, 11.5 mmol) was dissolved in CCl_4 (90 mL). AIBN (0.58 g) was added to the solution as a radical initiator, then *N*-bromosuccinimide (4.0 g, 22.5 mmol) was added portionwise over 30 min, then the solution was heated at reflux for 12 h. The reaction was allowed to cool to RT, then $CHCl_3$ (50 mL) was added and the mixture filtered through a Celite® pad, flushing with $CHCl_3$ (3 × 20 mL). The solvent was removed and the residue dried thoroughly *in vacuo*, then recrystallised from a minimum volume of hot ethanol. The recrystallisation solution was cooled in the freezer, then the solid was filtered off and washed with ice-cold ethanol (5 mL),

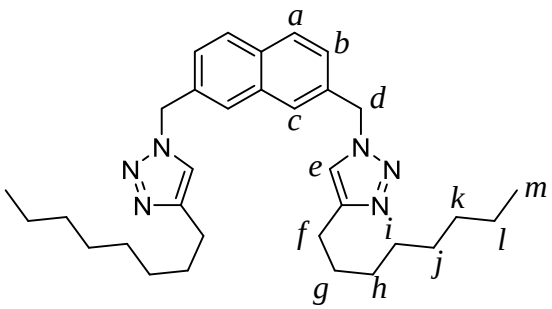
giving the product **78** as an off-white powder (1.89 g, 52%); **^{1}H NMR** (300 MHz, $CDCl_3$) δ ppm 7.83 (d, ^3J = 8.80 Hz, 2H, 2 × H_a), 7.82 (s, 2H, 2 × H_c), 7.53 (dd, ^3J = 8.51 Hz, ^4J = 2.05 Hz, 2H, 2 × H_b), 4.67 (s, 4H, 4 × H_d).

2,7-Bis(azidomethyl)naphthalene, 79



2,7-Bis(bromomethyl)naphthalene **78** (0.5 g, 1.6 mmol) was dissolved in DMSO (10 mL). NaN_3 (0.41 g, 6.4 mmol) was added and the solution stirred at RT under N_2 for 3 d. Water (60 mL) was then added to the mixture, and the product extracted with Et_2O (3 × 20 mL). The extracts were washed with water (3 × 20 mL), and brine (20 mL), dried ($MgSO_4$) and the solvent removed *in vacuo* to give the product **79** as an off-white powder (0.33 g, 87%); **^{1}H NMR** (300 MHz, $CDCl_3$) δ ppm 7.89 (d, ^3J = 8.21 Hz, 2H, 2 × H_a), 7.79 (s, 2H, 2 × H_c), 7.46 (dd, ^3J = 8.21, ^4J = 1.76 Hz, 2H, 2 × H_b), 4.53 (s, 4H, 4 × H_d); **^{13}C NMR** (76 MHz, $CDCl_3$) δ ppm 133.54, 133.10, 132.70, 128.63, 127.15, 126.34, 54.92.

Alkyl-substituted bis-triazole naphthalene, 80

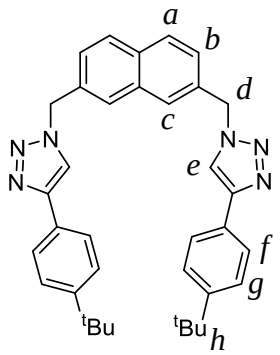


Method 1: 2,7-Bis(azidomethyl)naphthalene **79** (50 mg, 0.21 mmol), 1-decyne (61 mg, 0.08 mL, 0.44 mmol), $[Cu(CH_3CN)_4](PF_6)$ (39 mg, 0.11 mmol), TBTA (56 mg, 0.11 mmol) then DIPEA (81 mg, 0.11 mL, 0.63 mmol) were dissolved in dry CH_2Cl_2 (100 mL). The yellow solution was stirred at RT for 2 d under N_2. The solvent was then removed *in vacuo*, and the residue purified on a silica TLC plate (3% MeOH/CH_2Cl_2), giving the product **80** as a white powder (39 mg, 36%).

Method 2: 2,7-Bis(azidomethyl)naphthalene **79** (100 mg, 0.42 mmol) was dissolved in MeOH

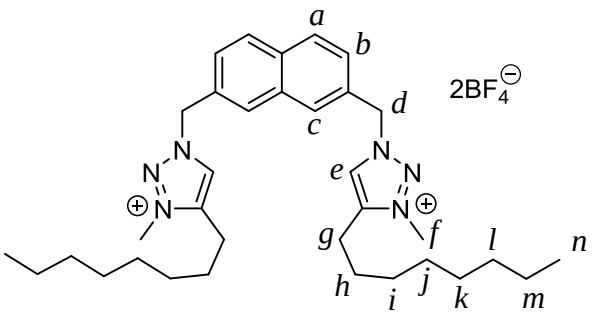
(15 mL). Sodium ascorbate (34 mg, 0.18 mmol), $CuSO_4$ (32 mg, 0.13 mmol) and 1-decyne (120 mg, 0.16 mL, 0.88 mmol) were added, and the solution stirred at RT for 3 d, after which time a precipitate had formed. The precipitate was filtered off and washed with MeOH (2 × 10 mL), giving the pure product **80** as a white powder (0.155 g, 72%); **^{1}H NMR** (300 MHz, $CDCl_3$) δ ppm 7.84 (d, ^3J = 8.80 Hz, 2H, 2 × H_a), 7.68 (s, 2H, 2 × H_c), 7.37 (d, ^3J = 8.21 Hz, 2H, 2 × H_b), 7.25 (br. s., 2H, 2 × H_e), 5.66 (s, 4H, 4 × H_d), 2.69 (br. s., 4H, 4 × H_f), 1.63 (br. s., 4H, 4 × H_g), 1.17–1.39 (m, 20H, 20 × $H_{h–l}$), 0.87 (t, ^3J = 6.80 Hz, 6H, 6 × H_m); **^{13}C NMR** (76 MHz, $CDCl_3$) δ ppm 133.22, 133.02, 132.78, 128.89, 127.15, 126.05, 54.11, 31.79, 29.28, 29.25, 29.17, 22.61, 14.07; **HRMS (ESI+)** *m/z*: 515.3840 ($[M+H]^+$, calc. for $[C_{32}H_{47}N_6]^+$ = 515.3857).

Aryl-substituted bis-triazole naphthalene, 81



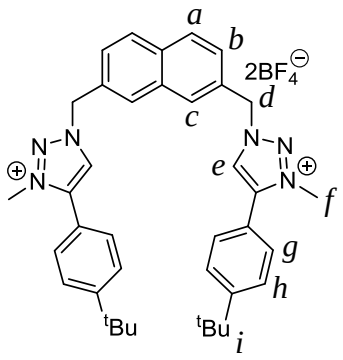
2,7-Bis(azidomethyl)naphthalene **79** (0.1 g, 0.42 mmol) was dissolved in MeOH (16 mL). Sodium ascorbate (34 mg, 0.17 mmol), $CuSO_4 \cdot 5H_2O$ (32 mg, 0.13 mmol) and 1-*tert*-butyl-4-ethynylbenzene (140 mg, 0.16 mL, 0.88 mmol) were added, and the solution stirred under N_2 at RT for 3 d, after which a precipitate had formed. The solid was filtered off, washed with MeOH (2 × 2 mL) and air-dried, giving the product **81** as a yellow powder (180 mg, 77%); **^{1}H NMR** (300 MHz, $CDCl_3$) δ ppm 7.87 (d, ^3J = 8.21 Hz, 2H, 2 × H_a), 7.76–7.70 (m, 6H, 2 × H_c, 4 × H_f), 7.67 (s, 2H, 2 × H_e), 7.46–7.40 (m, 6H, 2 × H_b, 4 × H_g), 5.75 (s, 4H, 4 × H_d), 1.33 (s, 18H, 18 × H_h); **^{13}C NMR** (76 MHz, $CDCl_3$) δ ppm 151.32, 148.33, 133.22, 133.05, 132.85, 129.01, 127.56, 127.10, 126.05, 125.70, 125.38, 119.32, 54.14, 31.23; **HRMS (ESI+)** *m/z*: 555.3209 ($[M+H]^+$, calc. for $[C_{36}H_{39}N_6]^+$ = 555.3231).

Alkyl-substituted bis-triazolium naphthalene receptor, 82·2BF$_4$



The neutral bis-triazole naphthalene precursor **80** (100 mg, 0.19 mmol) was dissolved in dry CH_2Cl_2 (10 mL). $Me_3O{\cdot}BF_4$ (58 mg, 0.39 mmol) was added and the solution stirred at RT overnight under N_2. The reaction was then quenched with a drop of MeOH, and stirred for 5 min. The solvent was removed *in vacuo* and the residue purified by preparative silica TLC plate (8% MeOH/CH_2Cl_2) to give the product **82**·2BF$_4$ as an off-white solid (48 mg, 36%); **^{1}H NMR** (300 MHz, $CDCl_3$) δ ppm 8.28 (s, 2H, 2 × H_e), 7.69 (s, 2H, 2 × H_c), 7.67 (d, ^3J = 9.39 Hz, 2H, 2 × H_a), 7.40 (dd, ^3J = 8.21 Hz, ^4J = 1.17 Hz, 2H, 2 × H_b), 5.70 (s, 4H, 4 × H_d), 4.12 (s, 6H, 6 × H_f), 2.72 (t, ^3J = 8.20 Hz, 4H, 4 × H_g), 1.66 (quin, ^3J = 7.60 Hz, 4H, 4 × H_h), 1.11–1.41 (m, 20H, 2 × $H_{i–m}$), 0.83 (t, ^3J = 6.50 Hz, 6H, 6 × H_n); **^{13}C NMR** (76 MHz, $CDCl_3$) δ ppm 145.28, 132.97, 132.93, 130.31, 128.64, 127.99, 126.32, 56.53, 37.33, 31.64, 29.00, 28.91, 26.53, 23.18, 22.52, 14.01; **HRMS (ESI+)** *m/z*: 272.2112 ([M – 2(BF$_4$)]$^{2+}$, calc. for $[C_{34}H_{52}N_6]^{2+}$ = 272.2121).

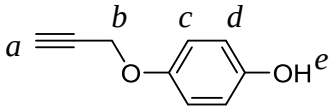
Aryl-substituted bis-triazolium naphthalene receptor, 83·2BF$_4$



The neutral bis-triazole naphthalene precursor **81** (100 mg, 0.13 mmol) was dissolved in dry CH_2Cl_2 (10 mL). $Me_3O{\cdot}BF_4$ (53 mg, 0.36 mmol) was added and the solution stirred at RT overnight under N_2. The reaction was then quenched with a drop of MeOH, and stirred for 5 min. The solvent was removed *in vacuo* and the residue purified by preparative silica TLC

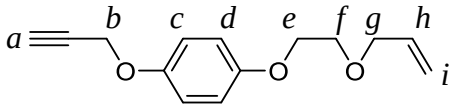
plate (8% MeOH/CH_2Cl_2) to give the product **83**·$2BF_4$ as an off-white solid (25 mg, 25%); **^{1}H NMR** (300 MHz, $CDCl_3$) δ ppm 8.43 (s, 2H, 2 × H_e), 7.80 (s, 2H, 2 × H_c), 7.60 (d, ^3J = 8.21 Hz, 2H, 2 × H_a), 7.43–7.54 (m, 8H, 4 × H_g, 4 × H_h), 7.41 (d, ^3J = 8.80 Hz, 2H, 2 × H_b), 5.73 (s, 4H, 4 × H_d), 4.16 (s, 6H, 6 × H_f), 1.24 (s, 18H, 18 × H_i); **^{13}C NMR** (76 MHz, $CDCl_3$) δ ppm 155.17, 143.73, 133.05, 132.94, 130.09, 129.19, 128.67, 128.41, 128.25, 126.61, 126.49, 119.00, 56.81, 38.40, 34.94, 30.97; **HRMS (ESI+)** *m/z*: 292.1800 ([M – 2(BF_4)]$^{2+}$, calc. for $[C_{38}H_{44}N_6]^{2+}$ = 292.1808).

Propargyl hydroquinone, 84



This compound has been previously reported in the literature.[42] To a degassed solution of NaOH (4.2 g, 105 mmol) and hydroquinone (5.8g, 52.5 mmol) in dioxane and water (1:1, 150 mL) was added dropwise a solution of propargyl bromide (6.23 g, 4.67 mL, 52.5 mmol) in degassed dioxane (25 mL). The resultant mixture was stirred for 2 d, degassing throughout. $HCl_{(aq.)}$ (1 M, 125 mL) was added and the mixture extracted into CH_2Cl_2 (2 × 50 mL). The combined organics were dried ($MgSO_4$), filtered and concentrated to dryness *in vacuo*. The residue was purified by column chromatography (1% MeOH/CH_2Cl_2) to give the desired product **84** (1.9 g, 27%) as a red oil; **^{1}H NMR** (300 MHz, $CDCl_3$) δ ppm 6.88–6.82 (m, 2H, 2 × H_c), 6.71–6.76 (m, 2H, 2 × H_d), 5.73 (s, 1H, 1 × H_e), 4.60 (d, ^4J = 2.35 Hz, 2H, 2 × H_b), 2.49 (t, ^4J = 2.35 Hz, 1H, 1 × H_a); **^{13}C NMR** (76 MHz, $CDCl_3$) δ ppm 151.43, 116.29, 115.92, 75.28, 67.03, 56.62.

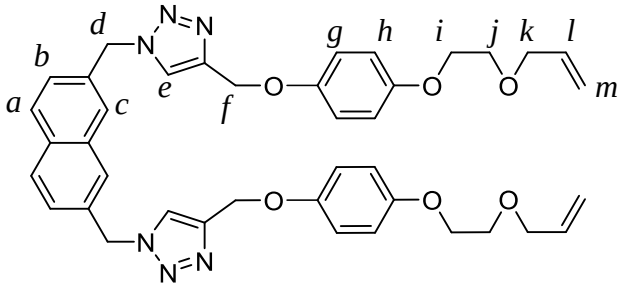
Propargyl-appended vinyl compound, 85



A suspension of propargyl-substituted hydroquinone **84** (0.5 g, 3.4 mmol), mesylate **46** (0.6 g, 3.4 mmol) and K_2CO_3 (4.0 g, 28.9 mmol) in dry CH_3CN (40 mL) was heated at 95 °C for 72 h. The mixture was allowed to cool to RT whereupon it was filtered and concentrated to dryness *in vacuo*. The resultant residue was dissolved in CH_2Cl_2 (10 mL), washed with $HCl_{(aq.)}$ (1 M, 2 × 10 mL), water (2 × 10 mL), $NaOH_{(aq.)}$ (10%, 2 × 10 mL), water (2 × 10 mL)

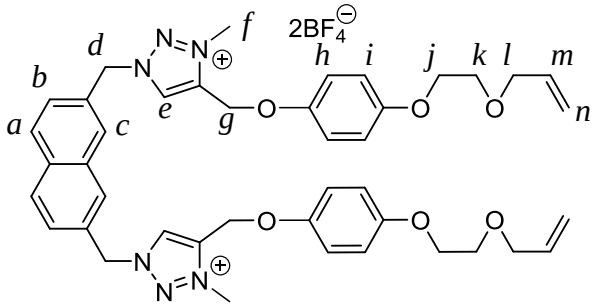
and brine (10 mL), dried ($MgSO_4$), filtered and the solvent removed *in vacuo*. The residue was purified by column chromatography (20% ethyl acetate/hexanes) to afford the desired product **85** (0.33 g, 42%); **^{1}H NMR** (300 MHz, $CDCl_3$) δ ppm 6.83–6.96 (m, 4H, 2 × H_c, 2 × H_d), 5.86–6.03 (m, 1H, 1 × H_h), 5.17–5.36 (m, 2H, 2 × H_i), 4.64 (d, ^4J = 2.35 Hz, 2H, 2 × H_b), 4.07–4.12 (m, 4H, 2 × H_e, 2 × H_g), 3.76–3.81 (m, 2H, 2 × H_f), 2.51 (t, ^4J = 2.64 Hz, 1H, 1 × H_a); **^{13}C NMR** (76 MHz, $CDCl_3$) δ ppm 153.63, 151.78, 134.53, 117.31, 115.98, 115.50, 78.83, 75.26, 72.32, 68.55, 67.97, 56.50; **HRMS (FI+)** *m/z*: 232.1095 ($[M]^+$, calc. for $[C_{14}H_{16}O_3]^+$ = 232.1099).

Vinyl-appended bis-triazole naphthalene, 86



2,7-bis(azidomethyl)naphthalene **79** (54 mg, 0.23 mmol) was dissolved in MeOH (10 mL). Sodium ascorbate (17 mg, 0.09 mmol), $CuSO_4{\cdot}5H_2O$ (16 mg, 0.07 mmol) and vinyl-appended alkyne **85** (102 mg, 0.46 mmol) were added, and the solution stirred under N_2 at RT for 3 d, after which a precipitate had formed. The solid was filtered off, washed with MeOH (2 × 2 mL) and air-dried, giving the product **86** as a yellow powder (130 mg, 83%); **^{1}H NMR** (300 MHz, $CDCl_3$) δ ppm 7.86 (d, ^3J = 8.21 Hz, 2H, 2 × H_a), 7.67 (s, 2H, 2 × H_c), 7.56 (s, 2H, 2 × H_e), 7.40 (dd, ^3J = 8.51, ^4J = 1.47 Hz, 2 H, 2 × H_b), 6.79–6.92 (m, 8 H, 4 × H_g, 4 × H_h), 5.86–6.02 (m, 2 H, 2 × H_l), 5.70 (s, 4H, 4 × H_d), 5.18–5.36 (m, 4H, 4 × H_m), 5.15 (s, 4H, 4 × H_f), 4.03–4.13 (m, 8H, 4 × H_i, 4 × H_k), 3.72–3.81 (m, 4H, 4 × H_j); **^{13}C NMR** (101 MHz, $CDCl_3$) δ ppm 153.41, 152.43, 145.05, 134.54, 133.05, 132.95, 132.90, 129.04, 127.25, 126.13, 122.65, 117.29, 115.78, 115.63, 72.33, 68.57, 68.05, 62.74, 54.19; **HRMS (ESI+)** *m/z*: 703.3229 ($[M + H]^+$, calc. for $[C_{40}H_{43}N_6O_6]^+$ = 703.3239).

Vinyl-appended bis-triazolium naphthalene, 87

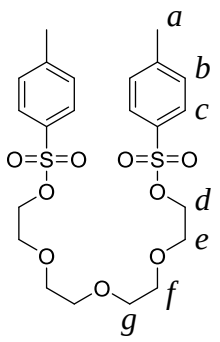


The neutral bis-triazole naphthalene precursor **86** (150 mg, 0.21 mmol) was dissolved in dry CH_2Cl_2 (20 mL). $Me_3O{\cdot}BF_4$ (79 mg, 0.53 mmol) was added and the solution stirred at RT overnight under N_2. The reaction was then quenched with a drop of MeOH, and stirred for 5 min. The solid was removed by filtration, washed with CH_2Cl_2 (2 × 10 mL), then the filtrate removed *in vacuo*, affording the product **87** as an brown oil (150 mg, 81%); **^{1}H NMR** (300 MHz, d_6-acetone) δ ppm 8.90 (s, 2H, 2 × H_e), 7.98 (s, 2H, 2 × H_c), 7.94 (d, ^3J = 8.21 Hz, 2H, 2 × H_a), 7.60 (dd, ^3J = 8.80, ^4J = 1.76 Hz, 2H, 2 × H_b), 6.75–6.95 (m, 8H, 4 × H_h, 4 × H_i), 6.09 (s, 4H, 4 × H_d), 5.72–5.88 (m, 2H, 2 × H_m), 5.39 (s, 4H, 4 × H_g), 4.98–5.22 (m, 4H, 4 × H_n), 4.41 (s, 6H, 6 × H_f), 3.90–4.00 (m, 8H, 4 × H_j, 4 × H_l), 3.67–3.60 (m, 4H, 4 × H_k).

Attempted synthesis of ring-closed bis-triazolium naphthalene macrocycle, 88

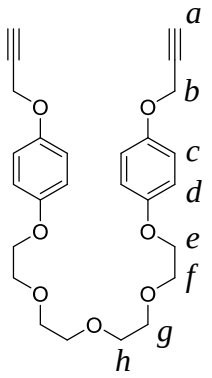
Bis-vinyl precursor **87** (30 mg, 0.033 mmol) and TBA·Cl template (4.6 mg, 0.017 mmol) were dissolved in dry CH_2Cl_2 (40 mL), and stirred at RT for 1 hr. Grubbs' II catalyst was added, and the solution stirred for 2 d. The solvent was then removed *in vacuo*, and the crude was analysed by ^{1}H NMR, which showed no evidence that the ring-closing metathesis reaction had taken place, as only the bis-vinyl precursor molecule **87** was observed. A repeated synthesis using Grubbs' I catalyst gave the same result.

Tosylated polyether, 89



Based on a literature procedure.[43] Tetraethylene glycol (4.46 g, 4.0 mL, 45.5 mmol) was dissolved in CH_2Cl_2 (100 mL), then tosyl chloride (17.5 g, 91.6 mmol) was added and the solution cooled to 0 °C. Powdered KOH (33.6 g, 600 mmol) was added portionwise, maintaining a temperature of 0 °C, and the reaction was stirred for 3 h at this temperature. CH_2Cl_2 (100 mL) was added, the mixture poured onto ice water (300 mL), and the organic layer separated. The aqueous layer was extracted with CH_2Cl_2 (3 × 100 mL), then the combined organic extracts were washed with H_2O (200 mL), dried ($MgSO_4$) and the solvent removed *in vacuo*. Impurities were removed from the residue by triturating with diethyl ether (2 × 50 mL), leaving the product **89** as a colourless oil (11.7 g, 63%); **^{1}H NMR** (300 MHz, $CDCl_3$) δ ppm 7.73–7.84 (m, 4H, 4 × H_c), 7.34 (d, ^3J = 8.21 Hz, 4H, 4 × H_b), 4.12–4.18 (m, 4H, 4 × H_d), 3.65–3.71 (m, 4H, 4 × H_e), 3.52–3.59 (m, 8H, 4 × H_f, 4 × H_f), 2.45 (s, 6H, 6 × H_a).

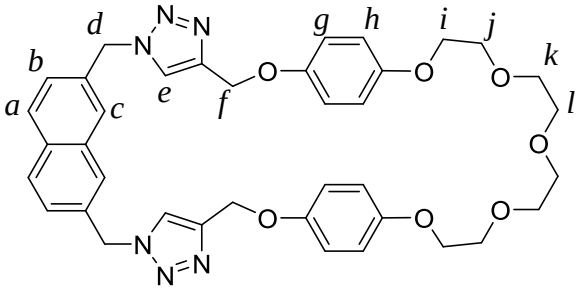
Bis-propargyl-terminated polyether, 90



A suspension of propargyl-substituted hydroquinone **84** (0.31 g, 2.1 mmol), tosylate **89** (0.37 g, 0.76 mmol) and K_2CO_3 (2.5 g, 18.1 mmol) in dry CH_3CN (40 mL) was heated at reflux for 3 d. The mixture was allowed to cool to RT whereupon it was filtered and concentrated to dryness *in vacuo*. The resultant residue was dissolved in CH_2Cl_2 (10 mL),

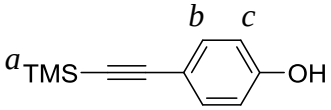
washed with $HCl_{(aq.)}$ (1 M, 2 × 10 mL) and H_2O (2 × 10 mL), dried ($MgSO_4$), filtered and the solvent removed *in vacuo*. The residue was purified by column chromatography (1.5% MeOH/CH_2Cl_2) to afford the desired product **90** as a brown oil (0.28 g, 69%); **^{1}H NMR** (300 MHz, $CDCl_3$) δ ppm 6.79–6.92 (m, 8H, 4 × H_c, 4 × H_d), 4.62 (d, ^3J = 2.35 Hz, 4H, 4 × H_b), 4.02–4.09 (m, 4H, 4 × H_e), 3.78–3.86 (m, 4H, 4 × H_f), 3.64–3.75 (m, 8H, 4 × H_g, 4 × H_h), 2.49 (t, ^3J = 2.35 Hz, 2H, 4 × H_a); **^{13}C NMR** (101 MHz, $CDCl_3$) δ ppm 153.65 129.78, 127.94, 116.03, 115.52, 78.86, 75.28, 70.78, 69.80, 68.00, 56.55; **HRMS (FI+)** *m/z*: 454.1986 ($[M]^+$, calc. for $[C_{26}H_{30}O_7]^+$ = 454.1992).

Hydroquinone-containing naphthalene macrocycle, 91



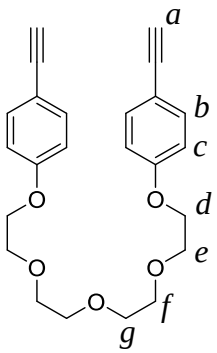
Bis-alkyne polyether **90** (76 mg, 0.17 mmol), bis(azidomethyl)naphthalene **79** (39 mg, 0.16 mmol), bis-amide pyridinium thread template **32a**·Cl (67 mg, 0.17 mmol), $[Cu(CH_3CN)_4](PF_6)$ (13 mg, 0.035 mmol) and TBTA (19 mg, 0.036 mmol) were dissolved in CH_2Cl_2 (125 mL) and stirred at RT for 1 h. DIPEA (0.018 mg, 0.025 mL, 0.14 mmol) was then added, and the solution stirred at RT for 4 d. The solvent was removed *in vacuo*, the residue triturated with MeOH (2 × 10 mL), then the solid was purified by column chromatography (4% MeOH/CH_2Cl_2), affording the product **91** as an off-white solid (27 mg, 23%); **^{1}H NMR** (300 MHz, $CDCl_3$) δ ppm 7.87 (d, ^3J = 8.80 Hz, 2H, 2 × H_a), 7.63 (s, 2H, 2 × H_c), 7.48 (s, 2H, 2 × H_e), 7.45–7.50 (m, 2H, 2 × H_b), 6.76–6.85 (m, 8H, 4 × H_g, 4 × H_h), 5.71 (s, 4H, 4 × H_d), 5.11 (s, 4H, 4 × H_f), 4.03 (dd, ^3J = 5.87, 4.11 Hz, 4H, 4 × H_i), 3.77–3.84 (m, 4H, 4 × H_j), 3.63–3.72 (m, 8H, 4 × H_k, 4 × H_l); **^{13}C NMR** (126 MHz, $CDCl_3$) δ ppm 153.33, 152.37, 145.17, 133.13, 132.98, 132.89, 129.09, 127.54, 126.59, 122.39, 115.75, 115.59, 115.56, 70.73, 69.68, 68.07, 62.84, 54.27; **HRMS (FI+)** *m/z*: 692.2881 ($[M]^+$, calc. for $[C_{38}H_{40}N_6O_7]^+$ = 692.2958).

4-TMS-ethynylphenol, 92



Based on a literature procedure.[44] To a degassed solution of 4-iodophenol (1.0 g, 5.8 mmol) and TMS-acetylene (0.68 g, 1.0 mL, 6.9 mmol) in dry triethylamine (15 mL) were added copper(I) iodide (26 mg, 0.14 mmol) and $Pd(PPh_3)_2Cl_2$ (96 mg, 0.14 mmol). The mixture was stirred for 3 h at 80 °C under N_2. The reaction mixture was allowed to cool to RT, whereupon the solids were filtered off and washed with diethyl ether, then the solvent was removed *in vacuo*. The residue was purified by column chromatography (1:1 EtOAc/pet. ether) to give the desired product **92** as a deep red oil (0.74 g, 90%); **^{1}H NMR** (300 MHz, $CDCl_3$) δ ppm 7.34–7.39 (m, 2H, 2 × H_b), 6.73–6.79 (m, 2H, 2 × H_c), 0.24 (s, 9H, 9 × H_a).

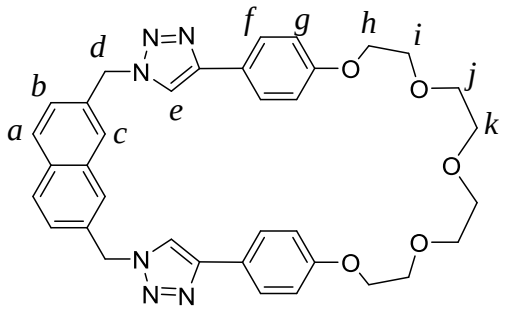
Bis-ethynylbenzene-terminated polyether, 93



A suspension of 4-TMS-ethynylphenol **92** (0.20 g, 1.4 mmol), tosylate **89** (0.28 g, 0.7 mmol) and K_2CO_3 (1.65 g, 11.9 mmol) in dry CH_3CN (20 mL) was heated at reflux for 3 d. The mixture was allowed to cool to RT whereupon it was filtered and concentrated to dryness *in vacuo*. The resultant residue was dissolved in $CHCl_3$ (10 mL), filtered and the solvent removed *in vacuo* to give the crude TMS-protected product as a yellow oil. The crude compound was deprotected by reacting with KOH (0.4 g, 7.1 mmol) in a solvent mixture of MeOH (30 mL) and H_2O (1 mL) for 16 h. After filtering off the solid and washing with MeOH (10 mL), the solvent was removed *in vacuo*, and the crude extracted with CH_2Cl_2 (3 × 10 mL) from H_2O (10 mL). The organic extracts were combined and the solvent once again removed under reduced pressure. The crude was purified by column chromatography (1% MeOH/CH_2Cl_2) to afford the desired deprotected product **93** as a yellow oil, which solidified on standing (0.13 g, 46%); **^{1}H NMR** (300 MHz, $CDCl_3$) δ ppm 7.37–7.45 (m, 4H,

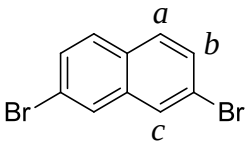
4 × H_b), 6.82–6.88 (m, 4H, 4 × H_c), 4.10–4.14 (m, 4H, 4 × H_d), 3.83–3.88 (m, 4H, 4 × H_e), 3.66–3.75 (m, 8H, 4 × H_f, 4 × H_g), 3.00 (s, 2H, 2 × H_a); **^{13}C NMR** (126 MHz, $CDCl_3$) δ ppm 159.13, 133.54, 114.57, 114.32, 83.60, 75.81, 70.84, 70.66, 69.66, 67.45; **HRMS (FI+)** *m/z*: 394.1783 ($[M]^+$, calc. for $[C_{24}H_{26}O_5]^+$ = 394.1780).

Phenol-containing naphthalene macrocycle, 94



Bis-alkyne polyether **93** (127 mg, 0.32 mmol), bis(azidomethyl)naphthalene **79** (77 mg, 0.32 mmol), bis-amide pyridinium thread template **32a**·Cl (123 mg, 0.32 mmol), $[Cu(CH_3CN)_4](PF_6)$ (25 mg, 0.067 mmol), TBTA (35 mg, 0.066 mmol) then DIPEA (0.053 mg, 0.074 mL, 0.41 mmol) were dissolved in CH_2Cl_2 (300 mL), and the solution stirred at RT for 4 d. The solvent was removed *in vacuo*, the residue triturated with acetone (2 × 10 mL), then the solid was purified by column chromatography (6% MeOH/CH_2Cl_2), affording the product **94** as an off-white solid (39 mg, 19%); **^{1}H NMR** (300 MHz, $CDCl_3$) δ ppm 7.91 (d, ^3J = 8.80 Hz, 2H, 2 × H_a), 7.61–7.67 (m, 4H, 4 × H_f), 7.57 (dd, ^3J = 8.80, ^4J = 1.76 Hz, 2H, 2 × H_b), 7.50 (s, 2H, 2 × H_e), 6.85–6.93 (m, 4H, 4 × H_g), 5.72 (s, 4H, 4 × H_d), 4.13 (dd, ^3J = 5.87, 4.11 Hz, 4H, 4 × H_h), 3.84 (dd, ^3J = 5.87, 4.11 Hz, 4H, 4 × H_i), 3.64–3.73 (m, 8H, 4 × H_j, 4 × H_k); **^{13}C NMR** (126 MHz, $CDCl_3$) δ ppm 158.76, 148.25, 133.34, 133.31, 132.98, 129.00, 127.41, 126.93, 126.87, 123.18, 118.77, 114.91, 70.79, 70.62, 69.45, 67.46, 54.21; **HRMS (FI+)** *m/z*: 632.2747 ($[M]^+$, calc. for $[C_{36}H_{36}N_6O_5]^+$ = 632.2747).

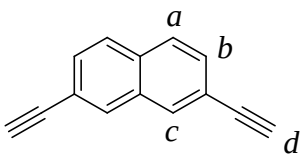
2,7-Dibromonaphthalene, 95



This method is based on a literature procedure.[45,46] Triphenylphosphine (14.41 g, 54.9 mmol)

was added to dry CH_3CN (20 mL) in a 250 mL 3-neck flask. The suspension was cooled to 0 °C, then bromine (2.8 mL, 54.9 mmol) was added dropwise over 1 h, such that the temperature remained < 5 °C, forming a very thick white slurry. 2,7-Dihydroxynaphthalene (4.00 g, 25 mmol) dissolved in CH_3CN (40 mL) was added in one portion, then the mixture was heated to 75 °C until the precipitate dissolves into solution. Once the solution was homogeneous, the CH_3CN was distilled off at atmospheric pressure, leaving a red oil. The temperature was then increased to 280−300 °C using a heating mantle, monitoring the temperature carefully, and the evolved HBr gas was trapped in a saturated $NaOH_{(aq.)}$ solution. This reaction temperature was maintained for 2 h. The reaction was cooled slowly to RT, and when the solution was at ~140 °C, the dark oil was poured into ethanol (40 mL) and allowed to sit at 4 °C overnight. The crude product was isolated by filtration, then purified by column chromatography (5% CH_2Cl_2/pet. ether), giving the product **95** as a colourless crystalline solid (4.95 g, 69%); **^{1}H NMR** (300 MHz, $CDCl_3$) δ ppm 7.92 (d, ^4J = 2.35 Hz, 2H, 2 × H_c), 7.69 (d, ^3J = 8.80 Hz, 2H, 2 × H_a), 7.57 (dd, ^3J = 8.80, ^4J = 1.76 Hz, 2H, 2 × H_b); **HRMS (FI+)** *m/z*: 285.8803 ($[M]^+$, calc. for $[C_{10}H_6Br_2]^+$ = 285.8816).

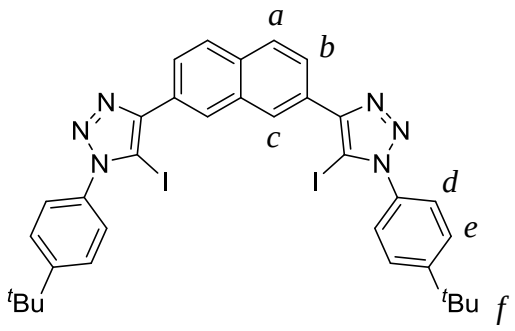
2,7-diethynylnaphthalene, 96



Based on a literature procedure.[47] A deaerated solution of 2,7-dibromonaphthalene **95** (0.345 g, 1.27 mmol) and trimethylsilyl-acetylene (0.31 g, 0.45 mL, 3.20 mmol) in dry triethylamine (10 mL) was treated with $Pd(PPh_3)_2Cl_2$ (30 mg, 0.43 mmol) and CuI (30 mg, 0.16 mmol). The mixture was heated at 85 °C in a closed vial for 3 days. The reaction was then cooled to RT, the solvent removed *in vacuo* and the residue suspended in CH_2Cl_2, which was filtered through a Celite® pad, and the pad rinsed with CH_2Cl_2 (2 × 20 mL). The filtrate solvent was removed *in vacuo*, and the residue dissolved in CH_3CN (20 mL) and water (1 mL), then KOH (0.36 g, 7.62 mmol) was added to deprotect the ethynyl groups. The solution was stirred at RT for 1 h, then the solvent removed *in vacuo*, and the residue partitioned between CH_2Cl_2 (25 mL) and $NH_4Cl_{(aq.)}$ (25 mL). The aqueous layer was extracted with CH_2Cl_2 (2 × 20 mL), and the combined organic layers were combined and dried over $MgSO_4$. The solvent was removed, and the residue purified by column chromatography

(5% CH_2Cl_2/pet. ether) to give the product **96** as an off-white solid (0.158 g, 71%); **^{1}H NMR** (300 MHz, $CDCl_3$) δ ppm 7.98 (s, 2H, 2 × H_c), 7.77 (d, ^3J = 8.80 Hz, 2H, 2 × H_c), 7.55 (dd, ^3J = 8.50, ^4J = 1.47 Hz, 2H, 2 × H_b), 3.18 (s, 2H, 2 × H_d); **^{13}C NMR** (76 MHz, $CDCl_3$) δ ppm 132.52, 132.23, 131.98, 129.56, 127.88, 120.25, 83.54, 78.01; **HRMS (FI+)** *m/z*: 176.0620 ($[M]^+$, calc. for $[C_{14}H_8]^+$ = 176.0626).

Bis-iodotriazole naphthalene, 97

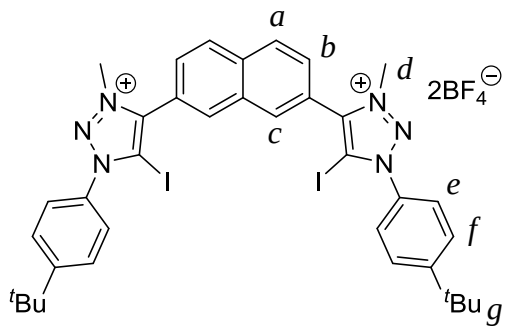


Method 1: This preparation involved adding the reagents directly to the reaction mixture for 2,7-bis(iodoethynyl)naphthalene **100** without purification the precursor, assuming quantitative yield. Firstly, CuI (190 mg, 1.0 mmol), triethylamine (105 mg, 0.14 mL, 1.0 mmol) and TBTA (0.1 g, 0.19 mmol) were stirred in dry THF (1 mL) for 20 min to dissolve. At the same time as the potassium *tert*-butoxide was added for the reaction to form iodoethynyl precursor **100**, azide **8** (193 mg, 1.10 mmol) and the CuI solution were added to the reaction mixture, and stirred at RT in the dark for 36 h. The reaction was then quenched with $NH_4OH_{(aq.)}$ (10%, 4 mL), and the THF removed *in vacuo*. H_2O (20 mL) was added, and the crude extracted with CH_2Cl_2 (3 × 40 mL). The organics were combined and the solvent removed *in vacuo*, then redissolved in 5% MeOH/CH_2Cl_2 (10 mL) and flushed through a silica plug, which was further rinsed with 5% MeOH/CH_2Cl_2 (3 × 20 mL). The reaction was then purified by preparative TLC plate (1% MeOH/CH_2Cl_2), giving the product **97** (53 mg, 14% over two steps).

Method 2: Azide **8** (79 mg, 0.45 mmol) was dissolved in CH_3CN (2 mL). Sodium iodide (0.24 g, 1.6 mmol) and $Cu(ClO_4)_2 \cdot 6H_2O$ (0.30 g, 0.80 mmol) were added to the reaction, which was covered in aluminium foil and stirred at RT for 3–5 min. TBTA (21 mg, 0.04 mmol) was added, then DBU (61 mg, 0.40 mmol) dissolved in THF (1 mL) was also added. The diethynyl naphthalene **96** (35 mg, 0.20 mmol) was added to the reaction last, then

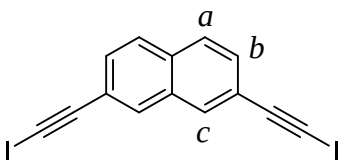
the mixture was stirred in the dark at RT overnight. The reaction was then diluted with CH_2Cl_2 (50 mL), then washed with $NH_4OH_{(aq.)}$ (25%, 25 mL), then brine (2 × 25 mL). The organic layer was separated, dried ($MgSO_4$) and the solvent removed *in vacuo*. The residue was then purified by column chromatography (1% MeOH/CH_2Cl_2) to give the product **97** as a white powder (67 mg, 43%); **^{1}H NMR** (300 MHz, $CDCl_3$) δ ppm 8.64 (s, 2H, 2 × H_c), 8.21 (dd, ^3J = 8.21, ^4J = 1.76 Hz, 2H, 2 × H_b), 8.02 (d, ^3J = 8.21 Hz, 2H, 2 × H_a), 7.61 (d, ^3J = 8.80 Hz, 4H, 4 × H_d), 7.52 (d, ^3J = 8.80 Hz, 4H, 4 × H_e), 1.39 (s, 18H, 18 × H_f); **^{13}C NMR** (76 MHz, $CDCl_3$) δ ppm 153.55, 149.89, 134.32, 132.93, 132.90, 128.14, 127.27, 126.26, 125.99, 125.96, 78.33, 34.93, 31.23; **HRMS (ESI+)** *m/z*: 779.0822 ($[M + H]^+$, calc. for $[C_{34}H_{33}I_2N_6]^+$ = 779.0851).

Bis-iodotriazolium naphthalene, 98·2BF$_4$



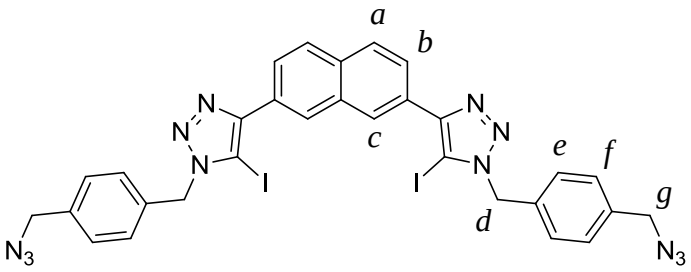
The neutral naphthalene bis-iodotriazole precursor **96** (67.0 mg, 0.0850 mmol) was dissolved in dry CH_2Cl_2 (10 mL). $Me_3O{\cdot}BF_4$ (38 mg, 0.257 mmol) was added and the solution stirred at RT overnight under N_2. The reaction was then quenched with a drop of MeOH, and stirred for 5 min. The solvent was removed *in vacuo* and the residue purified by column (5–7% MeOH/CH_2Cl_2) to give the product **98**·2BF_4 as an off-white solid (28 mg, 34%); **^{1}H NMR** (500 MHz, d_6-acetone) δ ppm 8.71 (s, 2H, 2 × H_c), 8.48 (d, ^3J = 8.39 Hz, 2H, 2 × H_a), 8.08 (dd, ^3J = 8.54, ^4J = 1.37 Hz, 2H, 2 × H_b), 7.86–7.90 (m, 4H, 4 × H_e), 7.82–7.85 (m, 4H, 4 × H_f), 4.59 (s, 6H, 6 × H_d), 1.44 (s, 18H, 18 × H_g); **^{13}C NMR** (126 MHz, d_6-acetone) δ ppm 157.02, 147.69, 136.29, 134.31, 133.72, 133.35, 130.76, 129.40, 128.14, 127.02, 123.25, 40.19, 35.97, 31.46; **HRMS (ESI+)** *m/z*: 404.0601 ($[M - 2(BF_4)]^{2+}$, calc. for $[C_{36}H_{38}I_2N_6]^{2+}$ = 404.0618).

2,7-Bis(iodoethynyl)naphthalene, 100



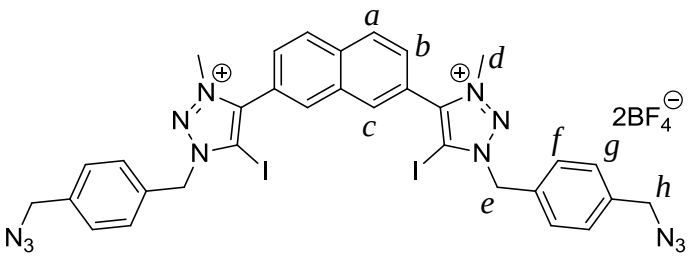
Based on a recently-reported one-pot procedure.[48] To a flame-dried 25 mL RBF fitted with a septum and stirrer bar was added solid NaHMDS (0.55 g, 3.0 mmol). The flask was covered in aluminium foil to exclude light, and the solid dissolved in dry THF (3.2 mL) and dry Et_2O (1.0 mL). The flask was cooled to −78 °C using a dry ice/acetone bath, and the solution stirred for 2 min. To a separate 10 mL RBF (also flame-dried, fitted with a septum and stirrer bar) was added iodoform (0.59 g, 1.5 mmol) and 2,7-bis(bromomethyl)naphthalene **78** (0.16 g, 0.5 mmol). These were dissolved in dry THF (1.0 mL) and stirred for 2 min to ensure complete dissolution. This solution was then added dropwise to the first, and the iodoform flask rinsed with dry THF (0.2 mL) and the solution added to the reaction. The mixture was slowly warmed to RT overnight, then potassium *tert*-butoxide was added, and the reaction stirred for another 24 h. It was discovered that the product was highly unstable to light, so once the reaction was finished, the product was either carefully isolated for characterisation with exclusion of light, or reacted on immediately without purification. To purify the product, the crude mixture was diluted with 1:1 Et_2O/hexanes (8 mL), then the suspension was filtered through a Celite® pad, which was subsequently rinsed with 1:1 Et_2O/hexanes (16 mL). The crude filtrate was evaporated to dryness, then purified by column chromatography (5% EtOAc/hexanes), giving the product **100** as an off-white powder (82 mg, 38%); **^{1}H NMR** (300 MHz, $CDCl_3$) δ ppm 7.89 (d, ^4J = 1.76 Hz, 2H), 7.74 (d, ^3J = 8.80 Hz, 2H), 7.48 (dd, ^3J = 8.40, ^4J = 1.60 Hz, 2H); **^{13}C NMR** (76 MHz, $CDCl_3$) δ ppm 132.23, 132.03, 129.73, 127.80, 121.50, 7.63.

Azide-appended naphthalene bis-iodotriazole, 101



Azide **35** (405 mg, 2.25 mmol) was dissolved in CH_3CN (2 mL). Sodium iodide (0.24 g, 1.6 mmol) and $Cu(ClO_4)_2 \cdot 6H_2O$ (0.30 g, 0.80 mmol) were added to the reaction, which was covered in aluminium foil and stirred at RT for 3–5 min. TBTA (21 mg, 0.04 mmol) was added, then DBU (61 mg, 0.40 mmol) dissolved in THF (1 mL) was also added. Diethynyl naphthalene **96** (35 mg, 0.20 mmol) was added to the reaction last, then the mixture was stirred in the dark at RT overnight. The reaction was then diluted with CH_2Cl_2 (50 mL), then washed with $NH_4OH_{(aq.)}$ (25%, 25 mL), then brine (2 × 25 mL). The organic layer was separated, dried over $MgSO_4$ and the solvent removed *in vacuo*. The residue was then purified by column chromatography (2% MeOH/CH_2Cl_2) to give the product **101** as a white powder (109 mg, 69%); **^{1}H NMR** (400 MHz, $CDCl_3$) δ ppm 8.53 (s, 2H, 2 × H_c), 8.13 (d, ^3J = 8.31 Hz, 2H, 2 × H_a), 7.97 (d, ^3J = 8.44 Hz, 2H, 2 × H_b), 7.42–7.30 (m, 8H, 4 × H_e, 4 × H_f), 5.73 (s, 4H, 4 × H_d), 4.36 (s, 4H, 2 × H_g); **^{13}C NMR** (101 MHz, $CDCl_3$): δ ppm 150.03, 135.90, 134.36, 132.92, 132.88, 128.71, 128.35, 128.16, 126.94, 125.78, 54.31, 54.11; **HRMS (ESI+)** *m/z*: 805.13 ($[M + H]^+$, calc. for $[C_{30}H_{23}I_2N_{12}]^+$ = 805.02.

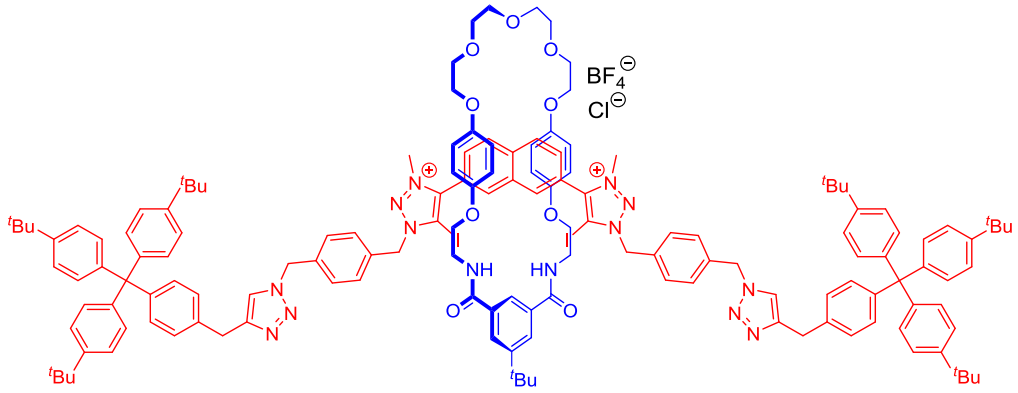
Azide-appended naphthalene bis-iodotriazolium, 102·2BF$_4$



The neutral naphthalene bis-iodotriazole precursor **101** (90.0 mg, 0.114 mmol) was dissolved in dry CH_2Cl_2 (50 mL). $Me_3O \cdot BF_4$ (42 mg, 0.285 mmol) was added and the solution stirred at RT overnight under N_2. The reaction was then quenched with a drop of MeOH, and stirred for 5 min. The solvent was removed *in vacuo* and the residue purified by column

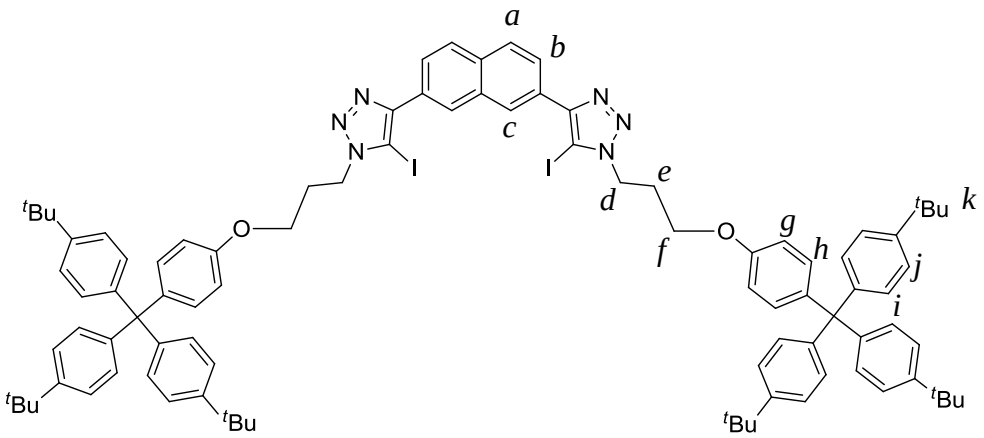
(7% MeOH/CH_2Cl_2) to give the product **102**·2BF_4 as an off-white solid (0.114 g, quant.); **^{1}H NMR** (300 MHz, CD_3CN) δ ppm 8.36–8.30 (m, 4H, 2 × H_a, 2 × H_c), 7.80 (dd, ^3J = 8.80, ^4J = 1.17 Hz, 2H, 2 × H_b), 7.56 (d, ^3J = 8.21 Hz, 4H, 4 × H_f), 7.48 (d, ^3J = 8.21 Hz, 4H, 4 × H_g), 5.89 (s, 4H, 4 × H_e), 4.46 (s, 4H, 4 × H_h), 4.22 (s, 6H, 6 × H_d); **^{13}C NMR** (76 MHz, CD_3CN) δ ppm 147.99, 138.55, 136.26, 133.18, 133.03, 132.47, 130.91, 130.51, 130.06, 129.34, 122.72, 90.86, 58.68, 54.65, 40.37; **HRMS (ESI+)** *m/z*: 921.0716 ($[M - BF_4]^+$, calc. for $[C_{32}H_{28}BF_4I_2N_{12}]^+$ = 921.0678.

Attempted synthesis of stoppered naphthalene rotaxane, 103·Cl·BF_4



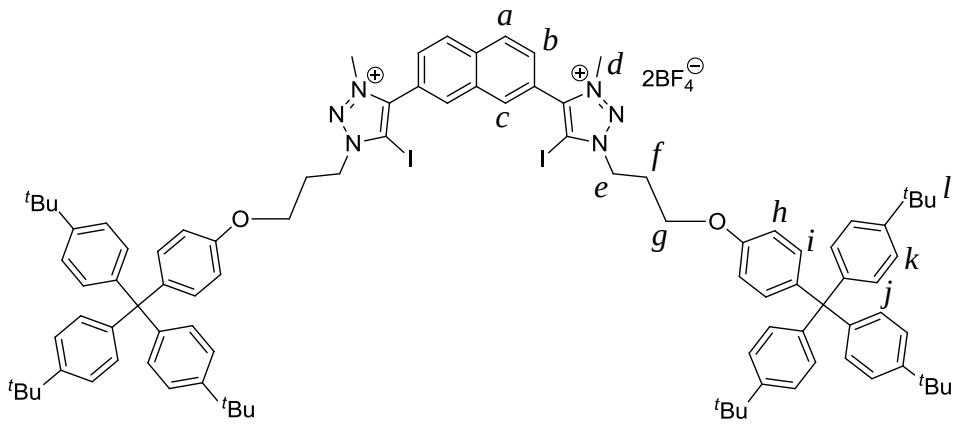
Macrocycle **34** (33 mg, 0.05 mmol) and TBA·Cl (14 mg, 0.05 mmol) were dissolved in dry CH_2Cl_2 (50 mL). Bis-iodotriazolium naphthalene thread precursor **102**·2BF_4 (50 mg, 0.05 mmol) dissolved in CH_3CN (1 mL) was added, and the solution stirred for 30 min at RT. To initially encourage formation of the mono-stoppered axle, alkyne stopper **42** (30 mg, 0.06 mmol) was added to the solution, with DIPEA (0.013 g, 0.017 mL, 0.1 mmol), TBTA (5 mg, 0.01 mmol) and $[Cu(CH_3CN)_4](PF_6)$ (4 mg, 0.01 mmol), and the solution stirred for 18 h. After this time, additional alkyne stopper **42** (30 mg, 0.06 mmol) was added to the solution with the aim of forming the bis-stoppered rotaxane. After stirring the mixture at RT for a further 3 d, there was no evidence for rotaxane formation, though the thread starting material had been consumed.

Bis-iodotriazole naphthalene axle precursor, 104



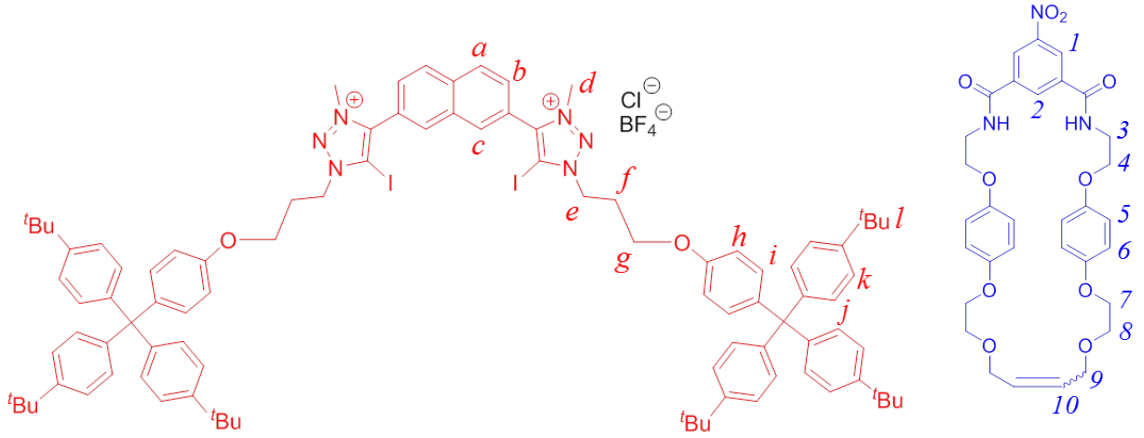
Azide stopper **54** (250 mg, 0.425 mmol) was dissolved in CH_3CN (2 mL). Sodium iodide (0.204 g, 1.36 mmol) and $Cu(ClO_4)_2 \cdot 6H_2O$ (0.255 g, 0.688 mmol) were added to the reaction, which was covered in aluminium foil and stirred at RT for 3–5 min. TBTA (18 mg, 0.033 mmol) was added, then DBU (52 mg, 0.34 mmol) dissolved in THF (1 mL) was also added. Diethynylnaphthalene **96** (30.0 mg, 0.170 mmol) was added to the reaction last, then the mixture was stirred in the dark at RT overnight. The reaction was then diluted with CH_2Cl_2 (50 mL), then washed with $NH_4OH_{(aq.)}$ (25%, 25 mL) and brine (2 × 25 mL). The organic layer was separated, dried over $MgSO_4$ and the solvent removed *in vacuo*. The residue was then purified by column chromatography (0.5% MeOH/CH_2Cl_2) to give the product **104** as a white powder (213 mg, 78%); **^{1}H NMR** (300 MHz, $CDCl_3$) δ ppm 8.53 (s, 2H, 2 × H_c), 8.12 (dd, ^3J = 8.80, ^4J = 1.60 Hz, 2H, 2 × H_b), 7.97 (d, ^3J = 8.80 Hz, 2H, 2 × H_a), 7.27–7.22 (m, 12H, 12 × H_i), 7.15–7.06 (m, 16H, 4 × H_h, 12 × H_j), 6.80 (d, ^3J = 8.80 Hz, 4H, 4 × H_g), 4.72 (t, ^3J = 7.00 Hz, 4H, 4 × H_f), 4.09 (t, ^3J = 5.70 Hz, 4H, 4 × H_d), 2.49 (quin, ^3J = 6.50 Hz, 4H, 4 × H_e), 1.23 (s, 54H, 54 × H_k); **^{13}C NMR** (126 MHz, $CDCl_3$) δ ppm 156.20, 149.56, 148.31, 144.07, 140.05, 132.92, 132.86, 132.31, 130.70, 128.26, 128.13, 126.99, 125.85, 124.05, 113.07, 64.01, 63.04, 48.09, 34.27, 31.36, 29.71; **HRMS (ESI+)** *m/z*: 1625.6180 ($[M + Na]^+$, calc. for $[C_{94}H_{104}I_2N_6NaO_2]^+$ = 1625.6202).

Bis-iodotriazolium naphthalene axle, 105·2BF$_4$



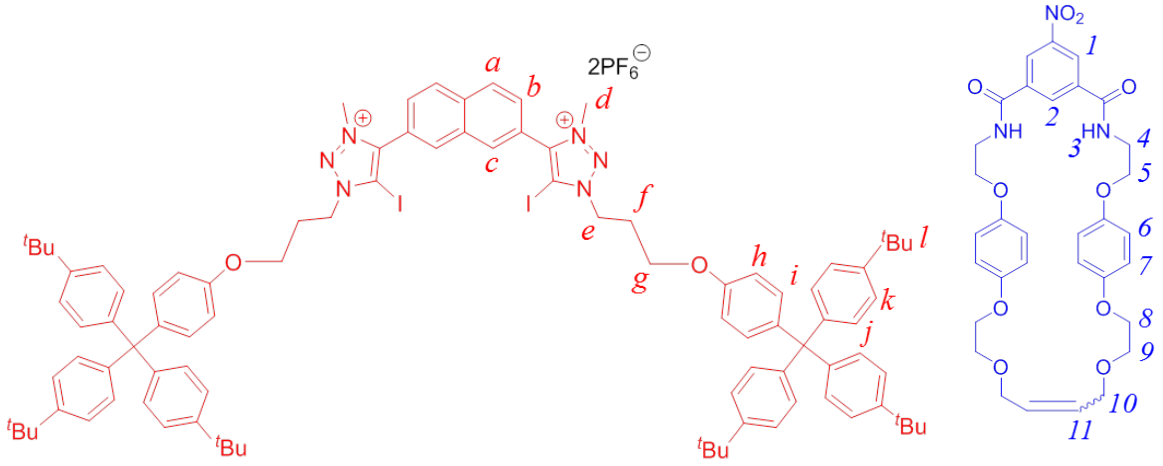
The neutral naphthalene bis-iodotriazole precursor **104** (149 mg, 0.0927 mmol) was dissolved in dry CH_2Cl_2 (25 mL). $Me_3O{\cdot}BF_4$ (34 mg, 0.232 mmol) was added and the solution stirred at RT overnight under N_2. The reaction was then quenched with a drop of MeOH, and stirred for 5 min. The solvent was removed *in vacuo* and the residue purified by column chromatography (7% MeOH/CH_2Cl_2) to give the product **105**·2BF$_4$ as an off-white solid (0.105 g, 63%); **^{1}H NMR** (400 MHz, DMSO-d_6) δ ppm 8.44 (s, 2H, 2 × H_c), 8.38 (d, ^3J = 8.68 Hz, 2H, 2 × H_a), 7.87 (dd, ^3J = 8.44, ^4J = 1.34 Hz, 2H, 2 × H_b), 7.29 (d, ^3J = 8.56 Hz, 12H, 12 × H_j), 7.15–7.00 (m, 16H, 4 × H_i, 12 × H_k), 6.87 (d, ^3J = 8.93 Hz, 4H, 4 × H_h), 4.90 (t, ^3J = 6.54 Hz, 4H, 4 × H_g), 4.21 (s, 6H, 6 × H_d), 4.17 (t, ^3J = 5.62 Hz, 4H, 4 × H_e), 2.47 (quin, ^3J = 5.90 Hz, 4H, 2 × H_f), 1.24 (s, 54H, 54 × H_l) **^{13}C NMR** (126 MHz, d_6-DMSO) δ ppm 155.76, 147.79, 145.51, 143.92, 139.28, 134.46, 131.67, 131.63, 131.50, 129.96, 129.45, 128.42, 124.37, 121.94, 113.44, 94.15, 94.10, 63.87, 62.58, 51.73, 34.04, 31.12, 28.19; **HRMS (ESI+)** *m/z*: 816.8424 ([M – 2(BF$_4$)]$^{2+}$, calc. for [$C_{96}H_{110}I_2N_6O_2$]$^{2+}$ = 816.8401).

Bis-iodotriazolium napthalene rotaxane, 106·Cl·BF_4



Bis-iodotriazolium naphthalene axle **105**·2BF_4 (0.100 g, 0.055 mmol), TBA·Cl (15 mg, 0.055 mmol) and macrocycle precursor **49** (54 mg, 0.083 mmol) were dissolved in dry CH_2Cl_2 (10 mL) and stirred at RT under N_2 for 30 min. Stewart–Grubbs' catalyst (5.4 mg, 10% w/w) was added and the solution stirred at RT for 3 days. The solvent was then removed *in vacuo* and the residue purified by two iterative TLC plates (1st: 5 × 1% MeOH/CH_2Cl_2, 2nd: 2 × EtOAc), to give the mixed chloride and tetrafluoroborate salt of the product as an off-white solid (19.5 mg, 15%); **^{1}H NMR** (500 MHz, 4:1 CD_2Cl_2/CD_3OD) δ ppm 8.67 (s, 1H, 1 × H_2), 8.61 (d, ^4J = 1.26 Hz, 2H, 2 × H_1), 8.06 (s, 2H, 2 × H_c), 7.97 (d, ^3J = 8.83 Hz, 2H, 2 × H_a), 7.50 (dd, ^3J = 8.51, 1.26 Hz, 2H, 2 × H_b), 7.21 (d, ^3J = 8.51 Hz, 12H, 12 × H_j), 7.14 (d, ^3J = 8.83 Hz, 4H, 4 × H_i), 7.07 (d, ^3J = 8.83 Hz, 12H, 12 × H_k), 6.82 (d, ^3J = 8.83 Hz, 4H, 4 × H_h), 6.53 (d, ^3J = 8.83 Hz, 4H, 4 × H_6), 6.39 (d, ^3J = 8.83 Hz, 4H, 4 × H_5), 5.87 (t, ^3J = 2.80 Hz, 2H, 2 × H_{11}), 4.69 (t, ^3J = 6.90 Hz, 4H, 4 × H_e), 4.23 (s, 6H, 6 × H_d), 4.18 (t, ^3J = 5.40 Hz, 4H, 4 × H_g), 4.12 (t, ^3J = 4.40 Hz, 4H, 4 × H_4), 3.93 (s, 4H, 4 × H_9), 3.85 (t, ^3J = 4.40 Hz, 4H, 4 × H_3), 3.74–3.77 (m, 4H, 4 × H_7), 3.64–3.67 (m, 4H, 4 × H_8), 2.55 (quin, ^3J = 6.30 Hz, 4H, 4 × H_f), 1.27 (s, 54H, 54 × H_l); **^{13}C NMR** (126 MHz, 4:1 CD_2Cl_2/CD_3OD) δ ppm 166.79, 157.35, 153.95, 153.78, 149.99, 149.76, 146.33, 145.50, 141.88, 137.49, 136.04, 133.72, 133.04, 132.88, 131.99, 131.16, 130.91, 130.53, 129.03, 127.03, 125.46, 122.43, 116.36, 115.46, 114.40, 72.12, 70.58, 69.13, 68.08, 65.04, 64.46, 53.82, 41.04, 40.79, 35.52, 32.45, 30.95, 29.35; **HRMS (ESI+)** *m/z*: 1127.4593 ($[M - Cl - BF_4]^{2+}$, calc. for $[C_{128}H_{145}I_2N_9O_{12}]^{2+}$ = 1127.4562).

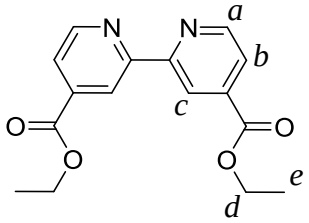
Bis-iodotriazolium napthalene rotaxane, 106·2PF$_6$



The naphthalene-based rotaxane **106**·Cl·BF$_4$ was anion exchanged for PF_6^- by dissolving it in CH_2Cl_2 (10 mL) and washing with $NH_4PF_{6(aq.)}$ (0.1 M, 6 × 10 mL) and water (3 × 10 mL), then removing the solvent and drying thoroughly *in vacuo* to give the product **106**·2PF$_6$ as an off-white solid (18.9 mg, 90%); **^{1}H NMR** (500 MHz, 4:1 CD_2Cl_2/CD_3OD) δ ppm 8.69 (d, ^4J = 1.22 Hz, 2H, 2 × H_1), 8.62 (s, 1H, 1 × H_2), 8.52 (t, ^3J = 6.00 Hz, 2H, 2 × H_3), 8.02 (s, 2H, 2 × H_c), 7.87 (d, ^3J = 8.70 Hz, 2H, 2 × H_a), 7.43 (dd, ^3J = 8.54, ^4J = 1.07 Hz, 2H, 2 × H_b), 7.20 (d, ^3J = 8.54 Hz, 12H, 12 × H_j), 7.13 (d, ^3J = 8.85 Hz, 4H, 4 × H_i), 7.07 (d, ^3J = 8.54 Hz, 12H, 12 × H_k), 6.80 (d, ^3J = 8.85 Hz, 4H, 4 × H_h), 6.55 (d, ^3J = 9.00 Hz, 4H, 4 × H_7), 6.41 (d, ^3J = 8.85 Hz, 4H, 4 × H_6), 5.83 (br. s., 2H, 4 × H_{11}), 4.60 (t, ^3J = 6.87 Hz, 4H, 4 × H_e), 4.19 (s, 6H, 6 × H_d), 4.11 (t, ^3J = 5.26 Hz, 4H, 4 × H_g), 4.05 (t, ^3J = 3.70 Hz, 4H, 4 × H_5), 3.91 (br. s., 4H, 4 × H_{10}), 3.84–3.80 (m, 4H, 4 × H_4), 3.77–3.74 (m, 4H, 4 × H_8), 3.66–3.63 (m, 4H, 4 × H_9), 2.48 (quin, ^3J = 6.10 Hz, 4H, 4 × H_f), 1.26 (s, 54H, 4 × H_l).

6.6 *Synthesis of Compounds from Chapter 4*

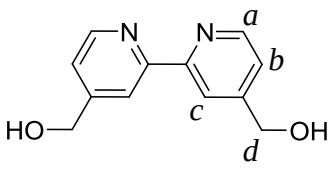
2,2′-Bipyridine-4,4′-dicarboxylic acid ethyl ester, 107



Based on a literature procedure.[49] To a suspension of 2,2′-bipyridine-4,4′-dicarboxylic acid

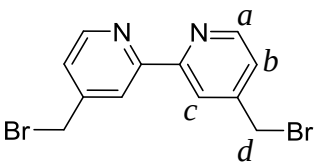
(2.0 g, 8.19 mmol) in ethanol (100 mL) was added dropwise thionyl chloride (4 mL). The solution was stirred at reflux under N_2 for 2 h. The reaction was allowed to cool to RT, then the solvent removed *in vacuo*. The residue was dissolved in CH_2Cl_2 (50 mL), washed with $NaHCO_{3(sat.\ aq.)}$ (50 mL), H_2O (50 mL), then dried ($MgSO_4$) and the solvent removed under reduced pressure, giving the product **107** as a white solid (2.15 g, 88%); **^{1}H NMR** (300 MHz, $CDCl_3$) δ ppm 8.96 (s, 2H, 2 × H_c), 8.88 (d, ^3J = 5.28 Hz, 2H, 2 × H_a), 7.93 (dd, ^3J = 4.99, ^4J = 1.47 Hz, 2H, 2 × H_b), 4.47 (q, ^3J = 7.04 Hz, 4H, 4 × H_d), 1.46 (t, ^3J = 7.04 Hz, 6H, 6 × H_e).

4,4′-Bis-hydroxymethyl-2,2′-bipyridine, 108



Based on a literature procedure.[50] Ethyl ester **107** (1.08 g, 3.6 mmol) was dissolved in ethanol (100 mL). $NaBH_4$ (3.0 g, 78 mmol) was added, and the solution stirred under reflux for 3 h. After cooling to RT, $NH_4Cl_{(sat.\ aq.)}$ (80 mL) was added, and the ethanol was removed *in vacuo*. The product was extracted with ethyl acetate (6 × 50 mL), then the organics were combined, dried ($MgSO_4$) and the solvent removed *in vacuo* to give the product **108** as a white solid (0.78 g, quant.); **^{1}H NMR** (300 MHz, CD_3OD) δ ppm 8.60 (d, ^3J = 5.28 Hz, 2H, 2 × H_a), 8.28 (s, 2H, 2 × H_c), 7.45 (d, ^3J = 5.10 Hz, 2H, 2 × H_b), 4.76 (s, 4H, 4 × H_d).

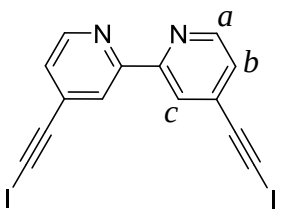
4,4′-Bis-bromomethyl-2,2′-bipyridine, 109



Based on a literature procedure.[50] Bis-alcohol precursor **108** (1.3 g, 6.0 mmol) was disolved in $HBr_{(aq.)}$ (48%, 40 mL) and $H_2SO_{4(aq.)}$ (18 M, 14 mL), and stirred at reflux for 6 h under N_2. The mixture was cooled to RT, and H_2O (70 mL) was added. The solution was then neutralised by cautious addition of $NaOH_{(aq.)}$ (10–1 M). The solid precipitate was then filtered off, washed with H_2O (3 × 10 mL), and the product dissolved in CH_2Cl_2, dried ($MgSO_4$) and the solvent removed *in vacuo* to afford the product **109** as a white powder (1.43 g, 69%);

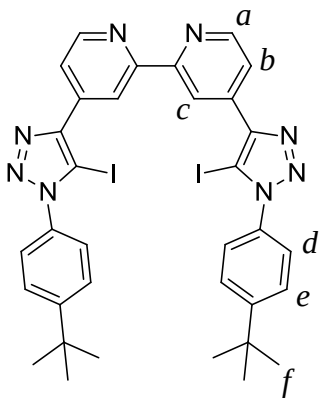
^{1}H NMR (300 MHz, $CDCl_3$) δ ppm 8.69 (d, ^3J = 5.28 Hz, 2H, 2 × H_a), 8.45 (s, 2H, 2 × H_c), 7.38 (dd, ^3J = 4.69, ^4J = 1.76 Hz, 2H, 2 × H_b), 4.50 (s, 4H, 2 × H_d).

4,4′-Bis-iodoethynyl-2,2′-bipyridine, 110



Based on a recently-reported one-pot procedure.[48] To a flame-dried 25 mL RBF fitted with a septum and stirrer bar was added solid NaHMDS (0.16 g, 0.88 mmol). The flask was covered in aluminium foil to exclude light, and the solid dissolved in dry THF (2.2 mL) and dry Et_2O (1.0 mL). The flask was cooled to −78 °C using an acetone/dry ice bath, and the solution stirred for 2 min. To a separate 10 mL RBF (also flame-dried, fitted with a septum and stirrer bar) was added iodoform (0.17 g, 0.44 mmol) and 4,4′-bis-bromomethyl-2,2′-bipyridine **109** (50 mg, 0.15 mmol). These were dissolved in dry THF (1.0 mL) and stirred for 2 min to ensure complete dissolution. This solution was then added dropwise to the first, and the iodoform flask rinsed with dry THF (0.2 mL) and the solution added to the reaction. The mixture was slowly warmed to RT overnight, then potassium *tert*-butoxide was added, and the reaction stirred for another 24 h. It was discovered that the product was highly unstable to light, so once the reaction was finished, the product was either carefully isolated for characterisation with exclusion of light, or reacted on immediately without purification. To purify the product, the crude mixture was diluted with THF (8 mL), then the suspension was filtered through a Celite® pad, which was subsequently rinsed with THF (16 mL). The crude filtrate was evaporated to dryness, then purified by column chromatography (5% MeOH/CH_2Cl_2), giving the product **110** as a red oily solid (10 mg, 15%); **^{1}H NMR** (300 MHz, d_8-THF) δ ppm 8.61 (d, ^3J = 5.28 Hz, 2H, 2 × H_a), 8.43 (s, 2H, 2 × H_c), 7.33 (dd, ^3J = 4.99 Hz, ^4J = 1.47 Hz, 2H, 2 × H_b).

2,2′-Bipyridyl bis-iodotriazole, 111

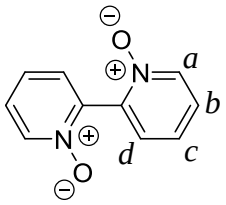


Method 1: This preparation involved adding the reagents directly to the reaction mixture for 4,4′-bis-iodoethynyl-2,2′-bipyridine **110** without purification of the precursor, assuming quantitative yield. After the potassium *tert*-butoxide was added for the reaction to form iodoethynyl precursor **110** and the solution had been stirring for 4 h, azide **8** (210 mg, 1.2 mmol), CuI–$P(OEt)_3$ (214 mg, 0.6 mmol) and triethylamine (210 mg, 0.28 mL, 2.0 mmol) were added to the reaction mixture, and stirred at RT in the dark for 36 h. The reaction was then flushed through a Celite® pad, which was rinsed with THF (2 × 25 mL), then 10% MeOH/CH_2Cl_2 (4 × 25 mL), collected separately. The solvent from the CH_2Cl_2 filtrate was removed *in vacuo*, then the residue was redissolved in THF (20 mL). $NH_4OH_{(aq.)}$ (25%, 30 mL) was added and the mixture stirred for 1 h. The THF was removed *in vacuo*, and the crude extracted into CH_2Cl_2 (3 × 40 mL). The organics were combined and washed with $NH_4OH_{(aq.)}$ (25%, 3 × 20 mL) until the washings were colourless, H_2O (40 mL) then brine (40 mL), dried ($MgSO_4$) then the solvent removed *in vacuo* to give the product **111** as a white powder (42 mg, 10% over two steps).

Method 2: Azide **8** (160 mg, 0.913 mmol) was dissolved in THF (2 mL). Sodium iodide (0.480 g, 3.20 mmol) and $Cu(ClO_4)_2 \cdot 6H_2O$ (0.600 g, 1.62 mmol) were added to the reaction, which was covered in aluminium foil and stirred at RT for 3–5 min. TBTA (42 mg, 0.079 mmol) was added, then DBU (122 mg, 0.801 mmol) dissolved in THF (1 mL) was also added. The diethynyl bipyridine **116** (82 mg, 0.40 mmol) was added to the reaction last, then the mixture was stirred in the dark at RT overnight. The reaction was then diluted with CH_2Cl_2 (200 mL), then washed with $NH_4OH_{(aq.)}$ (25%, 2 × 25 mL), then brine (50 mL). The organic layer was separated, dried ($MgSO_4$) and the solvent removed *in vacuo*. The residue

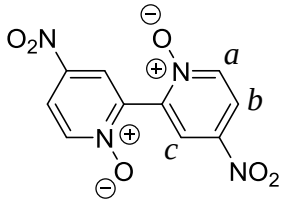
was then suspended in CH_3CN (25 mL) and heated at reflux for 1 h. The mixture was cooled to RT, the solid filtered off and washed with CH_3CN (20 mL) then Et_2O (20 mL), and air-dried to give the product **111** as a white powder (0.247 g, 77%); **^{1}H NMR** (300 MHz, $CDCl_3$) δ ppm 9.23 (s, 2H, 2 × H_c), 8.86 (d, ^3J = 4.69 Hz, 2H, 2 × H_a), 8.07 (dd, ^3J = 4.98, ^4J = 1.47 Hz, 2H, 2 × H_b), 7.63 (d, ^3J = 8.80 Hz, 4H, 4 × H_d), 7.51 (d, ^3J = 8.21 Hz, 4H, 4 × H_e), 1.41 (s, 18H, 18 × H_f); **^{13}C NMR** (126 MHz, $CDCl_3$) δ ppm 153.89, 149.74, 149.49, 134.12, 129.23, 128.13, 126.41, 126.03, 121.78, 119.02, 35.03, 31.27; **HRMS (ESI+)** *m/z*: 807.0911 ($[M + H]^+$, calc. for $[C_{34}H_{33}I_2N_8]^+$ = 807.0912).

2,2′-Bipyridine N-oxide, 112



Based on a literature procedure.[51] 2,2′-Bipyridine (10.0 g, 64.1 mmol) was dissolved in glacial acetic acid (75 mL). $H_2O_{2(aq.)}$ (30%, 25 mL) was added dropwise such that the solution temperature remained in the range 70–80 °C. The reaction was stirred at 75°C for 8 h, then cooled to RT. Acetone (375 mL) was added to precipitate the product, which was filtered off, washed with acetone (3 × 20 mL) and dried thoroughly, giving the product **112** as a white powder (10.29 g, 85%). **^{1}H NMR** (300 MHz, d_6-DMSO): δ ppm 8.35 (d, ^3J = 6.45 Hz, 2H, 2 × H_a), 7.63 (d, ^3J = 7.63 Hz, 2H, 2 × H_d), 7.52 (t, ^3J = 7.00 Hz, , 2 × H_b), 7.41 (t, ^3J = 7.60 Hz, 2H, 2 × H_c); **MS (ESI+)** *m/z*: 189.05 ($[M + H]^+$, calc. for $[C_{10}H_9N_2O_2]^+$ = 189.06).

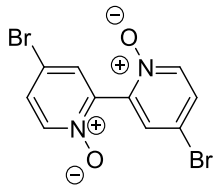
4,4′-Dinitro-2,2′-bipyridine N-oxide, 113



Based on a literature procedure.[51] 2,2′-Bipyridine N-oxide **112** (10.0 g, 53.2 mmol) was dissolved in fuming H_2SO_4 (30 mL) and cooled to 0 °C. Fuming HNO_3 (20 mL) was added

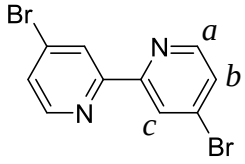
slowly and carefully, then the solution heated at 100 °C overnight. Once complete, the reaction was cooled to 0 °C, then poured on ice water (70 g). The suspension was filtered, and the solid washed with water until the washings were neutral, then washed with methanol (2 × 20 mL) and diethyl ether (2 × 20 mL), then air dried, giving the product **113** as a yellow powder (7.17 g, 48%); **^{1}H NMR** (300 MHz, DMSO-d_6) δ ppm 8.70 (d, ^4J = 3.52 Hz, 2H, 2 × H_c), 8.60 (d, ^3J = 7.20 Hz, 2H, 2 × H_a), 8.38 (dd, ^3J = 7.04, 3.52 Hz, 2H, 2 × H_b); **MS (ESI+)** *m/z*: 279.02 ($[M + H]^+$, calc. for $[C_{10}H_7N_4O_6]^+$ = 279.03).

4,4′-Dibromo-2,2′-bipyridine N-oxide, 114



Based on a literature procedure.[52] Bis-nitro precursor **113** (1.9 g, 6.83 mmol) was suspended in glacial acetic acid (30 mL). Acetyl bromide (20 mL) was added, and the reaction stirred at 100 °C for 4 h. The resulting yellow/brown solution was cooled to 0 °C, then poured onto ice (75 g) and neutralised with $NaOH_{(aq.)}$ (20%, ~150 mL). The precipitate was filtered off, washed with water (2 × 20 mL), MeOH (2 × 20 mL) and diethyl ether (2 × 20 mL), then dried to give the product **114** as an off-white powder (1.78 g, 76%). Insolubility of the product precluded obtaining NMR data. **MS (ESI+)** *m/z*: 346.85 ($[M + H]^+$, calc. for $[C_{10}H_7Br_2N_2O_2]^+$ = 346.88).

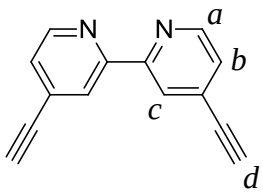
4,4′-Dibromo-2,2′-bipyridine, 115



Based on a literature procedure.[53] A suspension of N-oxide **114** (1.50 g, 4.33 mmol) and phosphorus tribromide (11.2 mL, 31.9 g, 118 mmol) were dissolved in dry CH_3CN (250 mL) and heated at reflux for 4 h. The resulting yellow/brown solution was poured into ice water (200 g) and $NaOH_{(aq.)}$ (20%, ~150 mL) was added to adjust the solution to pH 11. The resulting precipitate was extracted exhaustively into $CHCl_3$, then the combined organic layers

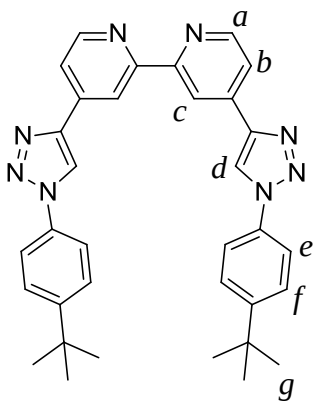
were dried ($MgSO_4$) and the solvent removed. The residue was recrystallised from water/ethanol, giving the product **115** as a yellow powder (1.19 g, 87%); **^{1}H NMR** (300 MHz, $CDCl_3$) δ ppm 8.62 (d, ^4J = 2.35 Hz, 2H, 2 × H_c), 8.50 (d, ^3J = 5.28 Hz, 2H, 2 × H_a), 7.52 (dd, ^3J = 5.28 Hz, ^4J = 1.76 Hz, 2H, 2 × H_b); **MS (ESI+)** *m/z*: 314.85 ($[M + H]^+$, calc. for $[C_{10}H_7Br_2N_2]^+$ = 314.89).

4,4′-Diethynyl-2,2′-bipyridine, 116



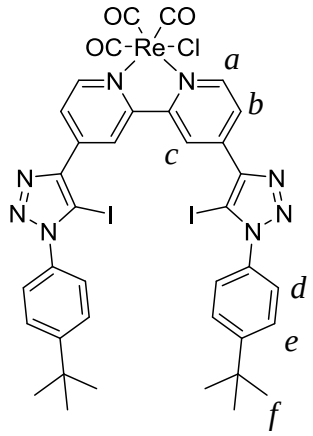
Based on a literature procedure.[54] A deaerated solution of bis-bromo precursor **115** (0.40 g, 1.27 mmol) and trimethylsilyl-acetylene (0.31 g, 0.45 mL, 3.20 mmol) in dry triethylamine (10 mL) was treated with $Pd(PPh_3)_2Cl_2$ (30 mg, 0.43 mmol) and CuI (30 mg, 0.16 mmol). The mixture was heated at 85 °C in a closed vial for 3 days. The reaction was then cooled to RT, the solvent removed *in vacuo* and the residue suspended in THF, which was filtered through a Celite® pad, and the pad rinsed with THF (2 × 10 mL). The filtrate solvent was removed *in vacuo*, and the residue dissolved in MeOH (20 mL), then KOH (0.36 g, 7.62 mmol) was added to deprotect the ethynyl groups. The solution was stirred at RT for 1 h, then the solvent was removed *in vacuo*, and the residue partitioned between CH_2Cl_2 (50 mL) and $NH_4Cl_{(aq.)}$ (50 mL). The aqueous layer was extracted with CH_2Cl_2 (2 × 20 mL), and the combined organic layers were combined and dried ($MgSO_4$). The solvent was removed, and the residue purified by column chromatography (3% MeOH/CH_2Cl_2) to give the product **116** as an off-white solid (0.162 g, 62%); **^{1}H NMR** (300 MHz, $CDCl_3$) δ ppm 8.67 (d, ^3J = 4.69 Hz, 2H, 2 × H_a), 8.49 (d, ^4J = 1.17 Hz, 2H, 2 × H_c), 7.39 (dd, ^3J = 4.69, ^4J = 1.76 Hz, 2H, 2 × H_b), 3.33 (s, 2H, 2 × H_d); **MS (ESI+)** *m/z*: 205.05 ($[M + H]^+$, calc. for $[C_{14}H_9N_2]^+$ = 204.07).

2,2′-Bipyridyl bis-triazole, 117



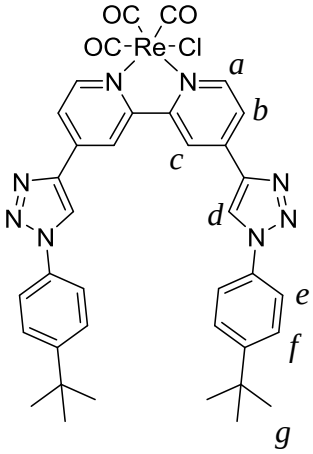
Diethynyl bipyridine **116** (41 mg, 0.20 mmol) and azide **8** (79 mg, 0.45 mmol) were dissolved in dry CH_2Cl_2 (20 mL). TBTA (0.116 g, 0.22 mmol), $[Cu(CH_3CN)_4](PF_6)$ (82 mg, 0.22 mmol) and DIPEA (64 mg, 0.5 mmol) were added and the solution stirred at RT under N_2 for 3 days. The reaction was then washed with $NH_4OH_{(aq.)}$ (25% w/w, 15 mL), brine (2 × 15 mL) and dried ($MgSO_4$), then the solvent removed *in vacuo*. The residue was then suspended in CH_3CN (25 mL) and heated at reflux for 1 h, then cooled to RT and the solid filtered off, washed with CH_3CN (10 mL), and diethyl ether (10 mL), then dried under vacuum to give the product **117** as a white solid (91.4 mg, 82%). **^{1}H NMR** (500 MHz, $CDCl_3$) δ ppm 8.93 (br. s, 2H, 2 × H_c), 8.83 (d, ^3J = 4.58 Hz, 2H, 2 × H_a), 8.64 (br. s, 2H, 2 × H_b), 8.15 (s, 2H, 2 × H_d), 7.77 (d, ^3J = 8.54 Hz, 4H, 4 × H_e), 7.60 (d, ^3J = 8.54 Hz, 4H, 4 × H_f), 1.40 (s, 18H, 18 × H_g); **^{13}C NMR** (126 MHz, $CDCl_3$) δ ppm 152.62, 149.52, 145.68, 134.32, 126.82, 120.51, 120.25, 120.02, 117.90, 34.87, 31.26; **HRMS (ESI+)** *m/z*: 555.2982 ($[M + H]^+$, calc. for $[C_{34}H_{36}N_8]^+$ = 555.2979.

Rhenium(I) bis-iodotriazole model receptor, 118



Bipyridyl precursor **111** (30 mg, 0.037 mmol) and $Re(CO)_5Cl$ (15 mg, 0.041 mmol) were suspended in $CHCl_3$ (30 mL) and heated at reflux for 3 days under N_2. The solvent was removed *in vacuo* and the residue purified by preparative TLC (silica, 1% $MeOH/CH_2Cl_2$) to give the product **118** as an orange solid (13 mg, 30%); **^{1}H NMR** (300 MHz, $CDCl_3$) δ ppm 9.19–9.13 (m, 4H, 2 × H_a, 2 × H_c), 8.36 (dd, ^3J = 5.86, ^4J = 1.76 Hz, 2H, 2 × H_b), 7.61–7.67 (m, 4H, 4 × H_d), 7.46–7.53 (m, 4H, 4 × H_e), 1.40–1.44 (m, 18H, 18 × H_f); **^{13}C NMR** (76 MHz, CD_2Cl_2) δ ppm 156.58, 154.95, 153.81, 145.45, 141.87, 134.32, 127.16, 126.51, 124.31, 120.97, 82.54, 35.53, 31.52, 16.48; **HRMS (ESI+)** *m/z*: 1134.9831 ($[M + Na]^+$, calc. for $[C_{37}H_{32}O_3N_8ClI_2NaRe]^+$ = 1134.9825.

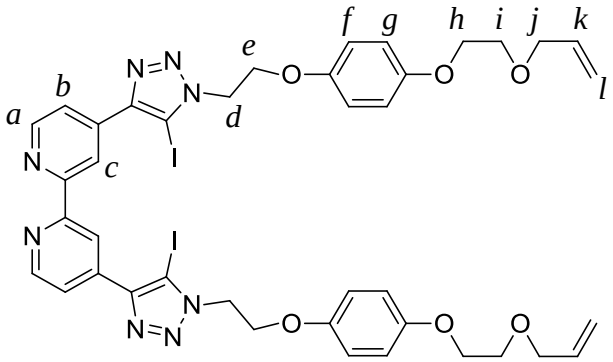
Rhenium(I) bis-prototriazole acyclic receptor, 119



Bipyridyl precursor **117** (30 mg, 0.054 mmol) and $Re(CO)_5Cl$ (20 mg, 0.054 mmol) were suspended in $CHCl_3$ (30 mL) and heated at reflux for 3 days under N_2. The resulting

precipitate was filtered off, washed with $CHCl_3$ (2 × 10 mL) and air-dried, giving the product **119** as a highly insoluble yellow powder (28 mg, 60%); **^{1}H NMR** (300 MHz, d_6-DMSO) δ ppm 9.83 (s, 2H, 2 × H_d), 9.28 (s, 2H, 2 × H_c), 9.15 (d, ^3J = 5.87 Hz, 2H, 2 × H_a), 8.25 (d, ^3J = 5.87 Hz, 2H, 2 × H_b), 7.92 (d, ^3J = 8.80 Hz, 4H, 4 × H_e), 7.71 (d, ^3J = 8.80 Hz, 4H, 4 × H_f), 1.36 (s, 18H, 18 × H_g). **HRMS (ESI+)** *m/z*: 883.1862 ($[M + Na]^+$, calc. for $[C_{37}H_{34}O_3N_8ClNaRe]^+$ = 883.1892.

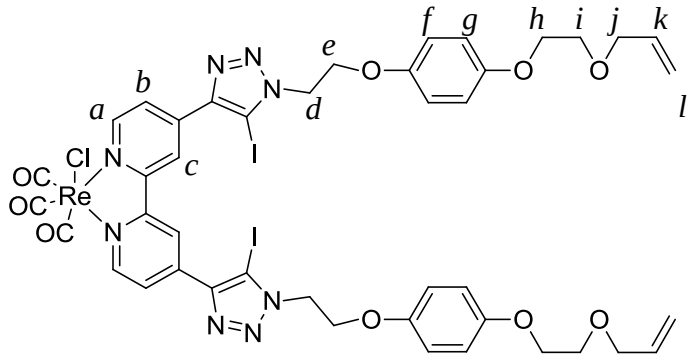
Allyl-appended 2,2′-bipyridyl bis-iodotriazole, 120



Allyl-appended azide **68** (0.290 g, 1.1 mmol) was dissolved in THF (2 mL). Sodium iodide (0.480 g, 3.2 mmol) then $Cu(ClO_4)_2 \cdot 6H_2O$ (0.600 g, 1.62 mmol) were added to the reaction, which was covered in aluminium foil and stirred at RT for 3–5 min. TBTA (42 mg, 0.079 mmol) was added, then DBU (122 mg, 0.801 mmol) dissolved in THF (1 mL) was also added. The diethynyl bipyridine **116** (82 mg, 0.40 mmol) was added to the reaction last, then the mixture was stirred in the dark at RT overnight. The reaction was then diluted with CH_2Cl_2 (50 mL), then washed with $NH_4OH_{(aq.)}$ (25%, 2 × 25 mL), then brine (50 mL). The organic layer was separated, dried ($MgSO_4$) and the solvent removed *in vacuo*. The residue was then suspended in CH_3CN (25 mL) and heated at reflux for 1 h. The mixture was cooled to RT, the solid filtered off and washed with CH_3CN (20 mL) then Et_2O (20 mL), and air-dried to give the product **120** as a white powder (0.286 g, 73%); **^{1}H NMR** (500 MHz, d_6-DMSO) δ ppm 9.14 (s, 2H, 2 × H_c), 8.85 (d, ^3J = 4.88 Hz, 2H, 2 × H_a), 8.07 (d, ^3J = 5.70 Hz, 2H, 2 × H_b), 6.85 (s, 8H, 4 × H_f, 4 × H_g), 5.93–5.81 (m, 2H, 2 × H_k), 5.28–5.10 (m, 4H, 4 × H_l), 4.87 (t, ^3J = 4.90 Hz, 4H, 4 × H_d), 4.46 (t, ^3J = 4.90 Hz, 4H, 4 × H_e), 4.04–3.95 (m, 8H, 4 × H_h, 4 × H_j), 3.66 (t, ^3J = 4.40 Hz, 4H, 4 × H_i); **^{13}C NMR** (126 MHz, d_6-DMSO) δ ppm 155.39, 152.91, 151.83, 150.08, 145.73, 139.20, 135.11, 121.18, 117.46, 116.47, 115.56, 115.37, 84.80, 71.08, 68.17, 67.47, 66.55, 49.88; **HRMS (ESI+)**

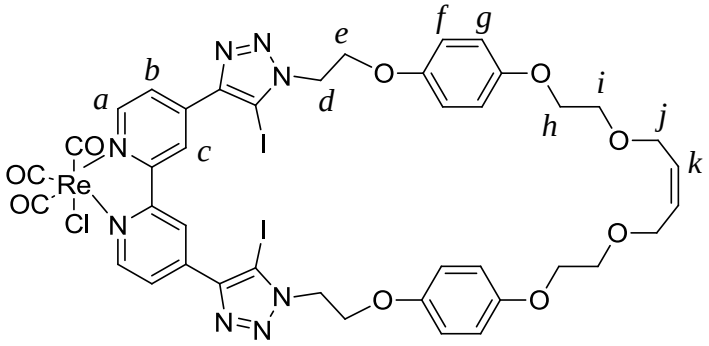
m/z: 1005.1080 ([M + Na]$^+$, calc. for [$C_{40}H_{40}I_2N_8NaO_6$]$^+$ = 1005.1052.

Allyl-appended Rhenium complex, 121



Bipyridyl precursor **120** (60 mg, 0.061 mmol) and $Re(CO)_5Cl$ (22 mg, 0.061 mmol) were suspended in $CHCl_3$ (30 mL) and heated at reflux for 3 days under N_2. The solvent was removed *in vacuo* and the residue purified by preparative TLC (silica, 3% MeOH/CH_2Cl_2) to give the product **121** as an orange solid (57 mg, 73%); **^{1}H NMR** (500 MHz, $CDCl_3$) δ ppm 9.10 (d, ^3J = 5.80 Hz, 2H, 2 × H_a), 9.05 (s, 2H, 2 × H_c), 8.26 (d, ^3J = 5.65 Hz, 2H, 2 × H_b), 6.85 (d, ^3J = 9.16 Hz, 4H, 4 × H_f), 6.80 (d, ^3J = 9.31 Hz, 4H, 4 × H_g), 5.87–5.99 (m, 2H, 2 × H_k), 5.16–5.34 (m, 4H, 4 × H_l), 4.88 (t, ^3J = 5.19 Hz, 4H, 4 × H_d), 4.46 (t, ^3J = 5.26 Hz, 4H, 4 × H_e), 4.01–4.11 (m, 8H, 4 × H_h, 4 × H_j), 3.76 (t, ^3J = 4.70 Hz, 4H, 4 × H_i); **^{13}C NMR** (126 MHz, $CDCl_3$) δ ppm 197.09, 156.04, 153.75, 153.24, 151.96, 144.40, 141.15, 134.52, 123.53, 120.29, 117.35, 115.71, 115.62, 72.34, 68.54, 68.06, 66.68, 50.85, 50.29, 29.67; **HRMS (ESI+)** *m/z*: 1311.0133 ([M + Na]$^+$, calc. for [$C_{43}H_{40}ClI_2N_8NaO_9Re$]$^+$ = 1311.0139.

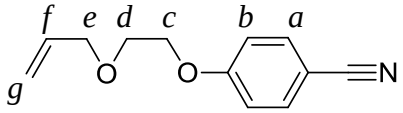
Allyl-appended Rhenium macrocycle, 122



Re complex **121** (57 mg, 0.044 mmol) was dissolved in dry CH_2Cl_2 (25 mL), and Stewart–Grubbs' catalyst (5.7 mg, 10% w/w) added. The solution was stirred at RT for 3 days, after

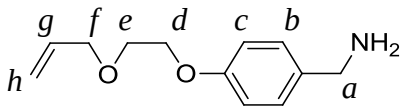
which the solvent was removed *in vacuo*. The residue was then purified by preparative TLC (silica, 3% MeOH/CH_2Cl_2) to give the product **122** as an orange solid (36 mg, 65%); **^{1}H NMR** (300 MHz, $CDCl_3$) δ ppm 9.12 (d, ^3J = 5.86 Hz, 2H, 2 × H_a), 9.05 (d, ^4J = 1.17 Hz, 2H, 2 × H_c), 8.27 (dd, ^3J = 5.86, ^4J = 1.76 Hz, 2H, 2 × H_b), 6.85–6.72 (m, 8H, 4 × H_f, 4 × H_g), 5.85–5.80 (m, 2H, 4 × H_k), 4.89 (t, ^3J = 4.98 Hz, 4H, 4 × H_d), 4.46 (t, ^3J = 4.98 Hz, 4H, 4 × H_e), 3.99–4.08 (m, 8H, 4 × H_h, 4 × H_j), 3.77–3.73 (m, 4H, 4 × H_i); **^{13}C NMR** (101 MHz, $CDCl_3$) δ ppm 156.03, 153.75, 153.26, 151.96, 144.47, 141.12, 129.21, 123.69, 120.31, 115.75, 115.66, 70.97, 68.45, 68.20, 66.91, 50.33, 29.68; **MS (MALDI+)** *m/z*: 1225.31 ($[M - Cl]^+$, calc. for $[C_{41}H_{36}I_2N_8O_9Re]^+$ = 1225.03).

Aryl nitrile-appended vinyl compound, 123



Based on a literature procedure.[34] Vinyl mesylate **46** (4.15 g, 23.0 mmol) and 4-cyanophenol (3.29 g, 27.6 mmol) were suspended in dry CH_3CN (100 mL). K_2CO_3 (6.36 g, 46.0 mmol) was added and the suspension heated at reflux under N_2 for 36 h. The reaction mixture was taken to dryness under reduced pressure. The residue was redissolved in CH_2Cl_2 (100 mL), washed with $HCl_{(aq.)}$ (1 M, 2 × 100 mL), brine (100 mL) and dried ($MgSO_4$), then the solvent removed under reduced pressure. The crude oil was purified by column chromatography (1:1 petrol/CH_2Cl_2) to give the product **123** as a colourless oil (2.99 g, 64%); **^{1}H NMR** (300 MHz, $CDCl_3$) δ ppm 7.62–7.51 (m, 2H, 2 × H_a), 7.02–6.92 (m, 2H, 2 × H_b), 6.01–5.83 (m, 1H, 1 × H_f), 5.34–5.19 (m, 2H, 2 × H_g), 4.21–4.14 (m, 2H, 2 × H_c), 4.08 (dt, ^3J = 5.86, ^4J = 1.47 Hz, 2H, 2 × H_e), 3.85–3.77 (m, 2H, 2 × H_d); **MS (ESI+)** *m/z*: 204.11 ($[M + H]^+$, calc. for $[C_{12}H_{14}NO_2]^+$ = 204.09)

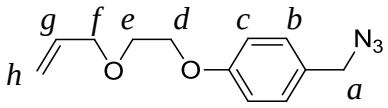
Amine-appended vinyl compound, 124



Based on a literature procedure.[34] Aryl nitrile compound **123** (2.03 g, 9.8 mmol) was dissolved in dry Et_2O (50 mL), then added dropwise to a suspension of $LiAlH_4$ (0.76 g, 20 mmol) in dry Et_2O (50 mL). Once the addition was complete, the suspension was heated at

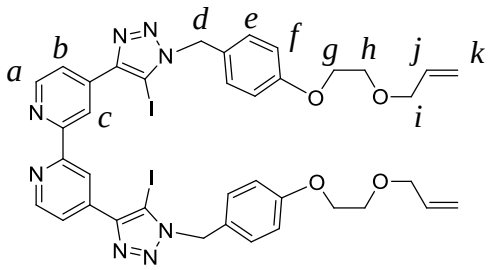
reflux under N_2 for 3 h, then subsequently cooled in an ice bath and quenched by addition of $MgSO_4 \cdot 10H_2O$. Once bubbling had ceased, the suspension was filtered and the colourless filtrate taken to dryness under reduced pressure, giving the pure product **124** as a light yellow oil (1.82 g, 90%); **^{1}H NMR** (300 MHz, $CDCl_3$): δ ppm 7.26–7.17 (m, 2H, 2 × H_b), 6.95–6.85 (m, 2 H, 2 × H_c), 6.04–5.86 (m, 1H, 1 × H_g), 5.37–5.14 (m, 2H, 2 × H_h), 4.17–4.08 (m, 4H, 2 × H_d, 2 × H_f), 3.84–3.74 (m, 4H, 2 × H_a, 2 × H_e).

Azide-appended vinyl compound, 125



To amine **124** (1.0 g, 4.83 mmol) dissolved in MeOH (30 mL) was added the HSO_4^- salt of imidazolesulfonyl azide (1.61 g, 5.90 mmol), K_2CO_3 (1.63 g, 11.8 mmol) and $CuSO_4 \cdot 5H_2O$ (15 mg, 0.06 mmol). The suspension was stirred at RT under a N_2 atmosphere for 3 days, then cautiously concentrated to ~5 mL under reduced pressure, diluted with $HCl_{(aq.)}$ (10%, 100 mL) and extracted with EtOAc (3 × 100 mL). The combined organic fractions were washed with brine (100 mL) and dried ($MgSO_4$), then the solvent removed under reduced pressure. The residue was purified by column chromatography (1:1 petrol:CH_2Cl_2) to give the product **125** as a colourless oil (0.865 g, 77%). **^{1}H NMR** (300 MHz, $CDCl_3$): δ ppm 7.17–7.28 (m, 2 H, 2 × H_b), 6.88–6.97 (m, 2 H, 2 × H_c), 5.86–6.01 (m, 1 H, 1 × H_g), 5.35–5.27 (m, 1 H, 1 × H_h), 5.16–5.25 (m, 1 H, 1 × H_h), 4.26 (s, 2H, 2 × H_a), 4.06–4.17 (m, 4H, 2 × H_d, 2 × H_f), 3.76–3.84 (m, 2H, 2 × H_e); **^{13}C NMR** (76 MHz, $CDCl_3$): δ ppm 158.80, 134.45, 129.67, 127.51, 117.37, 114.83, 72.33, 68.38, 67.42, 54.32; **HRMS (FI+)** *m/z*: 233.1158 ($[M]^+$, calc. for $[C_{12}H_{15}N_3O_2]^+$ = 233.1164).

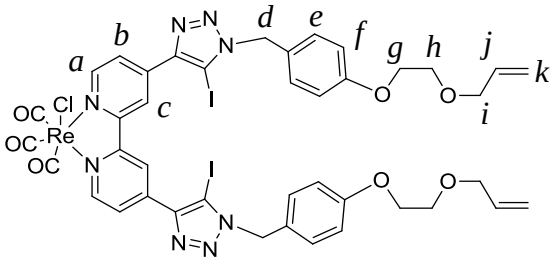
Bpy bis-iodotriazole allyl-appended compound, 126



Allyl-appended azide **125** (0.210 g, 0.90 mmol) was dissolved in THF (3 mL). Sodium iodide

(0.480 g, 3.2 mmol) then $Cu(ClO_4)_2 \cdot 6H_2O$ (0.590 g, 1.62 mmol) were added to the reaction, which was covered in aluminium foil and stirred at RT for 3–5 min. TBTA (42 mg, 0.079 mmol) was added, then DBU (121 mg, 0.801 mmol) dissolved in THF (1 mL) was also added. Diethynyl bipyridine **116** (82 mg, 0.40 mmol) was added to the reaction last, then the mixture was stirred in the dark at RT overnight. The reaction was then diluted with CH_2Cl_2 (50 mL), then washed with $NH_4OH_{(aq.)}$ (25%, 2 × 25 mL), then brine (2 × 25 mL). The organic layer was separated, dried ($MgSO_4$) and the solvent removed *in vacuo*. The residue was then suspended in CH_3CN (25 mL) and heated at reflux for 1 h. The mixture was cooled to RT, the solid filtered off and washed with CH_3CN (20 mL) and diethyl ether (20 mL), then air-dried to give the product **126** as a white powder (0.293 g, 80%); **^{1}H NMR** (300 MHz, $CDCl_3$): δ ppm 9.09 (d, ^4J = 1.76 Hz, 2H, 2 × H_c), 8.79 (d, ^3J = 5.20 Hz, 2H, 2 × H_a), 7.97 (dd, ^3J = 4.69, ^4J = 1.76 Hz, 2H, 2 × H_b), 7.34–7.26 (m, 4H, 4 × H_e), 6.96–6.85 (m, 4H, 4 × H_f), 6.03–5.86 (m, 2H, 2 × H_j), 5.65 (s, 4H, 4 × H_d), 5.35–5.27 (m, 2H, 2 × H_k), 5.24–5.19 (m, 2H, 2 × H_k), 4.18–4.06 (m, 8H, 4 × H_g, 4 × H_i), 3.85–3.75 (m, 4H, 4 × H_h); **^{13}C NMR** (76 MHz, $CDCl_3$): δ ppm 159.02, 149.69, 147.59, 134.54, 129.35, 126.23, 121.51, 118.71, 117.45, 114.99, 110.25, 72.38, 68.37, 67.48, 54.09; **HRMS (ESI+)** *m/z*: 923.1031 ($[M + H]^+$, calc. for $[C_{38}H_{37}I_2N_8O_4]^+$ = 923.1022)

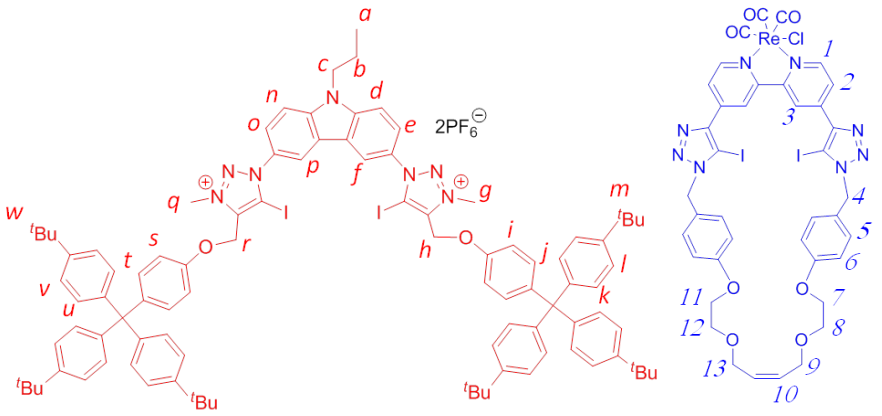
Allyl-appended Re complex, 127



Allyl-appended bpy compound **126** (138 mg, 0.15 mmol) and rhenium pentacarbonyl chloride (54 mg, 0.15 mmol) were dissolved in $CHCl_3$ and heated at reflux for 3 d under N_2. The solvent was then removed *in vacuo*, and the residue purified by preparative TLC plate (silica; 4% MeOH/CH_2Cl_2) to give the product **127** as an orange solid (138 mg, 75%); **^{1}H NMR** (300 MHz, $CDCl_3$): δ ppm 8.87 (d, ^3J = 5.86 Hz, 2H, 2 × H_a), 8.85 (s, 2H, 2 × H_c), 7.90 (dd, ^3J = 5.86, ^4J = 1.76 Hz, 2H, 2 × H_b), 7.25 (d, ^3J = 8.21 Hz, 4H, 4 × H_e), 6.99 (d, ^3J = 8.80 Hz, 4H, 4 × H_f), 5.81–6.03 (m, 2H, 2 × H_j), 5.44–5.72 (m, 4H, 4 × H_d), 5.09–5.37

(m, 4H, 4 × H_k), 4.20–4.17 (m, 4H, 4 × H_i), 4.09 (d, ^3J = 5.86 Hz, 4H, 4 × H_g), 3.84–3.81 (m, 4 H, 4 × H_h); **^{13}C NMR** (76 MHz, $CDCl_3$): δ ppm 196.94, 159.19, 155.76, 153.29, 144.03, 141.46, 134.41, 129.45, 125.84, 123.96, 118.94, 117.42, 115.10, 109.94, 82.40, 72.32, 68.34, 67.54, 54.17; **MS (MALDI+)** *m/z*: 1193.40 ([M − Cl]$^+$, calc. for $[C_{41}H_{36}I_2N_8O_7Re]^+$ = 1193.04).

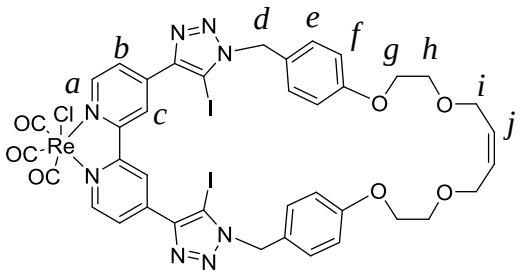
Rotaxane with carbazole-based axle and Re complex-based macrocycle, 128·2PF$_6$



Carbazole-based axle **51**·2BF_4 (59 mg, 0.032 mmol), TBA·Cl (9 mg, 0.032 mmol) and Re complex macrocycle precursor **127** (59 mg, 0.048 mmol) were dissolved in dry CH_2Cl_2 (10 mL) and the solution stirred for 30 min. Stewart–Grubbs' catalyst (dichloro[1,3-bis(2-methylphenyl)-2-imidazolidinylidene](2-isopropoxyphenylmethylene)ruthenium(II), 6 mg, 10% w/w cat.) was added and the solution stirred at RT for 3 days under N_2. The solvent was then removed *in vacuo*, and the residue purified by two preparative TLC plates (6% MeOH/CH_2Cl_2, then EtOAc) to give the product **128**·Cl·BF_4. This was anion exchanged for PF_6^- by dissolving in CH_2Cl_2 (10 mL) and washing with $NH_4PF_{6(aq.)}$ (0.1 M, 6 × 10 mL) and H_2O (2 × 10 mL), then the solvent was removed and the residue thoroughly dried *in vacuo*, to give **128**·2PF_6 as a yellow solid (6.7 mg, 7%); **^{1}H NMR** (500 MHz, 1:4 CD_3OD/CD_2Cl_2): δ ppm 9.04 (d, ^3J = 5.65 Hz, 2H, 2 × H_1), 8.04 (d, ^3J = 5.19 Hz, 2H, 2 × H_2), 7.58 (d, ^3J = 7.32 Hz, 4H, 4 × H_5), 7.56 (s, 2H, 2 × H_3), 7.37 (d, ^3J = 8.39 Hz, 2H, 2 × H_i), 7.32 (d, ^3J = 8.54 Hz, 2H, 2 × H_s), 7.28 (d, ^3J = 8.54 Hz, 6H, 6 × H_k), 7.25 (d, ^3J = 8.54 Hz, 6H, 6 × H_u), 7.19 (d, ^3J = 8.54 Hz, 6H, 6 × H_l), 7.16 (d, ^3J = 8.54 Hz, 6H, 6 × H_v), 7.13 (d, ^3J = 8.10 Hz, 2H, 2 × H_j), 7.08 (d, ^3J = 8.09 Hz, 2H, 2 × H_t), 6.79 (d, ^3J = 7.02 Hz, 4H, 4 × H_6), 5.74–5.70 (m, 4H, 2 × H_{10}, 2 × H_4), 5.63 (s, 2H, 2 × H_h), 5.56 (s,

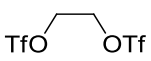
2H, 2 × H_r), 5.47 (d, ^2J = 14.80 Hz, 2H, 2 × H_4), 4.80 (s, 3H, 3 × H_g), 4.74 (s, 3H, 3 × H_q), 4.03 (s, 2H, 2 × H_{11}), 3.96 (s, 2H, 2 × H_{12}), 3.90–3.78 (m, 4H, 2 × H_9, 2 × H_{13}), 3.74 (s, 2H, 2 × H_7), 3.66 (s, 2H, 2 × H_8), 3.45 (t, ^3J = 7.48 Hz, 2H, 2 × H_c), 1.45–1.34 (m, 2H, 2 × H_b), 1.30 (s, 27H, 27 × H_m), 1.28 (s, 27H, 27 × H_w) 0.63 (t, ^3J = 7.32 Hz, 3H, 3 × H_a); **^{13}C NMR** (126 MHz, 1:4 CD_3OD/CD_2Cl_2): δ ppm 160.19, 155.71, 155.66, 154.08, 149.31, 145.84, 144.9, 144.85, 143.04, 142.93, 142.57, 142.29, 142.09, 133.11, 131.08, 130.23, 128.95, 127.88, 127.76, 125.91, 125.54, 125.06, 125.02, 122.13, 121.57, 119.23, 118.46, 115.3, 114.45, 114.4, 89.23, 71.31, 69.49, 68.67, 63.94, 63.89, 60.22, 59.85, 45.31, 40.59, 40.44, 34.82, 34.81, 32.56, 31.62, 31.46, 30.29, 29.98, 23.29, 22.19, 14.35, 11.5; **HRMS (ESI+)** *m/z*: 1429.8232 ($[M - 2(PF_6)]^{2+}$, calc. for $[C_{136}H_{141}ClI_4N_{15}O_9Re]^{2+}$ = 1429.8279).

Small Re Macrocycle



Significant quantities of the ring-closed macrocycle were also isolated from the above reaction; **^{1}H NMR** (500 MHz, $CDCl_3$) δ ppm 9.10 (d, ^3J = 5.80 Hz, 2H, 2 × H_a), 8.87 (s, 2H, 2 × H_c), 8.21 (dd, ^3J = 5.80, ^4J = 1.22 Hz, 2H, 2 × H_b), 7.24 (d, J = 8.54 Hz, 4H, 4 × H_e), 6.91 (d, ^3J = 8.54 Hz, 4H, 4 × H_f), 5.84 (br. s., 2H, 2 × H_j), 5.70 (d, ^2J = 15.11 Hz, 2H, 2 × H_d), 5.57 (d, ^2J = 15.11 Hz, 2H, 2 × H_d), 4.04–4.13 (m, 8H, 4 × H_g, 4 × H_i), 3.80 (t, ^3J = 4.50 Hz, 4H, 4 × H_h); **^{13}C NMR** (126 MHz, $CDCl_3$) δ ppm 159.21, 155.91, 153.36, 145.01, 144.40, 141.25, 129.39, 129.09, 125.72, 124.22, 119.66, 115.13, 80.08, 71.03, 68.37, 67.72, 54.33; **HRMS (ESI+)** *m/z*: 1222.9615 ($[M + Na]^+$, calc. for $[C_{39}H_{32}ClI_2N_8NaO_7Re]^+$ = 1222.9622).

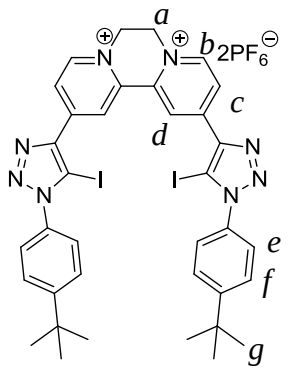
1,2-Bis(triflyl)ethane, 129



This synthetic procedure is based on a previously reported method.[55] Triflic anhydride (5.6 g, 3.3 mL, 20 mmol) dissolved in CH_2Cl_2 (20 mL) was added dropwise over 1 h into a solution

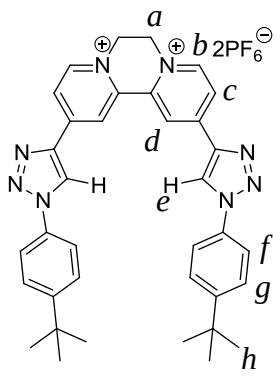
of ethylene glycol (0.62 g, 0.56 mL, 10 mmol) and pyridine (1.6 g, 1.6 mL, 20 mmol) in CH_2Cl_2 (8 mL) at 0 °C. Once addition was complete, the organics were washed with H_2O (10 mL) then dried ($MgSO_4$) and the solvent removed *in vacuo*. The residue was purified by column chromatography (CH_2Cl_2), giving the product **129** as a pink oil, which solidifies at room temperature (0.902 g, 31%); **^{1}H NMR** (400 MHz, $CDCl_3$): δ ppm 4.78 (s, 4H); **^{19}F NMR** (283 MHz, $CDCl_3$) δ ppm −74.35 (s, 6F)

Bis-iodotriazole diquat model, 130·2PF$_6$



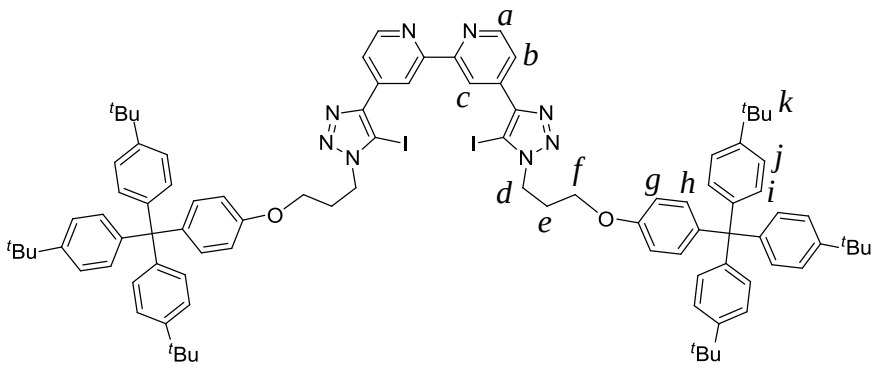
Bis-iodotriazole bpy precursor **111** (30 mg, 0.037 mmol) was dissolved in $CHCl_3$ (10 mL). 1,2-Bis(triflyl)ethane **129** (33 mg, 0.10 mmol) was added, and the solution stirred under N_2 in the dark at 40 °C for 3 days. The solvent was then removed, and the residue suspended in MeOH (20 mL) and stirred vigorously for 5 min. The solid was filtered off and the filtrate collected and reduced to ~5 mL. $NH_4PF_{6(sat.\ aq.)}$ (0.5 mL), then H_2O (10 mL) were slowly added, forming a precipitate which was filtered and washed with H_2O (3 × 10 mL), before being extracted with acetone (3 × 10 mL). The solvent was then removed *in vacuo*, giving the product **130**·2PF_6 as a brown solid (27 mg, 65%); **^{1}H NMR** (300 MHz, d_6-acetone) δ ppm 9.91 (s, 2H, 2 × H_d), 9.61 (d, ^3J = 6.45 Hz, 2H, 2 × H_b), 9.29 (d, ^3J = 6.45 Hz, 2H, 2 × H_c), 7.79 (d, ^3J = 8.40 Hz, 4H, 4 × H_e), 7.65 (d, ^3J = 8.21 Hz, 4H, 4 × H_f), 5.76 (s, 4H, 4 × H_a), 1.42 (s, 18H, 18 × H_g); **^{13}C NMR** (126 MHz, d_6-acetone) δ ppm 155.42, 149.82, 149.07, 144.45, 141.75, 135.04, 127.67, 127.28, 126.16, 125.49, 88.96, 53.78, 35.76, 31.53; **HRMS (ESI+)** *m/z*: 833.1078 ($[M - 2(PF_6) - H]^+$, calc. for $[C_{36}H_{35}I_2N_8]^+$ = 833.1069).

Bis-prototriazole diquat model, 131·2PF$_6$



Bis-triazole bipyridyl precursor **117** (40 mg, 0.072 mmol) was dissolved in $CHCl_3$ (20 mL). 1,2-Bis(triflyl)ethane **129** (64 mg, 0.20 mmol) was added, and the solution stirred under N_2 in the dark at 40 °C for 5 days. The solvent was then removed, and the residue suspended in MeOH (20 mL) and stirred vigorously for 5 min. The solid was filtered off and the filtrate collected and reduced to ~5 mL. $NH_4PF_{6(sat.\ aq.)}$ (0.5 mL), then H_2O (10 mL) were slowly added, forming a precipitate which was filtered and washed with H_2O (3 × 10 mL), before being extracted with acetone (3 × 10 mL). The solvent was then removed *in vacuo*, giving the product **131**·2PF$_6$ as a brown solid (25 mg, 40%); **^{1}H NMR** (300 MHz, d_6-acetone) δ ppm 9.68–9.74 (m, 4H, 2 × H_d, 2 × H_e), 9.51 (d, ^3J = 6.45 Hz, 2H, 2 × H_b), 9.01 (d, ^3J = 5.87 Hz, 2H, 2 × H_c), 7.94 (d, ^3J = 8.80 Hz, 4H, 4 × H_f), 7.75 (d, ^3J = 8.80 Hz, 4H, 4 × H_g), 5.69 (s, 4H, 4 × H_a), 1.40 (s, 18H, 18 × H_h); **^{13}C NMR** (76 MHz, d_6-acetone) δ ppm 154.10, 149.65, 148.92, 142.98, 141.93, 135.05, 127.97, 126.60, 125.49, 124.47, 121.32, 53.62, 31.54; **MS (MALDI+)** *m/z*: 582.51 ([M]$^+$, calc. for $[C_{36}H_{38}N_8]^+$ = 582.32).

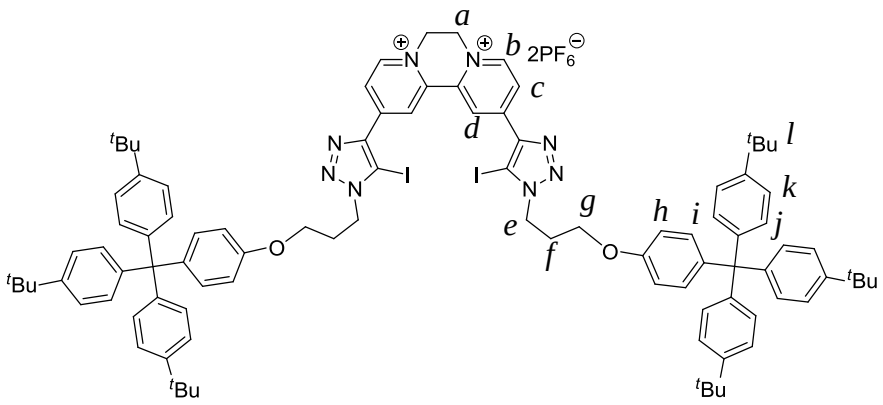
Bis-iodotriazole bipyridyl axle precursor, 132



Azide stopper **54** (186 mg, 0.32 mmol) was dissolved in THF (1.5 mL). Sodium iodide

(0.15 g, 1.0 mmol), then $Cu(ClO_4)_2 \cdot 6H_2O$ (0.19 g, 0.51 mmol) were added to the reaction, which was covered in aluminium foil and stirred at RT for 3–5 min. TBTA (13 mg, 0.024 mmol) was added, then DBU (39 mg, 0.26 mmol) dissolved in THF (1 mL) was also added. The diethynyl bipyridine **116** (26 mg, 0.13 mmol) was added to the reaction last, then the mixture was stirred in the dark at RT overnight. The reaction was then diluted with $CHCl_3$ (200 mL), then washed with $NH_4OH_{(aq.)}$ (25%, 2 × 25 mL) and brine (2 × 25 mL). The organic layer was separated, dried ($MgSO_4$) and the solvent removed *in vacuo*. The residue was then suspended in CH_3CN (10 mL) and heated at reflux for 1 h. The mixture was cooled to RT, the solid filtered off and washed with CH_3CN (2 × 5 mL), then Et_2O (2 × 5 mL), and air-dried to give the product **132** as an off-white powder (0.196 g, 95%); **^{1}H NMR** (400 MHz, $CDCl_3$): δ ppm 9.13 (s, 2H, 2 × H_c), 8.80 (d, ^3J = 4.89 Hz, 2H, 2 × H_a), 7.96 (d, ^3J = 4.03 Hz, 2H, 2 × H_b), 7.24 (d, ^3J = 8.44 Hz, 12H, 12 × H_i), 7.16–7.02 (m, 16H, 4 × H_h, 12 × H_j), 6.79 (d, ^3J = 8.68 Hz, 4H, 4 × H_g), 4.72 (t, ^3J = 7.21 Hz, 4H, 4 × H_d), 4.07 (t, ^3J = 5.40 Hz, 4H, 4 × H_f), 2.51–2.45 (m, 4H, 4 × H_e), 1.30 (s, 54H, 54 × H_k); **^{13}C NMR** (126 MHz, $CDCl_3$)**:** δ ppm 156.43, 156.14, 149.53, 148.32, 147.01, 144.06, 140.11, 139.85, 132.32, 130.70, 124.05, 121.64, 118.79, 113.07, 112.93, 63.87, 63.04, 48.12, 34.28, 31.37, 29.67; **HRMS (ESI+)** *m/z*: 1631.6416 ($[M + H]^+$, calc. for $[C_{94}H_{105}I_2N_8O_2]^+$ = 1631.6444).

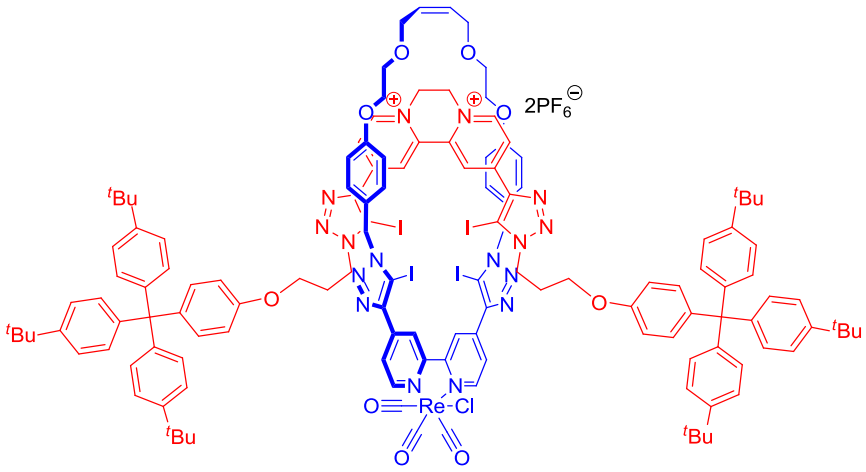
Bis-iodotriazole diquat axle, 133·2PF$_6$



Bis-iodotriazole bpy axle precursor **132** (100 mg, 0.061 mmol) was dissolved in $CHCl_3$ (60 mL), then the solvent carefully reduced *in vacuo* to ~10 mL. 1,2-Bis(triflyl)ethane (54 mg, 0.16 mmol) was added, and the solution stirred under N_2 in the dark at 40 °C for 5 d. The solvent was then removed, and the residue suspended in Et_2O (20 mL) and stirred vigorously for 5 min. The solid was filtered off, washed with Et_2O (2 × 10 mL), then

extracted with acetone (3 × 20 mL). The solvent was removed *in vacuo*, then the residue anion exchanged for PF_6^- by dissolving in CH_2Cl_2 (10 mL) and washing with $NH_4PF_{6(aq.)}$ (0.1 M, 6 × 10 mL). The solvent was then removed *in vacuo*, giving the product **133**·2PF_6 as a brown solid (54 mg, 46%); **^{1}H NMR** (300 MHz, d_6-acetone) δ ppm 9.75 (d, ^4J = 1.76 Hz, 2H, 2 × H_d), 9.53 (d, ^3J = 6.45 Hz, 2H, 2 × H_b), 9.16 (dd, ^3J = 6.45, ^4J = 1.76 Hz, 2H, 2 × H_c), 7.28–7.33 (m, 12H, 12 × H_j), 7.08–7.15 (m, 16H, 4 × H_i, 12 × H_k), 6.85 (s, 4H, 4 × H_h), 5.68 (s, 4H, 4 × H_a), 4.88 (t, ^3J = 7.00 Hz, 4H, 4 × H_e), 4.14 (t, ^3J = 5.90 Hz, 4H, 4 × H_g), 2.52 (quin, ^3J = 6.20 Hz, 4H, 4 × H_f), 1.29 (s, 54H, 54 × H_l); **^{13}C NMR** (126 MHz, d_6-acetone) δ ppm 157.61, 149.84, 149.31, 148.95, 145.30, 144.02, 141.65, 140.70, 132.94, 131.50, 125.79, 125.28, 125.17, 114.20, 87.17, 65.16, 64.00, 53.72, 49.62, 34.95, 31.74; **^{19}F NMR** (470 MHz, d_6-acetone) δ ppm −72.6 (d, $J_{P,F}$ = 709.19 Hz); **HRMS (ESI+)** *m/z*: 1804.6240 ([M − PF_6]$^+$, calc. for $[C_{96}H_{108}F_6I_2N_8O_2P]^+$ = 1803.6353).

Attempted synthesis of bis-iodotriazole diquat rotaxane, 134·Cl·PF_6



Bis-iodotriazole diquat axle **133**·2PF_6 (42 mg, 0.022 mmol), TBA·Cl (6 mg, 0.022 mmol), rhenium(I) bipyridyl-based macrocycle precursor **127** (40 mg, 0.033 mmol) and Hoveyda–Grubbs' catalyst (4 mg, 10% w/w cat.) were dissolved in dry CH_2Cl_2 (5 mL), and stirred in the dark under N_2 for 3 days. The solvent was then removed *in vacuo*, and the residue partially purified using size exclusion chromatography, as silica- or alumina-based chromatographic methods did not appear to be effective. Unfortunately it was discovered that the rotaxane was unstable, and it could not be isolated. **MS (ESI+)** *m/z*: 1429.82 ([M – 2(PF_6)]$^{2+}$, calc. for $[C_{135}H_{140}ClI_4N_{16}O_9Re]^{2+}$ = 1429.82).

References

(1) Hynes, M. J. *J. Chem. Soc., Dalton Trans.* **1993**, 311.
(2) Specfit v. 2.02 ed., Spectrum Software Associates Chapel Hill, NC, USA: 1997.
(3) Nowell, H.; Barnett, S. A.; Christensen, K. E.; Teat, S. J.; Allan, D. R. *J. Synch. Rad.* **2012**, *19*, 435.
(4) Cosier, J.; Glazer, A. M. *J. Appl. Cryst.* **1986**, *19*, 105.
(5) Palatinus, L.; Chapuis, G. *J. Appl. Cryst.* **1997**, *40*, 786.
(6) Betteridge, P. W.; Carruthers, J. R.; Cooper, R. I.; Prout, K.; Watkin, D. J. *J. Appl. Cryst.* **2003**, *36*, 1487.
(7) van der Sluis, P.; Spek, A. L. *Acta Cryst.* **1990**, *A46*, 194.
(8) Spek, A. L. *J. Appl. Cryst.* **2003**, *36*, 7.
(9) Carruthers, J. R.; Watkin, D. J. *Acta Cryst.* **1979**, *A35*, 698.
(10) Prince, E. *Mathematical Techniques in Crystallography and Materials Science*; Springer-Verlag, New York, 1982.
(11) Watkin, D. J. *Acta Cryst.* **1994**, *A50*, 411.
(12) Barbour, L. J. *Supramol. Chem.* **2001**, *1*, 189.
(13) Persistence of Vision Raytracer Pty. Ltd.: Williamstown, Victoria, Australia, 2004.
(14) Lee, B.-Y.; Park, S. R.; Jeon, H. B.; Kim, K. S. *Tetrahedron Lett.* **2006**, *47*, 5105.
(15) Goddard-Borger, E. D.; Stick, R. V. *Org. Lett.* **2007**, *9*, 3797.
(16) Fischer, N.; Goddard-Borger, E. D.; Greiner, R.; Klapötke, T. M.; Skelton, B. W.; Stierstorfer, J. *J. Org. Chem.* **2012**, *77*, 1760.
(17) Smith, K.; James, D. M.; Mistry, A. G.; Bye, M. R.; Faulkner, D. J. *Tetrahedron* **1992**, *48*, 7479.
(18) Xu, H.; Yin, K.; Huang, W. *J. Phys. Chem. C* **2009**, *114*, 1674.
(19) Zhao, T.; Liu, Z.; Song, Y.; Xu, W.; Zhang, D.; Zhu, D. *J. Org. Chem.* **2006**, *71*, 7422.
(20) Alvarez, S. G. A., Mijo T. *Synthesis* **1997**, *4*, 413.
(21) Guo, S.; Song, Y.; Huang, Q.; Yuan, H.; Wan, B.; Wang, Y.; He, R.; Beconi, M. G.; Franzblau, S. G.; Kozikowski, A. P. *J. Med. Chem.* **2009**, *53*, 649.
(22) Brotherton, W. S.; Clark, R. J.; Zhu, L. *J. Org. Chem.* **2012**, *77*, 6443.
(23) Ng, K.-Y.; Felix, V.; Santos, S. M.; Rees, N. H.; Beer, P. D. *Chem. Commun.* **2008**, 1281.
(24) Perepichka, I. F.; Besbes, M.; Levillain, E.; Sallé, M.; Roncali, J. *Chemistry of Materials* **2002**, *14*, 449.
(25) Wisner, J. A.; Beer, P. D.; Drew, M. G. B. *Angew. Chem. Int. Ed.* **2001**, *40*, 3606.
(26) O'Neil, E. J.; DiVittorio, K. M.; Smith, B. D. *Org. Lett.* **2006**, *9*, 199.
(27) Serpell, C. J.; Chall, R.; Thompson, A. L.; Beer, P. D. *Dalton Trans.* **2011**, *40*, 12052.
(28) Gibson, H. W.; Lee, S. H.; Engen, P. T.; Lecavalier, P.; Sze, J.; Shen, Y. X.; Bheda, M. *J. Org. Chem.* **1993**, *58*, 3748.
(29) Aucagne, V.; Hänni, K. D.; Leigh, D. A.; Lusby, P. J.; Walker, D. B. *J. Am. Chem. Soc.* **2006**, *128*, 2186.
(30) Bala, K.; Hailes, H. C. *Synthesis* **2005**, *2005*, 3423.
(31) Lankshear, M. D.; Evans, N. H.; Bayly, S. R.; Beer, P. D. *Chem. Eur. J.* **2007**, *13*, 3861.
(32) Sambrook, M. R.; Beer, P. D.; Lankshear, M. D.; Ludlow, R. F.; Wisner, J. A. *Org.*

Biomol. Chem. **2006**, *4*, 1529.
(33) Sodji, Q. H.; Patil, V.; Kornacki, J. R.; Mrksich, M.; Oyelere, A. K. *J. Med. Chem.* **2013**, *56*, 9969.
(34) White, N. G.; Costa, P. J.; Carvalho, S.; Félix, V.; Beer, P. D. *Chem. Eur. J.* **2013**, *19*, 17751.
(35) Gibson, V. C.; Spitzmesser, S. K.; White, A. J. P.; Williams, D. J. *Dalton Trans.* **2003**, 2718.
(36) Gee, H.-C.; Lee, C.-H.; Jeong, Y.-H.; Jang, W.-D. *Chem. Commun.* **2011**, *47*, 11963.
(37) White, N. G.; Beer, P. D. *Chem. Commun.* **2012**, *48*, 8499.
(38) Phipps, D. E.; Beer, P. D. *Tetrahedron Lett.* **2009**, *50*, 3454.
(39) Mercurio, J. M.; Tyrrell, F.; Cookson, J.; Beer, P. D. *Chem. Commun.* **2013**, *49*, 10793.
(40) Butterfield, A. M.; Gilomen, B.; Siegel, J. S. *Org. Process Res. Dev.* **2012**, *16*, 664.
(41) Rodriguez, A. L.; Tamrazi, A.; Collins, M. L.; Katzenellenbogen, J. A. *J. Med. Chem.* **2003**, *47*, 600.
(42) Srinivasan, M.; Sankararaman, S.; Hopf, H.; Dix, I.; Jones, P. G. *J. Org. Chem.* **2001**, *66*, 4299.
(43) Bonger, K. M.; van den Berg, R. J. B. H. N.; Heitman, L. H.; Ijzerman, A. P.; Oosterom, J.; Timmers, C. M.; Overkleeft, H. S.; van der Marel, G. A. *Bioorg. Med. Chem.* **2007**, *15*, 4841.
(44) Hirose, T.; Matsuda, K. *Chem. Commun.* **2009**, 5832.
(45) Porzi, G.; Concilio, C. *J. Organomet. Chem.* **1977**, *128*, 95.
(46) Talele, H. R.; Chaudhary, A. R.; Patel, P. R.; Bedekar, A. V. *ARKIVOC* **2011**, *2011*, 15.
(47) Neenan, T. X.; Whitesides, G. M. *J. Org. Chem.* **1988**, *53*, 2489.
(48) Pelletier, G.; Lie, S.; Mousseau, J. J.; Charette, A. B. *Org. Lett.* **2012**, *14*, 5464.
(49) Patterson, B. T.; Keene, F. R. *Aust. J. Chem.* **1998**, *51*, 999.
(50) Gillaizeau-Gauthier, I.; Odobel, F.; Alebbi, M.; Argazzi, R.; Costa, E.; Bignozzi, C. A.; Qu, P.; Meyer, G. J. *Inorg. Chem.* **2001**, *40*, 6073.
(51) Zhang, D.; Telo, J. P.; Liao, C.; Hightower, S. E.; Clennan, E. L. *J. Phys. Chem. A* **2007**, *111*, 13567.
(52) García-Lago, R.; Alonso-Gómez, J.-L.; Sicre, C.; Cid, M.-M. *Heterocycles* **2008**, *75*, 57.
(53) Staats, H.; Eggers, F.; Haß, O.; Fahrenkrug, F.; Matthey, J.; Lüning, U.; Lützen, A. *Eur. J. Org. Chem.* **2009**, *2009*, 4777.
(54) James, P. V.; Yoosaf, K.; Kumar, J.; Thomas, K. G.; Listorti, A.; Accorsi, G.; Armaroli, N. *Photochem. Photobiol. Sci.* **2009**, *8*, 1432.
(55) Lindner, E.; von Au, G.; Eberle, H.-J. *Chem. Ber.* **1981**, *114*, 810.

Appendices

Appendix A: Crystallography Data

Crystallographic Information Files (CIF)

The crystallographic information files (.cif) of the crystal structures presented in this thesis are given in the accompanying CD-ROM.

Compound	Space Group	File Name
64	$P2_1/n$	64_carb
65	$C2/c$	65_carb
Ni(**65**)$_2$	$P\bar{1}$	Ni(65)2_complex
81	Pa	81_ naph
83·2BF_4	$P2_1/n$	83-2BF4_ naph
128·2Cl	$P\bar{1}$	128-2Cl_rotax

Data Tables

Table A-1: Summary of the single crystal X-ray collection and refinement data for carbazole-based compounds **64**, **65** and Ni(**65**)$_2$.

	64	**65**	Ni(**65**)$_2$
Formula	$C_{40}H_{59}N_7$	$C_{44}H_{51}N_7$, CH_2Cl_2	$C_{88}N_{14}Ni$
F_w [g mol^{-1}]	637.96	762.84	1311.77
crystal size [mm^3]	0.02×0.10×0.70	0.10×0.20×0.40	0.02×0.02×0.55
crystal System	Monoclinic	Monoclinic	Triclinic
space group	$P2_1/n$	$C2/c$	$P\bar{1}$
a [Å]	23.0026(7)	16.6255(5)	14.2560(9)
b [Å]	5.7192(2)	14.8501(4)	16.8784(11)
c [Å]	28.6148(9)	17.1284(5)	18.4142(12)
α [°]	90	90	74.929(6)
β [°]	96.684(3)	104.8671(13)	73.440(6)
γ [°]	90	90	89.658(5)
V [Å^3]	3738.9(2)	4087.3(2)	4089.8(5)
Z	4	4	2
T [K]	150(2)	150(2)	150(2)
Radiation type	Cu Kα	Mo Kα	Cu Kα
λ [Å]	1.5418	0.71073	1.5418
μ [mm^{-1}]	0.518	0.200	0.738
F(000)	1392	1624	1308
θ [°]	3.87–76.52	5.12–27.53	2.72–44.56
index ranges	$-29 \le h \le 28$	$-21 \le h \le 20$	$-12 \le h \le 12$
	$0 \le k \le 6$	$0 \le k \le 19$	$-14 \le k \le 15$
	$0 \le l \le 35$	$0 \le l \le 22$	$0 \le l \le 16$
reflections collected	14663	20848	12344
independent reflections (R_{int})	7854 (0.0503)	4664 (0.033)	6163 (0.1072)
data/restraints/parameters	5585/0/424	4663/6/249	6103/0/413
GOF on F^2	1.0008	1.0551	1.0861
R_1 ($I > 2\sigma(I)$)[a]	0.0573	0.0576	0.1937
wR_2 ($I > 2\sigma(I)$)[b]	0.1421	0.1366	0.3607
R_1 (all data)	0.0797	0.0758	0.2624
wR_2 (all data)	0.1541	0.1533	0.3985

[a] $R_1 = \Sigma| |F_0| - |F_c| | / \Sigma |F_0|$. [b] $wR_2 = [\sum w(F_0^2 - F_c^2)^2 / \sum w(F_0^2)^2]^{1/2}$

Table A-2: Summary of the single crystal X-ray collection and refinement for naphthalene-based acyclic compounds **81** and **83**·2BF_4, and all-XB rotaxane **128**·2Cl.

	81	**83**·2BF_4	**128**·2Cl
Formula	2($C_{36}H_{38}N_6$)	$C_{38}H_{44}N_6$, 2(BF_4), 0.5($CHCl_3$)	$C_{97}H_{109}I_2N_7O_2$, $C_{39}H_{32}ClI_2N_8O_7Re$, 2Cl, 0.6($CDCl_3$)
F_w [g mol^{-1}]	1109.48	818.10	3001.69
crystal size [mm^3]	0.10×0.45×0.70	0.03×0.04×0.22	0.01×0.01×0.06
crystal System	Monoclinic	Monoclinic	Triclinic
space group	*Pa*	$P2_1/n$	$P\bar{1}$
a [Å]	14.9636(3)	25.2347(13)	13.5151(5)
b [Å]	10.3226(2)	6.0664(2)	21.9753(11)
c [Å]	20.2574(4)	30.3545(13)	35.6732(15)
α [°]	90	90	86.667(4)
β [°]	98.4678(7)	112.756(6)	82.971(3)
γ [°]	90	90	77.018(3)
V [Å^3]	3094.91(11)	4285.1(4)	10241.3(4)
Z	4	4	2
T [K]	150(2)	150(2)	100(2)
Radiation type	Mo Kα	Cu Kα	synchrotron
λ [Å]	0.71073	1.5418	0.68890
μ [mm^{-1}]	0.072	1.676	1.290
F(000)	1183	1700	3002.593
θ [°]	5.156–27.475	3.5018–75.9801	1.470–26.589
index ranges	−19 ≤ h ≤ 19 0 ≤ k ≤ 13 0 ≤ l ≤ 26	−31 ≤ h ≤ 28 0 ≤ k ≤ 7 0 ≤ l ≤ 37	−17 ≤ h ≤ 17 −27 ≤ k ≤ 27 0 ≤ l ≤ 46
reflections collected	32827	18129	123417
independent reflections (R_{int})	14203 (0.029)	8685 (0.0386)	38243 (0.204)
data/restraints/parameters	6968/86/813	8651/63/551	27405/6222/2233
GOF on F^2	0.9622	0.9602	1.0319
R_1 ($I > 2\sigma(I)$)[a]	0.0428	0.1130	0.1011
wR_2 ($I > 2\sigma(I)$)[b]	0.0951	0.3202	0.2408
R_1 (all data)	0.0570	0.1460	0.1760
wR_2 (all data)	0.1075	0.3500	0.3584

[a] $R_1 = \Sigma| |F_0| - |F_c| | / \Sigma |F_0|$. [b] $wR_2 = [\sum w(F_0^2 - F_C^2)^2 / \sum w(F_0^2)^2]^{1/2}$

Appendix B: Absorption and Luminescence Spectra

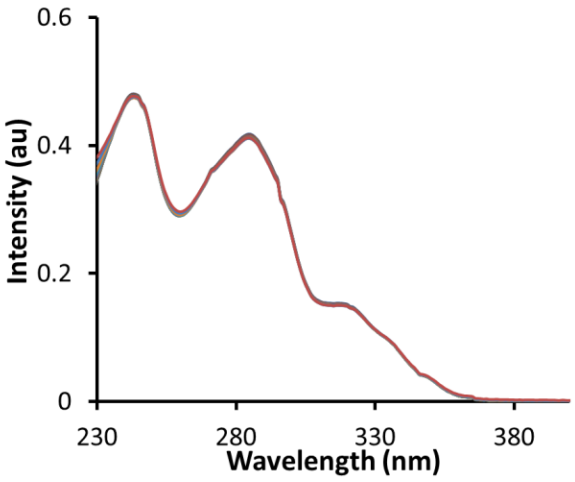


Figure B-1: UV-vis absorption spectra of **20**·2BF_4 upon addition of Cl^- (10 μM host, CH_3CN, 293 K).

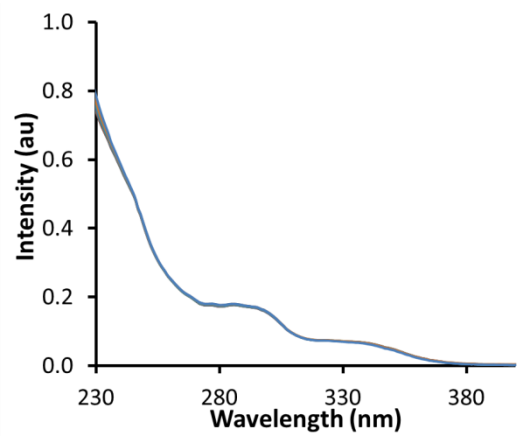


Figure B-2: UV-vis absorption spectra of rotaxane **60**·2PF_6 upon addition of TBA·Cl (10 μM host, CH_3CN, 293 K).

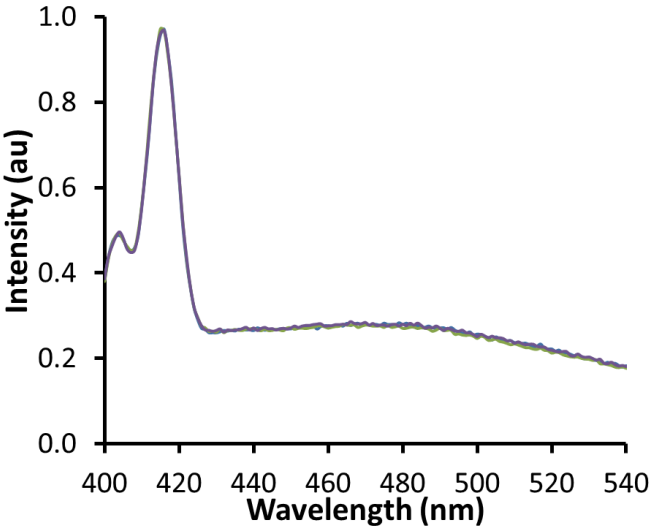


Figure B-3: Fluorescence emission spectrum of rotaxane **106**·2BF_4 upon addition of TBA·Cl (λ_{ex} = 370 nm, CH_3CN, 293 K).

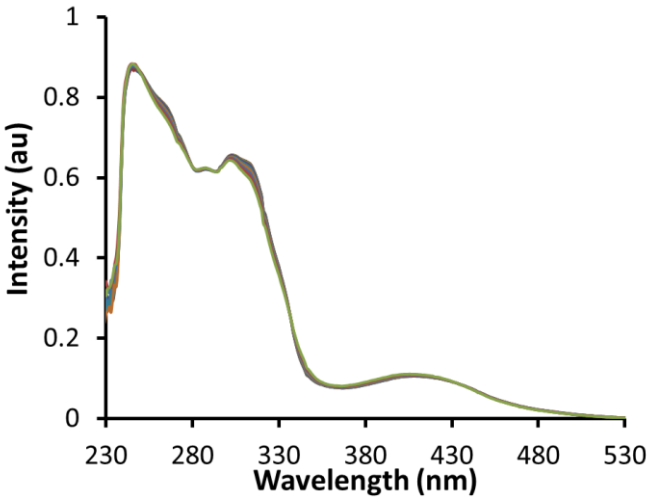


Figure B-4: UV-vis absorption spectra of **118** upon addition of TBA·Cl (15 μM host, $CHCl_3$, 293 K).

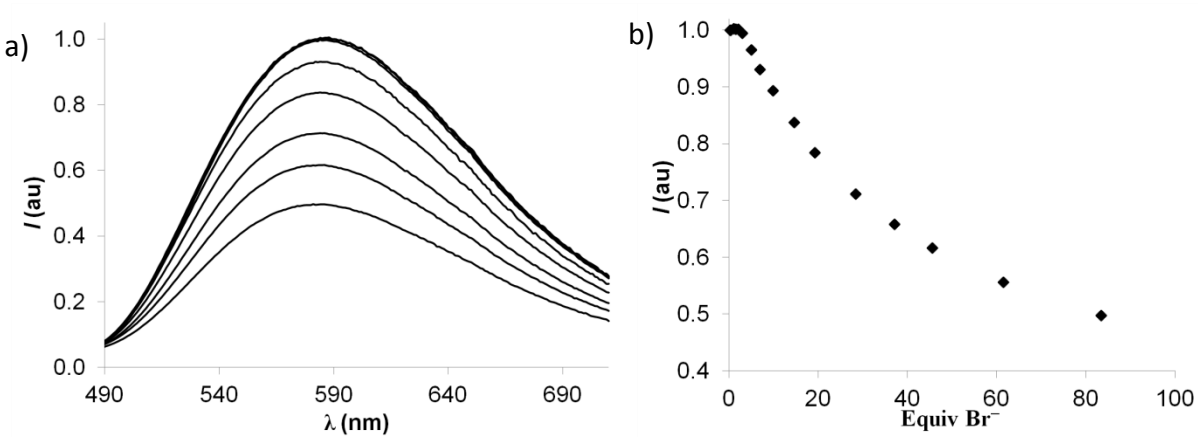


Figure B-5: a) Changes in the emission spectra of rotaxane **128**·2PF_6 (1×10^{-5} M in 10% H_2O/CH_3CN) upon addition of increasing equivalents of Br^-; **b)** Changes in the emission at 585 nm upon addition of Br^-.

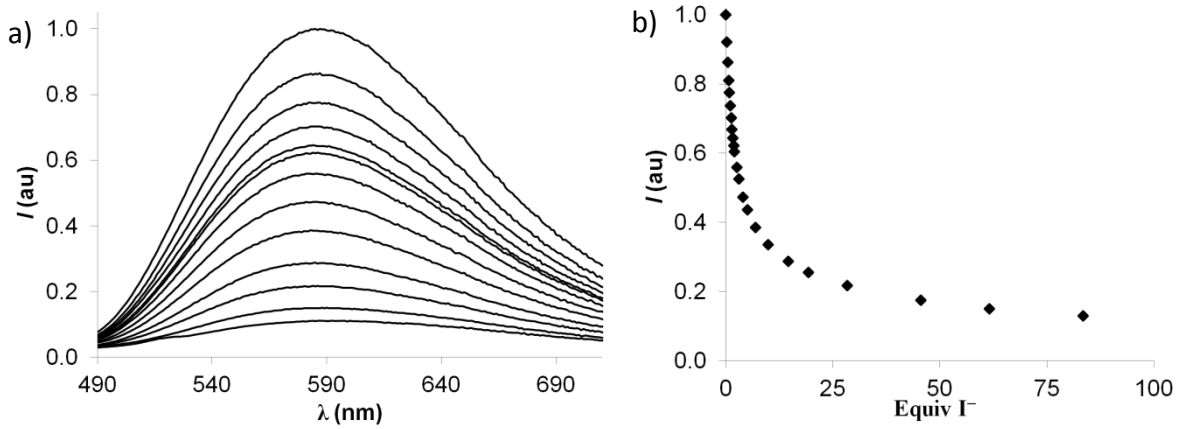


Figure B-6: a) Changes in the emission spectra of rotaxane **128**·2PF_6 (1×10^{-5} M in 10% H_2O/CH_3CN) upon addition of increasing equivalents of I^-; **b)** Changes in the emission at 585 nm upon addition of I^-.

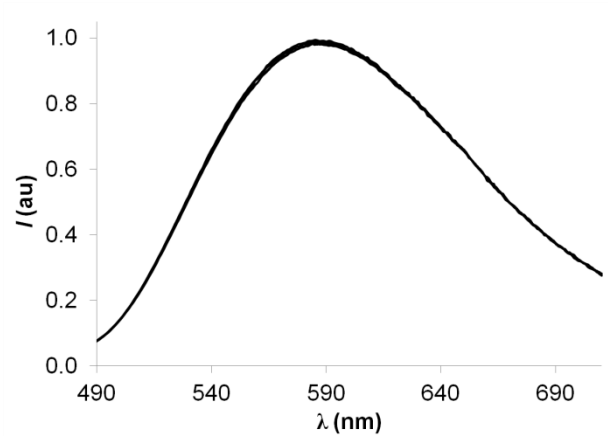


Figure B-7: The emission spectra of rotaxane **128**·$2PF_6$ (1×10^{-5} M in 10% H_2O/CH_3CN) upon addition of increasing equivalents of $H_2PO_4^-$.

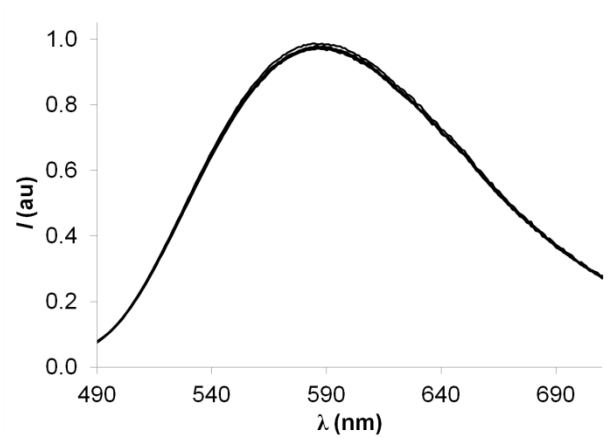


Figure B-8: The emission spectra of rotaxane **128**·$2PF_6$ (1×10^{-5} M in 10% H_2O/CH_3CN) upon addition of increasing equivalents of AcO^-.

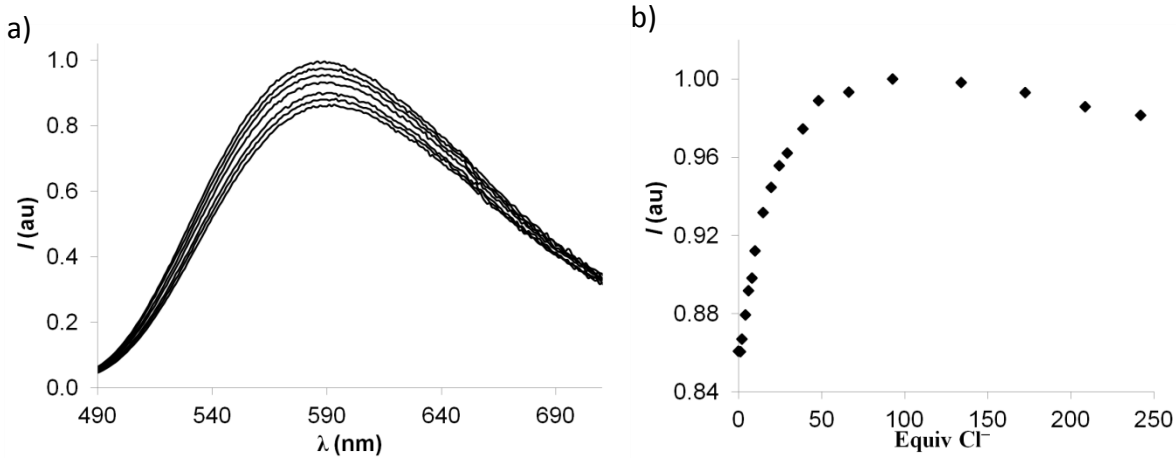


Figure B-9: a) Changes in the emission spectra of rotaxane **128**·$2PF_6$ (1×10^{-5} M in 20% H_2O/CH_3CN) upon addition of increasing equivalents of Cl^-; **b)** Changes in the emission at 585 nm upon addition of Cl^-.

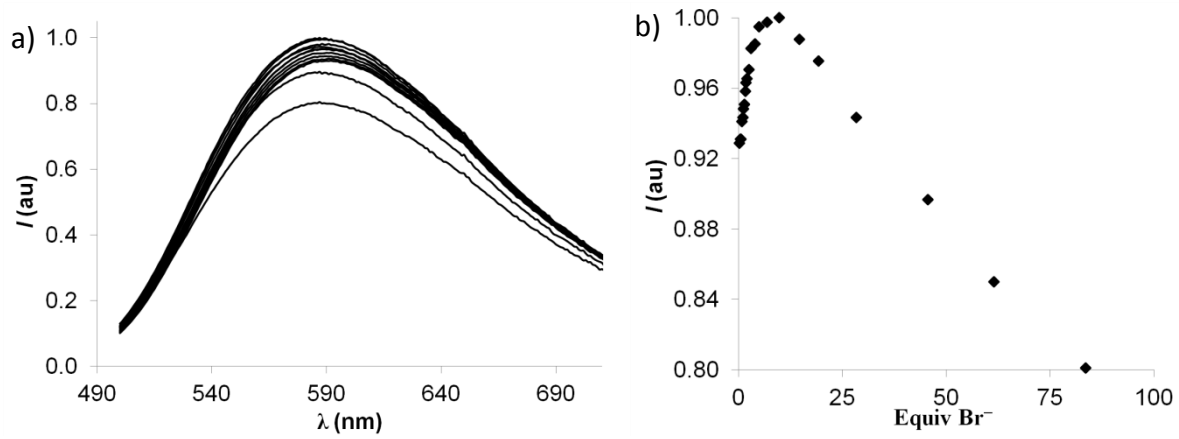


Figure B-10: a) Changes in the emission spectra of rotaxane **128**·2PF_6 (1×10^{-5} M in 20% H_2O/CH_3CN) upon addition of increasing equivalents of Br^-; **b)** Changes in the emission at 585 nm upon addition of Br^-.

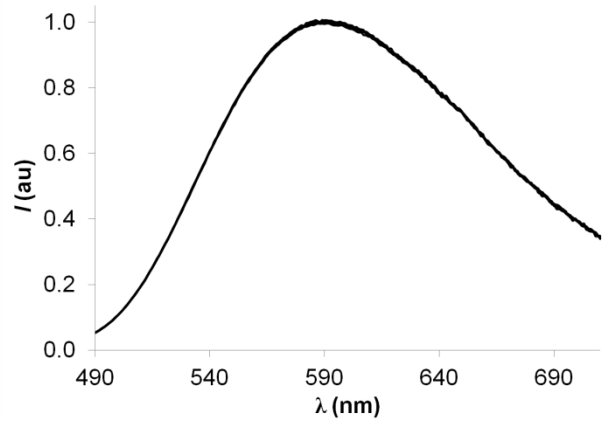


Figure B-11: The emission spectra of rotaxane **128**·2PF_6 (1×10^{-5} M in 20% H_2O/CH_3CN) upon addition of increasing equivalents of $H_2PO_4^-$.

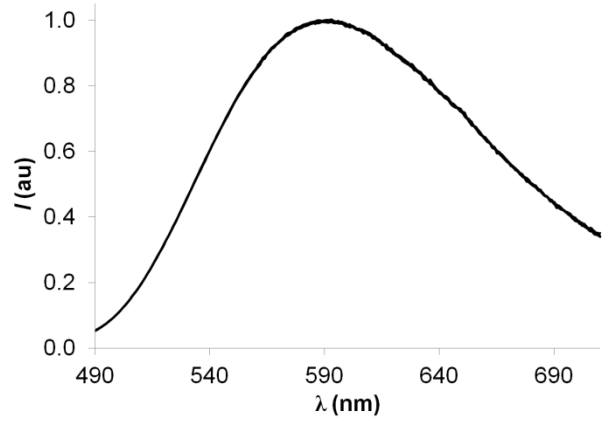


Figure B-12: The emission spectra of rotaxane **128**·2PF_6 (1×10^{-5} M in 20% H_2O/CH_3CN) upon addition of increasing equivalents of AcO^-.

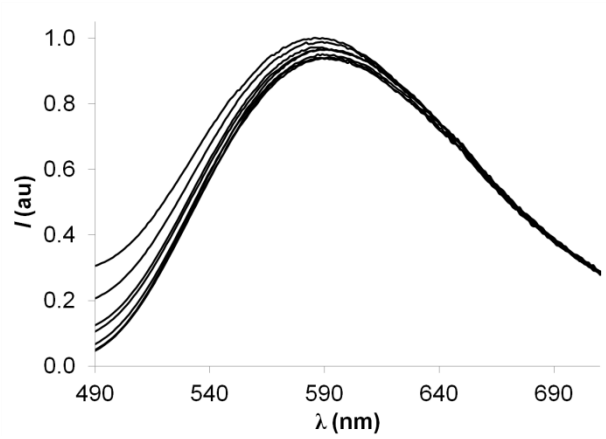


Figure B-13: Changes in the emission spectra of rotaxane **128**·2PF_6 (1×10^{-5} M in 20% H_2O/CH_3CN) upon addition of increasing equivalents of SO_4^{2-}.

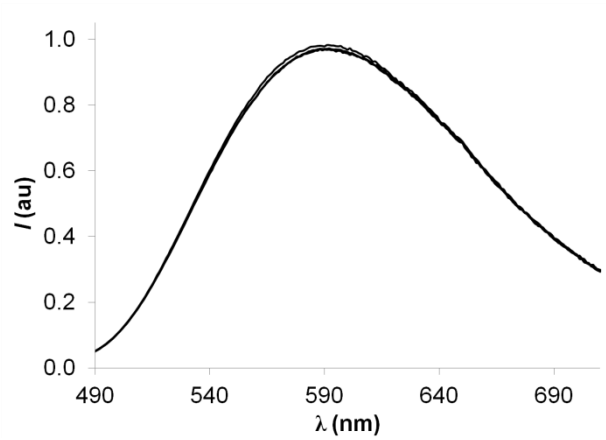


Figure B-14: The emission spectra of rotaxane **128**·2PF_6 (1×10^{-5} M in 20% H_2O/CH_3CN) upon addition of increasing equivalents of NO_3^-.

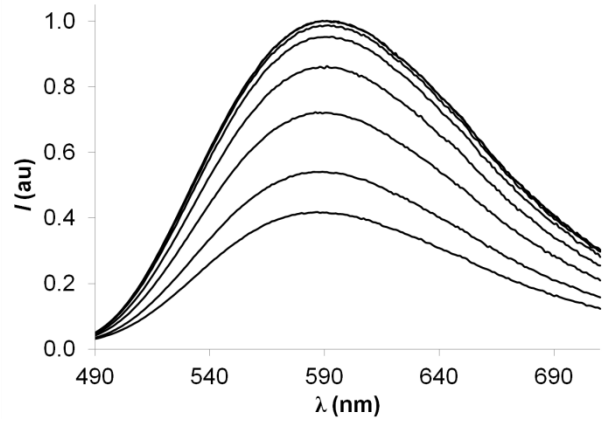


Figure B-15: Changes in the emission spectra of rotaxane **128**·2PF_6 (1×10^{-5} M in 20% H_2O/CH_3CN) upon addition of increasing equivalents of HCO_3^-.

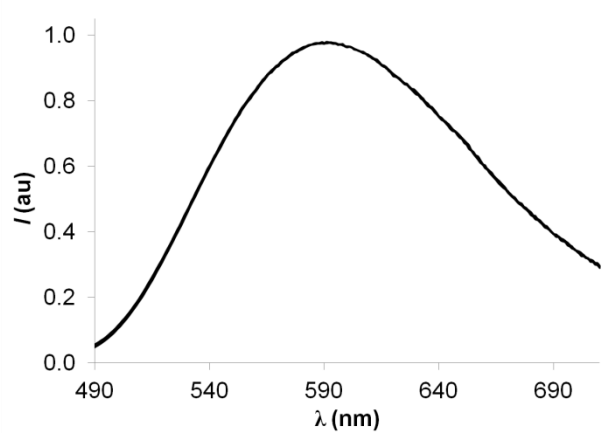


Figure B-16: The emission spectra of rotaxane **128**·2PF_6 (1×10^{-5} M in 20% H_2O/CH_3CN) upon addition of increasing equivalents of F^-.

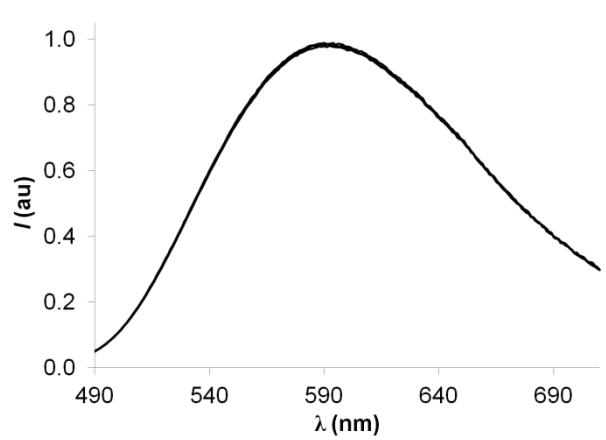


Figure B-17: The emission spectra of rotaxane **128**·2PF_6 (1×10^{-5} M in 20% H_2O/CH_3CN) upon addition of increasing equivalents of ClO_4^-.

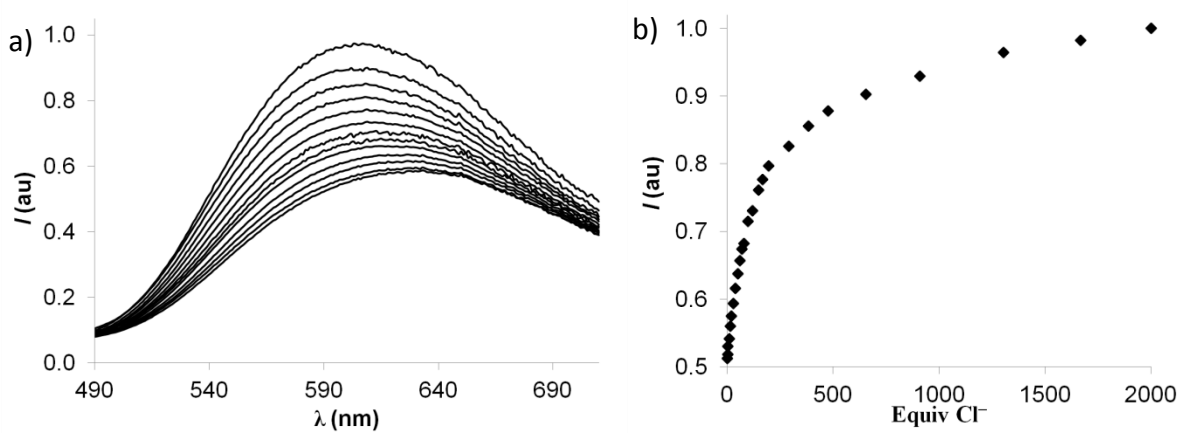


Figure B-18: a) Changes in the emission spectra of rotaxane **128**·2PF_6 (1×10^{-5} M in 50% H_2O/CH_3CN) upon addition of increasing equivalents of Cl^-; **b)** Changes in the emission at 555 nm upon addition of Cl^-.

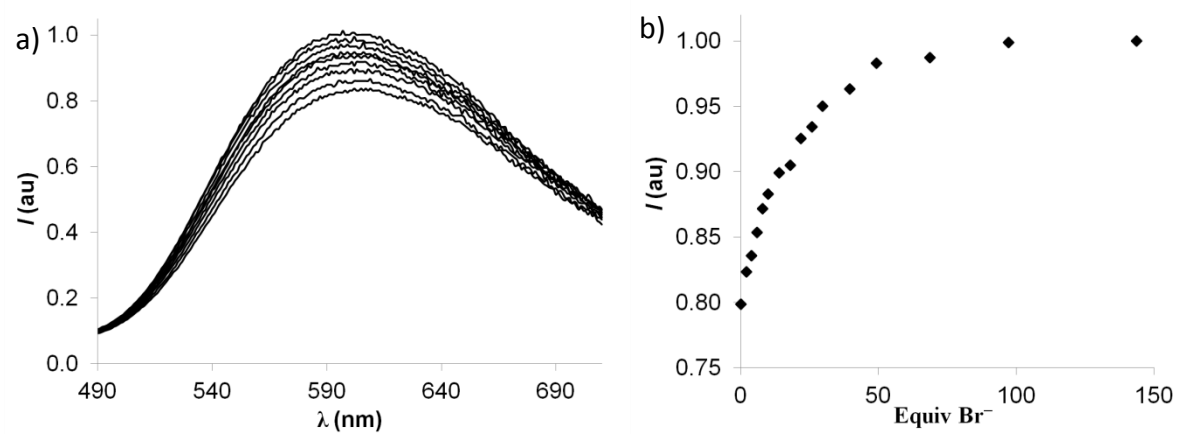


Figure B-19: a) Changes in the emission spectra of rotaxane **128**·2PF_6 (1×10^{-5} M in 50% H_2O/CH_3CN) upon addition of increasing equivalents of Br^-; **b)** Changes in the emission at 555 nm upon addition of Br^-.

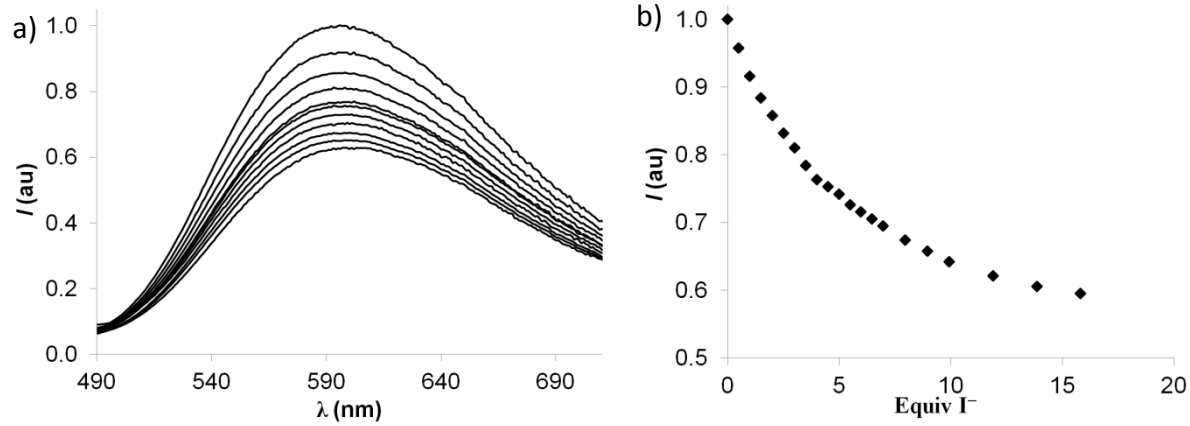


Figure B-20: a) Changes in the emission spectra of rotaxane **128**·2PF_6 (1×10^{-5} M in 50% H_2O/CH_3CN) upon addition of increasing equivalents of I^-; **b)** Changes in the emission at 555 nm upon addition of I^-. While spectra were also obtained with higher equivalents of anion added, they were not used for determining the association constant as the sample began to precipitate out of solution.

Appendix C: Electrochemical Data

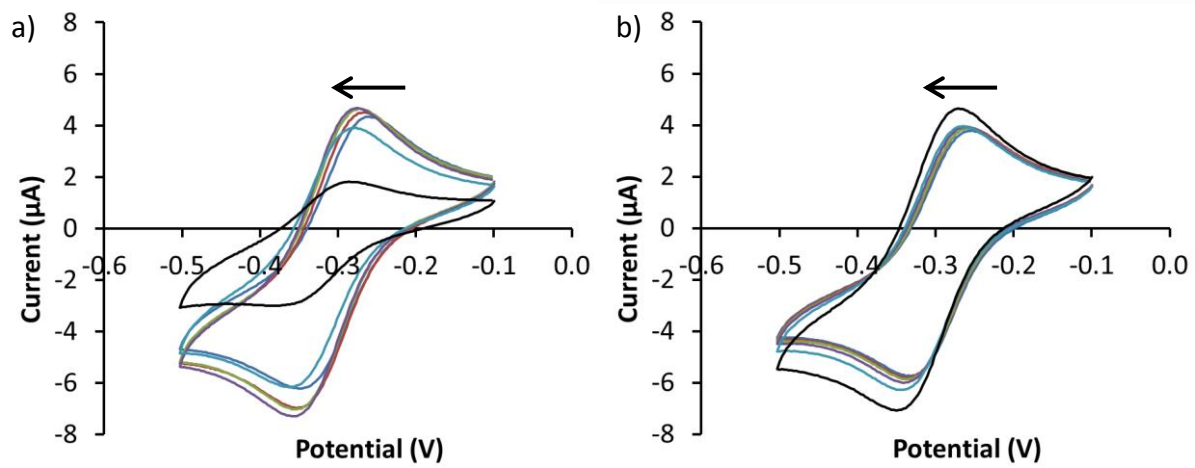


Figure C-1: Cyclic voltammograms of iodotriazole receptor **130**$^{2+}$ upon addition of **a)** Br^-; and **b)** I^- anions (electrolyte: 0.1 M $TBA{\cdot}PF_6$ in CH_3CN, 293 K, reference electrode: Ag/AgCl).

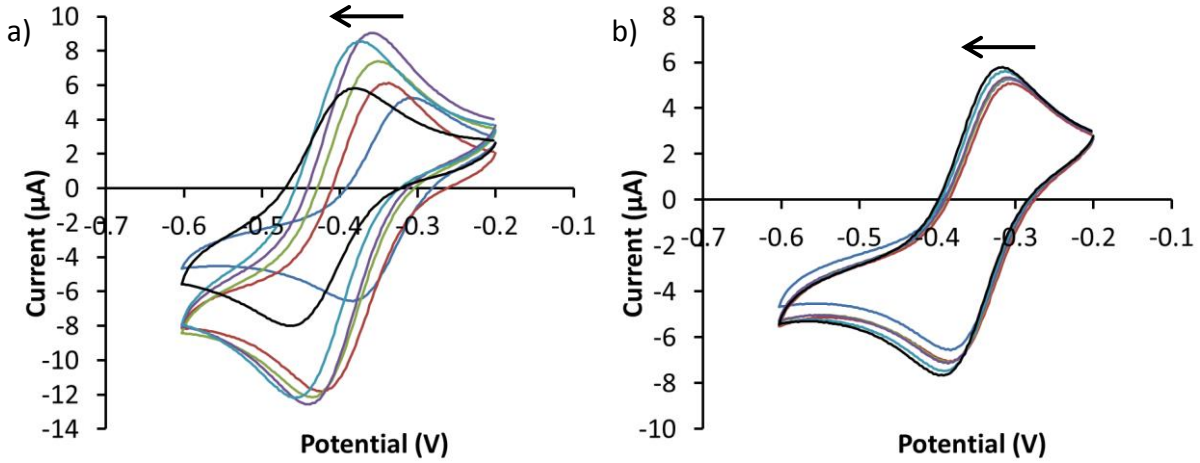


Figure C-2: Cyclic voltammograms of prototriazole receptor **131**$^{2+}$ upon addition of **a)** Cl^-; and **b)** I^- anions (electrolyte: 0.1 M $TBA{\cdot}PF_6$ in CH_3CN, 293 K, reference electrode: Ag/AgCl).

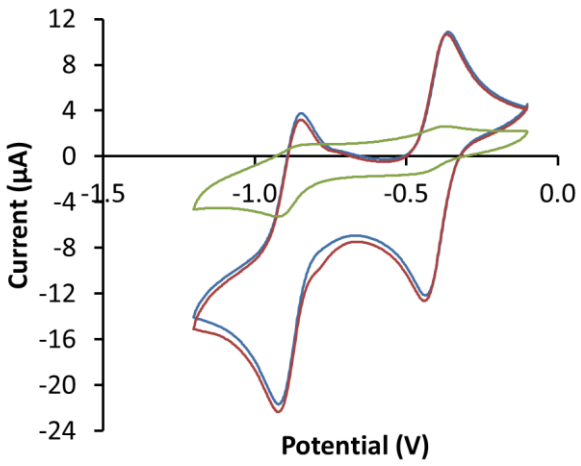


Figure C-3: Cyclic voltammograms of diquat upon addition of Cl^- anions. Note that partial precipitation had occurred at 5 equivalents (green line) (electrolyte: 0.1 M TBA·PF_6 in CH_3CN, 293 K, reference electrode: Ag/AgCl).